Landscape Series

Garik Gutman
Jiquan Chen
Geoffrey M. Henebry
Martin Kappas *Editors*

Landscape Dynamics of Drylands across Greater Central Asia: People, Societies and Ecosystems

Springer

Landscape Series

Volume 17

Aims and Scope

Springer's innovative Landscape Series is committed to publishing high-quality manuscripts that approach the concept of landscape from a broad range of perspectives. Encouraging contributions on theory development, as well as more applied studies, the series attracts outstanding research from the natural and social sciences, and from the humanities and the arts. It also provides a leading forum for publications from interdisciplinary and transdisciplinary teams.

Drawing on, and synthesising, this integrative approach the Springer Landscape Series aims to add new and innovative insights into the multidimensional nature of landscapes. Landscapes provide homes and livelihoods to diverse peoples; they house historic—and prehistoric—artefacts; and they comprise complex physical, chemical and biological systems. They are also shaped and governed by human societies who base their existence on the use of the natural resources; people enjoy the aesthetic qualities and recreational facilities of landscapes, and people design new landscapes.

As interested in identifying best practice as it is in progressing landscape theory, the Landscape Series particularly welcomes problem-solving approaches and contributions to landscape management and planning. The ultimate goal is to facilitate both the application of landscape research to practice, and the feedback from practice into research.

More information about this series at http://www.springer.com/series/6211

Garik Gutman • Jiquan Chen
Geoffrey M. Henebry • Martin Kappas
Editors

Landscape Dynamics of Drylands across Greater Central Asia: People, Societies and Ecosystems

Springer

Editors
Garik Gutman
Land-Cover/Land-Use Change Program
NASA Headquarters
Washington, DC, USA

Geoffrey M. Henebry
Department of Geography, Environment, and Spatial Sciences, Center for Global Change and Earth Observations
Michigan State University
East Lansing, MI, USA

Jiquan Chen
Department of Geography, Environment, and Spatial Sciences, Center for Global Change and Earth Observations
Michigan State University
East Lansing, MI, USA

Martin Kappas
Cartography, GIS & Remote Sensing Department, Institute of Geography
Georg-August University
Goettingen, Germany

ISSN 1572-7742 ISSN 1875-1210 (electronic)
Landscape Series
ISBN 978-3-030-30741-7 ISBN 978-3-030-30742-4 (eBook)
https://doi.org/10.1007/978-3-030-30742-4

This Springer imprint is published by the registered company Springer Nature Switzerland AG.
The registered company address is: Gewerbestrasse 11, 6330 Cham, Switzerland

Preface

Political and economic transformations, increasing populations, globalization, and climatic changes in the drylands of Greater Central Asia, which have been occurring over the past decades, have greatly affected the *people, societies, and ecosystems* of the region. Central Asia has experienced many drastic changes in land use from the Virgin Lands Campaign in mid-1950s to the abandonment of agricultural fields after the breakup of the Soviet Union in 1991 to their recultivation in more recent years. These and other changes over Greater Central Asia affected the environment and societies of the region, where water use by humans and water availability for crops, livestock, and other human uses have been the primary drivers of environmental changes. The most well-known (and analyzed) example in the region is the decades-long desiccation of the Aral Sea resulting from the diversion of two rivers for crop irrigation, specifically to increase cotton yields and combat soil salinization. Satellite observations that have accumulated during the last five decades provide a rich time series of the dynamic land surface, enabling systematic analysis of changes in land cover and land use from space. In the case of Aral Sea, Landsat satellite observations have allowed the continuous monitoring of its dynamics at spatial resolutions of tens of meters since early 1970s.

The breakup of the Soviet Union had huge impact on the structure of the society, local and regional economies, and the way people use the land. In some countries, state-owned and collectivized farms were transitioned to privately owned fields and enterprises. Some arable lands were abandoned, others idled or continued with cultivation; there were substantial changes in what was being produced and to whom it was being marketed. Space observations of nightlights, for example, have revealed that many cities and towns experienced significant shifts in population—both increasing and decreasing depending on country and region. During the economic boom in China that followed its accession to the World Trade Organization in 2001, the northwest drylands have experienced strong rural-to-urban migration, along with a dramatic expansion of urban infrastructure, while populations more than tripled.

This book describes and analyzes various patterns, processes, and consequences to the population and landscapes of the Greater Central Asia region. It is a compilation of results from studies on land-cover and land-use changes and their interactions with carbon, water and energy cycles, landscape dynamics, the role of institutional changes, as well as the consequences of global changes. The book is a truly interdisciplinary collaborative effort by an international team consisting of scholars from the USA, Europe, Central Asia, and elsewhere, under the auspices of the Northern Eurasia Earth Science Partnership Initiative (NEESPI) supported primarily by the NASA Land-Cover/Land-Use Change Program. It is of interest and directed to a broad range of scientists within natural and social sciences, those involved in studying recent and ongoing changes in drylands, be they senior scientists, early career scientists, or students. These studies provide the analysis of the dramatic changes in land uses triggered by an abrupt change in the economies of the region and land management. Lessons learned from these studies are additional evidence for the sustainability development of the drylands. The satellite data used for these studies were mostly from NASA and ESA optical sensors with coarse (~5 km to 250 m) and medium (100 m to 10 m) spatial resolutions.

In the context of the forthcoming Sixth Assessment Report (AR6) of the Intergovernmental Panel on Climate Change (IPCC) the IPCC Special report on Climate Change and Land published in 2019 provides a broad overview of the situation of Greater Central Asia.

In particular, the present book can help answer questions on the perception of risks and benefits of climate change, adaptation and mitigation options, and societal responses, including sociological aspects.

We warmly thank all the contributors of this book and acknowledge NASA's support. We also appreciate several colleagues for their constructive peer review of the drafts of the chapters. We thank Connor Crank for creating the webpage to facilitate communication among the authors and Kaylee Peterson for checking the format of all the chapters.

Washington, DC, USA Garik Gutman
January 2019

Contents

About the Editors

Dr. Garik Gutman is a Program Manager for the NASA Land-Cover/Land-Use Change (LCLUC) Program. He received his PhD in Climate Modeling in 1984. He was a National Research Council of the National Academy of Sciences Fellow at the National Oceanic and Atmospheric Administration (NOAA) and then worked there for 14 years as a Research Scientist. His research focused on remote sensing of the Earth's land surface and atmosphere from space. In 1996, for developing an original technique using satellite data for reliable analyses of the Earth's vegetation cover and its long-term variations, he received the US Department of Commerce Bronze Medal Award. During the last two decades, he has been leading the LCLUC program at NASA headquarters as well as Landsat-related activities. He is author of over 80 publications in peer-reviewed scientific journals and of several chapters in various climate- and land-cover related scientific volumes. He has been a chief editor or co-editor in several volumes on LCLUC-environment interactions including those for the Eurasian Arctic, in Siberia, and in Eastern Europe published by Springer.

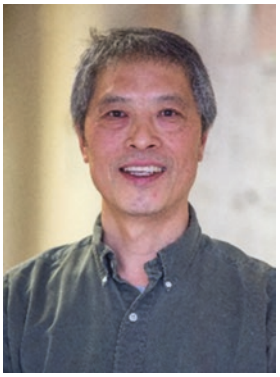

Dr. Jiquan Chen received his PhD in Ecosystem Analysis from the University of Washington and is currently a Professor at Michigan State University. He was a Bullard Fellow at Harvard University and on the faculty at Michigan Tech University and University of Toledo. He is broadly interested in ecosystem analysis, landscape ecology, conservation biology, biophysics, global change, land use, urban studies, and the sustainability of socioeconomic-ecological systems. He has conducted research on edge effects in fragmented landscapes, 3D canopy of forests, ecosystem carbon/water/energy fluxes, riparian zone management, agricultural and bioenergy crops, grassland (rangeland) ecology, dynamics of urban systems, and the role of institution in shaping landscapes and regions under the changing globe. He is a Fellow of the Ecological Society of America and of the American Association for the Advancement of Science and serves as the Editor in Chief for *Ecological Processes* and the book series Landscape Studies by Springer.

Dr. Geoffrey M. Henebry received his MS and PhD degrees in Environmental Sciences from The University of Texas at Dallas. He is a Full Professor in the Department of Geography, Environment, and Spatial Sciences at Michigan State University. He was a Senior Fulbright Research Fellow at Instituto Nacional de Pesquisas Espaciais (INPE) in Brazil and served on the faculties at Kansas State University, Rutgers University-Newark, University of Nebraska-Lincoln, and South Dakota State University. His research interests are broad and involve the use of remote sensing and geospatial technologies to study environmental patterns and processes, including quantitative analysis and modeling of land surface phenology and land-cover/land-use change. He is active in the American Geophysical Union and the North American Regional Chapter of the International Association for Landscape Ecology. He also serves as an Associate Editor for *Remote Sensing of Environment* and on the editorial boards of *Landscape Ecology* and *International Journal of Biometeorology*.

Dr. Martin Kappas is a University Professor of Geography and the Head of the Cartography, GIS, and Remote Sensing Section of the Georg-August University of Göttingen, Germany. His remote-sensing laboratory is a full member of EARSeL (European Association of Remote Sensing Laboratories). He is an active Member of DesertNET International (Competence Network for Research to Combat Desertification). His research interests are broad and include topics such as landscape evaluation using techniques of geoinformatics and ground truth data collection. His main research theme is the use of remote sensing and GIS to study land-cover/land-use changes. He is currently working on diverse interdisciplinary projects in Central Asia, Africa, Vietnam, and Europe. He is a Reviewer for the German Science Community (DFG) and the German Humboldt Foundation. Martin also serves actively inside various societies such as the German Society for Photogrammetry and Remote Sensing and the German International Institute for Applied Systems Analysis (IIASA). He currently serves on the editorial board of *Ecological Processes*.

Acronyms

%LCT	Percentage of Land Cover Type
NELDA	Northern Eurasia Land Dynamics Analysis
ADB	Asian Drylands Belt
AQI	Air Quality Indicator
AR4	Fourth Assessment Report
AR5	Fifth Assessment Report
ARS	Agricultural Research Service
AVHRR	Advanced Very High Resolution Radiometer
BCE	Before Common Era
BRDF	Bidirectional Reflectance Distribution Function
BRI	Belt and Road Initiative
CA	Central Asia
CAC	Central Asia Core
CARIN	Central Asia Regional Information Network
CE	Common Era
CLIGN	Climate Stochastic Weather Generator
CMG	Climate Modeling Grid
CNH	Coupled Natural and Human Systems
CNVM	Cropland-Natural Vegetation Mosaic
CO_2	Carbon Dioxide
DEA	Drylands of East Asia
DLB	Dry Land Belt
DLC	Dominant Land Cover
DTR	Diurnal Temperature Range
EA	East Asia
ECONSYS	Economic Systems
ECOSYS	Ecological Systems
EPI	Environmental Performance Index
ERA	Meteorological Reananalysis Data
ET	Evapotranspiration

FAO	Food and Agriculture Organization
FPAR	Fraction of Photosynthetically Active Radiation (400–700 nm) Absorbed by Green Vegetation
GCA	Greater Central Asia
GDP	Gross Domestic Product
GDPPC	Gross Domestic Product per Capita
GHSL	Global Human Settlement Layer
GLOBC	Climate Modelling and Global Change
GOFC-GOLD	Global Observation for Forest and Land Cover Dynamics
GPP	Gross Primary Production
HDI	Human Development Index
IPCC	Intergovernmental Panel on Climate Change
IVCI	Integral Vegetation Conditions Index
IVI	Integrated Vegetation Indices
KBG	Kara-Bogaz Gol
LAI	Leaf Area Index
LCC	Land Cover Change
LCLUC	Land-Cover and Land-Use Change
LE	Life Expectancy
LSK	Livestock
LSKD	Livestock Density
LSKPC	Livestock per Capita
LST	Land Surface Temperature
LST_{day}	Land Surface Temperature Day
LST_{night}	Land Surface Temperature Night
LUH	Land Use Harmonization
LUI	Land Use Index
MAP	Mean Annual Precipitation
MAT	Mean Annual Temperature
ME	Middle East
MODIS	Moderate Resolution Imaging Spectroradiometer
NASA	National Aeronautics and Space Administration
NBAR	Nadir BRDF Adjusted Reflectance
NDVI	Normalized Difference Vegetation Index
NEP	Net Ecosystem Production
NLCD	National Land Cover Dataset
NPP	Net Primary Production
NRCS	Natural Resource Conservation Service
NRI	National Resource Inventory
OED	Oxford English Dictionary
POP	Human Population Size
POPD	Population Density
REF S1	Reference State
RGB	Red, Green, Blue
RHEM	Rangeland Hydrology and Erosion Model

SAVI	Soil-Adjusted Vegetation Index
SCERIN	South-Central East European Regional Information Network
SD	Standard Deviation
SES	Social-Ecological Systems or Social-Environmental Systems
SOCSYS	Social Systems
SPOT-VGT	SPOT VEGETATION
STM	State-and-Transition Models
T	Soil loss Tolerance Rate
TC	Tasseled Cap
UN	United Nations
UNCCD	United Nations Convention to Combat Desertification
USGS	US Geological Survey
USSR	Union of Soviet Socialist Republics
VCI	Vegetation Condition Index
WBM	Water Balance Model
WRF	Weather Research and Forecasting
WTO	World Trade Organization

Chapter 1
Multiple Perspectives on Drylands Across Greater Central Asia

Geoffrey M. Henebry, Jiquan Chen, Garik Gutman, and Martin Kappas

More than a quarter of the planet's inhabitants live in drylands or above 2100 m above mean sea level. Yet, anthropogenic land dynamics in both mountain and arid landscapes have been understudied, despite the myriad global and regional changes occurring in recent decades, as well as their sensitivity and vulnerability to the changes. This volume of essays provides multiple complementary perspectives about how environmental change manifests in the drylands of Greater Central Asia. This belt of drylands (Lioubimtseva 2002; Groisman et al. 2018) includes several high mountain ranges (Azykova 2002; Merzlyakova 2002) that harvest water vapor from the atmosphere, bringing runoff, spring flow, and meltwaters from glaciers and seasonal snow melting water into the drylands through rivers that terminate in the big lakes of the region's several endorheic basins (Koronkevich 2002; Bai et al. 2011).

Where are these drylands? In this volume, there are multiple perspectives on this question from climatological, ecological, and geopolitical viewpoints. The core area, however, includes the five republics of Soviet Central Asia that emerged as nations in 1991 (Kazakhstan, Kyrgyzstan, Tajikistan, Turkmenistan, and Uzbekistan)

G. M. Henebry (✉) · J. Chen
Department of Geography, Environment, and Spatial Sciences,, Michigan State University, East Lansing, MI, USA
e-mail: henebryg@msu.edu; jqchen@msu.edu

G. Gutman
Land-Cover/Land-Use Change Program, NASA Headquarters, Washington, DC, USA
e-mail: ggutman@nasa.gov

M. Kappas
Cartography, GIS & Remote Sensing Department, Institute of Geography, Georg-August University, Goettingen, Germany
e-mail: mkappas@uni-goettingen.de

G. Gutman et al. (eds.), *Landscape Dynamics of Drylands across Greater Central Asia: People, Societies and Ecosystems*, Landscape Series 17,
https://doi.org/10.1007/978-3-030-30742-4_1

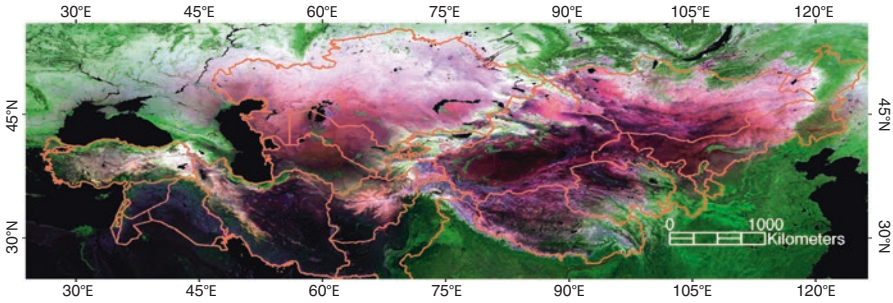

Fig. 1.1 False-color composite of the standard deviations of MODIS Tasseled Cap (TC) components from the NBAR product time series from 2001 through 2016. Orange outlines the 22 political entities of the Eurasian drylands. Red, green, blue displays the standard deviations of TC wetness, greenness, and brightness, respectively. Bodies of open water appear black

and seven arid administrative units of China (Gansu, Inner Mongolia, Ningxia, Qinghai, Shanxi, Tibet, and Xinjiang), and the nation of Mongolia constitute the drylands of East Asia. Together the Central Asia Core (CAC) and the Drylands of East Asia (DEA) spans some 74° of longitude. However, the drylands used in this volume can be extended, as in Chaps. 3 (Henebry et al. 2020) and 10 (Chen et al. 2020) to countries of the eastern Mediterranean to reach over a quarter of the way around the planet. Figure 1.1 portrays the drylands of Greater Central Asia and surrounding geographic context through the superposition of three interrelated spectral dimensions of a long time series of the NASA MODIS NBAR (Nadir-BRDF (Bidirectional Reflectance Distribution Function Adjusted Reflectance) product (MCD43C4, V006). Red, green, and blue display the standard deviations of the wetness, greenness, and brightness components of the MODIS Tasseled Cap transform (Lobser and Cohen 2007; de Beurs et al. 2015, 2016) of composites of the NBAR product from 2001 to 2016. Lighter (darker) hues indicate higher (lower) temporal variation in each component. The very dark regions along the southern drylands belt (especially, western Afghanistan and Pakistan, eastern Iran, and most of Iraq, Syria, Jordan, and Israel) indicate very low temporal variation in the TC components. In contrast, the mountainous areas embedded across the drylands show higher temporal variation, as do the steppes of northern Kazakhstan, China, and Mongolia where snow cover drives both strong seasonality in brightness and early season moisture to grow both grains and grasses.

There are two co-dominant land cover types across the drylands in Greater Central Asia (GCA): grasslands and barren lands. According to the NASA MODIS land cover product (MCD12C1, V006) (Table 1.1), these two types account for ~84% of the total area composed by the political entities identified in Chap. 10 (Chen et al. 2020) as composing the drylands of GCA. Croplands are <7%, but constitute the third most common land cover type and are increasing. Shrublands and savannas comprise 3.9% and 2.1%, respectively. Open water and wetlands register just above 1%, primarily due to the large lakes in the endorheic basins of

Table 1.1 Land cover composition (% of area) across Greater Central Asia (GCA), Central Asia Core (CAC), Drylands East Asia (DEA), and the Middle East (ME) according to the NASA MODIS land cover product. Groupings follow Chen et al. (2020) (Chap. 10)

	Forest	Shrub	Savanna	Grass	Wet	Crop	Urban	Mosaic	Snow	Barren	Water
GCA	1.5	3.9	2.1	47.5	0.1	6.6	0.4	0.1	0.5	36.2	1.1
CAC	0.2	5.7	0.9	57.4	0.2	7.6	0.5	<0.1	0.7	25.1	1.7
DEA	2.4	0.2	2.6	49.2	0.1	3.1	0.2	0.1	0.6	41.0	0.7
ME	1.8	9.0	3.5	26.1	0.2	12.3	0.9	0.2	<0.1	45.5	0.6

Central Asia. Forest cover is low (~1.5%) and patchily distributed. Urban and built-up areas across the Eurasian drylands is roughly equivalent to the area in persistent snow cover (<0.5%). Analyses of land surface dynamics appear in Henebry et al. (2020) (Chap. 3).

The "inbetweenness" of Central Asia (*cf* Frank 1992) – sometimes called Inner or Middle Asia (*cf* Cowan 2007) – has long been a region critical to connecting cultures in prehistory (Spengler et al. 2014; Jones et al. 2016), during the era of the Silk Road – 130 BCE to 1453 CE – (Beckwith 2009), and as a crossroads of imperial ambition in the modern era (Hopkirk 1994; Meyer and Brysac 2009). China's ambitious "One Belt One Road" initiatives aim to reinvigorate the economic, political, and social connections between China and its neighbors to the west (Du 2016; Yu 2017), but also pose potential threats to indigenous livelihoods and environmental conservation efforts in sensitive arid mountain landscapes (Foggin 2018). Yet, Central Asia remains a great unknown, at least scientifically.

In report of the Working Group II (Impacts of Climate Change) of the Fifth Assessment Report (AR5) of the Intergovernmental Panel on Climate Change (IPCC), Chapter 24 on Asia contains a revealing table comparing the state of knowledge about observed and projected impacts in more than two dozen sectoral issues by regions of Asia: North, East, Southeast, South, West, and Central (Hijioka et al. 2014). It states that no region contains more knowledge gaps than Central Asia. Indeed, of the 27 topics across the five relevant sectors (freshwater resources; terrestrial and inland water systems; food production systems and food security; human settlements, industry, and infrastructure; human health, security, livelihoods, and poverty), the report finds that "relatively abundant/sufficient information; knowledge gaps exist but conclusions can be drawn based on existing data" for only one topic for both observed and projected impacts: permafrost. Only one other sectoral topic is graded as sufficient information: projected impacts on farming area. For the remaining entries under Central Asia, the report finds there is "limited information/no data; critical knowledge gaps, difficult to draw conclusions", including *observed impacts* on farming area.

Although the AR5 report of the Working Group I (Physical Basis of Climate Change) demonstrates a consensus on a future of increasing temperatures in Central Asia (Christensen et al. 2013), projections of precipitation amount, timing, intensity are all highly uncertain (Flato et al. 2013; Hijioka et al. 2014). Indeed, the precipita-

tion projections for the AR5 were assessed – with a medium level of uncertainty – as no better than those from AR4 (Flato et al. 2013). We await the findings by Working Group I of the IPCC's Sixth Assessment Report to be released in April 2021 (http://www.ipcc.ch).

However, drylands are generally sensitive to climate change due to widespread moisture limitation (Lioubimtseva and Henebry 2009; von Wehrden et al. 2010; Fraser et al. 2011; Lioubimtseva et al. 2012; Huang et al. 2016; Groisman et al. 2018; Groisman et al. 2020, Chap. 2). In addition, areas with high elevations experience wider climatic variations (Rangwala and Miller 2012). Recent analysis of climatic extremes in long-term meteorological data from Central Asia finds significant increasing trends in both temperature and precipitation as well as a significant decreasing trend in annual maximum consecutive dry days (Zhang et al. 2019). An earlier study of precipitation trends and variability also found significant increasing trends in precipitation in much of Central Asia apart from western Kazakhstan (Xu et al. 2015). Trends in snow cover in Central Asia have shown mixed results – from significant decreases to no significant trends to significant increases in snow cover onset, melt, and/or duration – depending on the extent and elevation of the study area, and the source and resolution of the snow cover data (Zhou et al. 2013; Dietz et al. 2014; Liu et al. 2017; Tang et al. 2017; Tomaszewska and Henebry 2018). Furthermore, the weather in the Eurasian drylands, and Central Asia in particular, are susceptible to teleconnected forcings by climate oscillation modes, despite their distance from oceans (de Beurs and Henebry 2008; Henebry et al. 2013; Bothe et al. 2012; Wright et al. 2014; de Beurs et al. 2018; Zhang et al. 2019). It is not yet clear how climate change may influence the intensity, duration and frequency of climate oscillations and other circulation features (Mizuta 2012; Stevenson 2012; Jourdain et al. 2013; Lee et al. 2014).

In addition to manifold effects of climatic variability and change, drylands across Greater Central Asia have felt the repercussions of widespread socioeconomic, sociodemographic, and institutional changes in the wake of the formal disintegration of the Soviet Union at the end of 1991 and China's accession to the World Trade Organization a decade later (Chen et al. 2015, 2018). Socioeconomic development in the past quarter century in the drylands can be encapsulated by urban development, since many workers migrated from rural settings to urban environments within their country or to cities abroad.

The remaining chapters of this volume explore specific aspects of landscape dynamics in the drylands of Greater Central Asia. Groisman et al. (2020) (Chap. 2) highlights key environmental changes within and across the drylands belt, with an emphasis on climatic drivers. Henebry et al. (2020) (Chap. 3) brings together information about significant trends in land surface characteristics with the most recent collection of MODIS land cover data to explore potential linkages between land cover type and observed significant trends in land surface temperature. Sokolik et al. (2020) (Chap. 4) provides an overview of Central Asia with an emphasis on anthropogenic contributions to land surface disturbance and dust transport through storms. Qi et al. (2020) (Chap. 5) explores the food-water-energy nexus in Central

Asia. Abdullaev and Sokolik (2020) (Chap. 6) present the impact of dust storms on cotton production in Tajikistan. Chap. 7 (Fan et al. 2020) examines in detail the interplay between population and development in the cities of dryland China. Spaeth et al. (2020) (Chap. 8) drills down into a key constraint on development of grazing lands in Kazakhstan, namely soil erosion. Kappas et al. (2020) (Chap. 9) compares landscape dynamics in two large countries within the drylands – Kazakhstan and Mongolia – to identify opportunities for improving ecosystem stewardship of land resources. Chen et al. (2020) (Chap. 10) concludes the volume with a synoptic view of the drylands of Greater Central Asia and provides contrasts between the drylands of East Asia, Central Asia, and the Middle East.

Much of the interest in landscape dynamics is coming from the desire to understand how human activities have influenced landscapes, and how this understanding can inform future land planning and ecosystem stewardship for the drylands of the GCA. Much of the focus has been on how anthropogenic changes in disturbance regimes have altered landscape patterns and processes. For instance, changes in land use and management practices, such as grazing regimes, can alter the spatial arrangement of resources across the landscape, affecting the aboveground net primary production and influencing surface stability (Okin et al. 2009, 2015).

An important and unresolved question regarding landscape dynamics is whether changes in ecosystem functioning are only gradual processes. With the increasing length of earth observation time series, we have good opportunities to differentiate between gradual and abrupt changes. Tipping points in dynamical systems mark the abrupt transition in time and/or space from one dynamical regime to another. On either side of a tipping point the rules differ – a phase transition occurs leading to distinct landscape structure and ecosystem functioning. Transitions between dynamical regimes are frequently accompanied by hysteresis: the path up to and across the tipping point is very different from the path back across the tipping point. Some examples of dynamic regime switching and hysteresis in drylands include desertification of arid and semiarid lands (Saiko and Zonn 2000; Geist and Lambin 2004; Behnke 2008; Okin et al. 2015), increasing shrub encroachment (Archer et al. 1995; Eldridge et al. 2011; Brandt et al. 2013), and urban expansion (Angel et al. 2011; Güneralp et al. 2015; Fan et al. 2020).

The GCA drylands, as shown in this volume, is a region unique from an ecological point of view with a remarkable mix of climatic and edaphic conditions (Chaps. 3 and 4), vegetation types and land use patterns (Chaps. 3, 4, 6, and 9). Over the twentieth century, drastic changes occurred, both natural and anthropogenic (Chaps. 2, 3, 4, 7, and 10) that profoundly affected landscapes and their ecosystem functioning, including successive institutional changes with large impact on the agricultural sector, croplands, and grasslands (Chaps. 4, 5, 6, 8, 9, and 10) and global environmental change and major regional droughts (Chaps. 2 and 3).

While this volume of essays gathers the fruits of past and ongoing international interdisciplinary collaborations, the need for more research by scholars of multiple countries into the integrated social-environmental systems (SESs) of arid and mountain landscapes is pressing, if we are to understand the past and current changes,

evaluate their manifold impacts, and prepare to cope, ameliorate, and adapt in response to the unfolding future (Lesnikowski et al. 2015; Reyer et al. 2017).

Acknowledgements We would like to acknowledge the financial support from the National Aeronautics and Space Administration (NASA)'s Land-Cover and Land-Use Change (LCLUC) Program through a grant to South Dakota State University (NNX15AP81G) and a grant to Michigan State University (NNX15AD51G). Any opinions, findings, and conclusions or recommendations expressed in this paper are those of the authors and do not necessarily reflect the views of NASA.

References

Abdullaev SF, Sokolik IN (2020) Assessment of the influence of dust storms on the cotton production in Tajikistan. In: Gutman G et al (eds) Landscape dynamics of drylands across greater Central Asia: people, societies and ecosystems. Springer, Cham

Angel S, Parent J, Civco DL et al (2011) The dimensions of global urban expansion: estimates and projections for all countries, 2000–2050. Prog Plann 75(2):53–107

Archer S, Schimel DS, Holland EA (1995) Mechanisms of shrubland expansion: land use, climate or CO_2? Clim Chang 29(1):91–99

Azykova EK (2002) Geographysical and landscape characteristics of mountain territories. Mountains of Kyrgyzstan. Technology, Bishkek, pp 15–21

Bai J, Chen X, Li J, Yang L, Fang H (2011) Changes in the area of inland lakes in arid regions of Central Asia during the past 30 years. Environ Monit Assess 178(1–4):247–256

Beckwith CI (2009) Empires of the silk road: a history of central Eurasia from the bronze age to the present. Princeton University Press, Princeton

Behnke RH (ed) (2008) The socio-economic causes and consequences of desertification in Central Asia. Springer, Dordrecht

Bothe O, Fraedrich K, Zhu X (2012) Precipitation climate of Central Asia and the large-scale atmospheric circulation. Theor Appl Climatol 108(3–4):345–354

Brandt JS, Haynes MA, Kuemmerle T et al (2013) Regime shift on the roof of the world: alpine meadows converting to shrublands in the southern Himalayas. Biol Conserv 158:116–127

Chen J, John R, Shao C et al (2015) Policy shifts influence the functional changes of the CNH systems on the Mongolian plateau. Environ Res Lett 10:085003

Chen J, John R, Sun G et al (2018) Prospects for the sustainability of social-ecological systems (SES) on the Mongolian plateau: five critical issues. Environ Res Lett

Chen J, Ouyang Z, John R et al (2020) Social-ecological systems across the Asian Drylands Belt (ADB). In: Gutman G et al (eds) Landscape dynamics of drylands across greater Central Asia: people, societies and ecosystems. Springer, Cham

Christensen JH, Kumar KK, Aldrian E et al (2013) Intergovernmental panel on climate change (2014). Climate phenomena and their relevance for future regional climate change. In: Climate change 2013 – the physical science basis: Working Group I Contribution to the Fifth Assessment Report of the Intergovernmental Panel on Climate Change (pp. 1217–1308). : Cambridge University Press, Cambridge

Cowan PJ (2007) Geographic usage of the terms middle Asia and Central Asia. J Arid Environ 69(2):359–363

de Beurs KM, Henebry GM (2008) Northern annular mode effects on the land surface phenologies of northern Eurasia. J Clim 21:4257–4279

de Beurs KM, Henebry GM, Owsley BC, Sokolik I (2015) Using multiple remote sensing perspectives to identify and attribute land surface dynamics in Central Asia 2001–2013. Remote Sens Environ 170:48–61

de Beurs KM, Owsley BC, Julian JP (2016) Disturbance analyses of forests and grasslands with MODIS and Landsat in New Zealand. Int J Appl Earth Obs 45:42–54

de Beurs KM, Henebry GM, Owsley B, Sokolik I (2018) Large scale climate oscillation impacts on temperature, precipitation, and land surface phenology in Central Asia. Environ Res Lett 13:065018

Dietz AJ, Conrad C, Kuenzer C et al (2014) Identifying changing snow cover characteristics in Central Asia between 1986 and 2014 from remote sensing data. Remote Sens 6:12752–12775

Du MM (2016) China's "one belt, one road" initiative: context, focus, institutions, and implications. Chn J Glob Govern 2(1):30–43

Eldridge DJ, Bowker MA, Maestre FT et al (2011) Impacts of shrub encroachment on ecosystem structure and functioning: towards a global synthesis. Ecol Lett 14(7):709–722

Fan P, Ouyang Z, Chen JJ et al (2020) Population and urban dynamics in drylands of China. In: Gutman G et al (eds) Landscape dynamics of drylands across greater Central Asia: people, societies and ecosystems. Springer, Cham

Flato G, Marotzke J, Abiodun B et al (2013) Evaluation of climate models. In: Stocker et al (eds) Climate change 2013: the physical science basis. Contribution of Working Group I to the fifth assessment report of the Intergovernmental Panel on Climate Change. Cambridge University Press, Cambridge, pp 741–866

Foggin JM (2018) Environmental conservation in the Tibetan plateau region: lessons for China's belt and road initiative in the mountains of Central Asia. Land 7(2):52

Ford JD, Berrang-Ford L, Bunce A et al (2015) The status of climate change adaptation in Africa and Asia. Reg Environ Chang 15:801–814

Frank AG (1992) The centrality of Central Asia. Stud Hist 8(1):43–97

Fraser EDG, Dougill AJ, Hubacek K et al (2011) Assessing vulnerability to climate change in dryland livelihood systems: conceptual challenges and interdisciplinary solutions. Ecol Soc 16(3):3

Geist HJ, Lambin EF (2004) Dynamic causal patterns of desertification. Bioscience 54(9):817–829

Groisman P, Bulygina O, Henebry G et al (2018) Dry land belt of northern Eurasia: contemporary environmental changes and their consequences. Environ Res Lett 13:115008

Groisman PY, Bulygina ON, Henebry GM et al (2020) Dry land belt of Northern Eurasia: contemporary environmental changes. In: Gutman G et al (eds) Landscape dynamics of drylands across greater Central Asia: people, societies and ecosystems. Springer, Cham

Güneralp B, Güneralp İ, Liu Y (2015) Changing global patterns of urban exposure to flood and drought hazards. Global Environ Chang 31:217–225

Henebry GM, de Beurs KM, Wright CK et al (2013) Dryland East Asia in hemispheric context. In: Chen J, Wan S, Henebry G, Qi J, Gutman G, Sun G, Kappas M (eds) Dryland East Asia: land dynamics amid social and climate change. HEP/De Gruyter, Berlin

Henebry GM, de Beurs KM, John R et al (2020) Recent land surface dynamics across the drylands of Greater Central Asia. In: Gutman G et al (eds) Landscape dynamics of drylands across greater Central Asia: people, societies and ecosystems. Springer, Cham

Hijioka Y, Lin E, Pereira JJ et al (2014) Asia. In: Climate change 2014 – impacts, adaptation and vulnerability: part B: regional aspects: Working Group II contribution to the IPCC fifth assessment report. Cambridge University Press, Cambridge, pp 1327–1370

Hopkirk P (1994) The great game: the struggle for empire in Central Asia. Kodansha Globe

Huang J, Yu H, Guan X et al (2016) Accelerated dryland expansion under climate change. Nat Clim Chang 6(2):166

Immerzeel WW, van Beek LPH, Bierkens MFP (2010) Climate change will affect the Asian water towers. Science 328:1382–1385

Jones H, Lister DL, Cai D et al (2016) The trans-Eurasian crop exchange in prehistory: discerning pathways from barley phylogeography. Quatern Int 426:26–32

Jourdain NC, Gupta AS, Taschetto AS et al (2013) The indo-Australian monsoon and its relationship to ENSO and IOD in reanalysis data and the CMIP3/CMIP5 simulations. Clim Dynam 41(11–12):3073–3102

Kappas M, Degener J, Klinge M et al (2020) A conceptual framework for ecosystem stewardship based on landscape dynamics: case studies from Kazakhstan and Mongolia. In: Gutman G et al (eds) Landscape dynamics of drylands across greater Central Asia: people, societies and ecosystems. Springer, Cham

Koronkevich N (2002) Rivers, lakes, inlands seas, and wetlands. In: Shahgedanova (ed) The physical geography of northern Eurasia. Oxford University Press, New York, pp 122–148

Lee JY, Wang B, Seo KH et al (2014) Future change of northern hemisphere summer tropical–extratropical teleconnection in CMIP5 models. J Clim 27(10):3643–3664

Lesnikowski AC, Ford JD, Berrang-Ford LM et al (2015) How are we adapting to climate change? A global assessment. Mitig Adapt Strateg Glob Chang 20:277–293

Lioubimtseva E (2002) Arid environments. In: Shahgedanova M (ed) The physical geography of northern Eurasia. Oxford University Press, New York, pp 267–283

Lioubimtseva E, Henebry GM (2009) Climate and environmental change in arid Central Asia: impacts, vulnerability, and adaptations. J Arid Environ 73(11):963–977

Lioubimtseva E, Kariyeva J, Henebry GM (2012) Climate change in Turkmenistan. In: Zonn et al (eds) The Turkmen Lake "Altyn Asyr" and water resources in Turkmenistan. Springer, Berlin, pp 39–58

Liu J, Zhang W, Liu T (2017) Monitoring recent changes in snow cover in Central Asia using improved MODIS snow-cover products. J Arid Land 9(5):763–777

Lobser SE, Cohen WB (2007) MODIS tasselled cap: land cover characteristics expressed through transformed MODIS data. Int J Remote Sens 28(22):5079–5101

Merzlyakova I (2002) The mountains of Central Asia and Kazakhstan. In: Shahgedanova (ed) The physical geography of northern Eurasia. Oxford University Press, New York, pp 377–402

Meyer KE, Brysac SB (2009) Tournament of shadows: the great game and the race for empire in Central Asia. Hachette, London

Mizuta R (2012) Intensification of extratropical cyclones associated with the polar jet change in the CMIP5 global warming projections. Geophys Res Lett 39(19)

Okin GS, Parsons AJ, Wainwright J et al (2009) Do changes in connectivity explain desertification? Bioscience 59(3):237–244

Okin GS, Moreno-de las Heras M, Saco PM et al (2015) Connectivity in dryland landscapes: shifting concepts of spatial interactions. Front Ecol Environ 13(1):20–27

Qi J, Pueppke S, Kulmatov R et al (2020) The complexity and challenges and challenges of Central Asia's water-energy-food systems. In: Gutman G et al (eds) Landscape dynamics of drylands across greater Central Asia: people, societies and ecosystems. Springer, Cham

Rangwala I, Miller JR (2012) Climate change in mountains: a review of elevation-dependent warming and its possible causes. Clim Chang 114:527–547

Reyer C, Otto IM, Adams S et al (2017) Climate change impacts in Central Asia and their implications for development. Reg Environ Chang 17:1639–1650

Saiko TA, Zonn IS (2000) Irrigation expansion and dynamics of desertification in the Circum-Aral region of Central Asia. Appl Geogr 20(4):349–367

Sokolik IN, Shiklomanov A, Xi X et al (2020) Quantifying the anthropogenic signature in drylands of Central Asia and its impact on water scarcity and dust emissions. In: Gutman G et al (eds) Landscape dynamics of drylands across greater Central Asia: people, societies and ecosystems. Springer, Cham

Spaeth KE, Weltz MA, Guertin DP et al (2020) Hydrology and erosion risk parameters for grasslands in Central Asia. In: Gutman G et al (eds) Landscape dynamics of drylands across greater Central Asia: people, societies and ecosystems. Springer, Cham

Spengler R, Frachetti M, Doumani P et al (2014) Early agriculture and crop transmission among bronze age mobile pastoralists of Central Eurasia. Proc R Soc Lond B Biol Sci 281(1783):20133382

Stevenson SL (2012) Significant changes to ENSO strength and impacts in the twenty-first century: results from CMIP5. Geophys Res Lett 39(17)

Tang Z, Wang X, Wang J et al (2017) Spatiotemporal variation of snow cover in Tianshan Mountains, Central Asia, based on cloud-free MODIS fractional snow cover product, 2001–2015. Remote Sens-Basel 9(10):1045

Tomaszewska MA, Henebry GM (2018) Changing snow seasonality in the highlands of Kyrgyzstan. Environ Res Lett 13:065006

von Wehrden H, Hanspach J, Ronnenberg K, Wesche K (2010) Inter-annual rainfall variability in Central Asia–a contribution to the discussion on the importance of environmental stochasticity in drylands. J Arid Environ 74(10):1212–1215

Wright CK, de Beurs KM, Henebry GM (2014) Land surface anomalies preceding the 2010 Russian heat wave and a link to the North Atlantic oscillation. Environ Res Lett 9:124015

Xu L, Zhou H, Du L et al (2015) Precipitation trends and variability from 1950 to 2000 in arid lands of Central Asia. J Arid Land 7(4):514–526

Yu H (2017) Motivation behind China's 'one belt, one road' initiatives and establishment of the Asian infrastructure investment bank. J Contemp China 26(105):353–368

Zhang M, Chen Y, Shen Y, Li B (2019) Tracking climate change in Central Asia through temperature and precipitation extremes. J Geogr Sci 29(1):3–28

Zhao S, Liu S, Xu C et al (2018) Contemporary evolution and scaling of 32 major cities in China. Ecol Appl 28(6):1655–1668

Zhou H, Aizen E, Aizen V (2013) Deriving long term snow cover extent dataset from AVHRR and MODIS data: Central Asia case study. Remote Sens Environ 136:146–162

Chapter 2
Dry Land Belt of Northern Eurasia: Contemporary Environmental Changes

Pavel Ya. Groisman, Olga N. Bulygina, Geoffrey M. Henebry, Nina A. Speranskaya, Alexander I. Shiklomanov, Yizhao Chen, Nadezhda M. Tchebakova, Elena I. Parfenova, Natalia D. Tilinina, Olga G. Zolina, Ambroise Dufour, Jiquan Chen, Ranjeet John, and Peilei Fan

2.1 Introduction

The Dry Land Belt (DLB) of Northern Eurasia occupies the interior of the Earth's largest continent. It is dry because it receives little water vapor transport from the tropics due to the numerous mountain ranges and high plateaus of Central and South Asia (Fig. 2.1). Some parts of the DLB are fertile and, thus, densely populated (Chen et al. 2018, 2020; Fan et al. 2018, 2020). Widespread moisture limitation

Olga N. Bulygina was deceased at the time of publication.

P. Y. Groisman (✉)
North Carolina State University at NOAA National Centers for Environment Information, Asheville, NC, USA

P.P Shirshov Institute for Oceanology, RAS, Moscow, Russia

Hydrology Science and Services Corp., Asheville, NC, USA
e-mail: Pasha.Groisman@noaa.gov

O. N. Bulygina (deceased)
All-Russian Research Institute for Hydrometeorological Information, Obninsk, Russia

G. M. Henebry · J. Chen
Department of Geography, Environment, and Spatial Sciences, Michigan State University, East Lansing, MI, USA
e-mail: henebryg@msu.edu; jqchen@msu.edu

N. A. Speranskaya
State Hydrological Institute, Basil Island, St. Petersburg, Russia
e-mail: speran@mail.rcom.ru

A. I. Shiklomanov
Earth Systems Research Center, University of New Hampshire, Durham, NH, USA
e-mail: alex.shiklomanov@unh.edu

G. Gutman et al. (eds.), *Landscape Dynamics of Drylands across Greater Central Asia: People, Societies and Ecosystems*, Landscape Series 17,
https://doi.org/10.1007/978-3-030-30742-4_2

constrains productivity in rangelands and croplands. The DLB has a very limited fresh water supply, which is highly dependent upon both irregular extra-tropical cyclones and a shrinking regional cryosphere (Shver 1976; Bliss et al. 2014; Groisman et al. 2018). Increases in evapotranspiration (ET) arising from increases in warm season temperatures and expansions of the growing season in the DLB are generally not compensated by precipitation increases (IPCC AR5 WG1 2013). Further, spatio-temporal shifts in precipitation pattern increase the likelihood that various unusual or extreme events (e.g., heatwaves, dzuds, dust storms) will negatively affect the livelihoods of regional societies and their interactions with the global economy (*e.g.*, Henebry et al. 2020; Chen et al. 2014, 2015). The DLB region is a source of dust storms, which can adversely impact the environment, climate, and human well-being over the region and beyond including densely populated areas of East Asia (Goudie and Middleton 1992; Darmenova et al. 2009).

Over the past three decades, the DLB has gone through several major changes that drive regional changes in agricultural and pastoral lands. The regional population has increased at a moderate rate similar to the global population trend and, in the past three decades, there have been profound institutional shifts in the agricultural sector. Increased global demand for meat and dairy products have produced strong pressure on agro-pastoral lands where fragile developing economies with frequent institutional shifts, water resource scarcity, and changing climatic condi-

Y. Chen
Joint Innovation Center for Modern Forestry Studies, College of Biology and the Environment, Nanjing Forestry University, Nanjing, Jiangsu, China

Department of Geography, University of Cambridge, Cambridge, United Kingdom

N. M. Tchebakova · E. I. Parfenova
V.N. Sukachev Institute of Forest SB RAS, Akademgorodok, Krasnoyarsk, Russia
e-mail: ncheby@ksc.krasn.ru

N. D. Tilinina
P.P Shirshov Institute for Oceanology, RAS, Moscow, Russia
e-mail: tilinina@sail.msk.ru

O. G. Zolina
Centre for Scientific Research, Université Grenoble Alpes, Saint Martin d'Heres Cedex, France
e-mail: olga.zolina@univ-grenoble-alpes.fr

A. Dufour
Université Grenoble Alpes, Saint-Martin-d'Hères, Cedex, France
e-mail: ambroise.dufour@univ-grenoble-alpes.fr

R. John
Department of Biology, University of South Dakota, Vermillion, SD, USA
e-mail: ranjeet.john@usd.edu

P. Fan
School of Planning, Design, and Construction, Center for Global Change and Earth Observations, Michigan State University, East Lansing, MI, USA
e-mail: fanpeile@msu.edu

tions interact to alter DLB ecosystem services and the societies that rely on them (Groisman et al. 2017; Qi et al. 2012, 2017).

Following the abrupt institutional changes of the 1990s, the DLB region experienced multiple sociodemographic and socioeconomic shifts (Groisman et al. 2018; Chen et al. 2018, 2020; Fan et al. 2020). Framed by the DLB's multiple socioeconomic transformations, this chapter seeks to: (i) document current tendencies of ongoing changes in the diverse biogeophysical environments of the DLB, and (ii) distinguish, when possible, the natural from the regional anthropogenic signals of these changes.

2.2 Observed Climatic Changes

2.2.1 Changes in Regional Surface Air Temperature

Surface air temperature across the DLB region has rapidly increased in the past half-century (Fig. 2.1). Average rates of temperature change of 1.8 °C × (100 year)$^{-1}$ for winter and 1.6 °C × (100 year)$^{-1}$ for spring have been observed (Groisman et al. 2018). Interannual variation of winter temperatures has been higher than spring temperatures. In contrast, warming tendencies observed during summer and autumn have been much smaller: 0.4 °C × (100 year)$^{-1}$ in summer and 0.7 °C × (100 year)$^{-1}$ in autumn. Warming affects the timing of seasonal cycles in multiple ways in the transition from the cold to the warm season: earlier snowmelt (ACIA 2005; Bulygina et al. 2011; Tomaszewska and Henebry 2018), earlier onset of spring green-up, and earlier peaks in river discharge. In summer, warming exacerbates glacial retreat in mountains across Central Asia, Caucasus, and southern Siberia (Khromova et al. 2014), and it exacerbates water deficits in DLB landscapes, especially at lower elevations.

Were regional precipitation to increase, the myriad negative consequences of warming across the DLB might be attenuated. Oceanic warming must result in more evaporation and the additional water vapor could ameliorate water deficits in the drylands through increased precipitation, were the additional water vapor to be transported to the interior drylands by atmospheric circulation (Groisman et al. 2018).

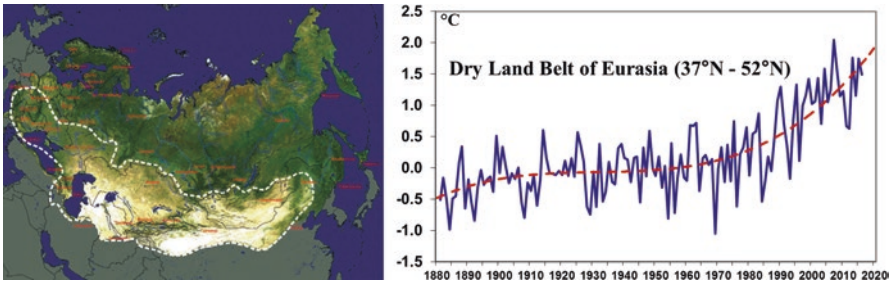

Fig. 2.1 **Left** Dry Land Belt (DLB) of Northern Eurasia (the dashed contour on the map from Groisman et al. 2018). **Right** Mean annual surface air temperature anomalies (°C) were area-averaged over the DLB with the polynomial trend shown in the graph describing 60% of the time series variation

2.2.2 Changes in Atmospheric Circulation

Planetary changes that affect radiative fluxes drive changes in circulation patterns in the atmosphere and the oceans circulation that generate downstream effects on the spatiotemporal distribution of water and energy exchanges between the land and ocean surfaces and the atmospheric boundary layer. Although the regional climates are predominately sunny, the DLB lacks sufficient moisture to retain the heat in soils, biomass, or water at and below the surface in both liquid and frozen states, resulting in large swings in daily air temperature. Water storage is limited throughout the DLB, including water storage in glaciers, inland and endorheic lakes, and permafrost, particularly at higher elevations, accumulated through earlier periods of higher precipitation and during the cold season.

Precipitation in the DLB in general and Central Asia, in particular, comes primarily from water vapor transported from outside of the region by two competing aspects of global warming. First, the weakening of thermal gradients from pole to equator weakens the westerlies flow and reduces water vapor transport (Bulygina et al. 2013; Groisman et al. 2018), which may result in atmospheric blocking patterns (Lupo et al. 2014; Mokhov et al. 2013) that produce anomalously warm or cold weather during the cold season (Schubert et al. 2014). During the warm season, the reduced westerlies result in extended periods with or without precipitation (Zolina et al. 2013; Groisman and Soja 2009; Lupo et al. 2014). Second, extratropical cyclones bring precipitation into the region (Tilinina et al. 2013). Groisman et al. (2018) calculated cyclone statistics for the Asian part of the DLB, reporting slight but significant tendencies toward more cyclones over Kazakhstan, Kyrgyzstan, northwestern China, and Mongolia. More research is required to understand the impact of these tendencies.

Calculation of the water vapor transport into the DLB provides an estimate of integral precipitation changes related to atmospheric circulation. Table 2.1 reports the results of processing of the ERA-Interim Reanalysis (Dee et al. 2011) data for the post-USSR period across two boundaries: (1) southward along 50°N from 60 to 110°E and (2) eastward along 50°E from 40 to 50°N. Integrating water vapor over the atmospheric column and calculating the fluxes, separately, across the northern (50°N) and western (50°E) borders reveals that almost all of the water vapor flows eastward with little flux coming southward. Note that there has been a decrease of nearly 15% in eastward water vapor flux since 1990, but erratic changes in the southward flux, from a decrease of more than 400% to an increase of nearly 700%, resulting in a more than nine fold decrease in the ratio of eastward to southward fluxes (Table 2.1). The diminishing eastward flux may be attributed both to weakening westerly flows and the desiccation of the Aral Sea (Zavialov 2007; Gaybullaev et al. 2012). Furthermore, large-scale climate oscillations affect precipitation patterns in Central Asia (Henebry et al. 2020; de Beurs et al. 2018) and elsewhere in the DLB (Gong et al. 2001; de Beurs and Henebry 2008; Jiang et al. 2011).

Table 2.1 Mean annual southward and eastward water vapor transport into Central Asia during the post-USSR period (1990–2017)

Analysis period	Mean annual southward flux across 50°N ($kg \times (m \times s)^{-1}$)	Change from 1990–1999 (%)	Mean annual eastward flux across 60°E ($kg \times (m \times s)^{-1}$)	Change from 1990 to 1999 (%)	Eastward to southward flux ratio
1990–1999	0.14	–	46.4	–	331.4
2000–2009	−0.48	−442.9	43.4	−6.5	−90.4
2010–2017	1.11	692.9	39.6	−14.7	35.7

2.2.3 Changes in Atmospheric Precipitation

Atmospheric precipitation in drylands is the most variable aspect of climate, and the DLB is no exception. However, there are manifold uncertainties about the precipitation record in the DLB. Uncertainties arise both from the sparse observational networks and from time-dependent systematic biases in precipitation records (Groisman and Legates 1995). Groisman et al. (2014) quantified these biases for Russia while Ding et al. (2007) did the same for China. They showed how each technological advance in rain gauge instrumentation (*e.g.*, wind shielding of gauges), and observing routines resulted in spurious increases of "observed" precipitation; whereas, the actual "ground-true" precipitation was substantially different and exhibited different decadal trends. Time-dependent bias-corrected precipitation records for the Russian part of DLB (*viz.*, steppes in southern West Siberia and in the Trans-Baikal Region) exhibit a long-term decrease in precipitation (SNCCA 2014). Using bias-corrected precipitation time series, Akhmadiyeva and Groisman (2008) reported a 4% increase in annual precipitation over Kazakhstan during the 1990–2006 period compared to previous three decades (1960–1989). Furthermore, significant discrepancies between a global precipitation reanalysis and a fuller representation of regional precipitation stations has been reported for Kazakhstan (Wright et al. 2009). Estimating summer rainfall totals over the DLB during the past 13 years compared to the previous 25 years using MERRA2 reanalysis data (Gelaro et al. 2017) reveals decreases in precipitation in the western end of the DLB, including Ukraine and European Russia (Groisman et al. 2018). The gradual drying of landscapes across this region (de Beurs et al. 2015) exacerbated the severe 2010 heat wave and extreme drought that arose from combination of atmospheric blocking (Schubert et al. 2014) and negative polarity of the North Atlantic Oscillation (Wright et al. 2014). At the eastern end of the DLB (Baikal Lake Basin, Trans-Baikal area, and northeastern China), heatwaves have been linked to increasing water deficit and severe forest fires centered on the Trans-Baikal area (Loboda and Chen 2017).

2.2.4 Changes in the Cryosphere

The cryospheric components of the DLB have been changing in recent decades, with most components exhibiting monotonic decreases (AMAP 2011; AMAP 2017). Duration of the spring season snow cover has been decreasing steadily, enabling an earlier onset to spring phenomena (Bulygina et al. 2011; SNCCA 2014). Permafrost at the edge of the permafrost zone, has begun to thaw (Romanovsky et al. 2017; Streletskiy et al. 2015). Active layer thickness of seasonally frozen ground has been increasing from the Arctic to the mountains of Central Asia, thereby damaging buildings and degrading infrastructure integrity (Shiklomanov et al. 2017). Changes in frozen ground has affected regional hydrology (Kalyuzhny and Lavrov 2012; Frauenfeld and Zhang 2011). Widespread changes in snow seasonality have been observed in Central Asia (Tomaszewska and Henebry 2018; Zhou et al. 2017). Area and volume of glaciers has been decreasing across the entire Northern Eurasia, including in the montane areas of DLB that are critical to river flows in endorheic basins (Aizen et al. 2006; Bliss et al. 2014; Farinotti et al. 2015; Khromova et al. 2014; Kotlyakov et al. 2015; Shahgedanova et al. 2010, 2014; Syromyatina et al. 2015). Ice storage on and below the ground is an important source of the water supply for DLB. For centuries (or millennia) water was transported to the remote mountains of the Eurasian continent and, instead of entering the global water cycle via runoff, was fixed and stored there in frozen form. This slow accumulation of the past is now changing to slow melting and, while it buffers the water balance in many foothills of montane DLB, it is not being replenished (Groisman et al. 2018).

2.2.5 Changes in River Discharge

Total runoff and river discharge are key measures for regional water supply. Annual river discharge throughout the territory of the Russian Federation averaged 5% higher in 1981–2012 than in 1936–1980 (Georgievsky et al. 2014), but the changes were not spatially uniform (Fig. 2.2). Southern Siberia and steppe regions of Western Siberia exhibit decreases in annual river discharge during 1978–2010, compared with 1946–1977 (Fig. 2.2a). This decline is mainly due to less runoff during spring and earlier summer due to less snow storage before spring snowmelt (Georgievsky et al. 2014; Shiklomanov and Lammers 2013). River flows during winter exhibit consistent and significant increases throughout the region. Significant increases (up to 100%) in winter runoff have been observed in southern Volga Basin and in southern East Siberia. Changes in annual and seasonal discharge across Eurasia are well documented (Holmes et al. 2016; Peterson et al. 2002; Shiklomanov et al. 2007; Smith et al. 2007; Shiklomanov and Lammers 2009, 2013; Troy et al. 2012); however, attribution to the sources of these changes remain unquantified (Bring et al. 2016).

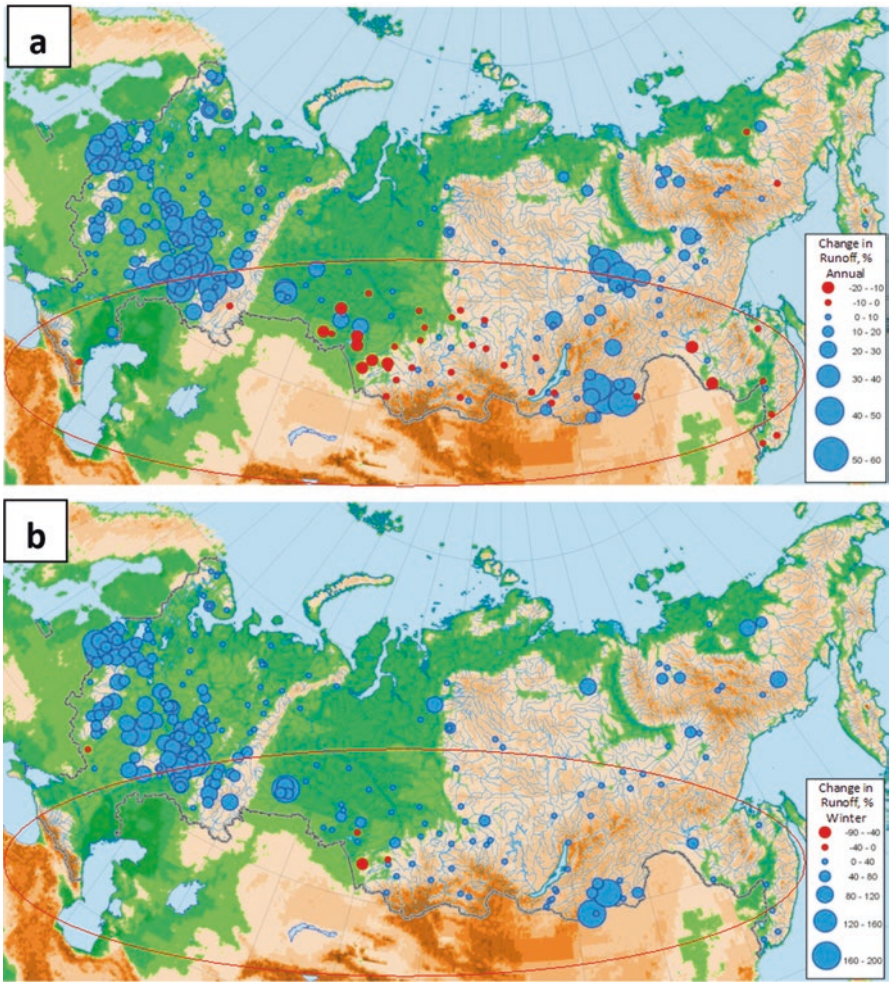

Fig. 2.2 Anomalies of (**a**) annual runoff and (**b**) winter runoff across the Russian Federation based on observational records from rivers minimally impacted by human activities during 1978–2010. Deviations of mean (**a**) annual runoff and (**b**) winter runoff during 1978–2010 were calculated against mean runoff during the prior observational period (1946–1977) and are shown in percent. Background colors show elevation above mean sea level with greens indicating lower elevations, browns higher elevations

Precipitation, the most important water source for runoff, does not show a significant change across the DLB (*cf.* Sect. 2.2.3) to support the observed increasing river discharge. However, spatial and seasonal changes in precipitation are highly variable. In contrast, the increase in air temperature across the DLB has been consistent and is projected to continue to rise in the future (IPCC AR5 WG1 2013). Increasing regional air temperatures leads to a retreating regional cryosphere (*cf.* Sect. 2.2.4). Regional studies have shown how changes in river ice affects river

discharge (Shiklomanov and Lammers 2014; Gurevich 2009). However, few comprehensive, larger scale studies of the region have explored the causes for the observed changes in discharge (*e.g.*, Bring et al. 2016).

To examine climatic signal in the annual and seasonal patterns of discharge in Central Asian rivers, we selected observational river gauge data from several montane rivers with minimal human impact located in the Syr Darya basin (http://neespi.sr.unh.edu; Shiklomanov et al. 2016). These small rivers flowing from the Tianshan Mountains show significant upward trends in annual discharge since 1970 (Fig. 2.3). The seasonal runoff variation for rivers in Tianshan Mountains have shown that the observed increasing tendencies in annual discharge are mainly due to the higher discharge rates during the spring and summer (data not shown), suggesting that snow and glacier melt due to increasing regional air temperature are the driving forces. A similar increasing tendency in river discharge starting in mid-1970s is evident for entire Syr Darya (data not shown). This pattern probably results both from decreases in water withdrawals after breakup of the Soviet Union and from increases in runoff from highland basins due to regional temperature increases. In contrast, no obvious trends in river discharge have been observed for the Pamir Mountains and the Amu Darya Basin (Chevallier et al. 2014).

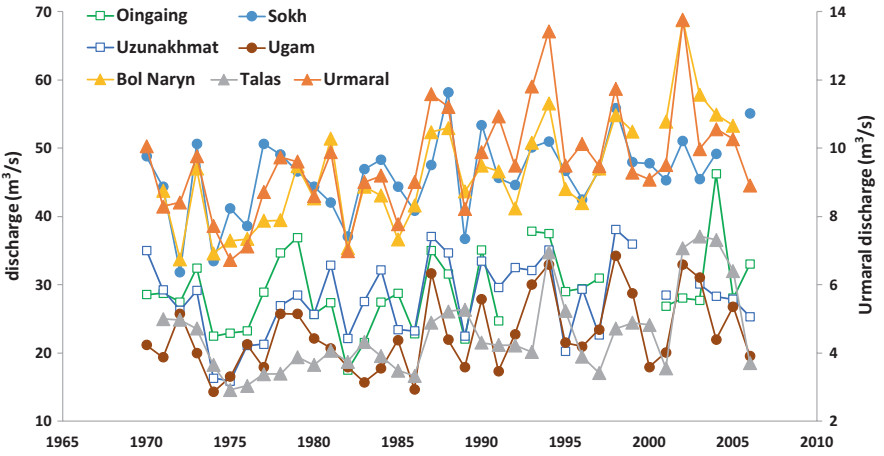

Fig. 2.3 Variation and trend in annual discharge for selected small rivers with minimal human impact in the Tianshan Mountains since 1970. Nonparametric Mann-Kendall (MK) test reveals positive trends in every river. Open squares show trends at $p < 0.1$; closed circles show trends at $p < 0.05$; closed triangles show trends at $p < 0.01$. Combined MK trend test on these discharge data indicates a positive trend at $p < 0.001$

2.3 Conclusions

Indisputable increases in surface air temperature, retreating cryosphere, increased discharge from small mountain rivers, and uncertainties in changes in precipitation have led to a generalized depletion of available water resources over much of the DLB, particularly in Central Asia. It is expected that increasing global and regional populations and a growing demand for land use and water resources will remain the major challenges for sustainable development across the DLB. Therefore, the role of conscientious human activity, policy development and implementation in land use, water management, construction, and consumption habits is crucial to advance environmental health and human well-being (Ford et al. 2015; Lesnikowski et al. 2015; Lioubimtseva and Henebry 2009).

Acknowledgements P. Groisman and G. Henebry were supported in part by NASA grant NNX15AP81G. N. Tchebakova acknowledges the Russian Foundation for Basic Research grant 16-05-00496 and the Russian Science Foundation grant 18-17-00069. O. Zolina, A. Dufour, and P. Groisman were partially supported through "ARCTIC-ERA: ARCTIC climate change and its impact on Environment, infrastructures, and Resource Availability" sponsored by ANR (France), RFBR (Russia), and US NSF (grants 1717770 and 1558389). Y. Chen was supported by National Youth Science Fund of China grant 1701227 and by the Priority Academic Program Development of Jiangsu Higher Education Institutions in China. Work of A. Shiklomanov was partially supported by U.S. NSF Grant 1602879 and Russian RFFI Grant 18-05-60240. Grant 14.B25.31.0026 of the Ministry of Education and Science of the Russian Federation provided support to P. Groisman, N. Tilinina, A. Shiklomanov, O. Bulygina, and O. Zolina for their work conducted at the P.P. Shirshov Institute of Oceanology. The synthesis workshop (Ulaan Baatar, June 2017) was partially sponsored by the "Dynamics of Coupled Natural and Human Systems" Program of the NSF (#1313761) and the LCLUC program of NASA (NNX15AD10G).

References

ACIA (Arctic Climate Impact Assessment) 2005 Scientific Report Chapter 2 "Arctic Climate: Past and Present" Cambridge University Press

Aizen VB, Kuzmichenok VA, Surazakov AB, Aizen EM (2006) Glacier changes in the central and northern Tianshan during the last 140 years based on surface and remote-sensing data. Ann Glaciol 43:202–213

Akhmadiyeva ZhK and Groisman PY (2008) General estimate of climatic change over Kazakhstan since 1990. Hydrol Ecol 2(3):46–54. (in Russian)

AMAP (Arctic Monitoring and Assessment Programme) (2011) Snow, water, ice and permafrost in the arctic (SWIPA): Climate change and the cryosphere report to the arctic council, AMAP Oslo Norway [Available at http://amap.no/swipa/]

AMAP (Arctic Monitoring and Assessment Programme) 2017 Snow, water, ice, permafrost in the arctic (SWIPA). Update. http://www.amap.no/swipa2017

Bliss A, Hock R, Radić V (2014) Global response of glacier runoff to twenty-first century climate change. J Geophys Res Earth Surf 119(4):717–730
Bring A, Fedorova I, Dibike Y et al (2016) Arctic terrestrial hydrology: a synthesis of processes, regional effects and research challenges. J Geophys Res Biogeosci 121:621–649
Bulygina ON, Groisman PY, Razuvaev VN and Korshunova NN (2011) Changes in snow cover characteristics over Northern Eurasia since 1966 Environ Res Lett 6:045204
Bulygina ON, Korshunova NN, Razuvaev VN (2013) Change of the near-surface winds over Russia during the past decades. Transact Voeikov Main Geophys Observ 568:156–172. (in Russian)
Chen J, Wan S, Henebry G et al (2014) Dryland East Asia: land dynamics amid social and climate change. Walter de Gruyter, Berlin, 467 p
Chen J, John R, Shao C et al (2015) Policy shifts influence the functional changes of the CNH systems on the Mongolian plateau. Environ Res Lett 10:085003
Chen J, John R, Sun G et al (2018) Prospects for the sustainability of social-ecological systems (SES) on the Mongolian Plateau: five critical issues. Environ Res Lett 13:123004
Chen J, Ouyang Z, John R et al (2020) Social-ecological systems across the Asian Drylands Belt (ADB). In: Gutman G et al (eds) Landscape dynamics of drylands across greater Central Asia: people, societies and ecosystems. Springer, Cham
Chevallier P, Pouyaud B, Mojaïsky M et al (2014) River flow regime and snow cover of the Pamir Alay (Central Asia) in a changing climate. Hydrol Sci J 59:1491–1506
Darmenova K, Sokolik IN, Shao Y et al (2009) Development of a physically-based dust emission module within the Weather Research and Forecasting (WRF) model: assessment of dust emission parameterizations and input parameters for source regions in Central and East Asia. J Geophys Res 114:D14201
de Beurs KM, Henebry GM (2008) Northern annular mode effects on the land surface phenologies of northern Eurasia. J Clim 21:4257–4279
de Beurs KM, Henebry GM, Owsley BC, Sokolik I (2015) Using multiple remote sensing perspectives to identify and attribute land surface dynamics in Central Asia 2001–2013. Remote Sens Environ 170:48–61
de Beurs KM, Henebry GM, Owsley B, Sokolik I (2018) Large scale climate oscillation impacts on temperature, precipitation, and land surface phenology in Central Asia. Environ Res Lett 13:065018
Dee DP, Uppalaa SM, Simmons AJ et al (2011) The ERA-interim reanalysis: configuration and performance of the data assimilation system. Quart J Roy Meteorol Soc 137:553–597
Ding Y, Yang D, Ye B, Wang N (2007) Effects of bias correction on precipitation trend over China. J Geophys Res 112:D13116
Fan P, Chen J, Ouyang Z et al (2018) Urbanization and sustainability under transitional economies: a synthesis for Asian Russia. Environ Res Lett 13:095007
Fan P, Ouyang Z, Chen J et al (2020) Population and urban dynamics in drylands of China. In: Gutman G et al (eds) Landscape dynamics of drylands across greater Central Asia: people, societies and ecosystems. Springer, Cham
Farinotti D, Longuevergne L, Moholdt G et al (2015) Substantial glacier mass loss in the Tianshan over the past 50 years. Nat Geosci 8(9):716
Ford JD, Berrang-Ford L, Bunce A et al (2015) The status of climate change adaptation in Africa and Asia. Reg Environ Chang 15:801–814
Frauenfeld OW, Zhang T (2011) An observational 71-year history of seasonally frozen ground changes in the Eurasian high latitudes. Environ Res Lett 6:044024
Gaybullaev B, Chen SC and Gaybullaev D (2012) Changes in water volume of the Aral Sea after 1960. Appl Water Sci 2:285
Gelaro R, McCarty W, Suárez MJ (2017) The modern-era retrospective analysis for research and applications, version 2 (MERRA-2). J Clim

Georgievsky VY, Georgievsky MV, Golovanov OF and Shalygin AL (2014) Land water systems, chapter: 4.1 in second assessment report of roshydromet on climate change and its consequences for territory of the Russian Federation Moscow, pp 350–361

Gong DY, Wang SW, Zhu JH (2001) East Asian winter monsoon and Arctic oscillation. Geophys Res Lett 28(10):2073–2076

Goudie AS, Middleton NJ (1992) The changing frequency of dust storms through time. Clim Chang 20:197–225

Groisman PY, Legates DR (1995) Documenting and detecting long-term precipitation trends: where we are and what should be done. Clim Chang 31:601–622

Groisman PY, Soja AJ (2009) Ongoing climatic change in Northern Eurasia: justification for expedient research. Environ Res Lett 4:045002

Groisman PY, Bogdanova EG, Alexeev VA et al (2014) Impact of snowfall measurement deficiencies on quantification of precipitation and its trends over Northern Eurasia. Ice and Snow 2(126):29–43

Groisman PY, Shugart HH, Kicklighter D et al (2017) Northern Eurasia Future Initiative (NEFI): facing the challenges and pathways of global change in the twenty-first century. Progress in Earth Planet Sci 4:41

Groisman P, Bulygina O, Henebry G et al (2018) Dry land belt of Northern Eurasia: contemporary environmental changes and their consequences. Environ Res Lett 13:115008

Gurevich E (2009) Influence of air temperature on the river runoff in winter (the Aldan river catchment case study). Russ Meteorol Hydrol 34:628–633

Henebry GM, de Beurs KM, John R et al (2020) Recent land surface dynamics across the Eurasian Drylands. In: Gutman G et al (eds) Landscape dynamics of drylands across greater Central Asia: people, societies and ecosystems. Springer, Cham

Holmes RM, Shiklomanov AI, Tank SE et al (2016) River discharge. In state of the climate in 2015. Bull Amer Meteorol Soc 97:S147–S149

IPCC AR5 WG1 (2013), Stocker TF et al. (eds) Climate change 2013: the physical science basis. Working Group 1 (WG1) Contribution to the Intergovernmental Panel on Climate Change (IPCC) 5th Assessment Report (AR5), Cambridge University Press

Jiang G, Zhao T, Liu J et al (2011) Effects of ENSO-linked climate and vegetation on population dynamics of sympatric rodent species in semiarid grasslands of Inner Mongolia, China. Canad J Zool 89(8):678–691

Kalyuzhny I, Lavrov A (2012) Basic physical processes and regularities of winter and spring river flow formation under the climate warming. Russ Meteorol Hydrol:68–81

Khromova T, Nosenko G, Kutuzov S et al (2014) Glacier area changes in Northern Eurasia. Environ Res Lett 9:015003

Kotlyakov VM, Khromova TY, Nosenko GA et al (2015) Recent glacier changes in mountain regions of Russia. KMK Scientific Press, Moscow, p 288

Lesnikowski AC, Ford JD, Berrang-Ford L et al (2015) How are we adapting to climate change? A global assessment. Mitig Adapt Strateg Glob Chang 20:277–293

Lioubimtseva E, Henebry GM (2009) Climate and environmental change in arid Central Asia: impacts, vulnerability, and adaptations. J Arid Environ 73:963–977

Loboda TV, Chen D (2017) Spatial distribution of young forests and carbon fluxes within recent disturbances in Russia. Glob Chang Biol 23(1):138–153

Lupo AR, Mokhov II, Chendev YG et al (2014) Studying summer season drought in Western Russia. Adv Meteorol 942027

Mokhov II, Akperov MG, Prokofyeva MA et al (2013) Blockings in the Northern hemisphere and Euro-Atlantic region: estimates of changes from reanalysis data and model simulations. Dokl Earth Sci 449:430–433

Peterson BJ, Holmes RM, McClelland JW et al (2002) Increasing river discharge to the Arctic Ocean. Science 298:2171–2173

Qi J, Chen J, Wan S, Ai L (2012) Understanding the coupled natural and human systems in dryland East Asia. Environ Res Lett 7:015202
Qi J, Xin X, John R et al (2017) Understanding livestock production and sustainability of grassland ecosystems in the Asian Dryland Belt. Ecolog Process 6(1):22
Romanovsky VE, Smith SI, Shiklomanov NI, Marchenko SS (2017) Terrestrial permafrost. Bull Amer Meteorol Soc 98(8):147–149
Schubert S, Wang H, Koster R et al (2014) Northern Eurasian heat waves and droughts. J Clim 27:3169–3207
Shahgedanova M, Nosenko G, Khromova T, Muravyev A (2010) Glacier shrinkage and climatic change in the Russian Altai from the mid-20th century: an assessment using remote sensing and PRECIS regional climate model. J Geophys Res – Atmos 115:D16107
Shahgedanova M, Nosenko G, Kutuzov S et al (2014) Deglaciation of the Caucasus Mountains, Russia/Georgia in the 21st century observed with ASTER satellite imagery and aerial photography. Cryosphere 8:2367–2379
Shiklomanov AI, Lammers RB (2009) Record Russian river discharge in 2007 and the limits of analysis. Environ Res Lett 4:045015
Shiklomanov AI and Lammers RB (2013) Changing discharge patterns of high-latitude rivers, in climate vulnerability: understanding and addressing threats to essential resources. Elsevier, pp 161–175
Shiklomanov AI, Lammers RB (2014) River ice responses to a warming Arctic – recent evidence from Russian rivers. Environ Res Lett 9:035008
Shiklomanov AI, Lammers RB, Rawlins MA et al (2007) Temporal and spatial variations in maximum river discharge from a new Russian data set. J Geophys Res – Biogeosciences 112:G04S53
Shiklomanov A, Prusevich A, Gordov E et al (2016) Environmental science applications with Rapid Integrated Mapping and analysis System (RIMS) IOP Conf Series Earth and Environ Sci 48 012034 November 2016
Shiklomanov NI, Streletskiy DA, Swales TB, Kokorev VA (2017) Climate change and stability of urban infrastructure in Russian permafrost regions: prognostic assessment based on GCM climate projections. Geograph Rev 107:125–142
Shver TA (1976) Atmospheric precipitation over the USSR territory (in Russian) Gidrometeoizdat Leningrad, 302 p
Smith LC, Pavelsky TM, MacDonald GM et al (2007) Rising minimum daily flows in northern Eurasian rivers suggest a growing influence of groundwater in the high-latitude water cycle. J Geophys Res Biogeosci 112:G04S47
SNCCA (Second National Climate Change Assessment for the Russian Federation) (2014). http://cc.voeikovmgo.ru/ru/publikatsii/2016-03-21-16-23-52. Moscow Roshydromet (in Russian)
Streletskiy D, Tananaev N, Ope T et al (2015) Permafrost hydrology in changing climatic conditions: seasonal variability of stable isotope composition in rivers in discontinuous permafrost. Environ Res Lett 10:095003
Syromyatina MV, Kurochkin YN, Bliakharskii DP, Chistyakov KV (2015) Current dynamics of glaciers in the Tavan Bogd Mountains (Northwest Mongolia). Environ Earth Sci 74:1905–1914
Tilinina N, Gulev SK, Rudeva I, Koltermann P (2013) Comparing cyclone life cycle characteristics and their interannual variability in different reanalyses. J Clim 26:6419–6438
Tomaszewska MA, Henebry GM (2018) Changing snow seasonality in the highlands of Kyrgyzstan. Environ Res Lett 13:065006
Troy TJ, Sheffield J, Wood EF (2012) The role of winter precipitation and temperature on northern Eurasian streamflow trends. J Geophys Res Atmos 117:D5
Wright CK, de Beurs KM, Akhmadiyeva ZK et al (2009) Reanalysis data underestimate significant changes in growing season weather in Kazakhstan. Environ Res Lett 4 045020
Wright CK, de Beurs KM, Henebry GM (2014) Land surface anomalies preceding the 2010 Russian heat wave and a link to the North Atlantic Oscillation. Environ Res Lett 9:124015

Zavialov PO (2007) Physical oceanography of the dying Aral Sea. Springer, 153 p
Zhou H, Aizen E, Aizen V (2017) Seasonal snow cover regime and historical change in Central Asia from 1986 to 2008. Glob Planet Chang 148:192–216
Zolina OG, Simmer C, Belyaev K et al (2013) Changes in the duration of European wet and dry spells during the last 60 years. J Clim 26:2022–2047

Chapter 3
Recent Land Surface Dynamics Across Drylands in Greater Central Asia

Geoffrey M. Henebry, Kirsten M. de Beurs, Ranjeet John, Braden C. Owsley, Jahan Kariyeva, Akylbek Chymyrov, and Mirasil Mirzoev

3.1 Introduction

As noted in Chap. 1 (Henebry et al. 2020), the IPCC's Fifth Assessment report (AR5; Hijioka et al. 2014) found that climate change impacts in Central Asia are not well characterized. Many key topics across broad sectors have too little information to document the manifold consequences of multi-dimensional climate change on drylands or to assess what these consequences may be under possible future climates. The dearth of information arises from complicated interactions of several

G. M. Henebry (✉)
Department of Geography, Environment, and Spatial Sciences,
Michigan State University, East Lansing, MI, USA
e-mail: henebryg@msu.edu

K. M. de Beurs · B. C. Owsley
Department of Geography and Environmental Sustainability, University of Oklahoma,
Norman, OK, USA
e-mail: kdebeurs@ou.edu; braden.owsley@ou.edu

R. John
Department of Biology, University of South Dakota, Vermillion, SD, USA
e-mail: ranjeet.john@usd.edu

J. Kariyeva
Alberta Biodiversity Monitoring Institute, University of Alberta, Edmonton, AB, Canada
e-mail: kariyeva@ualberta.ca

A. Chymyrov
Department of Geodesy and Geoinformatics, Kyrgyz State University of Construction,
Transport and Architecture, Bishkek, Kyrgyzstan

M. Mirzoev
Hydromelioration Faculty, Tajik Agrarian University, Dushanbe, Tajikistan

G. Gutman et al. (eds.), *Landscape Dynamics of Drylands across Greater Central Asia: People, Societies and Ecosystems*, Landscape Series 17,
https://doi.org/10.1007/978-3-030-30742-4_3

factors, including sparse population density, few resources to support national scientific investigations in the post-Soviet era, ethnic tensions and political situations that limit field investigations, and developing economies struggling to re-establish research capacity following a series of institutional and socio-economic shocks.

This chapter explores land surface dynamics of drylands in Greater Central Asia from complementary perspectives using different remote sensing products. Our aim here is not to provide a detailed accounting of changes in land cover types across time (*cf.* Chen et al. 2020). Rather, we seek to explore recent land surface dynamics in a threefold manner: (1) by visualizing spatiotemporal variation in major land cover types; (2) by identifying where there have been significant trends in land surface temperature at regional, national, and subnational scales; and (3) by linking observed trends to major land cover types.

3.1.1 Spatiotemporal Variation in Major Land Cover Types

Mapping of land cover and land use has been a mainstay application of remote sensing for decades. Any land cover/land use mapping effort is motivated by a set of questions that the product seeks to address. The map legend represents a model of the land surface with categories tuned to address those questions, such as the area and proportion of a few (*e.g.*, Anderson et al. 1976), a moderate number (*e.g.*, Loveland et al. 1991, 2000; Brown de Colstoun et al. 2003; Chymyrov et al. 2018) or numerous (*e.g.*, Johnson and Mueller 2010; Boryan et al. 2011) distinct categories. Traditional multinomial maps divide the plane using crisp sets of categories or types. Every point on the map belongs to only one cover type among several. Examples include the National Land Cover Dataset (NLCD) produced occasionally by the United State Geological Survey (Vogelmann et al. 2001; Homer et al. 2007, 2015), the Corine land cover data produced by the European Environment Agency (Büttner et al. 2004; Feranec et al. 2010), and the GlobeLand30 product from the National Geomatics Center of China (Chen et al. 2015). These finer spatial resolution products are generated infrequently due to the interaction of data acquisition tempo and cloud cover, and their class-specific accuracies can range widely, particularly when finer thematic resolutions are sought (Brovelli et al. 2015; Sun et al. 2016; Wickham et al. 2013, 2017; Wang et al. 2018).

While land cover change can be considered a local process (Sulla-Menashe et al. 2019), the proximate causes of local change may not be local. Indeed, the ideas of land use displacement (Meyfroidt and Lambin 2009; Meyfroidt et al. 2010) and telecoupling (Friis et al. 2016; Liu et al. 2014; Sun et al. 2017) explicitly address non-local influences on local land use transition and land cover change. Moreover, land cover and land use change can be occurring in the same area at different scales and tempos, due to differences in the driving forces. For example, while weather and climate can influence broad areas more slowly, direct human activity can shape

the landscape at finer scales more quickly (de Beurs et al. 2009; Kariyeva and van Leeuwen 2011, 2012; Wright et al. 2012; de Beurs and Henebry 2013).

Here we will use MODIS land cover product MCD12C1 with a spatial resolution of 0.05° (~5.3 km) to explore spatiotemporal variation in land surface dynamics. The most recent version of the MODIS land cover product suite (MCD12Q1 and MCD12C1 V006) is a substantial improvement over the previous iteration, and it includes algorithmic advances and post-classification processing to produce a richer, more accurate collection of data layers (Sulla-Menashe et al. 2019). The authors offer the caveat that the annual series of MODIS land cover products were "not designed to be used for mapping land cover changes" (Sulla-Menashe et al. 2019). Indeed, the 500 m resolution of MCD12Q1 would be too coarse to track finer scale changes in the landscape effectively, whether arising from direct human action (*e.g.*, land use conversion, land use intensification), natural processes (*e.g.*, succession, desertification, salinization), disturbance processes (*e.g.*, fire, drought, flood) or some combination of these. We contend, however, that MCD12C1 provides an appropriate resolution to identify potential areas of land-atmosphere interactions.

3.1.2 Significant Trends in Land Surface Temperature

Asymmetry in daytime and nighttime warming trends and the diurnal temperature range (DTR) have long been recognized as indicators of surface climate change (Karl et al. 1993; Gallo et al. 1999) that can also be used with climate projections (Braganza et al. 2004). Negative trends in DTR arise from multiple factors in addition to asymmetric warming, including clouds – especially low clouds – that reduce insolation, and soil moisture and precipitation that enable the surface to cool through evapotranspiration (Dai et al. 1999). Satellite observations of DTR are biased toward clear sky conditions, but studies have shown observations of the land surface temperature to agree well with station temperatures, although the latter lag in phase (Sun et al. 2006a, b).

Climate projections for Eurasian drylands broadly agree on warming, both at daytime and nighttime, but the projections for precipitation are highly uncertain (Reyer et al. 2017; Sillman et al. 2013; Yu et al. 2018; Zhang et al. 2019). Across the drylands, climate projections indicate an increasing number of "tropical nights" where the overnight temperate exceeds 20 °C as well as a shift in percentile exceedance rates (Sillmann et al. 2013). Increased temperatures overnight have been shown to be deleterious to the dominant C_4 grass species in semiarid US High Plains (Alward et al. 1999). However, the grasslands of Eurasia are dominated by C_3 grass species. Experimental manipulations in the steppes of northern China have demonstrated that nighttime warming can enhance belowground carbon sequestration in grasslands (Wan et al. 2009; Xia et al. 2009) and change the belowground microbial community that is critical to nutrient biogeochemistry in grasslands (Zhang et al. 2011). Thus, asymmetric effects in diurnal warming have broad implications for the

response of vegetation communities to environmental variation, change, and disturbance (Peng et al. 2013; Xia et al. 2014).

Here we use the MODIS Land Surface Temperature (LST) 8-day composites from Terra (MOD11C2) to identify statistically significant trends in the time series from 2001 to 2016 using a robust nonparametric trend test. An earlier analysis of changes in thermal time in Central Asia used the period 2000–2013 and an earlier version of the LST product (de Beurs et al. 2015).

There is lack of consensus in the scientific literature on what trend tests can – and cannot – reveal. Trend analysis evaluates whether an accumulation of separately non-significant step changes yields a step change over time that is significant at a specified level. Trend analysis is retrospective – it seeks to detect past change over a specific period (*cf.* Henebry 2019). Trends are not tendencies; despite sounding like similar words, they arise from different root meanings.

Used as a verb, the English word "trend" comes from Old English ("trend v.". OED Online 2017) word *trendan* that has the Anglo-Saxon root meaning of "to turn" or "to roll" (Bosworth 2010a) and is associated with the noun *trinda* that has the Anglo-Saxon root meaning of "a round lump" or "a ball" (Bosworth 2010b). The Anglo-Saxon roots of this older English word trend do not imply directionality. In contrast, used as a verb, the English word "tend" comes from the French *tend-re* and the Latin *tendĕre*, meaning to stretch, stretch out, extend, ("tend, v.2". OED Online. 2017), clearly implying directionality. Now consider the contemporary usage of "trending" in terms of social media: Twitter hashtags or Google search terms can trend up or down or wander around.

Trending is agnostic about direction, but tending implies some future behavior. Trends evaluate retrospectively, whereas tendencies project forward. Projecting a tendency is called forecasting, and it models the future rather than assesses the past.

Here what we seek is to identify *where* significant changes in the thermal regime have occurred in Greater Central Asian drylands. We use LST instead of air temperature for two reasons. First, LST is closer to what low-statured vegetation experiences than the air temperature measured at 2 m (Still et al. 2014). Second, these drylands, like many parts of the planet, have a low density of meteorological stations with underrepresentation in areas of high terrain (*e.g.*, Wright et al. 2009).

3.1.3 Linking Observed LST Trends to Major Land Cover Types

As mentioned earlier, it is reasonable to expect that large areas of change that emerge gradually is linked to atmospheric processes, such as climatic variation and change, as well as slow-onset extremes, such as drought. Thus, we seek to identify whether there are links between statistically significant trends – whether positive or negative – and the major land cover types occurring with these trend areas. The directionality of influence is not clear *a priori*: the observed changes in the thermal

environment may cause *or* may result from changes in the land cover types *or* both. It is beyond the scope of this chapter to conduct a study of change attribution (*cf.* Henebry 2019); rather, we are restricted here to identifying the associations of major land cover types with changes in the land surface temperature at different compositional thresholds.

3.2 Study Area

Here we take as the study area the entire drylands in Greater Central Asia (GCA) region and major subregions of Central Asia Core (CAC), Drylands East Asia (DEA), and Middle East (ME) as described in Chap. 10 (Chen et al. 2020). However, instead of the 22 political entities used in Chap. 10, we treat territories of the Palestinian National Authority (Gaza Strip and West Bank) as separate areas, yielding 24 political entities for the analysis.

3.3 Data

We used two Collection 6 MODIS products at 0.05° (~5.3 km) spatial resolution: MOD11C2 (Land Surface Temperature 8-day composites) and MCD12C1 (Land Cover Type Yearly). We analyzed land surface temperature (LST) separately for daytime (LST_{day}) and nighttime (LST_{night}). In addition, we calculated the diurnal temperature range (DTR) as the LST_{day} minus the LST_{night}. We used the IGBP (International Geosphere-Biosphere Programme) land cover scheme. However, we limited our analysis to the top four land cover types across the region: grasslands, barren lands, croplands, and open shrublands. These four types comprise nearly 94% of the land area in GCA, more than 96% in CAC, and more than 93% in DEA and ME (Table 3.1).

Table 3.1 Major land cover types in study regions by area and percentage

Region	Grass lands 10^3 km^2	%	Barren lands 10^3 km^2	%	Crop lands 10^3 km^2	%	Open shrublands 10^3 km^2	%	Other types 10^3 km^2	%	Total 10^3 km^2
GCA	10,293	50.0	7101	34.5	1332	6.5	743	3.6	1106	5.4	20,575
CAC	4660	61.3	1707	22.4	576	7.6	388	5.1	273	3.6	7604
DEA	4595	50.8	3599	39.8	274	3.0	9	0.1	565	6.3	9042
ME	1032	26.4	1792	45.9	479	12.3	345	8.8	257	6.6	3905

GCA Greater Central Asia, *CAC* Central Asia Core, *DEA* Drylands East Asia, *ME* Middle East

3.4 Methods

3.4.1 Visualizing Spatiotemporal Stability and Variation

The MCD12C1 product has a coarser spatial resolution (0.05°) built up from the native resolution of 500 m in the MCD12Q1 product. MCD12C1 includes a layer for each land cover type (LCT) reporting the percentage of that land cover type (%LCT) in each pixel. Thus, we can take the percentage layers across time (here 2003–2017) and calculate for each pixel the maximum, the mean, and the range (*i.e.*, maximum minus minimum) of percentages for each land cover type. Range of percentages for a specific land cover type serves as an indicator of land cover change over the period of study. It can also indicate instability in the product's algorithm or the impact of climatic variation in a water-limited ecosystem. It is beyond the scope of this analysis to attribute which explanation of high range in %LCT is more fitting.

We visualize regional stability and variation of land cover types in space and time in two ways. First, we form false color composites of the maximum, mean, and range displayed as red, green, and blue, respectively. Interpreting the resulting color mixtures is straightforward, but since the primary colors are not binary values but scaled from 0 to 100, there are many possible shades in the composite colors (Table 3.2). Yellows indicate stable core because the interannual range is low while the maximum and mean are high: %LCT is always high. Whites indicate unstable core because the range is high: %LCT is sometimes low but usually high. Magentas indicate an unstable but persistent periphery of the LCT, because the maximum and range are high but the mean is low: %LCT is sometimes high but usually low. Blues indicate unstable but ephemeral periphery, because maximum and mean are low, but range is high: %LCT is rare and erratic.

In addition to displaying LCT stability/variation for each of the top 4 LCTs, we visualize LCT variation across LCTs by forming false color composites of range values.

Table 3.2 Interpretation of false color composites indicating land cover type (LCT) stability/variation

Composite color	Red = Maximum %LCT	Green = Mean %LCT	Blue = Range %LCT	Interpretation of composite color
Yellows	High	High	Low	Stable core area of LCT
Whites	High	High	High	Unstable core area of LCT
Magentas	High	Low	High	Unstable but persistent periphery
Blues	Low	Low	High	Unstable but ephemeral periphery
Black	Zero	Zero	Zero	LCT absent

Modified from Henebry et al. (2013) and Alemu and Henebry (2016)

3.4.2 Detecting Significant Trends in the Thermal Regime and Linking to Political Entities

To detect and assess the cumulative effect of subtle changes through time, we applied the Seasonal Kendall trend analysis to the MOD11C2 data, conducting separate trend tests to LST_{day}, LST_{night}, and DTR). The Seasonal Kendall trend test is completely rank based and robust against non-normality, missing values, seasonality, and first-order autocorrelation (de Beurs and Henebry 2004).

Climate projections for Central Asia broadly agree on warming, both daytime and nighttime warming, and some project decreasing DTR (Zhang et al. 2019; Reyer et al. 2017; Silliman et al. 2013). Thus, we interrogated the results of significant trends ($p < 0.05$) using the following set of trends, separately and jointly: (1) significant positive trend in LST_{day}; (2) significant positive trend in LST_{night}; (3) significant negative trend in DTR; (4) significant positive trends in both LST_{day} and LST_{night}; and (5) significant positive trend in LST_{night} and significant negative trend in DTR. We tabulated the extent of significant trends in these five categories of occurrence for each of the 24 political entities as well as by subregion – CAC, DEA, ME – and the drylands of GCA.

3.4.3 Linking Changes in the Thermal Regime to Major Land Cover Types

We cross-tabulated the percentage of maximum (%max) and mean (%mean) land cover type through the study period for the four major LCTs (grasslands, barren lands, croplands, and open shrublands) with the trend pixels exhibiting one or more significant trends ($p < 0.05$). At 0.05° the Climate Modeling Grid (CMG) pixels are large relative to the native LCT product (500 m) and the percentage of an LCT within CMG pixel varies from 0 (absent) to 100 (complete coverage) at a nominal precision of 1%. If there is a strong linkage between an LCT and one or more of the thermal trends, then we expect to see proportional representation of the LCTs in trend pixels out of proportion to their occurrence in the larger landscape. An indication of this disproportionality is substantial asymmetry in the ratio of the significant thermal trend pixels of a particular LCT against its absence. Given the uncertainty in the MODIS LCT product, we evaluate the asymmetry in two ways. First, we look at the ratio $p1 = \Sigma x > 50\%/\Sigma x > 0\%$, where x is the percentage of area showing significant thermal trend for a given percentage of the LCT. If the LCT is strongly linked to the thermal trend, then we expect $p1 > 60\%$. Second, we look at the ratio $p2 = \Sigma x > 95\%/\Sigma x < 5\%$, where x is the percentage of area showing significant thermal trend for a given percentage of the LCT. If $p2 > 2.0$, then we deem the asymmetry substantial and conclude there is evidence for strong linkage between the LCT and the particular thermal trend or joint occurrence of significant thermal trends.

3.5 Results

3.5.1 Regional Stability and Variation of Major Land Cover Types

Grasslands and barren lands dominate the drylands of GCA, as evident in the yellow areas in Fig. 3.1 that exhibit high values of maximum and mean LCT percentages during the study period 2003–2017 combined with low range values, indicating stability. Areas of white indicate temporal variation: high values of maximum and mean LCT percentages coupled with high values of range LCT percentage. Note five large areas of white in Fig. 3.1a indicating high interannual variation in grassland percentage: (1) north-central Uzbekistan extending into south-central Kazakhstan; (2) south-east Turkmenistan extending into north-west Afghanistan; (3) north-central Kazakhstan; (4) eastern Iraq; and (5) north-east Pakistan. Areas of magenta indicate change in LCT: high maximum and range LCT percentages coupled with low mean LCT percentages. Note the magenta patches in Fig. 3.1b indicating changes in the coverage of barren lands around the Aral Sea and along the southern flank of the Zagros Mountains in Iraq and Iran and a comparable magenta corridor for open shrublands in Fig. 3.1d. Note, too, that Fig. 3.1d is composed mostly of magenta, indicating change and variation in open shrublands. Croplands can exist in limited areas in drylands; thus, Fig. 3.1c shows many slivers of yellow, white, and magenta located along rivers and floodplains, with the notable exception of the "Virgin Lands" region of northern Kazakhstan, where rainfed agriculture is prevalent.

LCT variation and change further portrayed in Fig. 3.2 where the ranges of LCT percentages are displayed for three different LCTs. Note that interpretation of the colors in Fig. 3.2 differs from Fig. 3.1. In both Fig. 3.2a and Fig. 3.2b, red indicates high variation in barren lands, green indicates high variation in grasslands, and yellow indicates high variation in both barren lands and grasslands over the period 2003–2017. Since blue displays variation in croplands in Fig. 3.2a and open shrublands in Fig. 3.2b, the interpretations of cyan and magenta differ between the two panels. In Fig. 3.2a, cyan indicates high variation in both grasslands and croplands and magenta is absent. In Fig. 3.2b, cyan indicates high variation in both grasslands and open shrublands, magenta indicates high variation in barren lands and open shrublands, and white indicates high variation in all three LCTs. Note the complexity of variation and change in south-central Kazakhstan and north-central Uzbekistan to the east of the shrinking Aral Sea and across Turkmenistan.

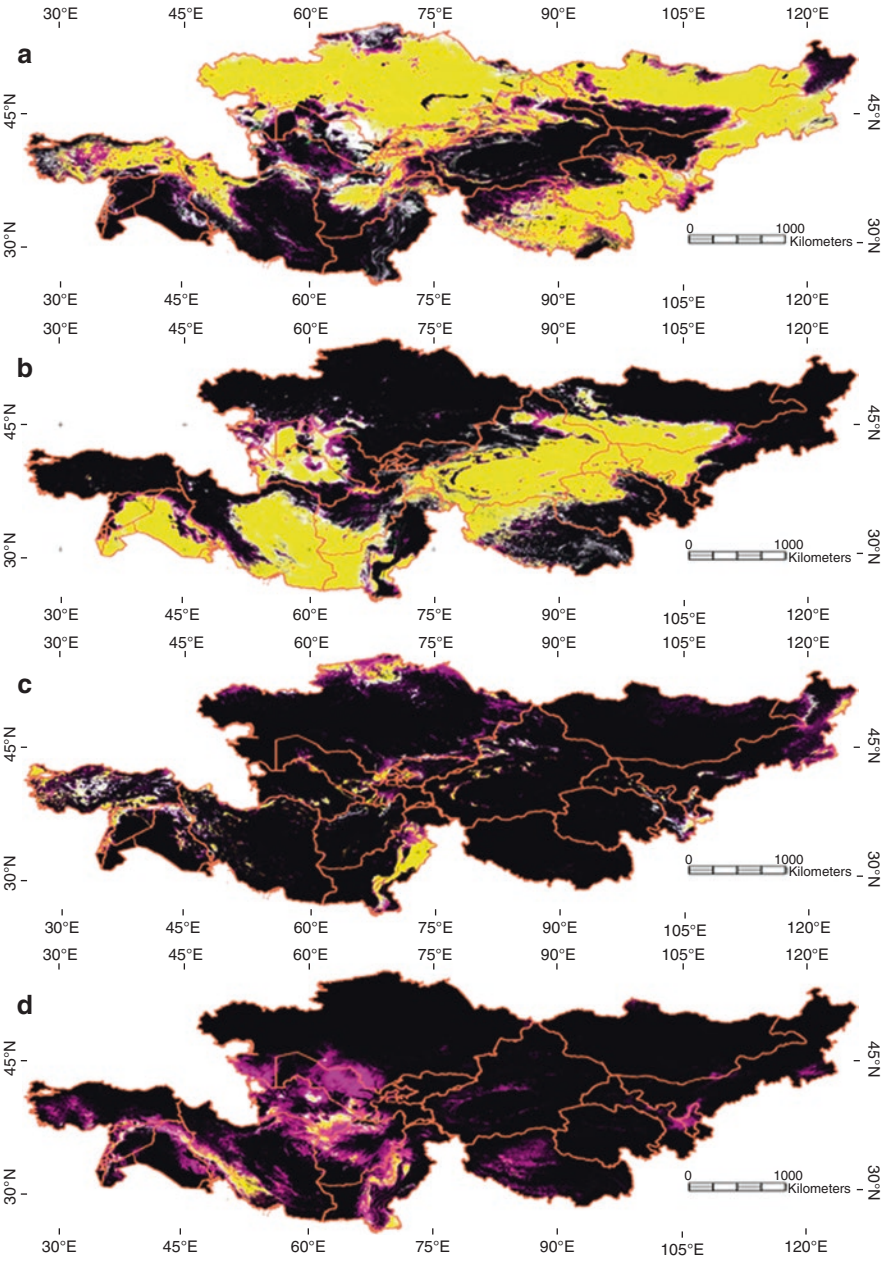

Fig. 3.1 False color composites displaying in RGB = %Max, %Mean, %Range for the four major LCTs: (**a**) Grasslands, (**b**) Barren Lands, (**c**) Croplands, and (**d**) Open Shrublands. (Note that Table 3.2 provides the key to interpreting the color combinations)

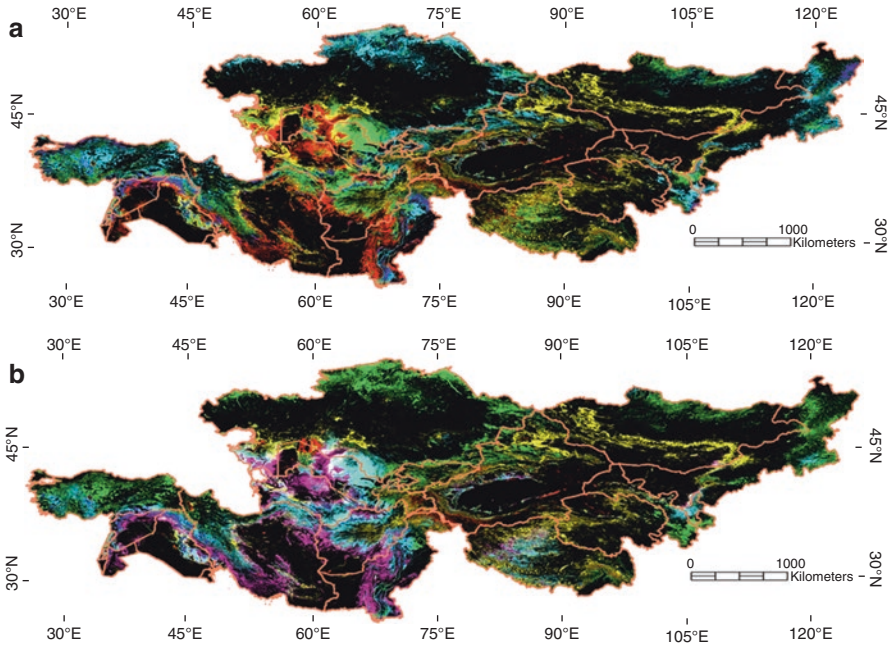

Fig. 3.2 False color composites displaying in RGB the %Ranges for three of the major LCTs: (**a**) Barren Lands, Grasslands, Croplands and (**b**) Barren Lands, Grasslands, and Open Shrublands

3.5.2 Significant Changes in the Thermal Regime Linked to Political Entities

Across GCA, the area exhibiting significant increases in nighttime land surface temperature was more than 2.5 times greater area than the area with significant increases in daytime land surface temperature (Table 3.3). Values of that ratio for CAC, DEA, and ME are, respectively, more than 2.8 times, nearly 2.3 times, and more than 3.0 times. Dryland East Asia shows the greatest extent of significantly increased LST_{night}, nearly 50% greater proportional area than in Central Asia Core. The diurnal temperature range has decreased significantly in each subregion, but substantially more (nearly one-third) in Middle East than in either CAC or DEA. Joint occurrence of significant increasing LST trends during both day and night is low across the subregions: from just over 1% in CAC to less than 2.5% in DEA. However, joint occurrence of increasing nighttime LST and decreasing DTR is more common, but still rare (all regions less than 5%), and the joint occurrence rate is comparable across subregions (the range is less than 1%).

Where across the vast region have these changes occurred? Figure 3.3 illustrates the spatial distributions of these changes in thermal regimes. It is apparent that rather than being distributed in a spatially random manner, the trends appear in large

Table 3.3 Percentage of area with significant Seasonal Kendall trends ($p < 0.05$)

Region/ Subregion	Positive LST_{day} (%)	Positive LST_{night} (%)	Negative DTR (%)	Positive $LST_{day} \cap$ Positive LST_{night} (%)	Positive $LST_{night} \cap$ Negative DTR (%)
GCA	5.55	14.13	8.06	1.86	3.65
CAC	3.90	10.97	7.52	1.12	4.18
DEA	7.18	16.35	7.58	2.36	3.23
ME	4.88	14.91	10.05	2.04	3.66

LST land surface temperature, *DTR* diurnal temperature range, *GCA* Greater Central Asia, *CAC* Central Asia Core, *DEA* Drylands East Asia, *ME* Middle East

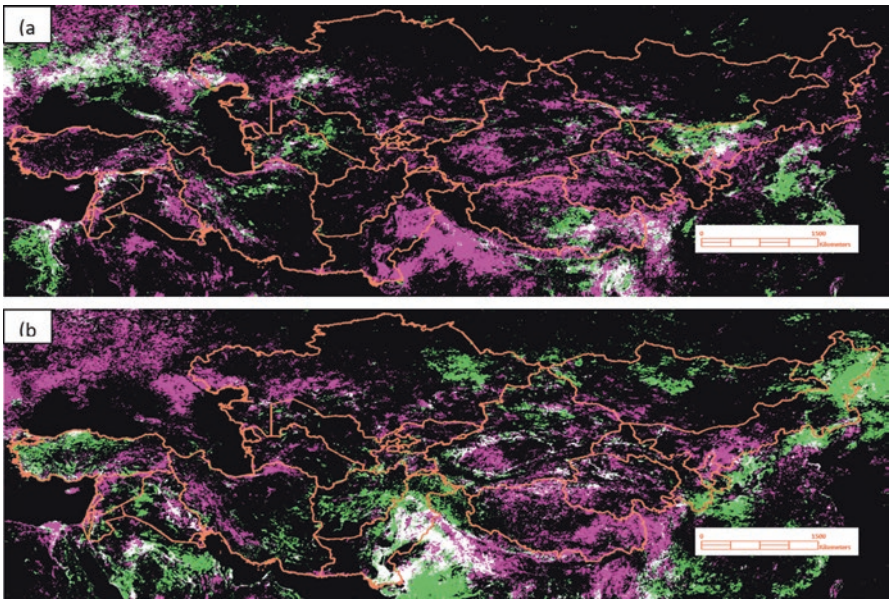

Fig. 3.3 False color composites displaying in RGB these significant ($p < 0.05$) thermal trends: (**a**) positive LST_{night}, positive LST_{day}, positive LST_{night}; and (**b**) positive LST_{night}, negative DTR, positive LST_{night}. Interpretation of these colors is straightforward. In both panels, magenta indicates significant ($p < 0.05$) positive trend in LST_{night}. Green indicates positive LST_{day} in panel (**a**) and negative DTR in panel (**b**). White indicates the joint occurrence of positive LST_{night} and LST_{day} in panel (**a**) and positive LST_{night} and DTR in panel (**b**). Black indicates the absence of the corresponding trends

patches of varying sizes. The prevalence of increased temperatures at night is striking. The joint occurrence of increased nighttime temperatures with increased daytime temperatures appears in several smaller patches, including just east of the remains of the Aral Sea in Kazakhstan, northwestern Syria, near Hohot in Inner Mongolia, in the Ural River delta in northwestern Kazakhstan, and in southern Tibet (Fig. 3.3a). In contrast, the joint occurrence with decreasing diurnal temperature range is restricted to just a few larger patches, particularly in eastern Pakistan and

northwest India and the northern rim of the Taklimakan desert in western China (Fig. 3.3b).

Which political entities (countries or administrative subunits) have been most affected, in terms of area, by these changes in land surface temperature? The next six tables examine the occurrence, joint occurrence, and absence of the three focal trends in thermal regime (*viz.*, positive LST_{day}, positive LST_{night}, and negative DTR) in the political entities composing the drylands of Greater Central Asia. Five of 24 political entities have more than 10% of their area affected by significantly increased LST_{day} between 2001 and 2016 (Table 3.4).

In contrast, significantly warmer nights were found in 19 of 24 political entities, where greater than 10% of their area was affected. In 5 of the 24, more than one-third of their affected area experienced warmer nights (Table 3.5). Note the most of these top five clustered in the eastern Mediterranean. Note also that only Ningxia appears in the top five for both LST_{day} and LST_{night} (*cf.* Tables 3.4 and 3.5).

The diurnal temperature range significantly decreased between 2001 and 2016 in 7 of 24 political entities with more than 10% of their area affected (Table 3.6).

Table 3.4 Political entities with the most area affected by significant ($p < 0.05$) positive trends in daytime land surface temperature (LST_{day})

Political entity	% area	km^2 area
Syria	17.5%	32,897
Inner Mongolia	15.4%	176,964
Tibet	15.3%	183,676
Turkmenistan	15.0%	70,278
Ningxia	12.4%	6366

Table 3.5 Political entities with the most area affected by significant ($p < 0.05$) positive trends in nighttime land surface temperature (LST_{night})

Political entity	% area	km^2 area
Gaza Strip	90.0%	282
Lebanon	58.6%	5958
West Bank	58.2%	3324
Ningxia	48.0%	24,712
Israel	36.1%	7495

Table 3.6 Political entities with the most area affected by significant ($p < 0.05$) negative trends in the diurnal temperature range (DTR)

Political entity	% area	km^2 area
Turkey	20.6%	1,610,645
Inner Mongolia	19.0%	218,077
[a]Pakistan	18.4%	153,256
Afghanistan	17.8%	114,558
Gansu	11.8%	47,981
Jordan	10.8%	9596
Iraq	10.8%	47,103

[a]Only northern Pakistan (834,552 km^2) was included in the analysis

Table 3.7 Political entities with the least area affected by the featured changes in thermal regime

Political entity	% area	km² area
Uzbekistan	86.4%	386,481
Mongolia	85.7%	1,340,515
Kyrgyzstan	85.1%	166,616
Kazakhstan	82.9%	2,253,498
Kuwait	81.4%	14,237

Table 3.8 Political entities with the most area affected by the joint occurrence of significant ($p < 0.05$) positive trends in both daytime and nighttime land surface temperature (positive LST_{day} ∩ positive LST_{night})

Political entity	% area	km² area
Syria	12.5%	23,426
Ningxia	6.8%	3512
Tibet	6.1%	73,821
Inner Mongolia	5.0%	57,232
Turkmenistan	2.5%	11,697

In addition to detecting where the thermal regime changed significantly, we can also identify were there was little, if any, significant change in daytime or nighttime land surface temperature or the diurnal temperature range. In 20 of 24 political entities, none of the featured changes in land surface temperature occurred in more than 50% of the area (data not shown). Note that more than 85% of Uzbekistan, Mongolia, and Kyrgyzstan and nearly 83% of Kazakhstan showed no significant changes in DTR or LST_{night} or LST_{day}, covering an area of more than four million km² – nearly 94% of the area of the European Union (Table 3.7).

Joint occurrence rates are lower, as might be expected. The top 5 countries with most area affected by significantly increased LST_{day} (Table 3.4) appear as the top 5 countries most affected by the joint occurrence of increased LST_{day} and LST_{night}, although the ordering differs apart from Syria, which occupies the top spot in both categories (Table 3.8). In 23 of 24 political entities, less than 10% of their area was affected by the joint occurrence of increased LST_{day} and LST_{night} (data not shown).

The joint occurrence of increased LST_{night} and decreased DTR (Table 3.9) appears as an interesting blend: Gaza Strip, Lebanon, Ningxia, and Israel from Table 3.5 joining northern Pakistan, Iraq, Turkey, and Jordan from Table 3.6. Although neither Xinjiang nor Qinghai appeared in the earlier tables, both exhibited trend joint occurrences in 5–6% of their territory – totaling nearly 130,000 km² (Table 3.9). In 14 of 24 political entities and in 22 of 24, less than 5% and less than 10% of their areas, respectively, were affected by the joint occurrence of positive trend in LST_{night} and negative trend in DTR (data not shown).

Table 3.9 Political entities with the most area affected by the joint occurrence of a significant ($p < 0.05$) positive trend in nighttime land surface temperature and a significant ($p < 0.05$) negative trend in diurnal temperature range (positive $LST_{night} \cap$ negative DTR)

Political entity	% area	km^2 area
Gaza Strip	40.0%	125
[a]Pakistan	21.4%	178,407
Lebanon	11.4%	1160
Iraq	8.0%	34,966
Ningxia	7.6%	3889
Israel	6.9%	1443
Turkey	6.9%	53,814
Xinjiang	5.7%	93,390
Jordan	5.5%	4892
Qinghai	5.1%	36,534

[a]Only northern Pakistan (834,552 km^2) was included in the analysis

Table 3.10 Area with significant thermal trends ($p < 0.05$)

Region/ Subregion	Positive LST_{day} (10^3 km^2)	Positive LST_{night} (10^3 km^2)	Negative DTR (10^3 km^2)	Positive $LST_{day} \cap$ Positive LST_{night} (10^3 km^2)	Positive $LST_{night} \cap$ Negative DTR (10^3 km^2)
GCA	1142	2907	1658	383	751
CAC	297	834	572	85	318
DEA	649	1478	685	213	292
ME	191	582	392	80	143

LST land surface temperature, *DTR* diurnal temperature range, *GCA* Greater Central Asia, *CAC* Central Asia Core, *DEA* Drylands East Asia, *ME* Middle East

3.5.3 Changes in the Thermal Regime Linked to Major Land Cover Types

As evident in Table 3.10, the areal extents of the significant trends are substantial, but they vary by trend type and region. Note that the areal extent of significantly increased LST at night is nearly 3 million km^2 across GCA (Table 3.10), with proportionally more of that area located in DEA (Table 3.11). Likewise, DEA has proportionally more area of significantly increased daytime LST. ME shows a disproportional area of significantly decreased diurnal temperature range. In contrast, CAC has disproportionally less area in any thermal trend except for the joint occurrence of positive LST_{night} and negative DTR (Table 3.11).

We present here the cross-tabulation results only for the %maximum coverage for each LCT as the results for the mean were comparable but weaker. The strongest land cover linkage was evident for grasslands, but only for particular (sub)regions and trends. Note that the joint occurrence of significant increases in both daytime and nighttime LST shows substantial asymmetry associated with grasslands across

Table 3.11 Ratio between the area exhibiting significant trends and the subregion area. If the ratio is greater than 1.0 (less than 1.0), then the subregion has disproportionally more (less) area displaying that thermal trend

Subregion	Positive LST_{day}	Positive LST_{night}	Negative DTR	Positive $LST_{day} \cap$ Positive LST_{night}	Positive $LST_{night} \cap$ Negative DTR
CAC	0.70	0.78	0.93	0.60	1.15
DEA	1.29	1.16	0.94	1.27	0.88
ME	0.88	1.06	1.25	1.10	1.00

GCA Greater Central Asia, *CAC* Central Asia Core, *DEA* Drylands East Asia, *ME* Middle East

Table 3.12 Maximum grasslands cover type as a percentage of total number of pixels with significant ($p < 0.05$) trend(s)

Grasslands in Region	Positive LST_{day} (%)	Positive LST_{night} (%)	Negative DTR (%)	Positive $LST_{day} \cap$ Positive LST_{night} (%)	Positive $LST_{night} \cap$ Negative DTR (%)
GCA	51.6	51.8	51.4	***62.2***	30.7
CAC	***62.2***	56.1	52.4	***82.0***	21.1
DEA	54.7	52.5	***65.0***	***69.4***	42.1
ME	27.2	44.9	29.2	25.7	28.9

Values in bold italics indicate that the ratio of pixels with cover type >95% to the pixel with cover type <5% is greater than 2.0
GCA Greater Central Asia, *CAC* Central Asia Core, *DEA* Drylands East Asia, *ME* Middle East

Table 3.13 Maximum barren lands cover type as a percentage of total number of pixels with significant ($p < 0.05$) trend(s)

Barren Lands in region	Positive LST_{day} (%)	Positive LST_{night} (%)	Negative DTR (%)	Positive $LST_{day} \cap$ Positive LST_{night} (%)	Positive $LST_{night} \cap$ Negative DTR (%)
GCA	45.0	37.2	26.2	26.2	35.7
CAC	44.5	17.8	28.9	18.2	15.3
DEA	48.0	53.8	13.3	34.3	59.6
ME	36.9	23.9	43.4	13.8	32.9

GCA Greater Central Asia, *CAC* Central Asia Core, *DEA* Drylands East Asia, *ME* Middle East

GCA, CAC, DEA, but not ME (Table 3.12). Increased daytime LST shows a strong linkage with grasslands only in CAC; and the negative trend of diurnal temperature range is linked to grasslands only in DEA.

In contrast to grasslands, the patterns associated with the other three LCTs – barren lands (Table 3.13), croplands (Table 3.14), and open shrublands (Table 3.15) – show no strong positive linkage with any thermal trend or joint occurrence of thermal trend. Indeed, the patterns associated with croplands (and open shrublands in Drylands East Asia) suggest negative linkages with the thermal trends.

Table 3.14 Maximum croplands cover type as a percentage of total number of pixels with significant ($p < 0.05$) trend(s)

Croplands in region	Positive LST_{day} (%)	Positive LST_{night} (%)	Negative DTR (%)	Positive $LST_{day} \cap$ Positive LST_{night} (%)	Positive $LST_{night} \cap$ Negative DTR (%)
GCA	7.4	14.5	18.8	12.5	33.7
CAC	3.1	27.7	16.3	2.5	59.6
DEA	2.5	3.6	19.9	1.9	10.9
ME	28.4	22.4	19.5	48.0	21.9

GCA = Greater Central Asia; CAC=Central Asia Core; DEA=Drylands East Asia; ME = Middle East

Table 3.15 Maximum open shrublands cover type as a percentage of total number of pixels with significant ($p < 0.05$) trend(s)

Open shrublands in region	Positive LST_{day} (%)	Positive LST_{night} (%)	Negative DTR (%)	Positive $LST_{day} \cap$ Positive LST_{night} (%)	Positive $LST_{night} \cap$ Negative DTR (%)
GCA	14.2	14.6	16.1	14.1	17.6
CAC	29.6	19.2	33.2	14.9	27.2
DEA	1.9	3.9	0.6	2.5	5.2
ME	31.9	34.4	18.4	41.9	24.4

GCA Greater Central Asia, *CAC* Central Asia Core, *DEA* Drylands East Asia, *ME* Middle East

3.6 Discussion

3.6.1 Regional Stability and Variation of Major LCTs

Most of the drylands in Greater Central Asia are either grasslands or barren lands, with the latter including sparsely vegetated lands. Thus, it is not surprising that pastoralism is widespread across the region (Kappas et al. 2020; Spaeth et al. 2020). The vast swaths of yellow (Fig. 3.1a–b) give way to relatively minor inclusions of magenta, mostly apparent at the edges. The area to the east of the Aral Sea shows how the contracting body of water has left a variable and changing landscape of barren lands, grasslands, and open shrublands (magenta and cyan patches in Fig. 3.2b). Although open shrublands are a relatively minor component they are widely distributed. The expanses of magenta (indicating high %maximum, low %mean, and high %range during the 2003–2017 period) in eastern CAC and ME (Fig. 3.1d) suggest that this LCT is difficult to map accurately or there has been a substantial land cover transition over this period or, most likely, both conditions pertain to differing degrees across the entire expanse.

In drylands, interannual variation in growing season weather can wreak havoc on classification algorithms relying in part on land surface phenology indicated by vegetation indices (Sulla-Menashe et al. 2019; Zhang et al. 2019). Parts of the drylands of GCA are strongly influenced by climate oscillation modes that shift precipitation amount and timing sufficiently to affect land surface phenology (de Beurs and Henebry 2008; de Beurs et al. 2018; Kariyeva et al. 2012; Wright et al. 2014).

That this part of the world is challenging to classify accurately is demonstrated by Sun et al. (2016), who conducted an accuracy assessment on the 2010 epoch of the GlobeLand30 product (Chen et al. 2015) in Central Asia using a combination of higher spatial resolution imagery and ground survey data. They found the overall accuracy of GlobeLand30 data was only 46% in Central Asia, despite other studies finding overall accuracies over 90% in other parts of the world (Sun et al. 2016). The biggest source of error was confusion between grassland and "bare land", which suggests that variation in growing season timing played a role in this poor accuracy metric.

In contrast to the other LCTs that are less intensively managed, croplands are more stable, particularly as they are often associated with riparian irrigation. However, where there is expansion, intensification, salinization, or abandonment during the study period (*e.g.*, Laiskhanov et al. 2016), such changes may manifest as areas of white (high values in %max, %mean, and %range). For example, substantial patches of white appear in Fig. 3.1c in Turkey and likely indicated increasing irrigation and/or cropland expansion (Alganci et al. 2014; Aslan and Gundogdu 2007; Ozdogan and Salvucci 2004).

3.6.2 Significant Thermal Trends Linked to Political Entities

Warmer nights can stress both plants and animals, especially in urbanized areas and during heat waves (Argüeso et al. 2015; Oleson et al. 2015; Prasad et al. 2008). It is notable that the populous eastern Mediterranean has experienced significant nighttime warming (Table 3.5 and Fig. 3.3a) and that a substantial fraction of western and northern Turkey has experience a significant decrease in the diurnal temperature range (Table 3.6 and Fig. 3.3b). Syria is notable for having more than 17% of the country affected by increased daytime land surface temperatures (Table 3.4) and an eighth of the country affected by both increased daytime and nighttime land surface temperatures (Table 3.8). While Syria's civil war has been attributed to climate change (Kelley et al. 2015) and the "Fertile Crescent" underwent an intense drought in 2007–2009 (Trigo et al. 2010), the linkage has been controversial (Kelley et al. 2017; Selby et al. 2017a, b). The changes in the thermal regime are clear, although the mechanism for their appearance is not clear in the eastern Mediterranean or elsewhere in the drylands of Greater Central Asia.

In an earlier trend analysis of Central Asia, de Beurs et al. (2015) used MOD11C2 V005 for 2000–2013 to evaluate the multiple trends, including positive and negative trends in LST_{day} and LST_{night} using a stricter significance threshold of $p < 0.01$. They

used equivalence testing to evaluate the influence of countries, major MODIS LCTs, and a grouping of anthropogenic biomes (anthromes) of Ellis and Ramankutty (2008) on thermal time trends. They found that Uzbekistan and Kazakhstan had equivalent areal proportions with increased LST_{day} (~10%) with another grouping of Turkmenistan, Kyrgyzstan, and Tajikistan with less than 5% of pixels exhibiting significantly increased daytime temperatures. While Kazakhstan had about 7% of its area showing increased LST_{night}, Uzbekistan had 3.5% of its pixels displaying increased nighttime temperatures, and the other three countries had less than 2%. In terms of equivalence, Kazakhstan was in one group, and Turkmenistan, Tajikistan, and Kyrgyzstan were in a second group, with Uzbekistan in both groups. Although these findings are not directly comparable with our results due to differences in data and methods, they are in general agreement.

3.6.3 Significant Thermal Trends Linked to Major LCTs

There is some evidence of linkages between the LCTs and the thermal trends in our results, particularly a positive linkage for grasslands and a negative linkage for croplands; however, the data are not compelling. In terms of increased LST_{day}, de Beurs et al. (2015) found shrublands and croplands with equivalent proportions (<4.5%) and grasslands and barren lands with equivalent proportions at more than twice the rate (<10.0%). In terms of increased LST_{night}, de Beurs et al. (2015) found two groupings with shrublands (<1.0%) forming one group and barren lands (4.6%) and grasslands (7.0%) forming the other, with croplands (3.2%) shared between them. Negative trends were very rare in LST_{night} (0.1%) and rare (<0.5%) in grasslands, barren lands, and croplands, with shrublands (2.7%) not considered in a separate group in terms of equivalence. Thermal time trends across the three anthrome aggregates – residential, populated, and remote – showed equivalence in every case.

One limitation of our analysis and that of de Beurs et al. (2015) is the mismatch in spatial scales between the finer grain of land cover composition and change and the coarser grain of atmospheric boundary layer processes. This limitation is a fundamental challenge common to the study of all land-atmosphere interactions. Analysis of the interannual variation in land surface phenology as a function of LCT instead of LCT directly may shed more light on why the thermal trends occur where they do.

A complementary approach could look at atmospheric teleconnections arising from climate oscillations to understand the spatial distribution of change patches. Although some studies have demonstrated the influence of climate modes on land surface processes (Chen et al. 2018; de Beurs and Henebry 2008; de Beurs et al. 2018; Hu et al. 2017; Kariyeva and van Leeuwen 2011, 2012; Kariyeva et al. 2012; Mariotti 2007; Wright et al. 2014), the temporal record of spaceborne observations is still short relative to the quasi-periodicity of major and regional climate oscillations.

3.7 Conclusions

We have been able to analyze time series of LST measurements to reveal important recent changes in the thermal regime across the vast region of drylands in Greater Central Asia. While these changes in warming, particularly at nighttime, are widespread, they are not evenly distributed in space. Some smaller political entities are disproportionally affected by the changes in land surface temperature. Urbanization is increasing rapidly across the drylands but it is still limited in extent (Fan et al. 2020). However, urbanized areas are at greater risk of deleterious health effects from warmer nights (Argüeso et al. 2015; Oleson et al. 2015).

While the possible and probable implications of these warming trends are outside the scope of this chapter, it is clear that there are significant implications for the water-energy-crop nexus (Qi et al. 2020; Abdullaev and Sokolik 2020), the use of grasslands for grazing (Kappas et al. 2020; Spaeth et al. 2020), and further changes in the climates across the drylands of Greater Central Asia (Groisman et al. 2018, 2020).

Acknowledgements This research was supported, in part, by NASA Science of Terra & Aqua project NNX14AJ32G entitled *Change in our MIDST: Detection and analysis of land surface dynamics in North and South America using multiple sensor datastreams*, by NASA's Land-Cover and Land-Use Change project NNX15AP81G entitled *How environmental change in Central Asian highlands impacts high elevation communities*, and by the Center for Global Change and Earth Observations at Michigan State University. Any opinions, findings, and conclusions or recommendations expressed in this paper are those of the authors and do not necessarily reflect the views of NASA.

References

Abdullaev SF, Sokolik IN (2020) Assessment of the influence of dust storms on the cotton production in Tajikistan. In: Gutman G et al (eds) Landscape dynamics of drylands across greater Central Asia: people, societies and ecosystems. Springer, Cham

Alemu WG, Henebry GM (2016) Characterizing cropland phenology in major grain production areas of Russia, Ukraine, and Kazakhstan by the synergistic use of passive microwave and visible to near infrared data. Remote Sens-Basel 8(12):1016

Alganci U, Ozdogan M, Sertel E, Ormeci C (2014) Estimating maize and cotton yield in southeastern Turkeywith integrated use of satellite images, meteorological data and digital photographs. Field Crop Res 157:8–19

Alward RD, Detling JK, Milchunas DG (1999) Grassland vegetation changes and nocturnal global warming. Science 283(5399):229–231

Anderson JR, Hardy EE, Roach JT, Witmer RE (1976) A land use and land cover classification system for use with remote sensor data: U.S. Geological Survey Professional Paper 964, 28 p

Argüeso D, Evans JP, Pitman AJ, Di Luca A (2015) Effects of city expansion on heat stress under climate change conditions. PLoS One 10(2):e0117066

Aslan ST, Gundogdu KS (2007) Mapping multi-year groundwater depth patterns from time-series analyses of seasonally lowest depth-to-groundwater maps in irrigation areas. Pol J Environ Stud 16(2):183–190

Boryan C, Yang Z, Mueller R, Craig M (2011) Monitoring US Agriculture: the US Department of Agriculture, National Agricultural Statistics Service, Cropland Data Layer Program. Geocarto Int 26(5):341–358

Bosworth J "An Anglo-Saxon Dictionary Online." Trendan. (ed) Thomas Northcote Toller and Others. Comp. Sean Christ and Ondřej Tichý. Faculty of Arts, Charles University in Prague, 24 Aug 2010a. Web. 28 June 2017. http://www.bosworthtoller.com/030992

Bosworth J "An Anglo-Saxon Dictionary Online." Trinda. (ed) Thomas Northcote Toller and Others. Comp. Sean Christ and Ondřej Tichý. Faculty of Arts, Charles University in Prague, 21 Mar 2010b. Web. 28 June 2017. http://www.bosworthtoller.com/031046

Braganza K, Karoly DJ, Arblaster JM (2004) Diurnal temperature range as an index of global climate change during the twentieth century. Geophys Rese Lett 31(13)

Brovelli M, Molinari M, Hussein E et al (2015) The first comprehensive accuracy assessment of GlobeLand30 at a national level: Methodology and results. Remote Sens-Basel 7(4):4191–4212

Brown de Colstoun EC, Story MH et al (2003) National Park vegetation mapping using multitemporal Landsat 7 data and a decision tree classifier. Remote Sens Environ 85(3):316–327

Büttner G, Feranec J, Jaffrain G et al (2004) The CORINE land cover 2000 project. EARSeL eProceedings 3(3):331–346

Chen J, Chen J, Liao A et al (2015) Global land cover mapping at 30 m resolution: A POK-based operational approach. ISPRS J Photogramm 103:7–27

Chen X, Wang S, Hu Z et al (2018) Spatiotemporal characteristics of seasonal precipitation and their relationships with ENSO in Central Asia during 1901–2013. J Geogr Sci 28(9):1341–1368

Chen J, Ouyang Z, John R et al (2020) Social-ecological systems across the Eurasian drylands. In: Gutman G et al (eds) Landscape dynamics of drylands across greater Central Asia: people, societies and ecosystems. Springer, Cham

Chymyrov A, Betz F, Baibagyshov E et al (2018) Floodplain forest mapping with sentinel-2 imagery: case study of Naryn River, Kyrgyzstan. In: Vegetation of Central Asia and Environs. Springer, Cham, pp 335–347

Dai A, Trenberth KE, Karl TR (1999) Effects of clouds, soil moisture, precipitation, and water vapor on diurnal temperature range. J Clim 12(8):2451–2473

de Beurs KM, Henebry GM (2004) Trend analysis of the Pathfinder AVHRR Land (PAL) NDVI data for the deserts of Central Asia. IEEE Geosci Remote S 1(4):282–286

de Beurs KM, Henebry GM (2008) Northern annular mode effects on the land surface phenologies of northern Eurasia. J Clim 21(17):4257–4279

de Beurs KM, Henebry GM (2013) Vegetation phenology in global change studies. In: Phenology: an integrative environmental science. Springer, Dordrecht, pp 483–502

de Beurs KM, Wright CK, Henebry GM (2009) Dual scale trend analysis for evaluating climatic and anthropogenic effects on the vegetated land surface in Russia and Kazakhstan. Environ Res Lett 4(4):045012

de Beurs KM, Henebry GM, Owsley BC, Sokolik I (2015) Using multiple remote sensing perspectives to identify and attribute land surface dynamics in Central Asia 2001–2013. Remote Sens Environ 170:48–61

de Beurs KM, Henebry GM, Owsley B, Sokolik IN (2018) Large scale climate oscillation impacts on temperature, precipitation and land surface phenology in Central Asia. Environ Res Lett 13(6):065018

Ellis EC, Ramankutty N (2008) Putting people in the map: Anthropogenic biomes of the world. Front Ecol Environ 6(8):439–447

Fan P, Ouyang Z, Chen J et al (2020) Population and urban dynamics in drylands of China. In: Gutman G et al (eds) Landscape dynamics of drylands across greater Central Asia: people, societies and ecosystems. Springer, Cham

Feranec J, Jaffrain G, Soukup T, Hazeu G (2010) Determining changes and flows in European landscapes 1990–2000 using CORINE land cover data. Appl Geogr 30(1):19–35

Friis C, Nielsen JØ, Otero I et al (2016) From teleconnection to telecoupling: taking stock of an emerging framework in land system science. J Land Use Sci 11(2):131–153
Gallo KP, Owen TW, Easterling DR, Jamason PF (1999) Temperature trends of the US historical climatology network based on satellite-designated land use/land cover. J Clim 12(5):1344–1348
Groisman P, Bulygina O, Henebry G et al (2018) Dryland belt of Northern Eurasia: contemporary environmental changes and their consequences. Environ Res Lett 13(11):115008
Groisman PY, Bulygina ON, Henebry GM et al (2020) Eurasian drylands: contemporary environmental changes. In: Gutman G et al (eds) Landscape dynamics of drylands across greater Central Asia: people, societies and ecosystems. Springer, Cham
Henebry GM (2019) Methodology II: remote sensing of change in grasslands. In: Gibson DJ, Newman J, (eds) Grasslands and climate change. Cambridge University Press, pp 40–64
Henebry GM, de Beurs KM, Wright CK, John R et al (2013) Dryland East Asia in hemispheric context. In: Chen J, Wan S, Henebry G, Qi J, Gutman G, Sun G, Kappas M (eds) Dryland East Asia: land dynamics amid social and climate change. HEP/De Gruyter, Berlin, pp 23–44
Henebry GM, Chen J, Gutman G, Kappas M (2020) Multiple perspectives on drylands across Greater Central Asia. In: Gutman G et al (eds) Landscape dynamics of drylands across greater Central Asia: people, societies and ecosystems. Springer, Cham
Hijioka Y, Lin E, Pereira JJ et al (2014) Asia. In: Climate change 2014 – impacts, adaptation and vulnerability: part B: regional aspects: Working Group II Contribution to the IPCC fifth assessment report. Cambridge University Press, Cambridge, pp 1327–1370
Homer C, Dewitz J, Fry J et al (2007) Completion of the 2001 national land cover database for the conterminous United States. Photogramm Eng Remote Sensing 73(4):337
Homer C, Dewitz J, Yang L et al (2015) Completion of the 2011 National Land Cover Database for the conterminous United States–representing a decade of land cover change information. Photogramm Eng Rem S 81(5):345–354
Hu Z, Zhou Q, Chen X, Qian C et al (2017) Variations and changes of annual precipitation in Central Asia over the last century. Int J Climatol 37:157–170
Johnson DM, Mueller R (2010) The 2009 Cropland data layer. Photogramm Eng Rem S 76(11):1201–1205
Kappas M, Degener J, Klinge M, Vitkovskaya I et al (2020) A conceptual framework for ecosystem stewardship based on landscape dynamics: case studies from Kazakhstan and Mongolia. In: Gutman G et al (eds) Landscape dynamics of drylands across greater Central Asia: people, societies and ecosystems. Springer, Cham
Kariyeva J and van Leeuwen W (2011) Environmental drivers of NDVI-based vegetation dynamics in Central Asia. Remote Sens-Basel 3(2):203–246
Kariyeva J and van Leeuwen W (2012) Phenological dynamics of irrigated and natural drylands in Central Asia before and after the USSR collapse. Agric Ecosyst Environ 162:77–89
Kariyeva J, van Leeuwen W and Woodhouse C (2012) Impacts of climate gradients on the vegetation phenology of major land use types in Central Asia (1981–2008). Front Earth Sci 6(2): 206–225
Karl TR, Jones PD, Knight RW et al (1993) A new perspective on recent global warming: asymmetric trends of daily maximum and minimum temperature. Bull Am Meteorol Soc 74(6):1007–1024
Kelley CP, Mohtadi S, Cane MA et al (2015) Climate change in the Fertile Crescent and implications of the recent Syrian drought. Proc Natl Acad Sci 112(11):3241–3246
Kelley C, Mohtadi S, Cane M et al (2017) Commentary on the Syria case: Climate as a contributing factor. Polit Geogr 30:1–3
Laiskhanov SU, Otarov A, Savin IY et al (2016) Dynamics of soil salinity in irrigation areas in South Kazakhstan. Pol J Environ Stud 25(6):2649–2475
Liu J, Hull V, Moran E, Nagendra H et al (2014) Applications of the telecoupling framework to land-change science. In: Rethinking global land use in an urban era. MIT Press, Cambridge, MA, pp 119–140

Loveland TR, Merchant JW, Ohlen DO, Brown JF (1991) Development of a land-cover characteristics database for the conterminous US. Photogramm Eng Remote Sensing 57(11):1453–1463
Loveland TR, Reed BC, Brown JF et al (2000) Development of a global land cover characteristics database and IGBP DISCover from 1 km AVHRR data. Int J Remote Sens 21(6–7):1303–1330
Mariotti A (2007) How ENSO impacts precipitation in southwest central Asia. Geophys Res Lett 34(16)
Meyfroidt P, Lambin EF (2009) Forest transition in Vietnam and displacement of deforestation abroad. Proc Natl Acad Sci 106(38):16139–16144
Meyfroidt P, Rudel TK, Lambin EF (2010) Forest transitions, trade, and the global displacement of land use. Proc Natl Acad Sci 107(49):20917–20922
Oleson KW, Monaghan A, Wilhelmi O et al (2015) Interactions between urbanization, heat stress, and climate change. Clim Chang 129(3–4):525–541
Ozdogan M, Salvucci GD (2004) Irrigation-induced changes in potential evapotranspiration in southeastern Turkey: Test and application of Bouchet's complementary hypothesis. Water Resour Res 40(4)
Peng S, Piao S, Ciais P et al (2013) Asymmetric effects of daytime and night-time warming on Northern Hemisphere vegetation. Nature 501(7465):88–92
Prasad PVV, Pisipati SR, Ristic Z et al (2008) Impact of nighttime temperature on physiology and growth of spring wheat. Crop Sci 48(6):2372–2380
Qi J, Kulmatov R, Bubochova T et al (2020) The complexity and challenges of water-energy-food systems in Central Asia. In: Gutman G et al (eds) Landscape dynamics of drylands across greater Central Asia: people, societies and ecosystems. Springer, Cham
Reyer CP, Otto IM, Adams S et al (2017) Climate change impacts in Central Asia and their implications for development. Reg Environ Chang 17(6):1639–1650
Selby J, Dahi OS, Fröhlich C, Hulme M (2017a) Climate change and the Syrian civil war revisited. Polit Geogr 60:232–244
Selby J, Dahi O, Fröhlich C, Hulme M (2017b) Climate change and the Syrian civil war revisited: A rejoinder. Polit Geogr 60:253–255
Sillmann J, Kharin VV, Zwiers FW et al (2013) Climate extremes indices in the CMIP5 multimodel ensemble: part 2. Future climate projections. J Geophys Res-Atmos 118(6):2473–2493
Spaeth KE, Weltz MA, Guertin DP et al (2020) Hydrology and erosion risk parameters for grasslands in Central Asia. In: Gutman G et al (eds) Landscape dynamics of drylands across greater Central Asia: people, societies and ecosystems. Springer, Cham
Still CJ, Pau S, Edwards EJ (2014) Land surface skin temperature captures thermal environments of C3 and C4 grasses. Glob Ecol Biogeogr 23(3):286–296
Sulla-Menashe D, Gray JM, Abercrombie SP, Friedl MA (2019) Hierarchical mapping of annual global land cover 2001 to present: the MODIS Collection 6 Land Cover product. Remote Sens Environ 222:183–194
Sun D, Pinker RT and Kafatos M (2006a) Diurnal temperature range over the United States: a satellite view. Geophys Res Lett 33(5)
Sun D, Kafatos M, Pinker RT, Easterling DR (2006b) Seasonal variations in diurnal temperature range from satellites and surface observations. IEEE Trans Geosci Remote Sens 44(10):2779–2785
Sun B, Chen X, Zhou Q (2016) Uncertainty assessment of GlobeLand30 land cover data set over central Asia. Int Arch Photogramm Remote Sens Spat Inf Sci 8:1313–1317
Sun J, Tong YX, Liu J (2017) Telecoupled land-use changes in distant countries. J Integr Agric 16(2):368–376
"tend, v.2". OED Online. 2017. Oxford University Press. http://www.oed.com/view/Entry/199030?rskey=QWVvbI&result=4&isAdvanced=false. Accessed 28 June 2017
"trend, v.". OED Online. 2017. Oxford University Press. http://www.oed.com/view/Entry/205545?result=1&rskey=RCbYG6&. Accessed 28 June 2017

Trigo RM, Gouveia CM, Barriopedro D (2010) The intense 2007–2009 drought in the Fertile Crescent: impacts and associated atmospheric circulation. Agric For Meteorol 150(9):1245–1257

Vogelmann JE, Howard SM, Yang L et al (2001) Completion of the 1990s National Land Cover Data Set for the conterminous United States from Landsat Thematic Mapper data and ancillary data sources. Photogramm Eng Remote Sensing 67(6)

Wan S, Xia J, Liu W, Niu S (2009) Photosynthetic overcompensation under nocturnal warming enhances grassland carbon sequestration. Ecology 90(10):2700–2710

Wang Y, Zhang J, Liu D et al (2018) Accuracy assessment of GlobeLand30 2010 land cover over China based on geographically and categorically stratified validation sample data. Remote Sens 10(8):1213

Wickham JD, Stehman SV, Gass L et al (2013) Accuracy assessment of NLCD 2006 land cover and impervious surface. Remote Sens Environ 130:294–304

Wickham J, Stehman SV, Gass L et al (2017) Thematic accuracy assessment of the 2011 national land cover database (NLCD). Remote Sens Environ 191:328–341

Wright CK, de Beurs KM, Akhmadieva ZK et al (2009) Reanalysis data underestimate significant changes in growing season weather in Kazakhstan. Environ Res Lett 4(4):045020

Wright CK, de Beurs KM and Henebry GM (2012) Combined analysis of land cover change and NDVI trends in the Northern Eurasian grain belt. Front Earth Science 6(2):177–187

Wright CK, de Beurs KM, Henebry GM (2014) Land surface anomalies preceding the 2010 Russian heat wave and a link to the North Atlantic oscillation. Environ Res Lett 9(12):124015

Xia J, Han Y, Zhang Z, Wan S (2009) Effects of diurnal warming on soil respiration are not equal to the summed effects of day and night warming in a temperate steppe. Biogeosciences 6(8):1361–1370

Xia J, Chen J, Piao S et al (2014) Terrestrial carbon cycle affected by non-uniform climate warming. Nat Geosci 7(3):173–180

Yu X, Zhao Y, Ma X et al (2018) Projected changes in the annual cycle of precipitation over central Asia by CMIP5 models. Int J Climatol 38(15):5589–5604

Zhang N, Xia J, Yu X et al (2011) Soil microbial community changes and their linkages with ecosystem carbon exchange under asymmetrically diurnal warming. Soil Biol Biochem 43(10):2053–2059

Zhang M, Chen Y, Shen Y, Li B (2019) Tracking climate change in Central Asia through temperature and precipitation extremes. J Geogr Sci 29(1):3–28

Chapter 4
Quantifying the Anthropogenic Signature in Drylands of Central Asia and Its Impact on Water Scarcity and Dust Emissions

Irina N. Sokolik, Alexander I. Shiklomanov, Xin Xi, Kirsten M. de Beurs, and Viatcheslav V. Tatarskii

4.1 Introduction: Anthropogenic Dust Assessments

Humans cause different impacts to the environment of Central Asia by modifying the water body and the land use which in turn resulted in emission of dust, known as the anthropogenic dust. The importance of anthropogenic impact to the global dust cycle has been increasingly recognized. However, it remains highly uncertain how much of the total dust emission or burden can be attributed to human activities in the atmospheric circulation and land surfaces (Tegen and Fung 1995; Sokolik and Toon 1996; Prospero et al. 2002; Mahowald and Luo 2003; Ginoux et al. 2012). Past estimates of the anthropogenic proportion of global dust vary from less than 10% to over 60% (Tegen and Fung 1995; Tegen et al. 2004; Mahowald and Luo 2003;

I. N. Sokolik (✉) · V. V. Tatarskii
School of Earth and Atmospheric Sciences, Georgia Institute of Technology, Atlanta, GA, USA
e-mail: isokolik@eas.gatech.edu; vvt@eas.gatech.edu

A. I. Shiklomanov
Earth Systems Research Center, University of New Hampshire, Durham, NH, USA
e-mail: alex.shiklomanov@unh.edu

X. Xi
Department of Geological and Mining Engineering and Sciences, Michigan Technological University, Houghton, MI, USA

K. M. de Beurs
Department of Geography and Environmental Sustainability, University of Oklahoma, Norman, OK, USA
e-mail: kdebeurs@ou.edu

G. Gutman et al. (eds.), *Landscape Dynamics of Drylands across Greater Central Asia: People, Societies and Ecosystems*, Landscape Series 17,
https://doi.org/10.1007/978-3-030-30742-4_4

Ginoux et al. 2012; Stanelle et al. 2014). There are a number of reasons for such large uncertainties (Xi and Sokolik 2016). Firstly, there is no consensus on the definition of anthropogenic dust that has been used by the scientific community. There is a number of human activities that can directly or indirectly contribute to dust emission, such as agricultural practices over croplands and pasture, industrial and transportation activities, desiccation of rivers and lakes, and changes of precipitation and atmospheric circulation (Zender et al. 2004). Past studies considered various anthropogenic processes. Whether or not a dust source should be classified natural or anthropogenic depends on the time scope of the study. Secondly, there exist large differences in the model estimates of the magnitude of dust emissions, with even larger differences in the spatiotemporal distributions (Huneeus et al. 2011).

The representation of dust sources and model treatments of dust emission processes are the main sources of model errors (Knippertz and Todd 2012). In addition, the models represent only some mechanisms that control the complex dust emission. Various challenges are involved in separating natural and anthropogenic dust source areas. Satellite observations of land and vegetation properties have been widely used to characterize the extent and severity of land degradation (Le et al. 2016). Given that increased wind erosion is a direct sign of the desertification, land degradation maps provide useful information for locating potential human-made dust source areas (Zhang et al. 2003). The assignment of land degradation to human disturbance, meanwhile, is difficult because of various confounding factors from rainfall and soil moisture variations, vegetation phenology, and land management practices (Le et al. 2016). Instead, most relevant studies to date used global gridded agricultural fraction data to identify dust source areas that are caused by cultivation and livestock grazing (*e.g.* Tegen et al. 2004; Ginoux et al. 2012). Fourth, it remains controversial on how to treat anthropogenic dust sources in models. Tegen et al. (2004) suggested to reduce the erosion threshold velocity for cultivated soils, assuming that human disturbances make the soil more susceptible to erosion. In contrast, Ginoux et al. (2012) and Stanelle et al. (2014) increased the threshold velocity for croplands in order to account for the effects of soil conservation practices. These practices are generally part of model tuning to maximize the agreement between models and observations.

Significant cases of land degradations have occurred in Central Asia in the past century. Under the Soviet Union agricultural collectivization, Central Asia has experienced the expansion of cultivation and irrigation of the virgin lands from the early 1950s (Xi 2014; Kappas et al. 2020, Chap. 9). The Virgin Lands Campaign (1954–1960) has resulted into conversion of large areas of natural steppe into farmlands. These actions have caused severe wind erosion and catastrophic dust bowls due to the monoculture farming practice (Stringer 2008). The degraded lands were abandoned as a result, while more lands that are new were reclaimed. In addition, the nomadic pastoralism practices have been replaced by state and collective farms. The pasture lands have been grazed by an increasing large number of the livestock above the carrying capacity, year-round without migration. This has led to the depletion of the vegetation cover and upper soil layers, making the soil vulnerable to the

wind erosion (Gintzburger et al. 2005; Robinson et al. 2003). Following the collapse of Soviet Union, the production of cereal and grain underwent significant declines (Lioubimtseva and Henebry 2009; de Beurs and Henebry 2004). The livestock production system crashed and resulted in very steep declines in the livestock numbers and a slow recovery of the degraded pasture lands (Gintzburger et al. 2005; Wilson 1997).

The spatial distribution of cropland and pasture fractions and their annual changes from the 1950s and 2010s are shown in Fig. 4.1. We used the agricultural data from the Land Use Harmonization project (hereafter as LUH dataset, http://luh.umd.edu/). This dataset includes annual cropland and pasture fractions for the period of 1700–2005 at 0.5° × 0.5° spatial resolutions (Hurtt et al. 2011, 2006). A dry (or rainfed) crop belt of wheat and barley spreads eastward from Ukraine to the Ural Mountains and eastern Siberia, and southward to the Volga valley and northern Caucasus (Fig. 4.1) (Kappas et al. 2020, Chap. 9). The desert and steppe landscapes are being used as pasture lands, including the semi-arid steppe, shrublands and mountainous rangelands (Gintzburger et al. 2005). Irrigated croplands (*e.g.*, cotton, rice) are mainly located in loess deposits and river deltas of southern and southeastern mountains. Figure 4.1b shows the increasing cropland fraction from 10% in 1950 to 14% in 1960, likely due to cultivation of virgin lands. The fraction of cropland remains nearly constant until 1990. The cropland fraction has decreased after

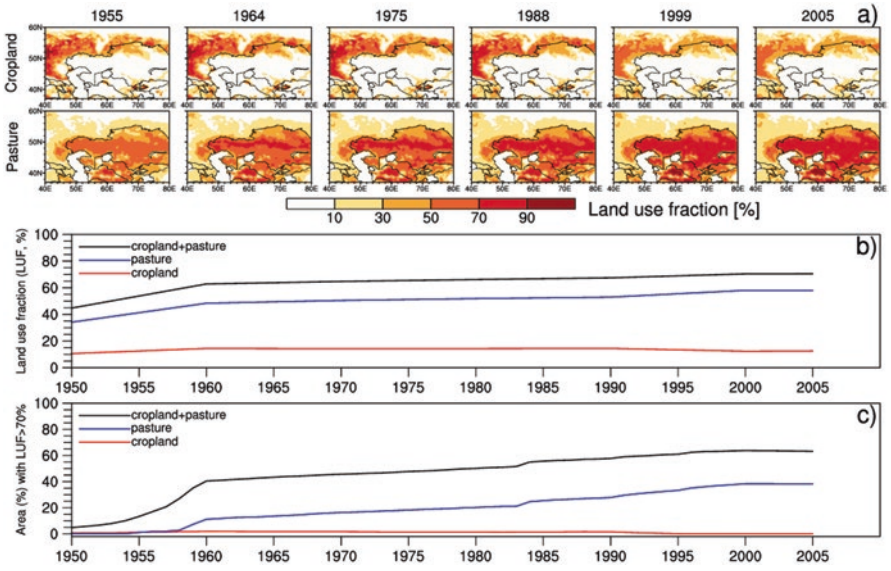

Fig. 4.1 (**a**) For selected years, shown are annual cropland and pasture fractions from the LUH dataset; (**b**) domain-average annual land-use fractions of cropland, pasture, and their sum (cropland+pasture), and (**c**) the percentage of land area with cropland plus pasture land-use fractions larger than 70%. (From Xi 2014)

1990, likely due to the Soviet Union collapse. In comparison, the pasture fraction has monotonically increased from 34% in 1950 to 48% in 1960 and to 58% in 2005. This indicates that the pasture fraction simply represents the fraction of the land area used for grazing, which does not reflect the decreasing trend of the grazing intensity following the Soviet Union collapse (Chen et al. 2020, Chap. 10). The cropland and pasture combined accounts for 45% of the total land surface in 1950 and 70% in 2005. Less than 2% of the total land area has a cropland fraction higher than 70%, whereas there are a lot more land areas that were mostly (fraction >70%) used as grazing lands.

Figure 4.2 shows the Landsat images for regional inland water bodies, illustrating significant water level variations in Central Asia (Le et al. 2016). As part of the agricultural collectivism policy, large-scale irrigation systems have been built to increase the soil fertility. As a result, the diversion of water from Amu Darya and Syr Darya caused the persistent shrinkage of the Aral Sea since the 1960s (Micklin 2007). By 2006, the Aral Sea has diminished by 90% in volume and 74% in area. The Aral Sea was separated into two parts in 1987: a small North Sea and a large south sea. The south Aral Sea includes a deep western basin and a shallow eastern basin with a narrow channel connecting them. The eastern basin suffered rapid desiccation in the last few years and became completely dry in 2014. The exposed sea bottom is a well-known dust source and is often referred to as Aralkum (Micklin

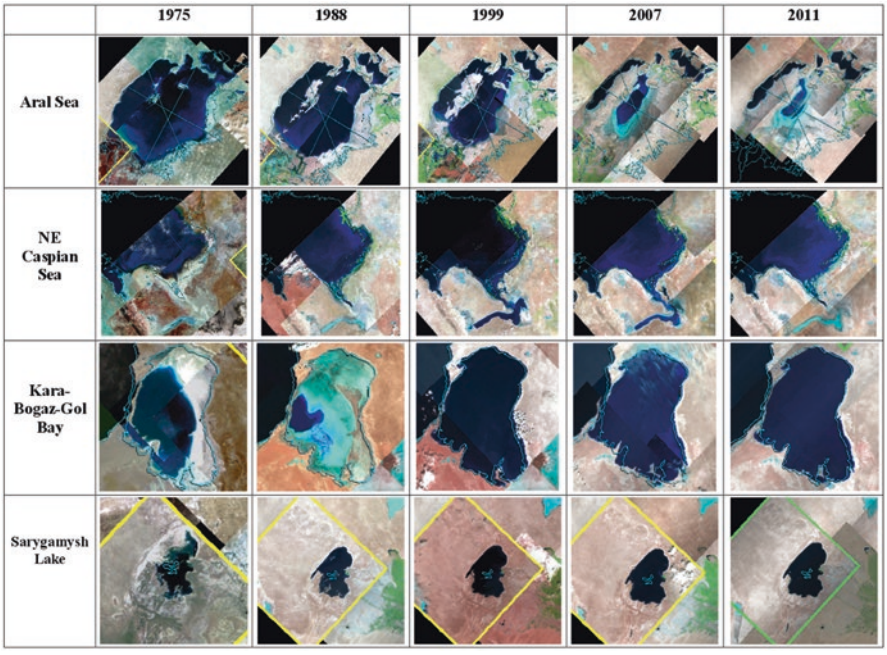

Fig. 4.2 Landsat images of surface water body changes. Shown are images for selected years (1975, 1988, 1999, 2007, and 2011). (From Xi 2014)

2007). The water level fluctuations of Caspian Sea has led to the drying (*e.g.*, 1975, 1988 and 2011) and inundation (*e.g.*, 1999, 2007) of the shallow northeast shoals (Kravtsova and Lukyanova 2000). As a result, the northeast Caspian coast turned into a dry solonchak desert which is undergoing wind erosion. A dam has been built in 1980 to block the water flow from Caspian Sea to the Kara-Bogaz-Gol bay, resulting in a dry salt flat prone to wind erosion *(*Leroy et al. 2006; Varushchenko et al. 2000). The Kara-Bogaz-Gol bay began to refill with water after the dam has been destroyed in 1992. In turn, the Sarygamysh Lake located to the southwest of Amu Darya has been progressively increasing in size due to the drainage water.

The land-use changes in Central Asia (*e.g.*, agriculture and water body) have significant consequence to the region's dust emission, due to their impacts on the regional climate and land surface properties (Groisman et al. 2018). We developed a regional dust model system WRF-Chem-DuMo by employing the community Weather Research and Forecasting with chemistry (WRF-Chem) model. This modeling system enable us to examine the relationship between dust, climate, and land-cover/land-use change (Sokolik et al. 2013; Darmenova et al. 2009; Xi and Sokolik 2015). In WRF-Chem-DuMo model, the land surface is represented by a discrete number of dominant land cover (DLC) types. The DLC is defined as the land type in each grid cell with the largest fraction based on the 24-category US Geological Survey (USGS) Global Land Cover Characteristics Database (hereinafter USGS24). The USGS24 dataset is developed from the 1-year (April 1992–March 1993) Advanced Very High Resolution Radiometer NDVI data (Eidenshink and Faundeen 1994). Figure 4.3a shows that USGS24 mainly focuses on natural land types with no categories dedicated for agriculture, but instead use the mosaic classes of cropland and pasture. Because of its static nature, the data set has major representation errors of the present-day areal extent of Aral Sea and the shallow lagoon of Caspian

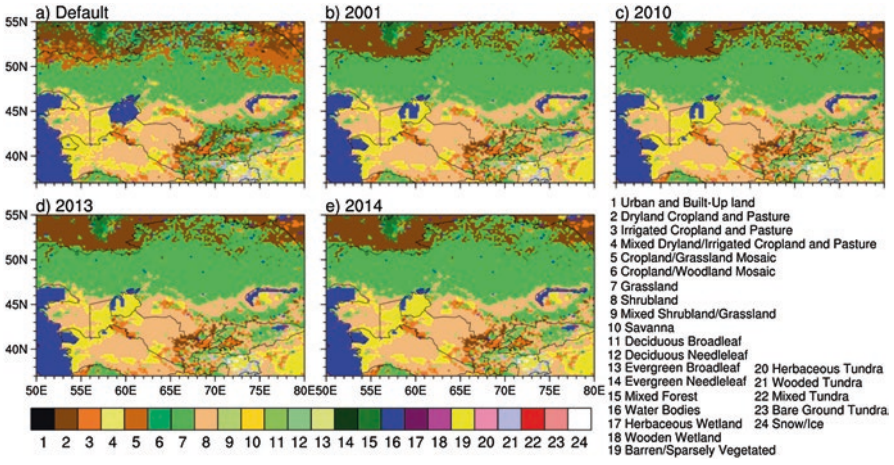

Fig. 4.3 (**a**) The default dominant land cover map in WRF-Chem-DuMo and (**b**–**e**) modifications for dust emission simulations (only 4 years are shown). (From Xi and Sokolik 2015)

Sea, the Kara-Bogaz-Gol (KBG) gulf (Xi and Sokolik 2016). The Aral Sea is incorrectly treated as a full lake, while the KBG gulf as a barren area. The KBG gulf was completely dry when a dam was built in 1980 to block water flow from the Caspian Sea. The dam was demolished in 1992, and after that the KBG gulf was refilled with water. As a result, the USGS24 data set needs to be modified to account for the changes in the land/water mask.

Here the LUH agricultural fraction data are used to reconstruct the spatial distribution of cropland and pasture in the USGS24 data set. The dust emission potential of the cropland and pasture lands depends on the threshold velocity as a function of the surface roughness properties and soil moisture. In the USGS24 DLC map, the cropland is presented as categories #2 "Dryland Cropland and Pasture" (hereafter referred to as CAT2) and #3 "Irrigated Cropland and Pasture" (CAT3), while pasture is represented by categories #7 "Grassland" (CAT7) and #8 "Shrubland" (CAT8). We modified the USGS24 cropland distribution based on the LUH cropland fraction. By considering all grid cells, the fraction of CAT2 or CAT3, depending on whether the grid is rainfed or irrigated cropland, is replaced by the LUH cropland fraction if the LUH cropland fraction is found to be larger than the CAT2 or CAT3 fraction (Xi and Sokolik 2015). Similarly, the fraction of CAT7 or CAT8 in each grid cell, depending on whether the grid is located north or south of 45°N, is replaced by the LUH pasture fraction, if the latter is found to be larger. Then, the fraction of the DLC type in each grid is subtracted to ensure that the fractions of all land types sum to 100%. Finally, a new DLC map is recomputed from the modified USGS24 land fractions. To correct the land/water mask, we modify the DLC type of the dried Aral Sea to "Barren/Sparsely Vegetated", and the soil texture to "Silty Clay Loam". We also modify the DLC type to "Water Bodies" in the KBG grid cells to reflect the restoration of KBG gulf. By modifying the cropland and pasture distributions and land/water mask, we are able to reconstruct the up-to-date USGS DLC maps. Figure 4.3 shows reconstructions for selected years (Table 4.1).

Our reconstructions include soil erosion at marginal lands under the Khrushchev's virgin lands program, soil salinization due to excessive irrigation and poor drainage in cotton monoculture, desiccation of the Aral Sea, overgrazing of rangelands, abandonment of cultivated lands, and rehabilitation of overgrazed rangelands during the post-Soviet era (Gupta et al. 2009). Additionally, the region has experienced

Table 4.1 List of modelling experiments, indicating the abbreviated name of the experiment, dust seasons considered, the dust scheme used, soil size distribution used in the modeling, and wind used as a threshold value

Experiment	Dust seasons	Dust source function	Dust scheme	Soil size distribution	Wind
MB_Dry	2000–2014	–	MB	Dry-sieved	u_*
MB_Wet	2000–2014	–	MB	Soil texture	u_*
Shao_Dry	2000–2014	–	Shao	Dry-sieved	u_*
TF_Sta	2000–2014	Static	TF	–	u_{10}
TF_Dyn	2000–2008	Dynamic	TF	–	u_{10}

significant warming, but mixed changes occurred in precipitation with large impacts on the region's glacier mass balance, streamflow, and agricultural production (Gupta et al. 2009; Lioubimtseva and Cole 2006). Although the enhanced wind erosion due to land-use activities in Central Asia is well documented (*e.g.* Orlovsky and Orlovsky 2002; Stringer 2008), there have been no quantitative assessments on its impacts on dust emission in the region.

Using the reconstructed land cover maps from multiple years (2000 to 2014), we conducted model simulations by employing the WRF-Chem-DuMo model to determine the contribution of direct land-use disturbance in agriculture and surface water bodies to the dust emission in Central Asia. We consider three dust emission schemes (including two physically based and one simplified), two soil size distributions, and two preferential dust source functions that for the five model experiments. Figure 4.4 shows the mapping of potential anthropogenic dust sources using four land use index (LUI) thresholds (80%, 85%, 90%, and 95%) at 1° × 1° grid resolution, as

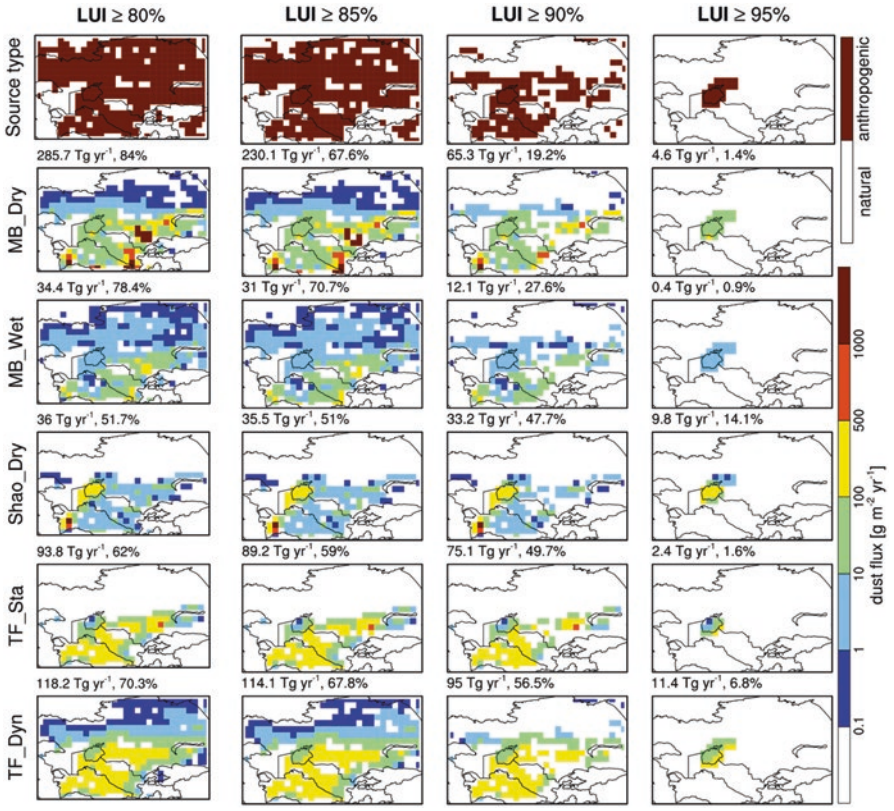

Fig. 4.4 Identification of anthropogenic dust source areas at 1° × 1° grid resolution based on four LUI thresholds (80%, 85%, 90%, and 95%) and the corresponding anthropogenic dust fluxes based on MB_Dry, MB_Wet, Shao_Dry, TF_Sta, and TF_Dyn experiments. The domain-integrated annual anthropogenic dust fluxes (Tg year) and proportions (%) are also shown. (From Xi and Sokolik 2016)

well as the estimated anthropogenic dust fluxes based on the MB_Dry, MB_Wet, and Shao Dry experiments (Xi and Sokolik 2016). The majority of land surfaces are mapped as anthropogenic sources when using LUI thresholds of 80% and 85%. The source area is significantly reduced using a threshold of 90%, which covers an area of the semiarid steppe belt, Karakum and Kyzylkum deserts, and Aralkum. Aralkum becomes the only anthropogenic source when using a threshold of 95%. Based on long-term (1981–2006) satellite NDVI data, Le et al. (2016) found that Central Asian countries were subject to varying extent of land degradation (*e.g.*, 8% of the total land area in Turkmenistan and Uzbekistan, 60% in Kazakhstan). They identified several land degradation hotspots over croplands and grazing lands located in north Kazakhstan, northwest Tajikistan, and south Uzbekistan and Turkmenistan (see also Chen et al. 2020, Chap. 10). These hotspots are consistent with the anthropogenic source areas derived using the 90% LUI threshold, although the dust source areas are shifted toward grazing lands that have a higher LUI than croplands. Nevertheless, we consider the LUI threshold of 90% to offer a reasonable estimate of the anthropogenic dust source area in Central Asia. Based on five model experiments, 18.3–56.5% dust emission can be considered anthropogenic in Central Asia with an optimal LUI threshold of 90%. On the other hand, for the LUI threshold in the range of 85–90%, the ADP shows significant variations in the MB scheme (18.3–70.2%), but small changes in the Shao (32.8–48.1%) and TF (49.7–67.8%) schemes. Clearly, the different dust emission parameterizations not only cause a wide spread in the estimated anthropogenic dust proportions, but they are also responsible for the varying sensitivities of anthropogenic dust to the LUI threshold.

We detected a large model disparity from the five experiments considered in: (1) the estimated anthropogenic proportion of total dust emissions that ranged from 18.3% to 56.5%, (2) the spatial distribution of anthropogenic dust, (3) the sensitivity of anthropogenic dust to land-use intensity in separating natural and human-made source areas (Fig. 4.5), and (4) the relative importance of agriculture versus the

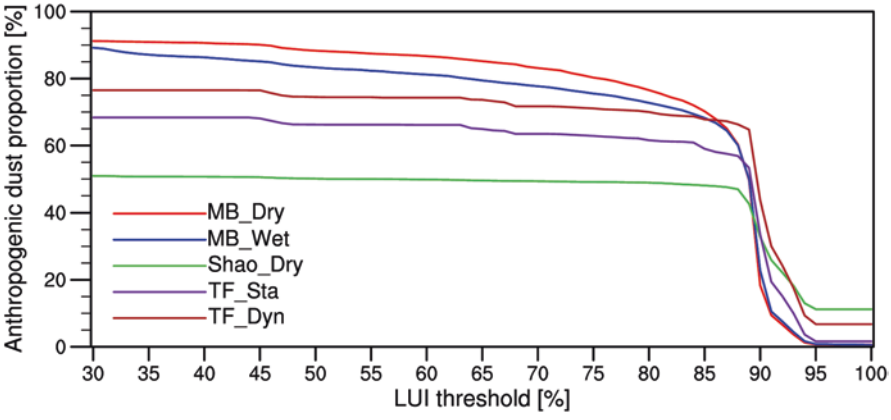

Fig. 4.5 The anthropogenic dust proportion as a function of the LUI threshold. (After Xi and Sokolik 2016)

desiccation of Aral Sea to the region's dust emission. We conclude that the parameterization of the model with erosion thresholds, particularly the vegetation effect on the threshold friction velocity, is a key source of model uncertainty in quantifying the contribution of human land use to dust emission. All model experiments show a negative trend in the anthropogenic dust proportion from 2000 to 2014, despite the continuous drying of Aral Sea that leads to enhanced dust activity in recent years. The decreasing trend points out to a shift of the dust emission toward natural source areas. Our model experiments also reveal consistent responses of anthropogenic dust to land-cover changes. We found that anthropogenic dust increases in response to the gain in the land type of open shrublands and decreases in response to the losses in grasslands and barren/sparsely vegetated. The overall resulting effect is a net decrease in the anthropogenic dust associated with land-cover changes over agricultural lands. In addition to the impacts of land-cover changes on dust emission, dust may also alter land cover by modifying the atmospheric radiation that affects the vegetation growth, and deposition processes, highlighting the need for an integrated understanding of human-dust-ecosystem interactions (*e.g.* Xi and Sokolik 2012; Farmer 1993).

4.2 Reconstruction of the Human Growth in the Region

World Bank (2017) reported a growth in more than 5000 cities in Eastern Europe and Central Asia in understanding city growth or decline (Restrepo Cadavid et al. 2017). The World Bank report included cities in Kazakhstan, Kyrgyzstan, Uzbekistan and Tajikistan, but most of the figures and graphs did not explicitly focus on these four countries. Here, we used the data from the World Bank report to explicitly investigate the urban growth in these four countries within our study area. We first investigated the urban growth between 1989 and 1999/2000; the population data is reported for slightly different years in these four countries. No population data for Tajikistan was available for the earliest time period (*i.e.*, no cities in this country in Fig. 4.6). We found that between 1989 and 1999/2000 most cities in Kazakhstan (51/73) declined in population, while the major hubs of Astana in the north and Almaty in the south experienced urban growth. Kyrgyzstan experienced a population decline in two thirds of its cities (18/27 cities). The situation appears very different in Uzbekistan, where a decline in the cities was only 10% (12/118).

During 1999/2000–2014, most cities in the study area grew (213/257), including Tajikistan (Fig. 4.7) and 88% growth in Uzbekistan. Kyrgyzstan and Kazakhstan cities also grew by 57% and 78%, respectively. While there is no data available for the first period in Tajikistan, there is data for this second period, which shows that 95% of the cities in Tajikistan grew between 2000 and 2014.

While increasing urban population is an indicator of growth, nightlight images can also illuminate human impact in a country. We downloaded the annual data for the years 1991, 2000 and 2013 from the version 4 DMSP OLS Nighttime Lights Time Series (NOAA Geophysical Data Center, 2018). This product presents persis-

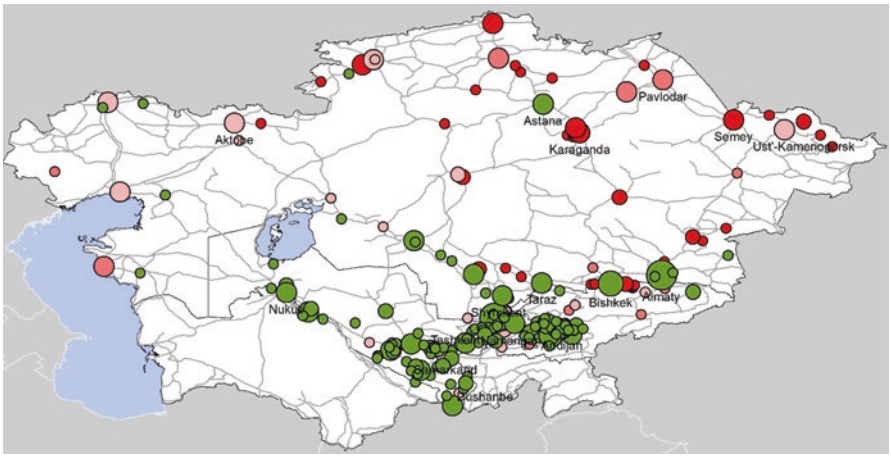

Fig. 4.6 City size based based on the data from 1999/2000, change from 1989 to 1999

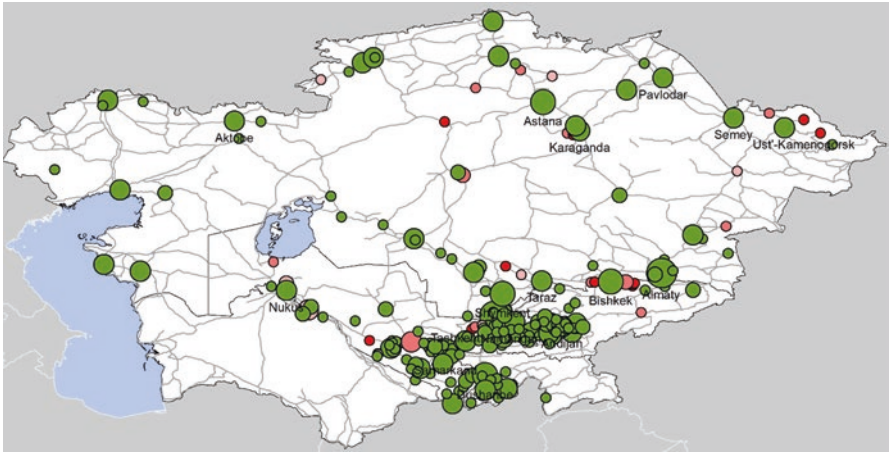

Fig. 4.7 City size based on data from 2014, change from 1999/2000 to 2014

tent lighting from cities, towns and other sites with background noise removed. The nightlight data shows that only a small portion of the land is lit at night in Central Asia, but rising from 4.5% in 1991 to 6.6% in 2013. It is interesting to note that the lit area grew in all countries between 1991 and 2000 in Central Asian countries, but between 2000 and 2013 both Tajikistan and Uzbekistan experienced a decline in the lit area (Table 4.2). At this point it is not clear why nightlights in these two countries declined.

We also investigated the rate of change in the intensity of the stable average lights product between 1991 and 2000 (Fig. 4.8-top) and from 2000 to 2013 (Fig. 4.8-bottom). We find that while the total percentage of lit land increased from

Table 4.2 Percentage of lit land area in Central Asian countries

	1991 (%)	2000 (%)	2013 (%)
Kazakhstan	3.1	3.4	5.0
Kyrgyzstan	3.4	6.0	9.0
Tajikistan	7.9	10.0	8.4
Turkmenistan	3.9	6.8	7.3
Uzbekistan	14.4	17.1	14.5
Central Asia	4.5	5.5	6.6

3.1% to 3.4% between 1991 and 2000 (Table 4.2), almost all lit areas in Kazakhstan declined in nightlight intensity (Fig. 4.8-top). The only areas with increasing nightlights are some of the core urban areas, the Kenkiyak oil fields south of Aktobe and another oil field to the north of Kyzylorda. This decline in night light intensity appears to match well with the decline in urban population in Kazakhstan during this period. Figure 4.4 also shows that the light intensity declined in Kyrgyzstan and Uzbekistan in both periods even though the urban population increased in almost all cities during that time (Fig. 4.7). In Kazakhstan on the other hand, the nightlight intensity increased between 2000 and 2013.

In a previous analysis, we applied the Seasonal Kendall trend test to time series of MODIS vegetation index data between 2001 and 2013 (de Beurs et al. 2015). We found a significant negative trend for almost 42% of the vegetated land surface in Kazakhstan. The other four Central Asian countries revealed much lower percentages of negative vegetation trends, with Uzbekistan presenting the next highest percentage (26.7%) and Tajikistan the lowest percentage of negative vegetation trends (4.1%). We found the highest percentage of negative vegetation trends (38.7%) in grasslands while the lowest percentage (22.4%) in areas with higher human influences (*e.g.*, croplands). We also mapped the vegetation index data against the human influence dataset (Wildlife Conservation Society-WCS and University 2005) and found that a majority of the negative changes occurred for areas with low/intermediate human influence. There were few areas with vegetation increases, but the areas that did increase were almost entirely collocated with areas of higher human influence.

4.3 Quantifying the Water Resources Used for the Agriculture

Central Asia and the Aral Sea drainage basin, in particular, have undergone devastating environmental alterations over the last half century due to land-use/land-cover change that resulted in severe ecological challenges. Water-related change involves all of the key agents of change: land-use/cover change, pollution, over-exploitation of surface and groundwater, and climate change/variability. The entire

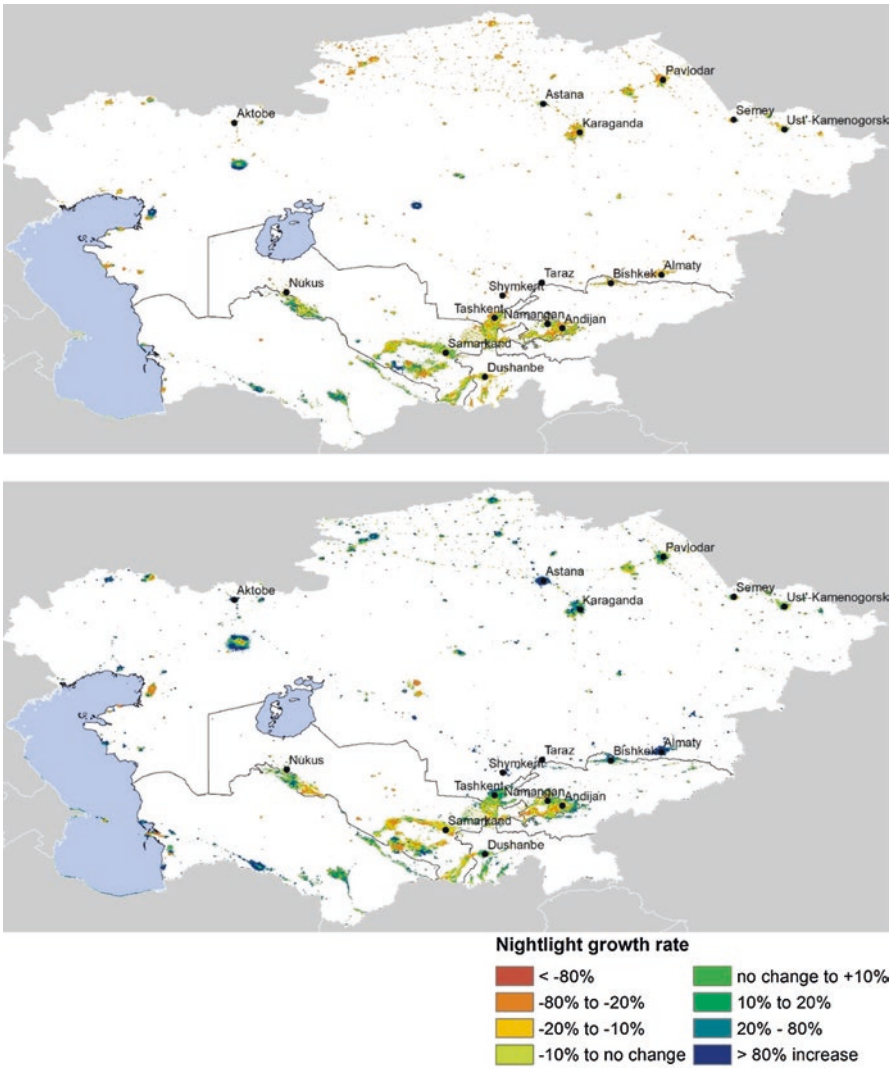

Fig. 4.8 (**Top**) Growth rate in nightlight intensity between 1991 and 2000; (**Bottom**) Growth rate in nightlight intensity between 2000 and 2013

Central Asian region is not water-scarce with total water resources and water availability per capita significantly greater than in the Northern Africa or the Near East. However, the territorial distribution of water resources in the region is spatially unequal. While the lowlands of the Aral Sea basin are characterized by deserts and semi-deserts, precipitation increases in the mountains, while the high mountains with their glaciers and permafrost areas serve as the "water towers" of the region. On average, 43% of the annual discharge in the basin originates in Tajikistan, 24%

in Kyrgyzstan, and approximately 19% in Afghanistan. However, the pattern of water usage is quite the opposite. The upstream mountain states use only about 17% of the water, while downstream Kazakhstan, Uzbekistan, and Turkmenistan use 83%.

The average total renewable water resources of the Central Asia is around 226 km^3/year, including 46 km^3/year inflow from neighboring countries, mainly China and Afghanistan (Shiklomanov and Rodda 2004). Most of regional renewable water resources are generated in the mountains where the largest regional rivers originate. Analysis of annual discharge variations for mountain rivers with relatively small human impact located in the Tianshan Mountains and the Syr Daria upstream basin showed significant upward trends for the most investigated rivers beginning in 90s (Chen et al. 2017). This tendency is observed downstream along the main channel of the Syr Daria River even though there is significant water use in the central part of the basin (Fig. 4.9). There are no, however, such obvious positive discharge trends for rivers located in the Pamir Mountains – Amu Daria upstream basin as well as for river gauges located along the main channel of the Amu Darya River (Fig. 4.9). The observed increasing tendencies in annual discharge of the Syr Daria river are mainly due to higher discharge rates in the spring and summer periods and are likely the result of more intensive snow and glacier melt driven by increasing regional air temperature in Tianshan mountains. Some decrease in area of irrigated lands especially in the Syr Daria river basin after the USSR breakup (Table 4.3) could also contribute to less agricultural water withdrawal and correspondingly higher streamflow (Qi et al. 2020, Chap. 5).

Climate change altering the regional hydrological cycle and fast population grows can significantly deteriorate the water availability in the region. Increase in

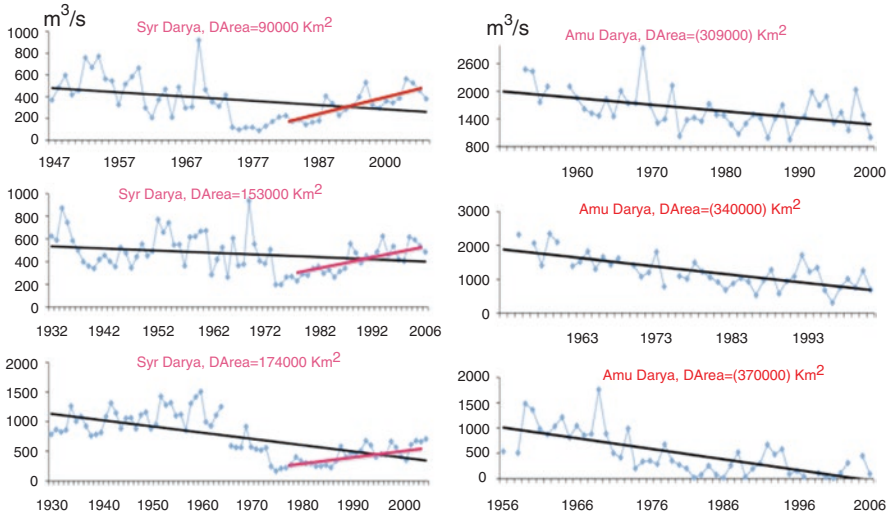

Fig. 4.9 Change in annual discharge along the main stem of Syr Darya (left panels) and Amu Darya rivers over the long-term period

Table 4.3 Area of irrigated lands by country (in thousand ha)

Country/year	1980	1990	1995	2000	2005	2010	2012
Kazakhstan	2690	2800	2681	2062	2127	2081	2100
Kyrgyzstan	1011	1004	1124	1064	1021	1021	1024
Tajikistan	671	751	747	750	800	762	748
Turkmenistan	850	1690	1780	1875	1990	1995	1995
Uzbekistan	3567	4187	4280	4256	4158	4350	4350
Total	8789	10,432	10,612	10,007	10,096	10,209	10,217

air temperature and associated accelerated glacier melt may eventually decrease river flows especially during vegetative period with serious consequences for regional agriculture, human security and development (Chen et al. 2020, Chap. 10). Recent estimate revealed the overall decrease from 1961 to 2012 in total glacier area and mass for the main regional mountain range – Tianshan to be 18 ± 6% and 27 ± 15%, respectively (Farinotti et al. 2015). Meltwater from snow, glaciers and permafrost supplies around 80% of the total river runoff in Central Asia (Sehring and Diebold 2012). The mountain cryosphere is, therefore, a crucial source of water for irrigation agriculture as well as for hydropower production in the region (Groisman et al. 2020, Chap. 2).

4.3.1 Water Use for Agriculture

During USSR period the water use in the region was controlled by central government in Moscow. However, after independence, the contradictions between upstream and downstream countries of the Aral Sea drainage basin for water use were escalated. The resource endowments of upper and downstream countries in the Central Asia are much different; the two upstream countries of Kyrgyzstan and Tajikistan lack of oil and gas resources but with abundant water resources to produce a cheap hydropower energy, which is most required during winter period. The downstream countries – Uzbekistan, Kazakhstan and Turkmenistan – are short of runoff yields but producing large quantities of coal, petroleum, natural gas and other mineral resources, and have extensive production, which requires lots of water for irrigation during vegetative period. Thus, different interests of upstream and downstream countries in use of transboundary water resources may lead to regional conflicts (Chen et al. 2020, Chap. 10).

The Central Asian countries have one of the largest irrigation schemes in the world. Around 22 million people depend directly or indirectly on irrigated agriculture in the region. Twelve to forty percent of the GDP of the Kazakhstan, Kyrgyzstan, Uzbekistan, Turkmenistan and Tajikistan is derived from agriculture, which is mostly irrigated. Without irrigation, much of the agricultural land would revert to desert scrub. While some areas have been irrigated for centuries, many

irrigational schemes were developed in the 1950s–1980s to irrigate desert or steppe areas and hundreds of thousands of people moved to the areas to work in agriculture. During 1970–1989 irrigated area expanded by 150% and 130% in the Amu Darya and Syr Darya river basins respectively (World Bank 2003). The extensive agricultural water use has led to significant decline in river inflow to the Aral Sea and associated dramatic decrease in sea water level. The Aral Sea area shrunk from 65,000 km^2 in 1970s to 8000 km^2 in 2015 and has lost 90% of its volume during this period (Izhitskiy et al. 2016). A new salt saturated desert (AralKum) was formed on the former sea bed providing an additional important source for dust and salt storms in the region (Low et al. 2013). Irrigation continues playing an important role in the economies of Central Asian countries. Table 4.3 demonstrates the changes in area of irrigated lands by country area over 1980–2013 based on information published in local statistical reports and provided by our local collaborators. The total irrigated area in the region slightly decreased between 1995 and 2005 after the USSR breakup and it started increasing again since 2005. There are, however, very different patterns of the change within the region reflecting various socio-economic, demographic and political influences (Fig. 4.10). Water for agricultural needs was and continues to be used highly inefficiently in the region. For example, according to World Bank data, farmers in Uzbekistan withdraw an average of 14,000 m^3/ha of water for irrigation, whereas rates in other countries with non-efficient irrigation such as Pakistan and Egypt are around 9000–10,000 m^3/ha. Central Asian countries have one of the highest rates of water consumption per capita in the world from 1304 m^3 in Kazakhstan to 5415 m^3 in Turkmenistan, whereas the rates in USA and Israel are 1550 m^3 and 281 m^3, respectively. Extensive and non-efficient irrigation led to reduce the quality of farmland through lowering water tables and salinization.

4.3.2 Analysis of Changes in Regional Water Stress

The analysis of changes in water stress for Central Asia was performed using data collections and tools available at the Water Systems Analysis Group of the University of New Hampshire. The Water Balance Model – (WBM) was applied to understand the consequences of changes in climate, water use (Fig. 4.10a), demography, and economy on various variables and indices characterizing regional water security. The WBM accounts for sub-pixel land-cover types, glacier and snow-pack accumulation/melt across sub-pixel elevation bands, anthropogenic water use (*e.g.*, domestic and industrial water consumption, irrigation for most of existing crop types), and hydro-infrastructure for large inter-basin water transfer (*e.g.* Karakum Canal in the Central Asia) and reservoir/dam regulations (Grogan et al. 2015). The map shows Central Asian countries and sub-country administrative units (Fig. 4.10b). The census data about land use, crops and irrigated area from 1980 to 2014 for the administrative units were combined with gridded MIRCA2000 rainfed and irrigated crop

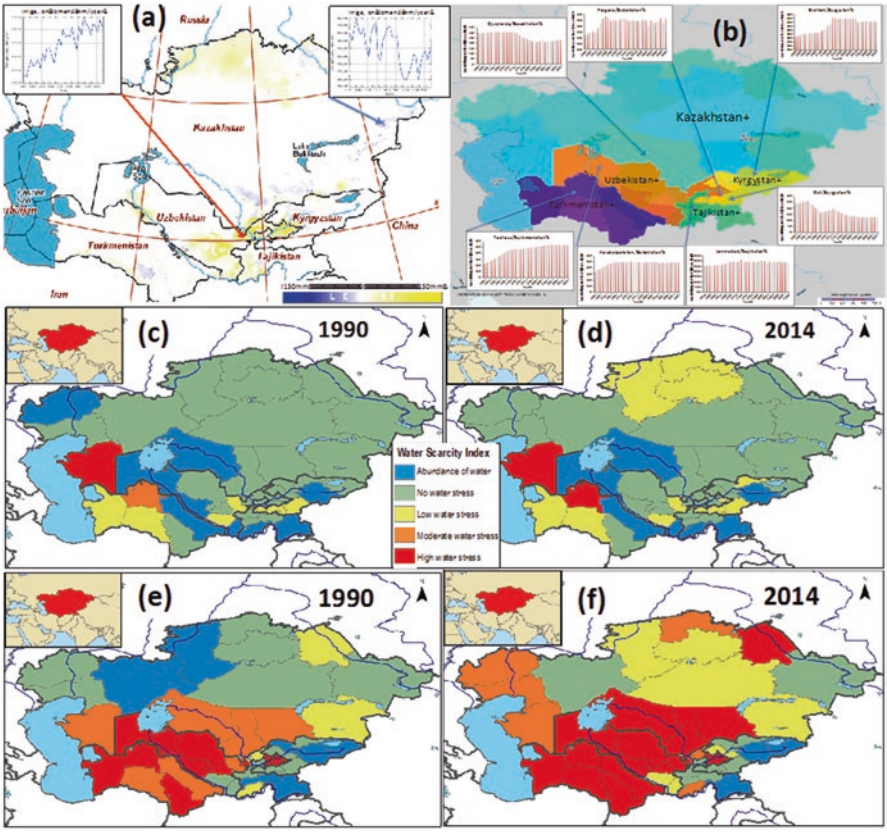

Fig. 4.10 Deviations in water use (irrigation, domestic, industrial, livestock) in mm/year between 2010–2014 and 1980–1985 are shown based on WBM simulations with 6 min spatial resolution; the embedded plots show opposite changes for two subregions (pixels) in annual water demand for irrigation (**a**); the map of administrative units of Central Asia and plots showing the dynamic of irrigated lands for several regions based on census data (**b**). Maps of Water Scarcity Index (WSI) based on total available water resources including inflow from other sub-regions (**c**, **d**), and only locally generated water resources (**e**, **f**) for 1990 and 2014. (From Shiklomanov et al. 2016)

data (Portmann et al. 2010) to provide variable land-use inputs for WBM simulations. The dynamics of water use for domestic, industrial and livestock needs were simulated in WBM using country-based statistical socio-economic information along with spatially distributed population density based on approach discussed in Shiklomanov and Rodda (2004).

The map (Fig. 4.10a) demonstrates the change in water use (via irrigation, domestic, industrial, livestock) across Central Asia between 2000–2012 and 1980–1985 based on WBM simulations using climatic data from MERRA- Modern Era Retrospective-Analysis for Research and Applications (Rienecker et al. 2011).

In general, the water use in the Central Asia has increased in 2000s from 1980 (yellow areas). Although in some regions of Kazakhstan, Kirgizstan and Turkmenistan the water use has declined, primarily due to decreased irrigation water demand. Two inserted plots show annual changes in irrigation water demand over 1980–2012 for two sub-regions (pixels) with opposite tendencies. Since 1980, irrigation water use significantly increased in Uzbekistan where the highest population growth rate has been observed. The barographs in Fig. 4.10b present official data about the changes in areas of irrigated lands for some administrative units. There are different patterns of the changes over 1980–2012, which reflect various socio-economic, demographic, and political issues. For example, significant drops in irrigated areas around 1990 in Osh region – Kyrgyzstan and Ferghana valley – Uzbekistan reflect the so-called Osh riots (ethnic conflict with numerous victims). Water Scarcity Index (WSI) (Brown and Matlock 2011) was estimated based on the WBM simulations using only locally generated water resources (Fig. 4.10e, f) and total available water resources (including inflow from other regions) (Fig. 4.10c, d). The index combines information about water abstractions and water availability. It is defined by the intensity of water resource use, *i.e.* the gross freshwater abstractions as percentage of the total renewable water resources or as percentage of internal water resources. This indicator is defined by the ratio WSI=W/Q, where W is the annual freshwater abstractions and Q is the annual available water. The severity of water stress is classified into several categories (from high water stress – red to abundance of water – blue Fig. 4.10c–f). This indicator neglects temporal and spatial variations as well as water quality. We also analyzed a number of other indexes and variables characterizing the water availability and water use in the region, including water availability index which compares all available water resources to the water demands (*i.e.* domestic, industrial and agricultural). There is general tendency towards significant decline in water availability by 2014 compared to 1990 (Fig. 4.10c–f). The water security situation in 2014 across the region is more stressful despite the significant political and socio-economic transformations in the region in 1990s, which led to a decrease in water use. This is primarily related to change in climatic conditions and population growth.

4.4 Conclusions

This chapter presents an analysis of the anthropogenic signature across the Central Asia. We examined the human influence on the LCLU dynamics and its consequences in the anthropogenic dust emission, water use, and the changes in urban growth. We used a regional dust modeling system WRF-Chem-DuMo to quantify the contribution of agricultural land use (*e.g.*, croplands and grazing lands) and desiccation of the Aral Sea to the dust emission in Central Asia between 2000 and 2014. We have also assessed the anthropogenic fraction of dust, defined as a fraction of dust that relates to various human activities.

Our findings suggest that the major source of uncertainties stems from the model parameterization of erosion thresholds, especially the vegetation effect on the threshold friction velocity. The model experiments reveal consistent responses of anthropogenic dust to occurring land-cover changes. In particular, the fraction of anthropogenic dust decreases in response to the gain in the land type of open shrublands and increases due to the losses in grasslands and barren/sparsely vegetated. The resulting effect is a net decrease in the anthropogenic dust associated with land-cover changes over agricultural lands. In addition to the impacts of land-cover changes on dust emission, dust may also alter land cover by influencing dryland ecosystems via radiative impacts and dust deposition processes, stressing the need for an integrated understanding of human-dust-ecosystem interactions.

We also investigated the rate of change in the intensity of the stable average lights product between 1991 and 2000 and from 2000 to 2013. Our analysis revealed that while the total percentage of lit land increased (3.1–3.4%) between 1991 and 2000 (Table 4.2) almost all lit areas in Kazakhstan declined in night light intensity (Fig. 4.8-top). The only areas with increasing nightlights are some core urban areas, the Kenkiyak oil fields south of Aktobe and another oil field to the north of Kyzylorda. This decline in night light intensity appears to match the decline in urban population in Kazakhstan during this period.

Water use has been a central factor in controlling the food security and the livelihood. Water is a key agent in Central Asia ultimately determining human well-being, food security, and economic development. There are complex interplays among the natural and anthropogenic drivers effecting the regional hydrological processes and water availability. Analysis of the data combined from regional censuses and remote sensing shows a decline in areas of arable and irrigated lands and a significant decrease in availability of arable and irrigated lands per capita across all Central Asian countries since the middle of 1990s as the result of post-Soviet transformation processes. This change could lead to considerable deterioration in food security and human system sustainability. The change of political situation in the region has also resulted in the escalated problems of water demand between countries in international river basins. Anthropogenic and Natural Systems (WBM-TrANS) has been used to understand the consequences of changes in climate, water and land use on regional hydrological processes and water availability. The model accounts for sub-pixel land-cover types, glacier and snow-pack accumulation/melt across sub-pixel elevation bands, anthropogenic water use (*e.g.,* domestic and industrial consumption, and irrigation for most of existing crop types), hydro-infrastructure for inter-basin water transfer and reservoir/dam regulations. We found that regional water availability is mostly impacted by the changes in extent and efficiency of crop field irrigation, especially in highly arid areas of Central Asia, changes in winter snow storage, and shifts in seasonality and intensity of glacier melt waters driven by climatic changes.

Acknowledgements This work has been supported by NASA LCLUC program, grant #NNX14AD88G.

References

Brown A, Matlock MD (2011) A review of water scarcity indices and methodologies. White paper 106:19

Chen Y, Li W, Fang G, Li Z (2017) Hydrological modeling in glacierized catchments of central Asia-status and challenges. Hydrol Earth Syst Sci 21(2):669

Chen J, Ouyang Z, John R et al (2020) Social-ecological systems across the Asian Drylands Belt (ADB). In: Gutman G et al (eds) Landscape dynamics of drylands across greater Central Asia: people, societies and ecosystems. Springer, Cham

Darmenova K, Sokolik IN, Shao Y, Marticorena B, Bergametti G (2009) Development of a physically based dust emission module within the Weather Research and Forecasting (WRF) model: assessment of dust emission parameterizations and input parameters for source regions in Central and East Asia. J Geophys Res 114(D14):D14201

de Beurs KM, Henebry GM (2004) Land surface phenology, climatic variation, and institutional change: analyzing agricultural land cover change in Kazakhstan. Remote Sens Environ 89(4):497–509

de Beurs KM, Henebry GM, Owsley BC, Sokolik I (2015) Using multiple remote sensing perspectives to identify and attribute land surface dynamics in Central Asia 2001–2013. Remote Sens Environ 170:48–61

Eidenshink JC, Faundeen JL (1994) The 1 km AVHRR global land data set: first stages in implementation. Int J Remote Sens 15(17):3443–3462

Farinotti D, Longuevergne L, Moholdt G, Duethmann D, Mölg T, Bolch T, Vorogushyn S, Güntner A (2015) Substantial glacier mass loss in the Tien Shan over the past 50 years. Nat Geosci 8(9):716

Farmer AM (1993) The effects of dust on vegetation – a review. Environ Pollut 79(1):63–75

Ginoux P, Prospero JM, Gill TE, Hsu NC, Zhao M (2012) Global-scale attribution of anthropogenic and natural dust sources and their emission rates based on MODIS Deep Blue aerosol products. Rev Geophys 50(3):0388

Gintzburger G, Le Houérou HN, Toderich K (2005) The steppes of Middle Asia: post-1991 agricultural and rangeland adjustment. Arid Land Res Manag 19(3):215–239

Grogan DS, Zhang F, Prusevich A, Lammers RB, Wisser D, Glidden S, Li C, Frolking S (2015) Quantifying the link between crop production and mined groundwater irrigation in China. Sci Total Environ 511:161–175

Groisman PY, Bulygina ON, Henebry GM et al (2020) Dry land belt of Northern Eurasia: contemporary environmental changes. In: Gutman G et al (eds) Landscape dynamics of drylands across greater Central Asia: people, societies and ecosystems. Springer, Cham

Gupta P, Kienzler K, Martius C et al (2009) Research prospectus: a vision for sustainable land management research in Central Asia. ICARDA Central Asia and Caucasus Program. Sustainable Agriculture in Central Asia and the Caucasus Series No.1. CGIAR-PFU, Tashkent

Huneeus N, Schulz M, Balkanski Y et al (2011) Global dust model intercomparison in AeroCom phase I. Atmos Chem Phys 11(15):7781–7816

Hurtt GC, Frolking S, Fearon MG et al (2006) The underpinnings of land-use history: three centuries of global gridded land-use transitions, wood-harvest activity, and resulting secondary lands. Glob Chang Biol 12(7):1208–1229

Hurtt GC, Chini LP, Frolking S et al (2011) Harmonization of land-use scenarios for the period 1500–2100: 600 years of global gridded annual land-use transitions, wood harvest, and resulting secondary lands. Clim Chang 109(1–2):117

Izhitskiy AS, Zavialov PO, Sapozhnikov PV et al (2016) Present state of the Aral Sea: diverging physical and biological characteristics of the residual basins. Sci Rep-UK 6

Kappas M, Degener J, Klinge M et al (2020) A conceptual framework for ecosystem stewardship based on landscape dynamics: case studies from Kazakhstan and Mongolia. In: Gutman G et al (eds) Landscape dynamics of drylands across greater Central Asia: people, societies and ecosystems. Springer, Cham

Knippertz P, Todd MC (2012) Mineral dust aerosols over the Sahara: meteorological controls on emission and transport and implications for modeling. Rev Geophys 50(1):RG1007
Kravtsova V, Lukyanova S (2000) Studies of recent changes in the Caspian coastal zone of Russia based on aerial and space imagery. J Coastal Res:196–206
Le QB, Biradar C, Thomas R et al (2016) Socio-ecological context typology to support targeting and upscaling of sustainable land management practices in diverse global dryland. Paper presented at the 8th International Conference on Environmental Modelling and Software, Toulouse, France, July 11, 2016
Leroy S, Marret F, Giralt S, Bulatov S (2006) Natural and anthropogenic rapid changes in the Kara-Bogaz Gol over the last two centuries reconstructed from palynological analyses and a comparison to instrumental records. Quatern Int 150(1):52–70
Lioubimtseva E, Cole R (2006) Uncertainties of climate change in arid environments of Central Asia. Rev Fish Sci 14(1–2):29–49
Lioubimtseva E, Henebry GM (2009) Climate and environmental change in arid Central Asia: impacts, vulnerability, and adaptations. J Arid Environ 73(11):963–977
Low F, Navratil P, Kotte K et al (2013) Remote-sensing-based analysis of landscape change in the desiccated seabed of the Aral Sea-a potential tool for assessing the hazard degree of dust and salt storms. Environ Monit Assess 185(10):8303–8319
Mahowald N, Luo C (2003) A less dusty future? Geophys Res Lett 30(17):017880
Micklin P (2007) The Aral Sea disaster. Annu Rev Earth Plant Sci 35(1):47–72
Orlovsky N, Orlovsky L (2002) White sandstorms in Central Asia, Global alarm: dust and sandstorms from the world's drylands. In: Youlin Y, Squires V, Qi L (eds) . UNCCD United Nations, Bangkok, pp 169–196
Portmann FT, Siebert S, Döll P (2010) MIRCA2000 – global monthly irrigated and rainfed crop areas around the year 2000: a new high-resolution data set for agricultural and hydrological modeling. Global Biogeochem Cy 24(1)
Prospero JM, Ginoux P, Torres O et al (2002) Environmental characterization of global sources of atmospheric soil dust identified with the NIMBUS 7 Total Ozone Mapping Spectrometer (TOMS) absorbing aerosol product. Rev Geophys 40(1):1002
Qi J, Pueppke S, Kulmatov R et al (2020) The complexity and challenges and challenges of Central Asia's water-energy-food systems. In: Gutman G et al (eds) Landscape dynamics of drylands across greater Central Asia: people, societies and ecosystems. Springer, Cham
Restrepo Cadavid P, Cineas G, Quintero LE, Zhukova S (2017) Cities in Eastern Europe and Central Asia: a story of urban growth and decline
Rienecker MM, Suarez MJ, Gelaro R et al (2011) MERRA: NASA's modern-era retrospective analysis for research and applications. J Clim 24(14):3624–3648
Robinson S, Milner-Gulland EJ, Alimaev I (2003) Rangeland degradation in Kazakhstan during the Soviet era: re-examining the evidence. J Arid Environ 53(3):419–439
Sehring J, Diebold A (2012) Water unites: from the glaciers to the aral sea. Trescher Verlag
Shiklomanov IA, Rodda JC (2004) World water resources at the beginning of the twenty-first century. Cambridge University Press
Shiklomanov A, Prusevich A, Gordov EP et al (2016) A Environmental science applications with Rapid Integrated Mapping and analysis System (RIMS). IOP Conf Ser Earth Environ Sci 1:012034
Sokolik IN, Toon OB (1996) Direct radiative forcing by anthropogenic airborne mineral aerosols. Nature 381(6584):681–683
Sokolik IN, Darmenova K, Huang J et al (2013) Examining changes in land cover and land use, regional climate and dust in dryland East Asia and their linkages within the Earth system. In: Chen J, Wan S, Henebry G et al (eds) Dryland East Asia: land dynamics amid social and climate change. HEP – De Gruyer, Berlin, pp 185–213
Stanelle T, Bey I, Raddatz T et al (2014) Anthropogenically induced changes in twentieth century mineral dust burden and the associated impact on radiative forcing. J Geophys Res Atmos 119(23):13526–13546

Stringer LC (2008) From global environmental discourse to local adaptations and responses: a desertification research agenda for Central Asia. In: The socio-economic causes and consequences of desertification in Central Asia. Springer, Dordrecht, pp 13–31
Tegen I, Fung I (1995) Contribution to the atmospheric mineral aerosol load from land surface modification. J Geophys Res-Atmos 100(D9):18707–18726
Tegen I, Werner M, Harrison SP, Kohfeld KE (2004) Relative importance of climate and land use in determining present and future global soil dust emission. Geophys Res Lett 31(5):n/a–n/a
Varushchenko AN, Lukyanova SA, Solovieva GD et al (2000) Evolution of the Gulf of Kara-Bogaz-Gol in the past century. In: Lulla KP, Dessinov LV (eds) Dynamic earth environments: remote sensing observations from Shuttle-Mir Missions. Wiley, pp 201–210
Wildlife Conservation Society-WCS, University CFIESINCC (2005) Last of the wild project, Version 2, 2005 (LWP-2): global human influence Index (HII) Dataset (Geographic). NASA Socioeconomic Data and Applications Center (SEDAC) Palisades, NY
Wilson RT (1997) Livestock, pastures, and the environment in the Kyrgyz Republic, Central Asia. Mt Res Dev:57–68
World Bank (2003) The World Bank Annual Report 2003 (English). The World Bank, Washington, DC
World Bank (2017) The World Bank Annual Report 2017. The World Bank
Xi X (2014) Examination of mineral dust variability and linkages to climate and land-cover/land-use change over Asian drylands. Disertation, Georgia Institute of Technology
Xi X, Sokolik IN (2012) Impact of Asian dust aerosol and surface albedo on photosynthetically active radiation and surface radiative balance in dryland ecosystems. Adv Meteorol 2012
Xi X, Sokolik IN (2015) Dust interannual variability and trend in Central Asia from 2000 to 2014, and their climatic linkages. J Geophys Res Atmos
Xi X, Sokolik IN (2016) Quantifying the anthropogenic dust emission from agricultural land use and desiccation of the Aral Sea in Central Asia. J Geophys Res-Atmos 121(20):12270–12281
Zender CS, Miller RLRL, Tegen I (2004) Quantifying mineral dust mass budgets:terminology, constraints, and current estimates. Eos Trans AGU 85(48):509–512
Zhang X-Y, Gong S, Zhao T et al (2003) Sources of Asian dust and role of climate change versus desertification in Asian dust emission. Geophys Res Lett 30(24)

Chapter 5
The Complexity and Challenges of Central Asia's Water-Energy-Food Systems

Jiaguo Qi, Steven Pueppke, Rashid Kulmatov, Temirbek Bobushev, Shiqi Tao, Tlektes I. Yespolov, Marat Beksultanov, and Xi Chen

5.1 Introduction

The region that we now recognize as Central Asia has a complex political and cultural history that traces back to antiquity and is deeply interwoven with struggles to access water and achieve food security in an unforgiving climate. Genghis Khan consolidated control over almost all of this area in the thirteenth century, but his Mongol Empire soon disintegrated into a patchwork of successor states that ascended and fell over the centuries. Those that survived into the late nineteenth century were all eventually integrated into Imperial Russia, which coveted the natural resources of the region (Carrère d'Encausse 2009; Olcott 1987; Peyrouse 2013).

J. Qi (✉)
Department of Geography, Environment, and Spatial Sciences, Center for Global Change and Earth Observations, Michigan State University, East Lansing, MI, USA
e-mail: qi@msu.edu

S. Pueppke
Asia Hub, Nanjing Agricultural University, Nanjing, China
e-mail: pueppke@msu.edu

R. Kulmatov
Department of Biology, National University of Uzbekistan, Tashkent, Uzbekistan

T. Bobushev
Department of Capacity Development and Scientific Cooperation, Central-Asian Institute for Applied Geosciences, Bishkek, Kyrgyzstan

S. Tao (✉)
Department of Geography, Environment, and Spatial Sciences, Center for Global Change and Earth Observations, Michigan State University, East Lansing, MI, USA
e-mail: taoshiqi@msu.edu

G. Gutman et al. (eds.), *Landscape Dynamics of Drylands across Greater Central Asia: People, Societies and Ecosystems*, Landscape Series 17,
https://doi.org/10.1007/978-3-030-30742-4_5

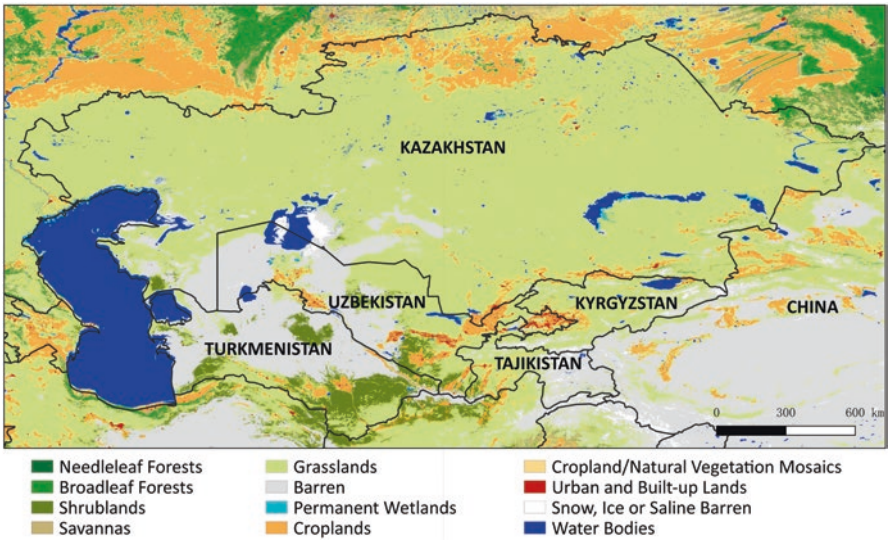

Fig. 5.1 Land use and land cover in Central Asia and surrounding countries as of 2017. The map is derived from MODIS products

The Central Asian lands were reorganized into five republics during the Soviet period. With the collapse of the Soviet Union in the early 1990s, all five became independent. For our purposes, it is these five independent republics – Kazakhstan, Kyrgyzstan, Tajikistan, Turkmenistan, and Uzbekistan – that constitute Central Asia (Lioubimtseva and Henebry 2009).

Lying far from the sea, Central Asia is a vast and isolated area characterized by seemingly endless steppes. But the region also contains high mountains that are blanketed with forests and topped with glaciers, as well as inhospitable deserts and other barren zones that are scarcely able to support life (Fig. 5.1). Six percent of Tajikistan's entire surface area – more than 8400 km^2 – is covered by almost 8500 glaciers (Kayumov 2010), and 70% of Turkmenistan is given over to the enormous Karakum Desert, which extends across 350,000 km^2. The climate is for the most

T. I. Yespolov
Kazakh National Agrarian University, Almaty, Kazakhstan
e-mail: rector@kaznau.kz

M. Beksultanov
AgriTech Hub Kaz, Almaty, Kazakhstan
e-mail: maratb@precisionagro.com

X. Chen
Xinjiang Institute of Ecology and Geography, Chinese Academy of Science Xinjiang Branch, Urumqi, China
e-mail: chenxi@ms.xjb.ac.cn

part distinctively continental. Summer days are often cloudless and can be searingly hot, but winters, especially in the north, are usually frigid and harsh. Annual precipitation generally decreases along a gradient from east to west, but it is localized and variable, ranging from as much as 900 mm on windward mountain slopes to just 5–10 mm in the western lowlands of Kazakhstan (Böhner 2006; Bolch 2007; Groisman et al. 2020, Chap. 2; Pilifosova et al. 1997; Qi et al. 2012).

Although Central Asia is arid, the landscape is interrupted by several significant lakes, including the Caspian Sea, the earth's largest inland body of water. A few of the region's lakes such as Kyrgyzstan's Issyk-kul, are at higher elevation, but like the Caspian Sea, most lie in the arid lowlands. Waterbodies such as the Aral Sea and Lake Balkhash are fed not by localized precipitation, but by rivers the descend from the surrounding highlands. The Aral Sea thus receives its major inflows from the Syr Darya and Amu Darya, with inflows from the Ili and Karatal rivers sustaining Lake Balkhash. Many other rivers and smaller streams course down from Central Asia's mountain highlands. Some form tributaries of the region's main rivers but others simply flow onto the deserts and steppes, where they dry up and disappear.

5.2 Water-Energy-Food in Central Asia

5.2.1 Perspective

Water has always been the most precious resource for human existence across Central Asia, because it limits the availability of locally produced food and thus governs political and cultural stability in a region that until recently had few options for reliable access to food from elsewhere (Horsman 2018; Pueppke et al. 2018c; Wittfogel 1957). Constraints imposed by water-food interrelationships are consequently deeply embedded, long standing issues in the region. These constraints were partially lifted when transportation systems such as the Trans-Caspian railway and steamship travel were extended into the area by the Russians in the 1880s, allowing for efficient movement of food and other products to and from Central Asia (Carrère d'Encausse 2009).

These developments accentuated the linkages between water-food and a third factor: energy. Originally important as a means of transporting food and other agricultural products, energy later assumed importance in redirecting the flow of the region's water and releasing it from the constraints of gravity. This greatly increased the potential for irrigation in Central Asia and cemented the close linkage between management of water resources and production of food that defines the naturally arid region today. The ability of impounded water to produce energy hydroelectrically adds other dimensions to the equation, some beneficial and some negative. All are important for closing the circle on Central Asia's water-energy-food (WEF) system.

5.2.2 Interrelationships

Transhumance is the most defining factor in the Central Asia's food system (Olcott 1987). For millennia, the region's much celebrated nomads have taken advantage of seasonal weather cycles to find pasturage for their herds, which supply protein to meet basic human nutritional needs. Relying on instinct and intuition, herders learned to match the right kinds of animals in the right numbers with the seasonal availability of forages on the rain-fed steppes and along Central Asia's rivers. This practice, which places few demands on technology and infrastructure, has been optimized over the centuries to take advantage of what the environment offers. Although most nomads have now settled, transhumance and exploitation of natural grasslands remains as a key enabler of food security in Central Asia (Wiens 1969).

Options for sedentary, crop-based agriculture in Central Asia are few in the absence of irrigation water, which at first was simply diverted from rivers and streams and allowed to flow onto fields by gravity (Lattimore 1940; Lewis 1966; Pueppke et al. 2018c). It was the Czars who built the initial large-scale irrigation works in the region. Although much of it was to expand production of cotton near the Aral Sea (Beckert 2017), hydraulic infrastructure for food production was constructed by the Russians in the late eighteenth century (Poujol and Fourniau 2005). It has been estimated that by 1900, 300,000 hectares of land in just the Ili River basin, an area not known for cotton production, were equipped for irrigation (Redakiivey and Samkovoy 2003). The Soviets greatly accelerated diversion of water to irrigate food crops and cotton in Central Asia. Plans were drawn up soon after they had consolidated power in the 1920s, and irrigation infrastructure, much of it at a mammoth scale, was constructed over the following decades. Examples include the Great Ferghana Canal (1939), the Karakum Canal (1954), Kapchagai Dam (1969), Toktogul Dam (1978), and Nurek Dam (1980). Food production was not the first priority for much of the Soviet irrigation infrastructure in Central Asia. Energy security was a more pressing problem, and so structures such as Kapchagai Dam were engineered to optimize power production, with irrigation considered to be a collateral benefit (Chida 2013).

Kapchagai Dam provides a striking illustration of the challenges inherent in achieving a balance between water, energy, and food in Central Asia (Chida 2013; Pueppke et al. 2018b, c). Damage to the downstream ecosystem became apparent soon after the dam was closed in December of 1969. Insufficient inflows caused the level of downstream Lake Balkhash to drop, and the Ili River delta, a traditional site of forage production for livestock, began to desiccate (Starodubtsev and Truskavetskiy 2011). The repercussions were so severe that filling of Kapchagai Reservoir was halted in the mid-1980s, permanently constraining energy production (Dostaj et al. 2006; Petr 1992). Power is predominately needed for heat in the winter, so the level of the reservoir was allowed to rise in the summer and then fall during the cold months as water was released through the turbines. This inverted the annual flow cycle of the Ili River, substituting counter cyclical pulses of water in the

winter for the spring and summer flows needed during the growing season (Akiyama et al. 2012; Kezer and Matsuyama 2006; Nurtazin et al. 2019). Irrigation water from Kapchagai Reservoir nevertheless did facilitate food production on several tracts of land that had been non-arable (Dostaj et al. 2006; Pueppke et al. 2018c), but this was offset by catastrophic damage to Lake Balkhash fisheries, which rely on natural seasonal flows to promote spawning (Graham 2016; Graham et al. 2017; Pueppke et al. 2018a; Thorpe and Van Anrooy 2010).

Although the details may differ, similarly complex, often unintended consequences are associated with every attempt to manage water, energy, and food in Central Asia. A few examples will suffice. In Uzbekistan, diversion of the Amu Darya and Syr Darya rivers has led to the near destruction of the Aral Sea, which was once Central Asia's fourth largest lake (Micklin et al. 2014). Today's much reduced Aral Sea is universally considered to be a poster child for environmental destruction triggered by ill-advised diversion of water for agriculture. Construction of Turkestan's Turkmen Lake, which began in 2000, threatens to divert even more water from the Amu Darya. A huge desert reservoir, it has been justified as a means to increase production of wheat and cotton, livestock, and fisheries. If completed, Ragun Dam in upstream Tajikistan will only exacerbate the situation. Under construction on a major tributary of the Amu Darya, it is designed to facilitate irrigation and generate enough hydropower to allow Tajikistan to meet all of its internal electricity needs with excess available for export (Fields et al. 2013). In the process, it has drawn renewed attention to regional WEF conflicts.

5.3 A Systems Approach

5.3.1 Perspective

Although rarely treated as such when management decisions are made, water, energy, and food are interdependent components of what can be called the WEF nexus (Keairns et al. 2016; Rakhmatullaev et al. 2017) or the WEF system (Fig. 5.2). It is possible to isolate the individual components on paper, but as the above examples confirm, this never occurs in the real world (Chen et al. 2020, Chap. 10). Tradeoffs and synergies are always lurking, in time and in space, and so although the details of nexus thinking remain unresolved, there is value in adopting an approach that acknowledges system interdependencies and seeks to avoid the occurrence of undesirable consequences in practice. It is the much maligned Soviet Union that may have conducted the first WEF system test under real world conditions (Bekchanov and Lamers 2016), and it did so in Central Asia, where it actively managed the water-energy relationship, in the process indirectly managing food as well (Abdullaev and Rakhmatullaev 2016; Wegerich 2011).

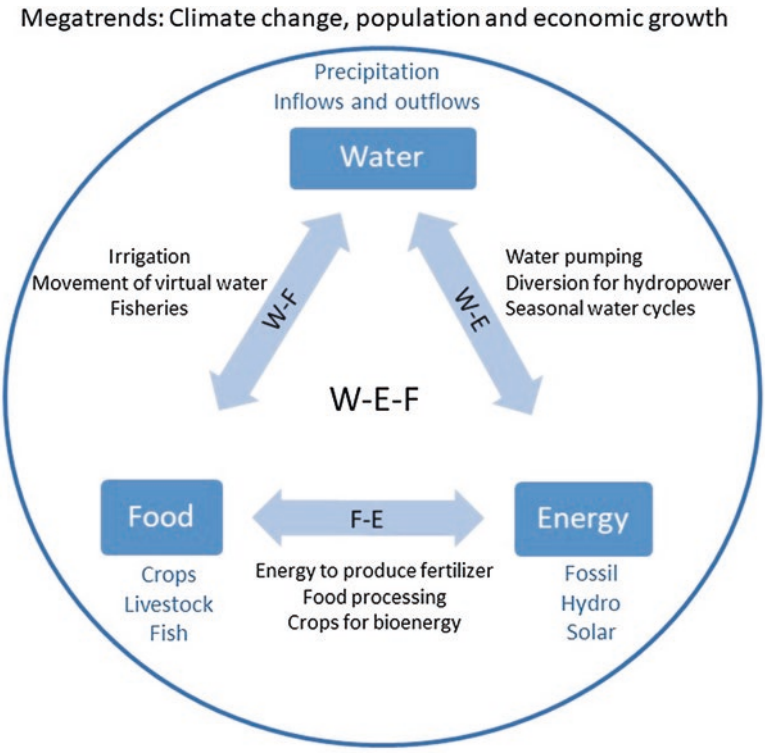

Fig. 5.2 Conceptual depiction of the WEF system in Central Asia. The diagram emphasizes the complexity and challenges at the interfaces of the three system components: water, energy, and food

5.3.2 The Soviet Experiment and Its Aftermath

The five Central Asian republics share common borders and a regional geography, but they differ greatly in resource distribution (Fig. 5.3). Tajikistan and Kyrgyzstan are mountainous with relatively abundant water resources but very limited fossil energy reserves. Turkmenistan and Uzbekistan are the opposite; they are dependent on water inflows from other countries but have some fossil energy. Kazakhstan has immense fossil fuel reserves and is to a significant extent dependent on water inflows from other countries. These disparities were balanced centrally during the Soviet period such that energy flowed from energy-rich to water-rich regions in return for water flows in the opposite direction (Granit et al. 2012; Horsman 2018; Rahaman 2012; Rakhmatullaev et al. 2017). Although environmental damage was severe, especially at the Aral Sea, the Soviet governmental structure ensured that Moscow could enforce these policies and that water and energy were equitably distributed and used to ensure food security for all five republics. This argument was generally accepted by all (Rakhmatullaev et al. 2017).

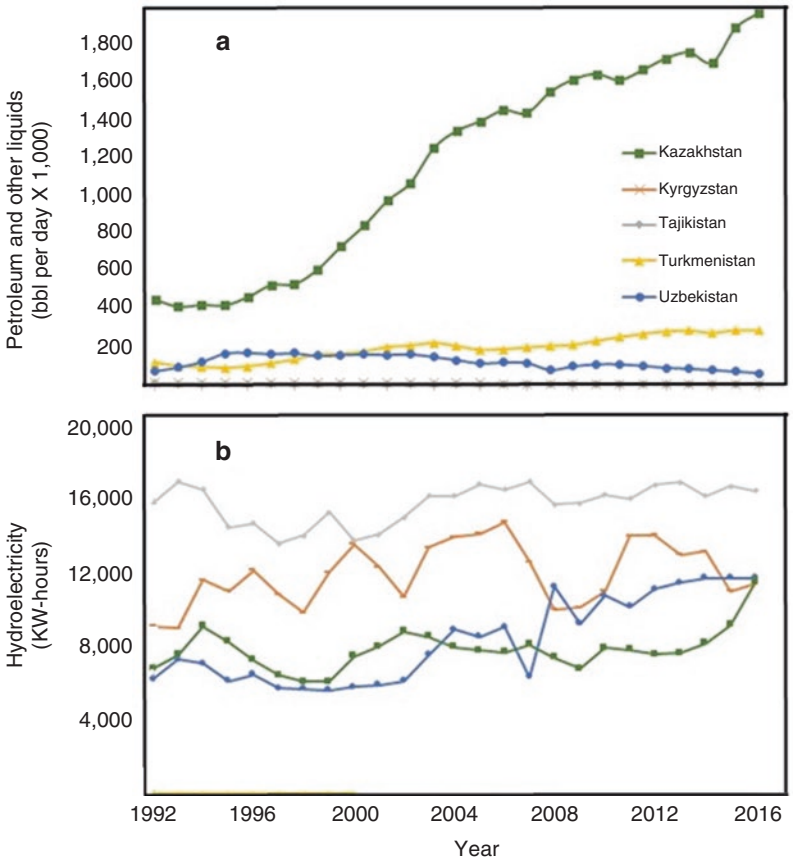

Fig. 5.3 Changes in the production of (**a**) petroleum and other liquid forms of energy and (**b**) hydroelectric energy by the five Central Asian republics between 1992 and 2016. Note that production by Kyrgyzstan and Tajikistan in (**a**) and Turkmenistan in (**b**) lies along the x-axis. The statistics are from UN data (2019)

The consensus in water and energy usage changed with the dissolution of the Soviet Union in 1991, which abolished the WEF system enforcement mechanism and created five independent states. Some had abundant energy, and others had abundant water. All were financially insecure and exposed to unfamiliar market forces. Each new republic experienced heightened concern for its own security and weakened concern for the welfare of its neighbors. Upstream republics consequently set out to develop and monetize their water resources, with insufficient attention given to the consequences for food and water security of downstream states. Downstream republics did the same with their fossil energy resources. The result has been a protracted series of transboundary disagreements over resource use, primarily along the water-energy axis (Horsman 2018; Stone 2012).

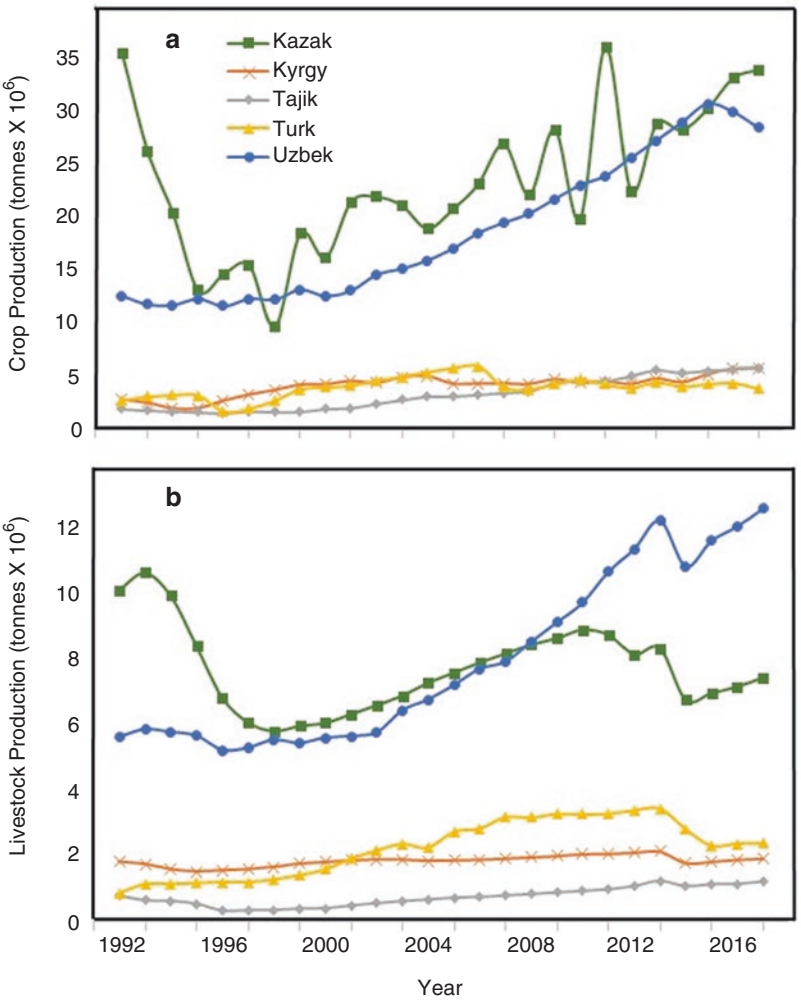

Fig. 5.4 Changes in the primary production of crops (**a**) and livestock (**b**) by the five Central Asia republics countries between 1992 and 2016. The statistics are from UNdata (2019)

The food consequences of these and other developments are shown in Fig. 5.4, which charts changes in crop and livestock production in the five Central Asian republics for which at least partial data are available after 1991. A quarter century after independence, it is apparent that crop and livestock production has stagnated in three of the five Central Asian republics at levels marginally greater than and occasionally below those seen just after the collapse of the Soviet Union. Kazakhstan forfeited more than two-thirds of its crop production during its first decade of independence and lost nearly half of its livestock production capacity during the same period. Uzbekistan managed to increase livestock production for a few years, but progress then faltered. Although Uzbekistan and Kazakhstan are exceptions to gen-

erally discouraging regional trends, progress in increasing crop and animal production has generally slowed since 2010.

5.4 WEF Challenges

It is not our purpose here to consider all aspects of Central Asia's WEF system in comprehensive detail. Rather, we have pointed out the unique features of the region's environment, introduced key WEF system drivers, and related them to one another. We conclude by identifying priority, system-wide challenges that must be addressed if the WEF system is to be sustained into the future. For convenience, these are organized under the headings of water, energy, and food; in the real world, they all grade into one another.

5.4.1 Water

Many water resources of Central Asia are not permanent features of the landscape, and so although water is widely distributed across the mountainous and lowland areas of the region, there is evidence of change over a 30-year period ending in 2015 (Fig. 5.5). This is most striking in the permanent contraction of the Aral Sea (Sokolik et al. 2020, Chap. 4), but also visible in the apparently permanent enlargement of Garabogaz Bay

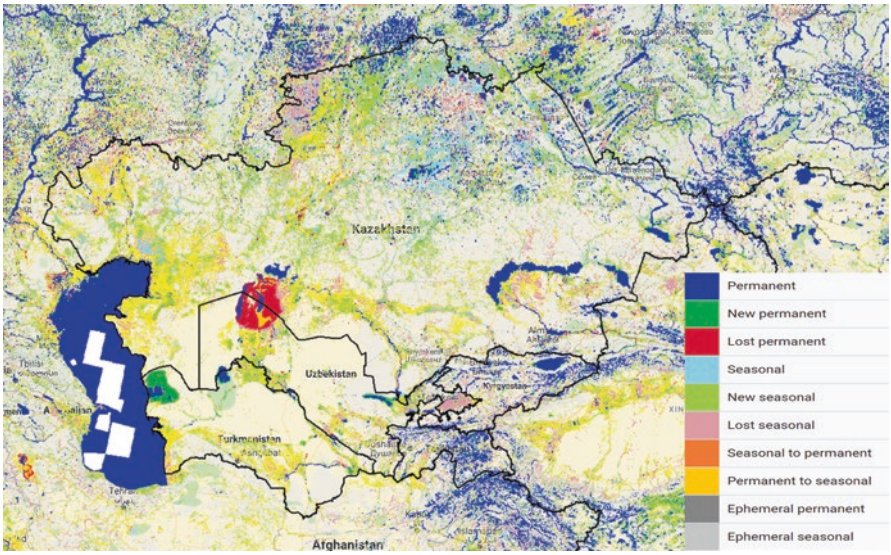

Fig. 5.5 Central Asian surface water distribution and changes from 1984 to 2015. (The data are derived from JRC Surface Water Products (Pekel et al. 2016))

in far northwestern Turkmenistan. Seasonal water losses are most evident in the fertile Ferghana Valley, in far northern Kazakhstan, and in areas adjacent to Lake Balkhash. In contrast, new seasonal water appears along both irrigated and non-irrigated reaches of the Amu Darya, Chu, and Syr Darya rivers in Kazakhstan, Uzbekistan, and Turkmenistan. Additional changes will almost certainly occur in the future.

In light of the above changes and those anticipated in the future, it is crucial to ensure an adequate supply of water for Central Asia in the face of multiple challenges: a modified environment that threatens to decrease water availability in the future, transboundary disputes over distribution of water, and economic developments that will likely lead to increasing consumptive use of water. Environmental change in Central Asia is primarily manifested as a warming trend conditioned by climate change, which is leading to glacier retreat and increasing evaporative water loss (Groisman et al. 2018; Lioubimtseva et al. 2005; Qi et al. 2012). In addition, shifts in regional precipitation patterns have intensified the frequency of rainstorms, even as the number of rainy days and total annual rainfall have decreased (Groisman et al. 2020, Chap. 2). The immediate consequences of these environmental changes are difficult to precisely predict, but over the short term, they may elevate water inflows into the region; over the long term, they will likely permanently reduce Central Asia's water resources (Sorg et al. 2012, 2014).

Although the Central Asia's transboundary water issues first became apparent with the breakup of the Soviet Union almost 30 years ago (Zhiltsov et al. 2018), transboundary disputes are not limited to those among the five former Soviet republics (Abdolvand et al. 2015; Chen et al. 2020, Chap. 10; Ho 2017; Stone 2012). Several of the region's major rivers, notably the Ili and the Irtysh, have their origin to the east, in neighboring Xinjiang, China, where withdrawals are increasing, primarily for irrigated food production (Christiansen and Schöner 2004; Thevs et al. 2017). This has led to as of yet unsuccessful attempts to forge a binding and comprehensive water sharing agreement between the two neighbors (Eritja et al. 2016; Xie and Jia 2018). Tension consequently persists, and this will likely be influenced by regional developments such as China's Belt Road Initiative, which is leading to massive investment in infrastructure, increased population, and vastly improved transportation networks along a corridor between China and Western Europe. These investments will increase demand for energy, facilitate trade, including the export of virtual water from the region, and almost certainly have other profound WEF system effects (Dave and Kobayashi 2018; Martens 2019). Among them is the potential to ease tensions between Kazakhstan and China and facilitate cooperation on transboundary water issues.

5.4.2 Energy

The distinctions between Central Asian republics with and without access to fossil fuels are striking. Today, Kazakhstan produces roughly five times the amount of petroleum and other liquid fossil fuels as the other four republics combined (Fig. 5.3a). Coal production figures are even more skewed, with Kazakhstan's pro-

duction now more than ten times that of the sum of the other states (UNdata 2019). Moreover, in the case of both liquid and solid fossil fuels, production by Kazakhstan but not the other states, has been rapidly rising. As the Soviets clearly understood, the picture is different when hydroelectric power is considered (Fig. 5.3b). Tajikistan produced almost twice as much hydropower as Kazakhstan and Uzbekistan during the Soviet era, but this remained more or less stable thereafter, as Uzbekistan and Kazakhstan – and to a lesser extent Kyrgyzstan – have steadily increased their hydropower capacity. Due to its flat, low terrain, the hydropower potential of Turkmenistan is virtually nil.

From the perspective of the WEF system, the most crucial energy challenge is the optimization of water management for two interconnected goals: hydroelectric power generation and irrigated food production. Energy also plays a direct, often essential role in making water available for thirsty crops. Several irrigation districts in Kazakhstan have in fact been decommissioned due to lack of energy to elevate water to them (Pueppke et al. 2018c), and in Uzbekistan, an astonishing three-quarters of the annual budget of the Ministry of Agriculture and Water Resources goes to purchasing energy to power irrigation pumps (Abdullaev and Rakhmatullaev 2016). The key issue is not just the amount of water available for irrigation from a dammed river, but as we have seen with Kapchagai Dam, the seasonal timing of its availability with respect to fisheries, animal agriculture, and crop production. All three interact and are affected by annual water cycles. This often generates internecine conflicts within the WEF system, as when the natural cycle is disrupted to divert water for irrigation and discharge its downstream later for hydropower generation (Pueppke et al. 2018b).

Unlike Kazakhstan's Kapchagai Dam, structures such as Tajikistan's immense Rogun are being constructed by upstream countries to address their own interests, yet each directly affects the water resources available to a nearby downstream country (Sabonis-Helf 2018; Zhiltsov et al. 2018). This overlays the complexity of a transboundary energy element onto the transboundary water disputes discussed above. In the case of Rogun Dam, construction of which was begun by the Soviets more than four decades ago and is not yet completed, the tension has been such that armed conflict between Tajikistan and Uzbekistan was briefly considered (Graham 2016).

5.4.3 Food

Central Asia's food system rests on three components: fisheries, animal herding, and crop-based agriculture. Complementary on the one hand, on the other they have distinct requirements for resources and often find themselves in competition for access to resources such as energy and water (Pueppke et al. 2018b). Although important for local communities near the Caspian Sea, Aral Sea, Lake Balkhash, and other larger water bodies, fisheries have traditionally been a minor, and in recent decades a neglected element of the region's food system. Fish capture declined

precipitously after the dissolution of the Soviet Union, and fish have generally lost out when natural water flows were redirected for other purposes (Graham et al. 2017; Petr 1992; Pueppke et al. 2018a; Thorpe and Van Anrooy 2010). It may not be feasible to resurrect fisheries as a viable contributor to food security in the region, but aquaculture does offer potential to substitute for fisheries, as illustrated by the post-Soviet progress made by Uzbekistan (Graham et al. 2017).

Animal herding, on the other hand, represents the traditional food production system across the region. Although constrained in some areas by lack of access to water, herding exploits the availability of spring and summer pastures on Central Asia's grassy steppes and along piedmont and higher mountain slopes (Fig. 5.1). Hay and other forages near rivers and streams serve to carry the animals over winter. It is noteworthy that Central Asia's grasslands receive little or no management, to the extent that animal agriculture is minimally dependent on water and energy inputs other than those needed to produce feed that is grown on irrigated land. The system remains viable, but there is significant potential to introduce improved management practices to the region's pastures and to supplement livestock grazing with high quality feed from forages grown on cropland.

Although a relatively recent phenomenon, extensive cultivation of crops has become the third component of Central Asia's food system. With the exception of areas such as Northern Kazakhstan, where rainfall is sufficient for dryland cultivation of grains, most food crops require irrigation and as the Soviets learned, attention to crop management. Much of the region's irrigation infrastructure was constructed during Soviet times and is now decaying, inefficient, and in many cases no longer functional. The level of modern management in the form of agricultural inputs, use of advanced plant genetics, and optimized irrigation schedules is nonetheless comparatively high, and hydraulic infrastructure is being revamped. Large tracts of irrigated lands nevertheless remain devoted to low value commodity crops such as rice and wheat. Immense tracts of irrigated lands near the Aral Sea are still reserved for production of cotton, a low value crop that competes with food crops. Cotton need not occupy valuable irrigated land that is also suitable for food production (Rakhmatullaev et al. 2017), and when such land is available, there is much potential to upgrade it with modern and efficient irrigation technology and exploit it for the production of high value food crops.

5.5 Conclusions

Central Asia's complex WEF system dynamics pose a series of challenges that are relatively simple to articulate but much more difficult to address given the region's socioeconomic and geopolitical status. Political will and significant investment clearly will be required. Systems thinking that weighs what appear to be isolated management decisions against potential tradeoffs, synergies, and unforeseen outcomes across time and space is also desirable. The same is true for acknowledgment that Central Asia, although divided into separate republics that must take their own

interests into account, depends on a common resource base for its ultimate security and sustainability. These issues, notwithstanding the fundamental sustainability challenge for the region, may well be finding the right balance and sense of primacy for use of the region's scarce water resources to produce food and generate energy while addressing the competing priorities of a globalizing world.

Acknowledgements We would like to acknowledge the financial support from NASA's Land-Cover and Land-Use Program grant (NNX15AD51G), NASA IDS grant (80NSSC17K0259), and the United States Department of Agriculture (MICL02264) through AgBioResearch at Michigan State University. We thank Shuxin Li and Yachen Xie for assistance in the creation of figures used in this chapter.

References

Abdolvand B, Mez L, Winter K (2015) The dimension of water in Central Asia: security concerns and the long road of capacity building. Environ Earth Sci 73:897–912

Abdullaev I, Rakhmatullaev S (2016) Setting up the agenda for water reforms in Central Asia. Does the nexus approach help? Environ Earth Sci 75:870

Akiyama T, Li J, Kubota J et al (2012) Perspectives on sustainability assessment: an integral approach to historical changes in social systems and water environment in the Ili River basin of Central Eurasia, 1900-2008. World Futures 68:595–627

Beckert S (2017) Empire of cotton: a global history. Vintage Books, New York

Bekchanov M, Lamers PA (2016) Economic costs of reduced irrigation availability in Uzbekistan (Central Asia). Regional Environ Change 16:2369–2387

Böhner J (2006) General climatic controls and topoclimatic variations in central and high Asia. Boreas 35:279–295

Bolch T (2007) Climate change and glacier retreat in northern Tien Shan (Kazakhstan/Kyrgyzstan) using remote sensing data. Glob Planet Chang 56:1–12

Carrère d'Encausse H (2009) Islam and the Russian empire. Tauris, London, UK

Chen J, Ouyang Z, John R et al (2020) Social-ecological systems across the Asian Drylands Belt (ADB). In: Gutman G, Chen J, Henebry GM et al (eds) Landscape dynamics of drylands across greater Central Asia: people, societies and ecosystems. Springer, Cham

Chida T (2013) Science, development and modernization in the Brezhnev time. The water development in the Lake Balkhash basin. Cahiers du Monde Russe 54:239–264

Christiansen T, Schöner U (2004) Irrigation areas and irrigation water consumption in the upper Ili catchment, NW-China. Justus-Liebig-Universität, Giessen

Dave B, Kobayashi Y (2018) China's silk road Economic Belt initiative in Central Asia: economic and security implications. Asia-Europe J 16:267–281

Dostaj ZD, Giese E, Hagg W (2006) Wasserressourcen und deren Nutzung im Ili-Balchas Becken. Justus-Liebig-Universität, Giessen

Eritja MC, Estapa JS, Rafols XP (2016) Towards improved regional co-operation over water issues in Central Asia: the case of hydroelectric energy and inland fisheries. Asian J Int Law 6:119–158

Fields D, Kochnakyan A, Mukhamedova T et al (2013) Tajikistan's Winter energy crisis: electricity supply and demand alternatives. World Bank, Washington, DC

Graham NA (2016) The prospect for regional governance of inland fisheries in Central Eurasia. In: Taylor WW, Bartley DM, Goddard CI et al (eds) Freshwater, fish and the future: proceedings of the global cross-sectoral conference. FAO, Rome, pp 333–341

Graham NA, Pueppke SG, Uderbayev T (2017) The current status and future of Central Asia's fish and fisheries. Confronting a wicked problem. Water 9:701
Granit J, Jägerskog A, Lindström A et al (2012) Regional options for addressing the water, energy and food nexus in Central Asia and the Aral Sea Basin. Int J Water Res Dev 28:419–432
Groisman PY, Bulygina ON, Henebry GM et al (2018) Dry Land Belt of Northern Eurasia: contemporary environmental changes and their consequences. Environ Res Lett 13:115008
Groisman PY, Bulygina ON, Henebry GM et al (2020) Eurasian drylands: Contemporary environmental changes. In: Gutman G, Chen J, Henebry GM et al (eds) Landscape dynamics of drylands across greater Central Asia: people, societies and ecosystems. Springer, Cham
Ho S (2017) China's transboundary river policies towards Kazakhstan: issue-linkages and incentives for cooperation. Water Int 42:142–162
Horsman S (2018) Transboundary water management and security in Central Asia. In: Sperling J, Kay S, Papacosma SV (eds) Limiting institutions? The challenge of Eurasian security governance. Manchester University Press, Manchester, pp 86–104
Kayumov A (2010) Glacier resources of Tajikistan in conditions of the climate change. State Agency for Hydrometeorology of Committee for Environmental Protection under the Government of the Republic of Tajikistan, Dushanbe, Tajikistan
Keairns DL, Darton RC, Irabien A (2016) The energy-water-food nexus. Annu Rev Chem Biomol Eng 7:239–262
Kezer K, Matsuyama H (2006) Decrease of river runoff in the Lake Balkhash basin in Central Asia. Hydrol Process 20:1407–1423
Lattimore O (1940) Inner Asian Frontiers of China. American Geographical Society, New York
Lewis RA (1966) Early irrigation in West Turkestan. Ann Assoc Am Geograph 56:467–491
Lioubimtseva E, Henebry GM (2009) Climate and environmental change in arid Central Asia: impacts, vulnerability, and adaptations. J Arid Environ 73:963–977
Lioubimtseva E, Cole R, Adams J et al (2005) Impacts of climate and land-cover changes in arid lands of Central Asia. J Arid Environ 62:285–308
Martens P (2019) The political economy of water insecurity in Central Asia given the belt and road initiative. Central Asian J Water Res 4:79–94
Micklin P, Aladin N, Plotnikov I (eds) (2014) The Aral Sea: the devastation and partial rehabilitation of a great lake. Springer, Cham
Nurtazin S, Thevs N, Iklasov M et al (2019) Challenges to the sustainable use of water resources in the Ili River basin of Central Asia. E3S Web Conf 81:01009
Olcott M (1987) The Kazakhs. Hoover Institution Press, Stanford
Pekel JF, Cottam A, Gorelick N, Belward AS (2016) High-resolution mapping of global surface water and its long-term changes. Nature 540(7633):418
Petr T (1992) Lake Balkhash, Kazakhstan. Int J Salt Lake Res 1:21–46
Peyrouse S (2013) The hydroelectric sector in Central Asia and the growing role of China. China Eurasia Forum Q 5:131–148
Pilifosova O, Eserkepova I, Dolgih S (1997) Regional climate change scenarios under global warming in Kazakhstan. Clim Chang 36:23–40
Poujol C, Fourniau V (2005) Trade and economy (second half of nineteenth century to early twentieth century). In: Palat MK, Tabyshalieva A (eds) History of civilizations of Central Asia. UNESCO Publishing, Paris, pp 51–77
Pueppke SG, Iklasov MK, Beckmann V et al (2018a) Challenges for sustainable use of the fish resources from Lake Balkhash, a fragile lake in an arid ecosystem. Sustainability 10:1234
Pueppke SG, Nurtazin ST, Graham NA et al (2018b) Central Asia's Ili River ecosystem as a wicked problem: unraveling complex interrelationships at the interface of water, energy, and food. Water 10:541
Pueppke SG, Zhang Q, Nurtazin ST (2018c) Irrigation in the Ili River basin of Central Asia: from ditches to dams to diversion. Water 10:1650
Qi J, Bobushev T, Kulmatov R et al (2012) Addressing global change challenges for central Asian socio-ecosystems. Frontiers Earth Sci 6:115–121

Rahaman MM (2012) Principles of transboundary water resources management and water-related agreements in Central Asia: an analysis. Int J Water Res Dev 28:475–491
Rakhmatullaev S, Abdullaev I, Kazbekov J (2017) Water-energy-food-environmental nexus in Central Asia: from transition to transformation. In: Zhiltsov SS, Zonn IS, Kostianoy AG et al (eds) Water resources in Central Asia: international context. Springer, Cham, pp 103–120
Redakiivey P, Samkovoy AB (2003) Problems of hydroecological stability in the basin of Lake Balkhash. Kazhydromet, Almaty, Kazakhstan. (In Russian)
Sabonis-Helf T (2018) Tajikistan's Roghun dam: understanding Rahmon's "palace of light". In: Burghart DL, Sabonis-Helf T (eds) Central Asia in the era of sovereignty. The return of Tamerlane. Lexington Books, Lanham, pp 429–452
Sokolik IN, Shiklomanov A, Xi X et al (2020) Quantifying the anthropogenic signature in drylands of Central Asia and its impact on water scarcity and dust emissions. In: Gutman G, Chen J, Henebry GM et al (eds) Landscape dynamics of drylands across greater Central Asia: people, societies and ecosystems. Springer, Cham
Sorg A, Bolch T, Stoffel M et al (2012) Climate change impacts on glaciers and runoff in Tien Shan (Central Asia). Nat Clim Chang 2:725–731
Sorg A, Huss M, Rohrer M et al (2014) The days of plenty might soon be over in glacierized central Asian cathcments. Environ Res Lett 9:104018
Starodubtsev VM, Truskavetskiy SR (2011) Desertification processes in the Ili River delta under anthropogenic pressure. Water Res 38:253–256
Stone R (2012) For China and Kazakhstan, no meeting of the minds on water. Science 337:405–407
Thevs N, Nurtazin S, Beckmann V et al (2017) Water consumption of agriculture and natural ecosystems along the Ili River in China and Kazakhstan. Water 9:207
Thorpe A, Van Anrooy R (2010) Strategies for the rehabilitation of the inland fisheries sector in Central Asia. Fisheries Mgmt Ecol 17:134–140
UNdata (2019) Coal production statistics for Central Asian countries. Available at: www.data.un.org
Wegerich K (2011) Water resources in Central Asia: regional stability or patchy make-up? Central Asia Survey 2:275–290
Wiens HJ (1969) Change in the ethnography and land use of the Ili Valley and region, Chinese Turkestan. Ann Assoc Am Geograph 59:753–775
Wittfogel KA (1957) Oriental despotism. A comparative study of total power. Yale University Press, New Haven
Xie L, Jia S (2018) China's international transboundary rivers. Politics, security and diplomacy of shared water resources. Routledge, London
Zhiltsov SS, Zonn IS, Grishin OE et al (eds) (2018) Water resources in Central Asia: international context. Springer, Cham

Chapter 6
Assessment of the Influences of Dust Storms on Cotton Production in Tajikistan

Sabur F. Abdullaev and Irina N. Sokolik

6.1 Introduction

Mineral dust is the dominant atmospheric aerosol in Central Asia (Buseck and Pósfai 1999; Jish Prakash et al. 2015; Xi and Sokolik 2012) It plays an important role in the Earth's climate system of the region, although the magnitude (and even the sign) of its radiative effect at the top of the atmosphere remains uncertain. Most airborne dust is generated in desert and semi desert areas and transported across local to global scales. Dust storms can lift millions of tons of dust into the atmospheric boundary layer. Large quantities of airborne dust cause severe air pollution, reduce visibility, shut down airports, increase traffic and aircraft accidents, and affect crop productivity (Abdullaev et al. 2012a, b, 2013; Chung and Yoon 1996; Hagen and Woodruff 1973; Middleton 1986a, b; Middleton and Chaudhary 1988; Morales 1979). Other environmental impacts of dust include reduced soil fertility, crop damage, reduced insolation at the surface and, as a consequence, decreased output from solar devices, damaged telecommunications and mechanical systems, and increased occurrence of respiratory diseases and other human health impacts (Bennett et al. 2006; Bennion et al. 2007; Fryrear 1981; Hagen and Woodruff 1973; Liu and Ou 1990; Longstreth et al. 1995; Mitchell 1971; Nihlén and Olsson 1995; Sokolik and Golitsyn 1993; Sokolik et al. 1998, 2001).

S. F. Abdullaev (✉)
Physical-Technical Institute Academy of Sciences of Republic of Tajikistan, Dushanbe, Tajikistan

I. N. Sokolik
School of Earth and Atmospheric Sciences, Georgia Institute of Technology, Atlanta, GA, USA
e-mail: isokolik@eas.gatech.edu

G. Gutman et al. (eds.), *Landscape Dynamics of Drylands across Greater Central Asia: People, Societies and Ecosystems*, Landscape Series 17,
https://doi.org/10.1007/978-3-030-30742-4_6

6.2 Dust Storms, Dust Hazes, and Their Effects

Dust storms are an active factor depleting soil through wind erosion. Initiation and development of dust storms depend on increasing aridity, fragmentation of the upper layers of soil, and the lack of vegetated cover. During dust storms, wind blows the top layer of soils, often mixed with seeds and young plants. Soil particles detach from the surface. Lighter dust particles are transported over large distances, while heavier ones fall and strike other particles that are then also involved in the overall movement of the storm. Plant roots exposed by wind erosion can desiccate, and leaves can be damaged to the extent that recovery is not possible. Dust particles suspended in the air can deposit on plant canopies through both gravitational settling and static electrical forces. Dust coatings then impair the ecophysiological functioning of the plants.

Atmospheric dust absorbs sunlight, so surface insolation under dusty conditions decreases by about 20% in the summer and about 50% in the winter (Kondratiev 1965). Dust haze (suspended dust particles) can reduce the solar radiation in the ultraviolet wavelengths by five to ten times. Dust effects can be divided into physical and chemical effects.

Physical effects, associated with the formation of a dust storm, include impeding the normal exchanges of heat and moisture between the leaves and atmosphere. Dust can disrupt stomatal apparatus, limit transpiration, contribute to the rise in leaf temperature by 2–4 °C (even by 8–10 °C in some circumstances), slow photosynthesis, especially under low light, lower the sugar level in plant tissues, reduce crop yield, and degrade crop quality. Particularly strong impacts of dust occur in hot, dry summers when leaf surfaces are bombarded with loose dust particles, causing physical damage. Chemical effects are associated with the composition of water-soluble compounds in the dust (Fig. 6.1). These compounds can enter plants and affect their photosynthetic metabolism (Abdullaev et al. 2001).

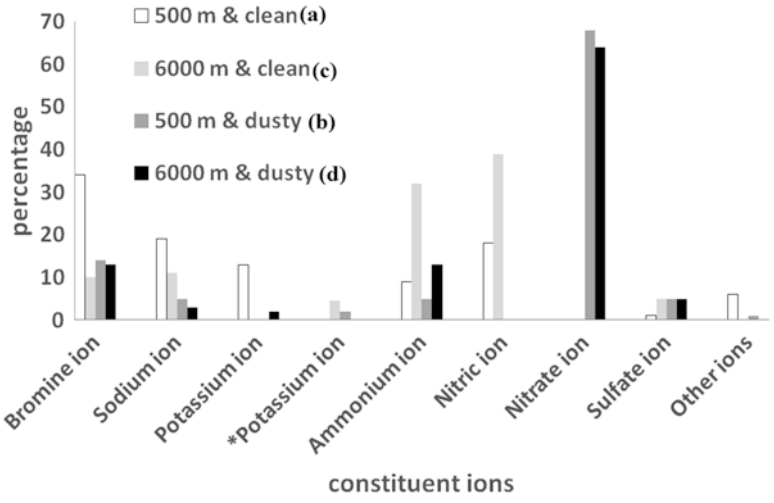

Fig. 6.1 Relative contents of soluble components (**a**–**d**) of aerosols at a height of 500 m (**a**, **b**) and 6000 m (**c**, **d**) in "clean" conditions (**a**, **c**) and during dust storms (**b**, **d**). (After Belan et al. 1993)

In general, the composition of an average dust aerosol in Central Asia includes the following chemical compounds and their percentages: SiO_2 (54%), $CaCO_3$ (11%), Al_2O_3 (10%), Fe_2O_3 (4%), MgO (2%), K_2O (2%), and Na_2O (2%), with other measured compounds at <1% (Nazarov et al. 2007). Samples of dust aerosol that were collected during dust storms at the weather station Ayvadj, Tajikistan over the period 2007–2015 have the following average content of minerals: quartz SiO_2 (44%), calcite $CaCO_3$ (17%), potassium mica $KAl_2([AlSi_3O10](OH,F)_2$ (13%), dolomite-2 $CaMg(CO_3)_2$ (8%), dolomite $CaOMgCO_3CO_3$ (6%), albite $NaAlSi_3O_8$ (6%) and clinochlore $(Mg,Al)6[Si_3, 1–2, Al)0,9–1,2O_{10}](OH)_8$ (4%) (Nazarov et al. 2007). The comparison of the values of elements in the atmospheric aerosol in a relatively clean atmosphere (09/27/2014) and in a period of dust intrusion (10/16/2014) appears in Table 6.1. Note the marked increase in most elements (aside from S and Ag) in the dusty sample.

Table 6.1 Elemental composition of atmospheric dust aerosols from Dushanbe. On relatively clean day (9/27/2014) and on a relatively dusty day (10/16/2014)

Element	9/27/2014 clean	10/16/2014 dusty	Ratio of dusty/clean
Si	16.953	**33.218**	2.0
Al	7.384	**15.669**	2.1
Ca	6.959	**30.172**	4.3
Fe	3.45	**20.426**	5.9
Na	2.24	**25.05**	11.2
K	2.116	**6.003**	2.8
S	1.713	0.963	0.6
Mg	0.915	**1.274**	1.4
Cl	0.341	**0.497**	1.5
Ti	0.309	**1.355**	4.4
Zn	0.126	**1.471**	11.7
Mn	0.086	**0.526**	6.1
Ba	0.053	**0.413**	7.8
Sr	0.03	**0.231**	7.7
Pb	0.027	**0.216**	8.0
Rb	0.013	**0.094**	7.2
Ce	0.013	**0.055**	4.2
Br	0.009	**0.036**	4.0
Co	0.008	**0.058**	7.3
V	0.006	**0.053**	8.8
Ni	0.004	**0.023**	5.8
As	0.004	**0.016**	4.0
Ag	0.004	**0.004**	1.0
Cd	0.004	**0.013**	3.3
Ga	0.003	**0.019**	6.3
Cr	0.002	**0.008**	4.0
Cs	0.002	0.014	7.0
Cu	0.001	**0.026**	26.0
Sb	0.001	0.005	5.0

Units are $\mu g/m^3$. Numbers in bold indicate high means of elements

6.3 Cotton Production and Dust Impacts on Yields

Cotton is the most ancient crop grown for fiber. A valuable plant, more than 60 countries cultivate cotton over an area of 35 Mha (India 8 Mha, USA 6.8 Mha, Brazil 2.6 Mha, Pakistan – 1.4 Mha) (Singh et al. 2007). Cotton grows in different climatic conditions and at different latitudes, from 47° north to 30° south. The average yield of raw cotton is 2810 kg/ha.

Figure 6.2a presents the sown area of cotton in the period 1913–2013. In the Soviet Union, Tajikistan annually produced more than 800,000–900,000 tons of cotton. In 1980, a record harvest was gathered of more than 1 million tons (Fig. 6.2b). Figure 6.2c illustrates the dynamics of the cotton yield, C/ha, from 1913 to 2013 in Tajikistan, and Fig. 6.2d shows the average duration of dust storms (dust haze) in the period from 1913 to 2013 in Tajikistan. During the period from 1913 to 1991, the area sown to cotton, gross cotton harvest, and productivity of cotton increased nearly monotonically. After the disintegration of the Soviet Union in 1991, all these indicators decreased due to several reasons: the civil war in the country, increasing the amount of dust events and their duration (Fig. 6.2d), and institutional changes and policy reforms by the government of Tajikistan.

Cotton is a heat-loving and light-loving plant. The temperature range is 18–30 °C, with a minimum of 14 °C and with a maximum of 40 °C (Al-Khatib and Paulsen 1990; Kramer 1980; Levit 1980), with the optimal temperature for the growth is 27–32 °C, especially during budding and flowering phases. Seeds germinate at a soil temperature of 12–15 °C, but even faster at 22–25 °C. Growth slows when the temperature drops below 12 °C at night and below 25 °C during the day. The lack of

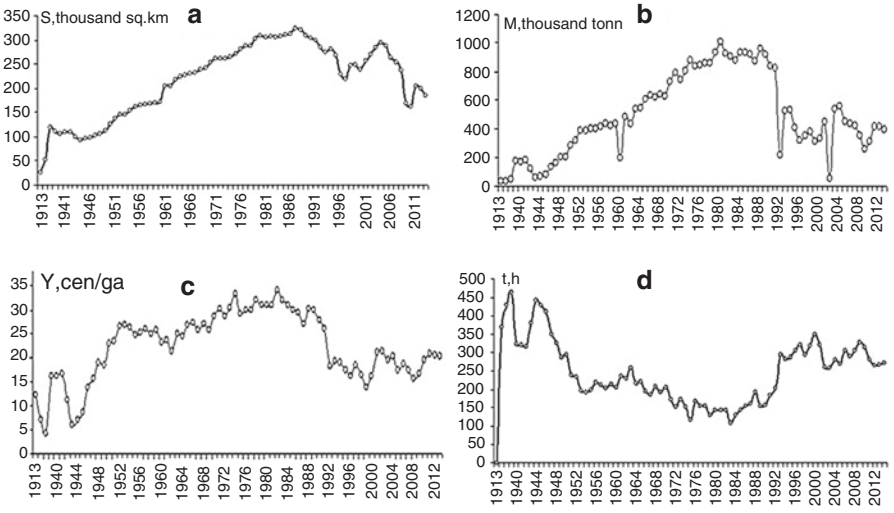

Fig. 6.2 Changes in sown areas of cotton (**a**), gross harvest of raw cotton (**b**), cotton yield (**c**) and duration of dust storms (dust haze) (**d**) from 1913 to 2013 in Tajikistan

heat begins to be especially noticeable at temperatures below 20 °C, and at 17 °C and below, the development of plants is strongly inhibited (Kuznetsov et al. 2003). However, if the temperature stays above 38° for a long time, it may cause flowers and seed pods to fall off. Timing of heat is important: a temperature increase of 1 °C in the spring or autumn months is more influential than during the summer.

Defining the length of the cotton growing season from germination to pod maturity, there are several cotton varieties: early maturity (100–110 days), medium-maturing (115–120 days), medium-late maturing (130–135 days), and late- maturing (150–170 days). Late-maturing cottons are fine-fiber varieties (Al-Khatib and Paulsen 1990; Bohnert and Sheveleva 1998; Bray et al. 2000; Kramer 1980; Kuznetsov et al. 2003; Levit 1980; McMichael et al. 1972; Pervez et al. 2004). Cotton possesses a strong root system; thus, it can use moisture from deeper soil layers, which explains its drought tolerance. Irrigation can significantly increase cotton yields. For successful growth of cotton, the following conditions must be met: (1) a long period for growth (180–200 days without frost); (2) adequate soil moisture; (3) abundant direct insolation (cloud cover above 50% slows growth); and (4) relatively high temperatures throughout the growing period (Pervez et al. 2004).

Day length has a strong influence on cotton development, but different varieties of cotton have different photoperiodic responses. During longer days, cotton development slows down and the transition to the reproductive phase lags. On a sunny day, the assimilation rate for 1 h of 1 m^2 of the leaf surface in a middle- maturing variety was 1.46 g versus early maturing variety of 1.45 g (Arutyunova et al. 1980). Thus, dust haze during and after a dust storm can limit photosynthesis by decreasing insolation that reaches the surface as well as coating the leaf surface to limit photon flux density reaching the leaves in the cotton canopy.

The temperature difference between soil and air affects plant growth and development: the larger the difference is, the better the plants grow, up to the thermal stress point of the leaves (Hatfield and Prueger 2015). Growth effects occur through temperature fluctuations and diurnal progression of temperature. The volumetric heat capacity of the air in and around the plant canopy is 0.0013 kJ/K. In contrast, the volumetric heat capacity of the ground ranges 2.05–2.43 kJ/K, depending on soil structure and composition. After the sunrise, the soil surface heats, and this heat is transferred both to the air and the soil, but the heating of the air takes place quickly and much more slowly the heating of the soil generating a soil-air temperature gradient. By noon, the difference decreases with the soil temperature approaching the ambient air temperature; before the sunset, the temperature difference reaches its minimum; and after sunset, the temperature difference grows, as the air loses heat more quickly. At night, the temperature gradually converges and then begins to diverge again as solar radiation increases. During the day, the air is warmer than the soil and the opposite at night.

There is a hypothesis that the plants grow better in the morning than in the afternoon, or after the sunset. From experience, we know that the growth and development of plants is affected by the ambient air temperature and the temperature difference between the soil and the air (Abdullaev et al. 2013; Hatfield and Prueger 2015).

Dust storms and associated strong winds leading to the destruction of the soil surface and soil erosion, which can strongly influence the course of the growing season in multiple ways, including the following: (1) depressing the ambient air temperature; (2) reducing the soil-air temperature differential; (3) smoothing sharp fluctuations in the temperature difference between soil and air; and (4) weakening photosynthesis.

Figure 6.3 shows the course of the monthly maximum and minimum air temperature and soil temperature, as well as their difference. While under normal conditions the magnitude of this contrast (difference between soil and air temperature) is an average of 23–25 °C, in the case of dust storm this contrast decrease to 0–8 °C.

In summary, it should be observed that prolonged dust storms during the growing season results in a slowing of growth and development and this, in turn, delays crop maturity, constraining the harvest period. The fluctuations of the gradient of the electric field of the earth has the following characteristic: from the temperate zone to the equator, there is a gradual fall. Under natural conditions, temperature of soil and air associated with electric factors that influence plants are shown in Fig. 6.4.

From an electrical point of view, the plant is a conductor of the second kind. With the air flowing around it on all sides, it is an excellent conductor. The plant is in a

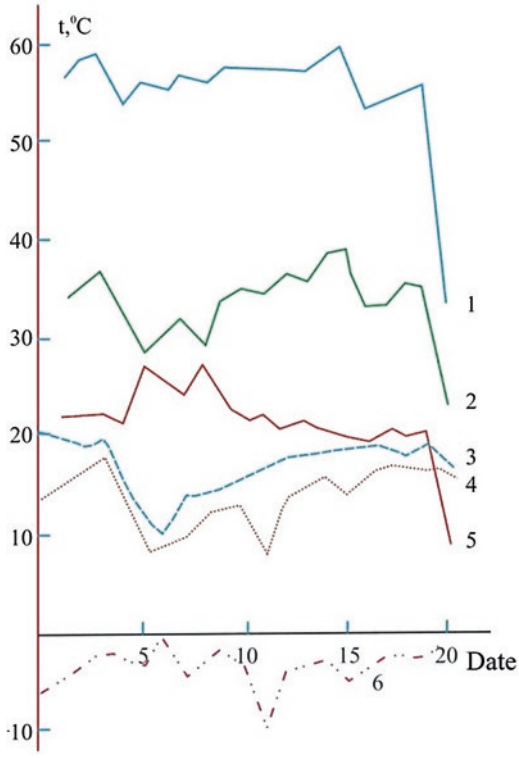

Fig. 6.3 The monthly behavior of the maximum and minimum temperatures of the air and soil and their difference (1-maximum soil temperature, 2-maximum air temperature, 3-minimum temperature of the soil, 4-minimum air temperature, 5-difference between maximum of oil and air temperature, 6-difference between minimum of soil and air temperature)

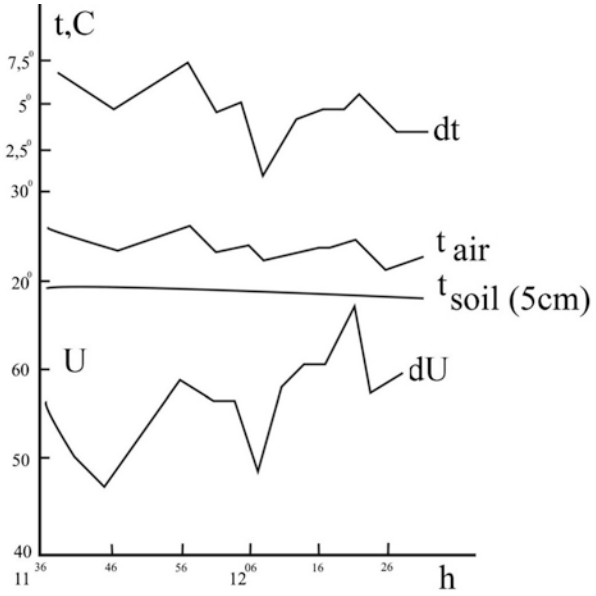

Fig. 6.4 Typical variations of the air and soil temperature, their difference, and the voltage difference under the representative natural condition

close contact with the soil, the soil takes power, as well as soil stresses, the voltage discharges from the air.

The distribution of the dust haze across the territory of Tajikistan depends on the origin of the dust, the type of synoptic processes, and surface characteristics. The annual number of days with haze from the north to the south is increasing. Hazy days are more likely during July through October, and least likely during the winter months (Abdullaev 2014). The duration of the haze, i.e., the number of days with the haze increases from the north to the south. In the north, its average duration is not more than 40 h, in the Gissar valley it rises to 200–400, and in the south up to 500–600 h per year (Abdullaev 2014).

Damages to cotton production caused by dust storms and dust haze can be divided into two parts: mechanical (or direct) damage and biological damage. Mechanical damage is associated with high wind speeds. Usually dust storms are accompanied by strong winds (speeds of more than 15 m/s). As a result of strong winds, plants may lose leaves, stems, and branches. We have considered the influence of strong winds with dust storms for the Shaartuz region in (Abdullaev et al. 2012a). The literature provides some direct results regarding the impact of dust on the development of cotton. In (Usmanov 1998) it is shown that the intensity of the transpiration of dusty leaves in the daytime is reduced to 62–69%, and the transmission of solar radiation through dust-laden leaves to the lower parts of the plant is reduced to 50–60%, so the surface temperature of the leaves increases. Losses in cotton yields due to the influence of dust aerosol reach 5–15% (Usmanov 1998).

Puri et al. (1992) investigated the positive effect of shelterbelts on the growth of cotton in India. Shelterbelts reduce wind speed by about 15–45%, depending on the season. Observations of morphological characters of plants and yield showed that the growth and yield of cotton increased by a distance four times the height of the trees downwind of the shelterbelt. Depending on the orientation of the shelterbelt, an increase from 4% to 10% in cotton yields was detected.

With wind speeds of 19–20 m/s (with gusts of 25–28 m/s) on June 20, 1987 in Kurgan-Tube, a large portion of cotton was dried and mechanically damaged up to 80% leaves, and 20% of plants were brought down. An area of 35 ha at the farm "Ayvadj" almost completely lost the cotton fields that were sown in April and early May: 80% of the plants were damaged, up to 30% of leaves were lost, as well as 50% mature fruits. Yield reduction was estimated at 10%. For cotton fields protected by forested shelterbelts, 80% of the plants were damaged, and up to 30% of leaves from individual plants were brought down growth point. Yield reduction was estimated at 5% (Abdullaev et al. 2012a).

The development of cotton is affected by dust storms and haze events in the period from the beginning of the mass flowering and before the ripening. In the beginning of this period, dust storms accompanied by strong winds have a negative influence on the formation of buds. The accumulation of sympodial branches and the formation of their bolls are the foundation for the future harvest of raw cotton. The dust haze, occurring in the flowering period of cotton, deposits large amounts of dust on the surface of the bodies of flowering of the cotton plant, slows down the fertilization process, and, thus, reduces the number of formed bolls. The effect of dust storms and haze in the southern regions of Tajikistan is stronger than in the northern districts. We have considered these effects in Kurgan-Tyube, Gissar, and Shaartuz districts of the Tajikistan (Fig. 6.5).

From all of these areas, the impact of dust storms and haze can be seen very clearly in the Shaartuz district, where the frequency of the occurrence of these dust phenomena during the growing season is very large. A downward trend in average yields is apparent due to the duration of darkness in the Shaartuz district.

Figure 6.6 shows the relationship between the yield of upland cotton varieties and the duration of the dust haze over the period of the emergence of the first leaf. The correlation coefficient of this relationship is $r = -0.77$. During 1972–1985, the greatest number of hours (206) with the haze was observed in 1983. The average yield of cotton in 1983 was the lowest (2.16 t/ha), and the smallest number of hours with haze (82) for the period of the appearance of the leaves 1 opening of cotton bolls was noted in 1973 and, therefore, the productivity of cotton was very high (3.47 t/ha). In the Shaartuz district, same dependencies were observed for the fine-fibered varieties of cotton (Figs. 6.6 and 6.7).

The majority of fine-fiber cotton varieties are local varieties, i.e., they are derived from breeding in the Kurgan-Tyube region, and so they are more resistant to such adverse phenomena like dust storms and haze than upland varieties (Figs. 6.8 and 6.9). The correlation coefficient, depending on the yield of fine-fiber cotton varieties with the duration of the period of the occurrence of haze and leaves first capsules opening, is $r = -0.65$.

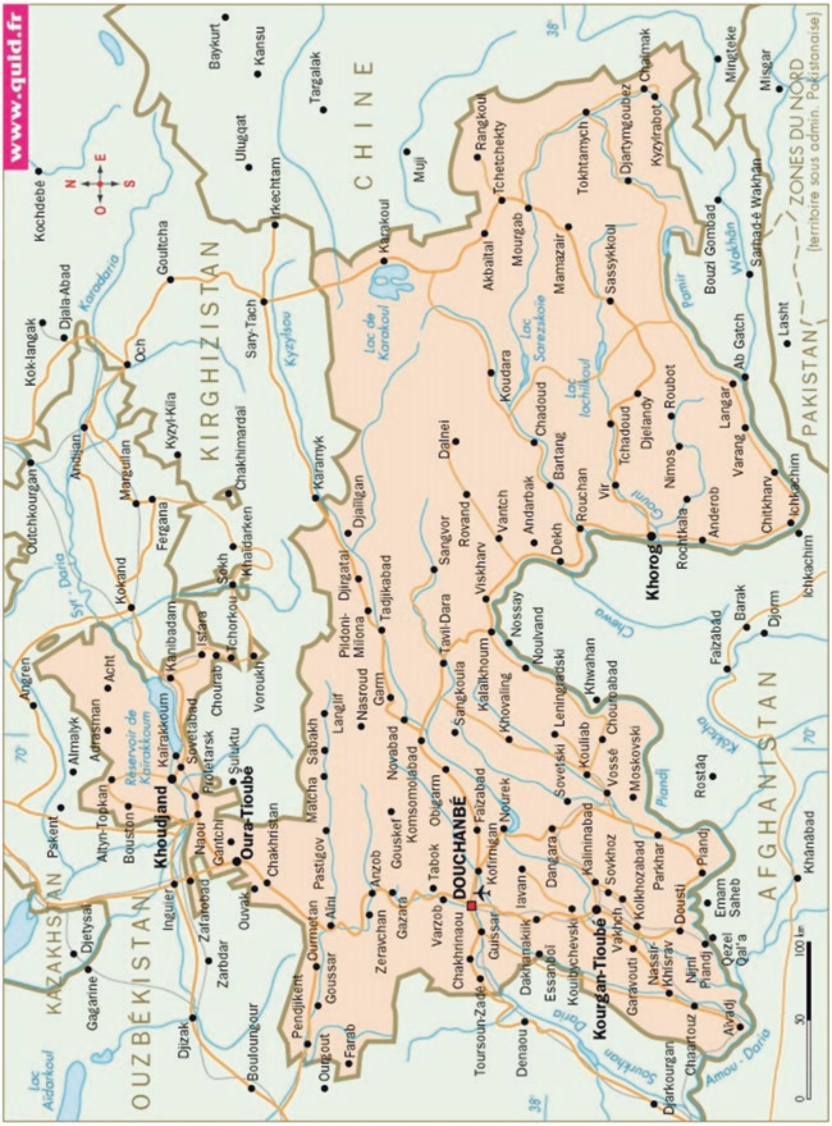

Fig. 6.5 Geographical map of Tajikistan (https://www.google.com/searchTajikistan)

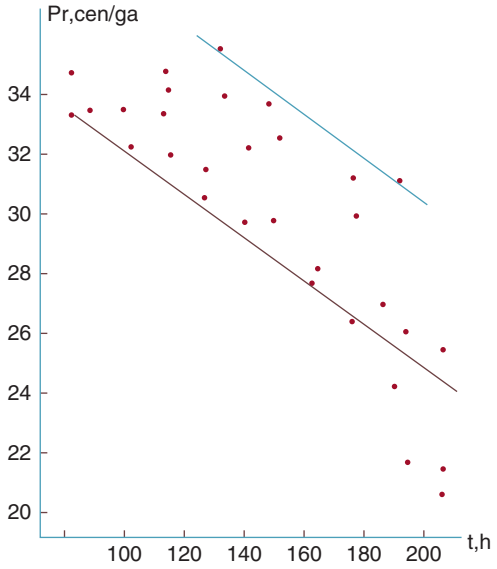

Fig. 6.6 Dependence of the cotton yield by the haze duration at the Shaartuz district for 1958–1989

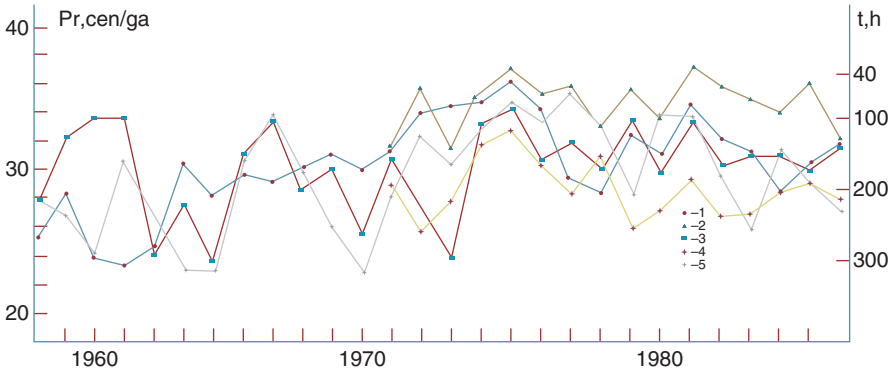

Fig. 6.7 Dynamics of the yield and the duration of the dust haze in some areas of the Republic of Tajikistan (*1* – Shaartuz-district, *2*-Kulob district, a *3*-Gissar district, *4*-Ordzhenekidzievsky district, *5*-Matcha district)

Figure 6.8 shows the average yields of upland cotton and fine-fiber varieties versus the duration of dust storms during May–September months.

Figures 6.8, 6.9, and 6.10 show the dependence of cotton yield on dust haze duration for different regions of Tajikistan.

We used the data of the yield of middle grade cotton for 1971–1986 and 1971–1983 for the fine-fiber varieties.

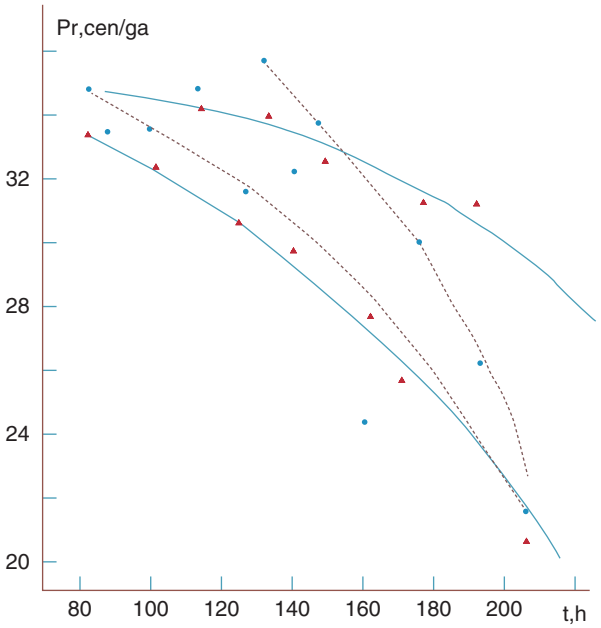

Fig. 6.8 Dependence of the yield of medium and fine-fiber cotton varieties on the total duration of the dust haze for *1*-medium (blue curves), *2*-fine fiber (red curves) for Shaartuz district for 1958–1989

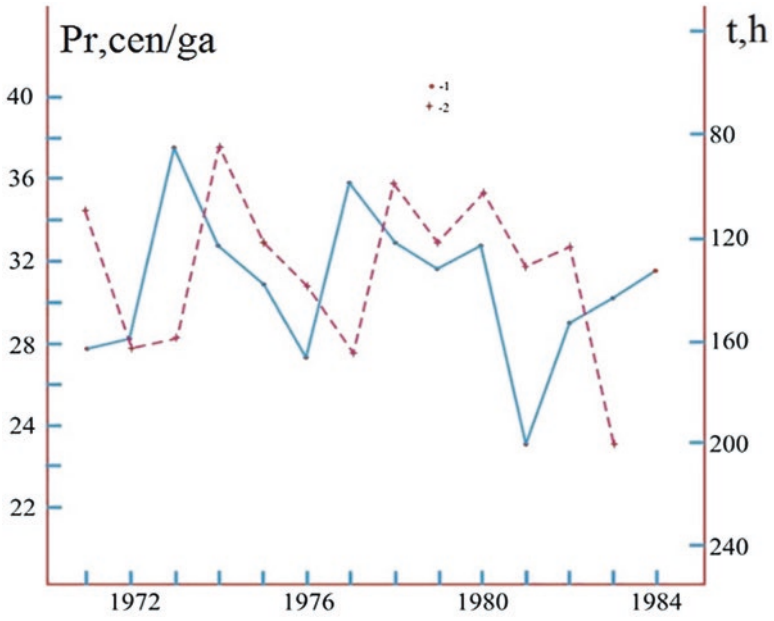

Fig. 6.9 The time series of the yield of medium and fine-fiber cotton varieties in the period from 1971 to 1984 in Tajikistan: *1*-medium fiber (red), *2*- fine fiber (blue)

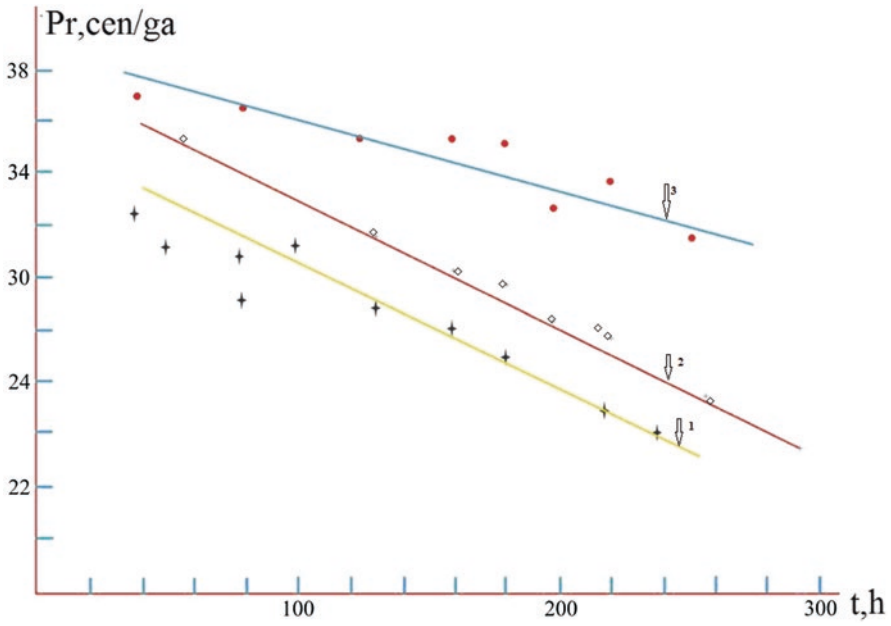

Fig. 6.10 The dependence of the cotton yield averaged for the three districts of the Republic of Tajikistan (*1* – Kulob district, *2* – Shaartuz district, and *3* – Matcha district)

As can be seen in Fig. 6.10, the yield upland varieties closely correlate with the duration of dust storms. The high cotton yields are obtained during this period that has no observed dust storms, and if observed, then with a weak intensity at the beginning of the period (1975). In 1975, cotton yield was 3.3 t/ha, and in May–September there were four times more dust storms compared to an average number. These dust storms do not have a strong intensity and occurred in May–July. Naturally, there has been a loss of the crop, but due to other soil and climatic resources and good farming practices losses were reduced. Therefore, in the soviet era in the district of the Kurgan-Tyube, the high yield of 3.5 t/ha or more was obtained when the dust storms in May and September did not occur. The harvest 3.2–3.5 t/ha was obtained when dust storms were not observed with a duration of 6 h at a weak intensity (at maximum wind speeds of 5–10 m/s). The lowest cotton yields 2.3–2.8 t/ha were obtained in the years when the dust storms were observed with a duration of 2–8 h with a strong intensity (with a wind speed of 12–16 m/s, or higher). The lowest yield of upland varieties of 2.49 t/ha, and fine-fiber grades of 2.3 t/ha were obtained in 1983, when dust storms with a moderate intensity and wind speed of 11–14 m/s were observed during the mass flowering of cotton. Thus, the yields of cotton depend on the duration of dust storms, and the correlation coefficient between upland cotton varieties and the duration of dust storms is $r = -0.84$, and for the fine-fiber varieties is $r = -0.66$.

Shaartuz and Bokhtar districts were used to investigate the influence area of haze on the productivity and yield of cotton addressing the Gissar district, but the connection was found to be very low because the haze frequency and its intensity in this region is very low. The correlation coefficient depending on the weight of 100 cotton bolls on the duration of the dust haze for the flowering period was $r = -0.55$, and the bond yields of cotton on the duration of the flowering period of the haze was $r = -0.45$.

Cumulative active temperatures (temperature more than 15 °C), expressed by the sum of long-term average temperatures and characterizing the security of a warm growing season, deviate significantly from year to year. In some years, these deviations in some areas (namely, Kurgan-Tyube, Shaartuz, and Gissar, TJ), can reach 300–500 °C, which dramatically affects the timing of the development and the productivity of plants. Thus, in years with a wide range of the heat, many crops cannot ripen at a large positive heat anomaly. Figure 6.11 shows the maximum air temperature for Kurgan-Tyube in June 1983 and July 1983 and the duration of dust storms.

During the dust storm, the maximum air temperature decreases sharply. Figure 6.12 illustrates the intensity of direct and diffuse solar radiation during a single month at Kurgan-Tyube, TJ. It shows how the intensity of direct radiation compared with the average value decreased almost twice. The intensity of the scattered radiation tends to increase over the average value of two or more times, because of the increased light scattering by dust particles (Tables 6.2 and 6.3).

Figure 6.13 presents the monthly sum of active temperatures for Shaartuz, Kurgan-Tyube, and Gissar in 2015 during the cotton growing season. The sum of active temperatures for Shaartuz, Kurgan-Tyube, and Gissar in 2015 during the growing season of cotton was 2741, 2613, and 2329 °C, respectively.

The correlations between the sum of active air temperatures and the duration of haze and dust storms shows only a modest relationship between the sums of active temperatures and the duration of the darkness, but it points to the association between a longer duration of haze and higher sum of active air temperatures (Table 6.4). Including a third factor that links the association to a specific time of year (date at which 10 °C is reached in the spring), substantially increases the strength of the correlation (Table 6.5).

In summary, these analyses provide a need for making recommendations to mitigate the impact of dust storms on crop yields: the creation of shelterbelts around agricultural crops; the establishment of forest belts near sources of dust storms; the development and the greening of desert zones; planting seedlings, steadily developing in conditions of desert areas; the creation of information stations reporting the occurrence of dust storms in areas along the path of the propagation of dust storms.

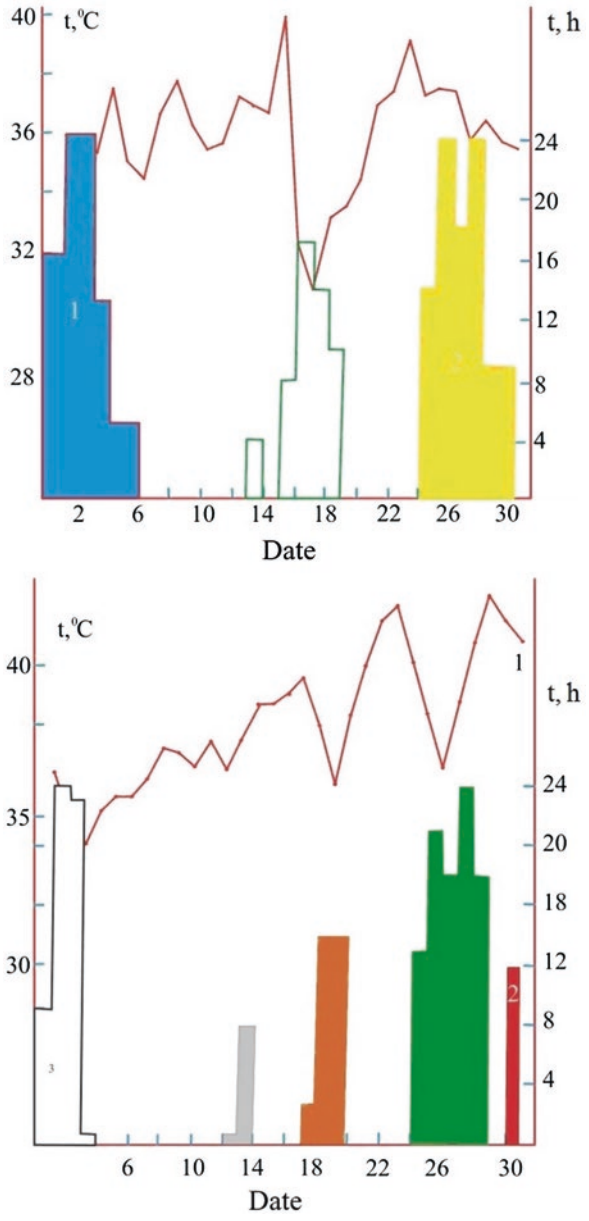

Fig. 6.11 Dependence of the maximum air temperature for the city of Kurgan-Tyube, TJ in June and July 1983 on the dust storm duration. The solid red line shows temperature, color boxes show the occurrence of dust storms

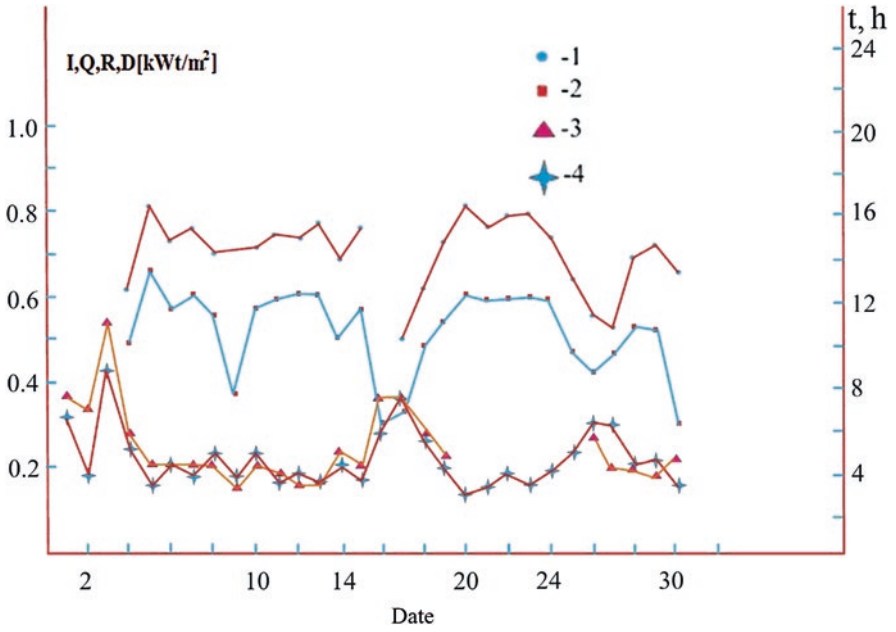

Fig. 6.12 Dependence of the intensity of direct and scattered radiation in a single month for the city of Kurgan-Tyube (*1*-total radiation Q, *2*-direct radiation I, *3*-scattered radiation D, *4*-reflected radiation R)

6.4 Conclusions

Tajikistan is in the global dust belt on the way of transport routes of dust from some major various dust sources. Dust storms significantly reduce the visibility and pose a human health threat, influence the air quality, and the quantity and quality of agricultural products. Dust plays an important role in the Earth's climate system, although the magnitude and even the sign of its radiative effect at the top of the atmosphere remain uncertain. Dust also causes a significant impact on radiative regime and temperatures. As a result, dust storms may cause a decrease in the temperature during daytime of up to 16 °C and an increase in the temperature during night time up to 7 °C compared to a clear day. In the period of Soviet Union, Tajikistan annually produced more than 800,000–900,000 tons of cotton, and in 1980 Tajikistan gathered a record harvest of more than 1 million tons. If one calculates the damage caused by strong winds and dust storms, the agriculture of Tajikistan is losing a few hundred million US dollars each year. The issues in the Tajikistan cotton production, such as water shortages, severe natural disasters, rapid increases in cultivation costs and overdependence on chemical fertilizers, should draw a greater attention of agronomists and the government. Water-saving irrigation techniques, disaster prevention measures, and mechanized manufacturing technologies should be further implemented and improved. Aim to resolve the issues of current cotton purchasing and storage policies, a new policy with references to the

Table 6.2 The cotton yield and duration of the dust haze in three districts of the Republic of Tajikistan

	Shaartuz district		Gissar district		Vahdat district	
Years	Y, 100 kg/ha	t, hour	Y100kg/ha	t, hour	Y, 100 kg/ha	t, hour
1958	25.3	260	28	208	28	208
1959	26.9	230	28.5	198	32.2	120
1960	23.8	290	24.1	282	33.5	90
1961	23.3	300	30.8	150	33.5	90
1962	24.8	270	20	180	24	185
1963	23	305	30.3	160	26.5	258
1964	22.9	308	28.2	202	22.5	315
1965	29.6	172	30.5	158	31	145
1966	29.2	182	33.6	90	33.2	98
1967	30	165	29.6	172	28.5	198
1968	30.9	149	25.9	244	29.9	168
1969	22.6	310	29.9	168	25.5	256
1970	28	208	33	145	30.5	155
1971	32	120	33.7	88	30	80
1972	30.2	160	34.2	80	23.8	290
1973	34.7	82	34.4	75	32.8	105
1974	34.4	75	35.9	49	34	83
1975	33	100	34	83	30.5	158
1976	29.2	182	35	65	30.6	132
1977	28.1	200	32.5	111	29.7	170
1978	28.2	202	32.1	120	33	100
1979	30.8	150	33.5	92	29.4	178
1980	32.8	108	33.3	95	34.1	80
1981	29.1	180	31.6	130	39.9	165
1982	25.4	259	30.8	150	30.5	155
1983	21.6	206	30.9	149	30.5	155
1984	28.6	192	30.2	160	29.7	170
1985	26.9	230	31.5	138	31	145
r	−0.94		−0.86		−0.78	
σ	3.70	69.66	3.48	55,61	3,64	62,84

foreign successful experience will need to be developed in the future, especially for the cotton subsidy policy in Tajikistan, which shall not only protect the interests of cotton farmers and take into account the interests of all aspects in the cotton industry, but also improve the market competitiveness of the entire cotton industry in Tajikistan, especially for the textile industry.

Table 6.3 Dynamics of the yield and the duration of the dust haze for the southern (Kulob) and northern (Matcha) areas of the Republic of Tajikistan

	Matcha district		Kulob district	
Years	Y, 100 kg/ha	t, hour	Y, 100 kg/ha	t, hour
1970	31.4	80	28.6	192
1971	35.3	59	25.5	156
1972	31.5	90	27.8	210
1973	34.7	70	31.4	138
1974	36.8	25	32.4	115
1975	35	65	30	165
1976	35.4	58	28.2	202
1977	32.8	65	30.5	158
1978	35.2	60	24.5	275
1979	33	65	26.8	228
1980	36.8	30	28.9	188
1981	35.2	60	26.2	240
1982	34.5	72	26.4	235
1983	33.5	92	28.2	202
1984	35.2	60	28.6	192
1985	31.9	65	27.5	215
<Y>	32.26	72.15	27.03	184.33
r	−0.76		−0.82	
σ	2.02	13.31	1.76	14.52

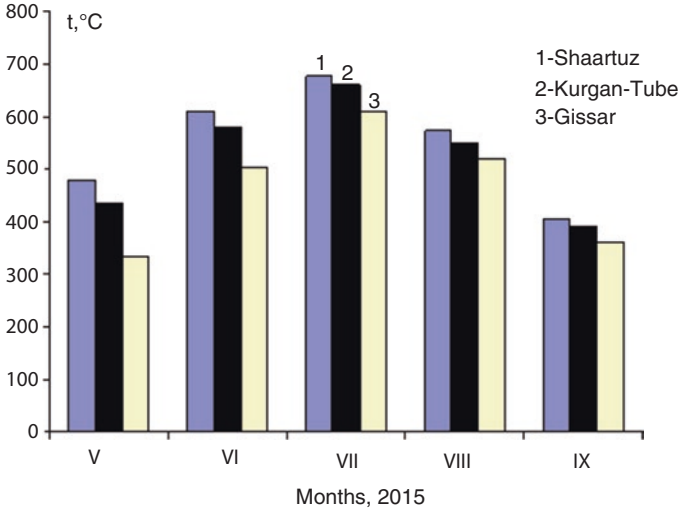

Fig. 6.13 The monthly sum of active temperatures for Shaartuz, Kurgan-Tyube and Gissar in 2015 during the growing season of cotton

Table 6.4 Simple correlation between active air temperature and duration of haze and dust storms

Location	Pearson correlation (r)
Gissar, TJ	0.56
Kurgan-Tyube, TJ	0.51
Shaartuz, TJ	0.56

Table 6.5 Multiple correlation between active air temperature, transition date of 10 °C in the spring, and duration of haze events and dust storms

Location	Pearson correlation (r)
Gissar, TJ	0.85 ± 0.05
Kurgan-Tyube, TJ	0.80 ± 0.09
Shaartuz, TJ	0.84 ± 0.08

Acknowledgments The authors are grateful to the support by the NASA LCLUC project, entitled "Multiscale synthesis of land cover and land use, climatic and societal changes in drylands of Central Asia" (NNX14AD88G) and from ISTC projects T-1688 and T-2076.

References

Abdullaev SF (2014) Complex research of the dust and gases in the arid zones and their influence on the regional climate on the south-East Central Asia. Doctoral thesis, Institute of Atmospheric Sciences, RAS, Moscow

Abdullaev AA, Abdurakhmanova ZN, Djumaev BB (2001) Photosynthetic carbon metabolism in cotton. Donish, Dushanbe

Abdullaev SF, Maslov VA, Nazarov BI (2012a) Influence of dust haze on the yield of cotton. Agric Sci 5:23–25

Abdullaev SF, Maslov VA, Nazarov BI (2012b) Influence of dust storms on the yield of pistachios and pasture grasses. Agric Sci 12:21–22

Abdullaev SF, Maslov VA, Nazarov BI (2013) Agriculture consequences dusty haze in arid zone. Agric Sci 5:4–5

Al-Khatib K, Paulsen GM (1990) Photosynthesis and productivity during high-temperature stress of wheat genotypes from major world regions. Crop Sci 30(5):1127–1132

Arutyunova LG, Ibragimov SI, Avtonomov AA (1980) Cotton biology. Kolos, Moscow

Belan BD, Kabanov DM, Panchenko MV (1993) Aircraft sounding of atmospheric parameters in the dust experiment. In: Soviet-American experiment on arid aerosol. Hydrometeoizdat, St. Petersburg, pp 26–28

Bennett C, McKendry I, Kelly S et al (2006) Impact of the 1998 Gobi dust event on hospital admissions in the lower Fraser Valley, British Columbia. Sci Total Environ 366(2–3):918–925

Bennion P, Hubbard R, O'hara S et al (2007) The impact of airborne dust on respiratory health in children living in the Aral Sea region. Int J Epidemiol 36(5):1103–1110

Bohnert HJ, Sheveleva E (1998) Plant stress adaptations – making metabolism move. Curr Opin Plant Biol 1(3):267–274

Bray E, Bailey-Serres J, Weretilnyk E (2000) Biochemistry and molecular biology of plants. Rockville: Plant Physiol:1158–1203

Buseck PR, Pósfai M (1999) Airborne minerals and related aerosol particles: effects on climate and the environment. Proc Natl A Sci 96(7):3372–3379

Chung Y-S, Yoon M-B (1996) On the occurrence of yellow sand and atmospheric loadings. Atmos Environ 30(13):2387–2397

Fryrear DW (1981) Long-term effect of erosion and cropping on soil productivity. Geol Soc Am 186:253–259
Hagen L, Woodruff N (1973) Air pollution from duststorms in the Great Plains. Atmos Environ (1967) 7(3):323–332
Hatfield JL, Prueger JH (2015) Temperature extremes: effect on plant growth and development. Weather Clim Extrem 10:4–10
Jish Prakash P, Stenchikov GL, Kalenderski S et al (2015) The impact of dust storms on the Arabian Peninsula and the Red Sea. Atmos Chem Phys 15(1):199–222
Kondratiev KY (1965) The interpretation of meteorological satellite radiation data (Meteorological satellite terrestrial UV radiation and cloud formation photographic data interpretation)
Kramer PJ (1980) Drought, stress, and the origin of adaptations. In: Tuerner, Kramer (eds) Adaptation of plants to water and high temperature stress. Wiley, New York, pp 7–20
Kuznetsov VV, Kholodova V, Kuznetsov VV, Yagodin B (2003) Selenium regulates the water status of plants exposed to drought. Dokl Biol Sci 1-6:266–268
Levit J (1980) Chilling, freezing and high temperature stress. In: Responses of plants to environmental stresses. Academic, New York
Liu C-M, Ou S (1990) Effects of tropospheric aerosols on the solar radiative heating in a clear atmosphere. Theor Appl Climatol 41(3):97–106
Longstreth JD, FRd G, Kripke ML (1995) Effects of increased solar ultraviolet radiation on human health. Ambio 24(3):153–165
McMichael BL, Jordan WR, Powell RD (1972) An effect of water stress on ethylene production by intact cotton petioles. Plant Physiol 49(4):658–660
Middleton N (1986a) Dust storms in the Middle East. J Arid Environ 10(2):83–96
Middleton N (1986b) A geography of dust storms in South-West Asia. Int J Climatol 6(2):183–196
Middleton N, Chaudhary Q (1988) Severe dust storm at Karachi, 31 May 1986. Weather 43(8):298–301
Mitchell J (1971) The effect of atmospheric particles on radiation and temperature. In: Man's inspection on the climate. MIT Press, Cambridge, pp 295–301
Morales C (1979) Saharan dust. Scope 14. Wiley, New York
Nazarov BI, Maslov VA, Abdullaev SF (2007) On influence of the dust aerosol on air temperature. Rep Acad Sci Repub Tajikistan 50(4):340–344
Nihlén T, Olsson S (1995) Influence of eolian dust on soil formation in the Aegean area. Z Geomorphol 39(3):341–361
Pervez H, Ashraf M, Makhdum M (2004) Influence of potassium nutrition on gas exchange characteristics and water relations in cotton (Gossypium hirsutum L.). Photosynthetica 42(2):251–255
Puri S, Singh S, Khara A (1992) Effect of windbreak on the yield of cotton crop in semiarid regions of Haryana. Agrofor Syst 18(3):183–195
Singh RP, Prasad PVV, Sunita K, Giri SN, Reddy KR (2007) Influence of high temperature and breeding for heat tolerance in cotton: a review. Adv Agron 93:313–385.
Sokolik IN, Golitsyn G (1993) Investigation of optical and radiative properties of atmospheric dust aerosols. Atmos Environ 27(16):2509–2517
Sokolik IN, Toon OB, Bergstrom RW (1998) Modeling the radiative characteristics of airborne mineral aerosols at infrared wavelengths. J Geophys Res 103(D8):8813–8826
Sokolik IN, Winker DM, Bergametti G et al (2001) Introduction to special section: outstanding problems in quantifying the radiative impacts of mineral dust. J Geophys Res 106(D16):18015–18027
Usmanov VO (1998) Estimation of the influence of dusty salt trensfer on the pruductivity of agricultureal crops in the Priaral region. Probl Desert Dev (3–4):147–151
Xi X, Sokolik IN (2012) Impact of Asian dust aerosol and surface albedo on photosynthetically active radiation and surface radiative balance in dryland ecosystems. Adv Meteorol 2012

Chapter 7
Population and Urban Dynamics in Drylands of China

Peilei Fan, Zutao Ouyang, Jiquan Chen, Joseph Messina, Nathan Moore, and Jiaguo Qi

7.1 Introduction

Since the launch of economic reforms in 1978, China has experienced rapid urbanization, raising its urbanization ratio threefold, from just 18% of the total population in 1978 to about 57% in 2016. This unprecedented urbanization has been fueled by a large influx of rural-to-urban migrants and accompanied by the dramatic transformation of urban landscapes across China. While most literature on China's population and urban dynamics focus on national level analysis, many have identified disparities between the east coastal, inland, and western regions (*e.g.*, Deng et al. 2008; Ma 2002; Xie and Hannum 1996; Zhang and Song 2003). However, most regional studies and city-level case studies have focused on the east coastal region (*e.g.*, Gaubatz 1999; Long et al. 2009; Yue et al. 2013).

This imbalance of regional development and studies on population and urban dynamics in Western China is due primarily to three causes. First, China's east coastal region has traditionally been the focal area for national population and economic development. Second, China's economic reforms started with the preferential policies for a number of coastal cities and provinces from the late 1970s to the 1990s, resulting in a faster pace of economic development, attracting migrants from non-coastal provinces, thus leading to a more rapid pace of urbanization in the east

P. Fan (✉)
School of Planning, Design, and Construction, Center for Global Change and Earth Observations, Michigan State University, East Lansing, MI, USA
e-mail: fanpeile@msu.edu

Z. Ouyang · J. Chen · J. Messina · N. Moore · J. Qi
Department of Geography, Environment, and Spatial Sciences, Center for Global Change and Earth Observations, Michigan State University, East Lansing, MI, USA
e-mail: yangzuta@msu.edu; jqchen@msu.edu; jpm@msu.edu; moorena@msu.edu; qi@msu.edu

G. Gutman et al. (eds.), *Landscape Dynamics of Drylands across Greater Central Asia: People, Societies and Ecosystems*, Landscape Series 17,
https://doi.org/10.1007/978-3-030-30742-4_7

coastal region than in the rest of the country. Third, the east coastal region hosts more elite research institutes and is more readily accessible to both local and international researchers, thus leading to more studies on population and urban dynamics in the east coastal region.

However, there is an urgent need to conduct studies in western China – in particular, the drylands region of Northwest China. First, urbanization has had severe environmental impacts in the drylands region, where the environment is more vulnerable to disturbance and disruption (Sietz et al. 2011; Qi et al. 2012). Second, China has gradually shifted its national developmental focus to the western region, addressing the imbalanced regional development and enhancing the role of the drylands region within its global strategy. In 2000 the central government started the National Western Development Program (Fan and Qi 2010). Recently, it advocated the high-profile One Belt One Road Initiative – a development strategy that focuses on the collaboration and connectivity between China and the Eurasian countries along the ancient Land Silk Road and Maritime Silk Road. Third, the multi-ethnicity of China's drylands region together with its rich natural resources have made the region a sensitive component for China's political stability, with its urbanization and population dynamics particularly deserving of closer examination.

This chapter will examine the region's population dynamics and urbanization from the middle of the twentieth century until 2015, with a particular focus on the period after the start of economic reforms. It will also focus on the experiences of provincial capital cities in the region, *i.e.*, Hohhot, Lanzhou, Yinchuan, and Urumqi. So far, just a few studies in English have examined population dynamics and urbanization in the drylands region (Chen et al. 2013; Dong et al. 2007; Dong and Zhang 2010; Fan et al. 2014, 2016; Li et al. 2017; Luo et al. 2010; Park et al. 2017; Sternberg 2017; Zhen et al. 2007). Some Chinese scholars have examined urbanization patterns and drivers, particularly in terms of land use change, for cities such as for Hohhot (Du 2003; Li et al. 2008; Sheng 2004), Lanzhou (Bai et al. 2008; Liang et al. 2010; Wang et al. 2007; Zhang et al. 2005), Urumqi (Dong et al. 2006; Hang and Chang 2006; Xiong et al. 2010) and Yinchuan (Chen and Gao 2007; Du 2007). Others have also studied the ecological impacts of urbanization, including formation of urban heat islands, for Hohhot (Zhang et al. 2008), Lanzhou (Huang and Zhang 2009), Urumqi (Xiong et al. 2010), and Yinchuan (Li and Tan 2009; Zhu and Zhang 2010), as well as for the whole region (Ren et al. 2006).

Based on the current literature, the main questions for this chapter are the following: (1) What are the spatiotemporal patterns of population dynamics in the drylands region of China? (2) What are the spatial and temporal dynamics of urban population change and urbanization of the region? (3) What are the spatiotemporal patterns of urban expansion of major cities in the drylands region of China over the past two decades? We also discuss the major socio-economic and institutional drivers of migration and urbanization.

7.2 Methods

7.2.1 Study Area

Administratively, China's northwestern region includes five provinces/autonomous regions: the provinces of Shan'xi, Gansu, Qinghai, Ningxia Hui Autonomous Region, and Xinjiang Uyghur Autonomous region. Here, we follow Chen et al. (2013) to identify drylands China as a region including four provinces in northwestern China: Inner Mongolia, Gansu, Ningxia, and Xinjiang (Fig. 7.1 and Table 7.1). With a total land area of 3,340,197 km^2, drylands China occupies 35% of the national territory. The annual total precipitation of the four drylands provinces are far below 500 mm, indicating that the region is a typical region for drylands farming (FAO 2018), with ~154 mm for Xinjiang, ~200 mm for Ningxia, ~220 mm for Inner Mongolia, and ~300 mm for Gansu in 2010. The dominant land cover types are barren and sparsely vegetated land, temperate grasslands, and croplands (Chen et al. 2013).

The region hosts a total population of 82 million people, *i.e.*, 6% of the national total, in its vast territory, leading to a low population density of 24 persons/km^2 that is less than one-fifth of national average. The drylands region lagged behind the average economic development level of China with a Gross Domestic Product per

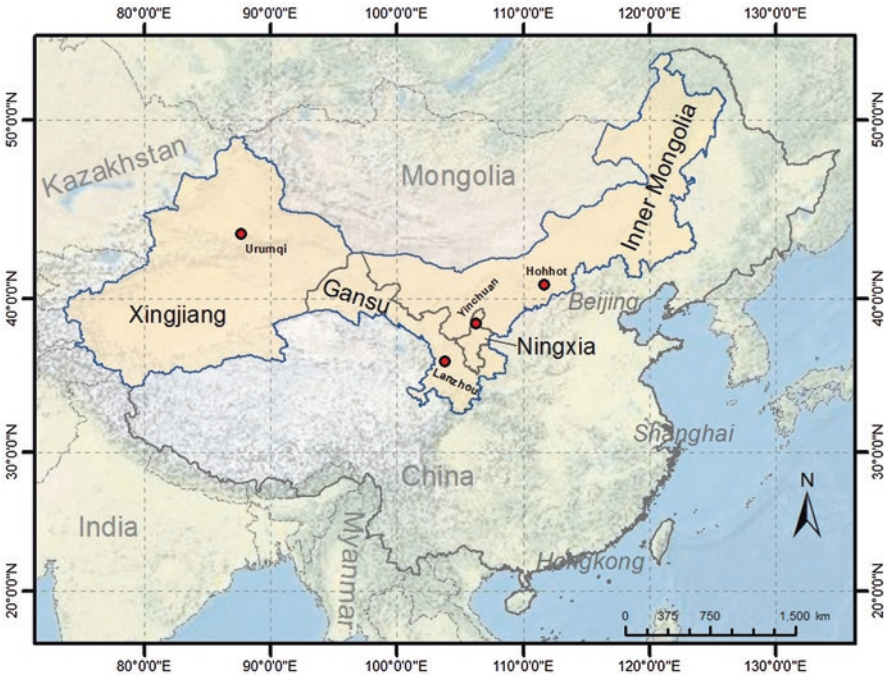

Fig. 7.1 Drylands China and its four provinces: Inner Mongolia, Gansu, Ningxia, and Xinjiang

Table 7.1 Profile of study area: drylands China and the four drylands provinces in 2016

	Land area (km^2)	Capital city	Population (million)	Urbanization (%)	Ethnic minority (%)	GDPpc (US$)
Inner Mongolia	1,183,000	Hohhot	25.2	61.2	24.7	10,853
Gansu	425,900	Lanzhou	26.1	44.7	9.9	4163
Ningxia	66,400	Yinchuan	6.75	56.3	36.9	7108
Xinjiang	1,664,897	Urumqi	23.98	48.4	63.5	6109
Total	3,340,197	*n.a.*	82.03	51.8	32.2	7004
% of China	34.8	*n.a.*	5.9	5.4	22.1	86.2
China	9,596,900	Beijing	1382.71	57.4	8.5	8130

Source: Various statistical yearbooks of the four provinces. Data on ethnic minorities are from 2015

capita (GDPpc) of $7004 in 2016 in contrast to the national average of $8130. However, the economic development level of the provinces in the region can be sorted in decreasing order – Inner Mongolia, Ningxia, Xinjiang, and Gansu – with a GDPpc of Inner Mongolia 33% greater than the national average. Three of the four drylands provinces are ethnic autonomous regions: Mongols in Inner Mongolia, Huis in Ningxia, and Uyghurs in Xinjiang. The drylands region thus hosts 22% of ethnic minorities in China. Also, nearly one-third (32%) of its total population is comprised of ethnical minorities.

All provincial capitals of drylands China feature semi-arid climates with low annual temperature and precipitation. All four have long cold winters, but the summers differ. While Yinchuan and Hohhot have hot and humid summers, Urumqi has hot, dry summers, and Lanzhou has short summers that are mild. Most of the cities are surrounded by mountains and developed their urban areas along rivers. Surrounded by Daqing Mountain to its north and the Yellow River and Hetao plains to its south, Hohhot is located on the Tumuochuan Plain, the south-central part of Inner Mongolia. Bounded by mountains on the south and north sides, Lanzhou is located in the upper course of the Yellow River and over the years its urban core developed into a dumbbell shape; the distance between the west and east ends of the city is ~35 km and ranges between 2 and 8 km north to the south. Lying between mountains to its southwest and northeast and the Toutun River in the north, Urumqi is located at the northern slope of the Tianshan Mountains and the southern edge of the Junggar Basin in the central north part of Xinjiang. With Helan Mountain to its west and the Yellow River running through the city from southwest to northeast, Yinchuan is located in the middle of the Yinchuan Plain.

These cities serve as the provincial centers for economic development and political and cultural activities (Table 7.2). All four cities are prefecture-level cities, or province-controlled cities, *i.e.*, the second level administrative units under the first level of administrative units of the provinces, autonomous regions, and municipalities. In China, prefecture-level cities include not only the urban built-up area as its core, but also a vast surrounding rural area. Similarly, a prefecture-level city's population includes not only urban population but also non-urban population. Except

Table 7.2 Profile of provincial capital cities: total and urban population, Gross Domestic Product per capita (GDPpc), and population density

	1995			2016				
							Pop. density	
	Total pop.	Urbanization	GDPpc	Total pop.	Urbanization	GDPpc	Total	City
City	Million	%	US$	Million	%	US$	Persons/km^2	Persons/km^2
Hohhot	1.8	44	850	3.1	68	15,473	139	630
Lanzhou	2.7	53	1629	3.7	81	9218	280	1691
Yinchuan	0.9	54	1126	2.2	76	11,188	194	272
Urumqi	1.4	82	1413	3.5	62	10,481	243	608

Total population refers to population with household registration (Hukou) in 1995, but residential population in 2016. Since 2008, China has used residential population as a base to calculate GDPpc at the regional and local level levels. Therefore, GDPpc in 2016 is based on residential population whereas GDPpc in 1995 is based on Hukou population. Population density, both population density of total and city proper, of Lanzhou and Urumqi are figures of 2015

Yinchuan, each city had over three million people in 2016, with more than 60% as urban population. The provincial capital cities had much higher GDPpc than the province averages, ranging from 1.4 times in Hohhot to 2.2 times in Lanzhou. Not surprisingly, population density of each city proper is much larger than the respective total administrative areas, especially for Lanzhou at 1691 persons/km^2, which is two times greater than that of Hohhot or Urumqi (~600 persons/km^2), and eight times higher than that of Yinchuan (272 persons/km^2). All have experienced rapid urbanization and vast urban sprawl in the recent decades with the main land use conversions being urban land converted from agricultural land and the conversion of other non-urban types of lands to agricultural usages (Fan et al. 2013).

7.2.2 Data and Methods

7.2.2.1 Urban Built-Up Land of the Drylands Region and the Provincial Capital Cities

For urban built-up land data, we used the Global Human Settlement Layer (GHSL) product (http://ghsl.jrc.ec.europa.eu/datasets.php), which provides global urban built-up distribution at 38 m, 250 m, and 1 km spatial resolution for the years 1975, 1990, 2000, and 2014. We used the 250 m resolution GHSL product for computing the total urban built-up area for each province of our study area. To demonstrate the detailed distribution within the administrative boundary of the cities, we used the 38 m resolution GHSL product. The GHSL built-up grid was assessed to have an overall accuracy of 89% (Pesaresi et al. 2016) using 3826 sample raster tiles collected from cartography data (which covers an area of 133,909 km^2 with a total built-up area of 4656 km^2). A comparison of multiple human settlement products from two Central European test sites also suggests that the GHSL not only preserves the fine-scale complexity of global human settlement patterns beyond urban core areas, but also greatly enhances pixel-based absolute accuracy (>80% overall accuracy) compared to previous products such as MODIS 500 m Map of Global Urban Extent (MOD500) (Schneider et al. 2010) and Globcover (GLOBC) (Bontemps et al. 2013; Klotz et al. 2016).

7.2.2.2 Demographic, Socio-Economic, and Environmental Data and Analysis

We also collected other data such as statistics on economic, demographic, and environmental indicators from a variety of sources, including the China Statistical Yearbook and statistical yearbooks from the Bureau of Statistics for each province.

We calculated migration for each province from 1950 to 2015 by using the annual population change, birth rate, and death rate. After we obtained data on the urban and total population of each province from 1950 to 2015, we calculated the overall degree of urbanization for drylands China.

To have a deeper understanding of the population and urbanization of drylands China, local experts in the four provinces and case cities were consulted on data and possible drivers for the changes in migrant and urban populations and urban built-up land at both province and city levels. We divided total population by total administrative area to obtain the population density of a city. Similarly, we divided the population of a city proper by its area to obtain the population density of the city proper, which can be used as a proxy of urban population density. We also obtained data on air quality of the cities from various annual editions of the China Statistical Yearbook.

7.3 Findings

7.3.1 Population Dynamics

From 1950 to 2015, drylands China increased its total population by 3.6 times, from 22 million in 1950 to 81 million in 2015. With the exception of Gansu, the region and its provinces have increased their populations steadily in recent decades (Fig. 7.2a). In 2015, Gansu and Inner Mongolia were the two most populous provinces with 26 and 25 million people, respectively. Ningxia is a small province with a population of 6.6 million in 2015, which is only about a quarter of Gansu's population.

There are several characteristics of immigration, defined here as net population moving into the province (Fig. 7.2b). First, the region generally experienced migrant inflow except for 2001–2004 and 2009–2013. Second, during or right after China experienced the great famine from 1958 to 1962, three provinces experienced a huge outflow of migrants: Gansu from 1960 to 1963, Inner Mongolia from 1961 to 1962, and Xinjiang from 1962 to 1963. Different provinces experienced differential levels of impact: while Gansu was seemingly the most seriously affected with about 925,000 emigrants from 1960 to 1963, Inner Mongolia had 666,000 people move out from 1961 to 1962. Xinjiang experienced 304,000 people moving out of the province from 1962 to 1963, which was the only period of net emigration that occurred before 1980s. Third, after the economic reform, Inner Mongolia had two extended periods – a total of 16 years – that experienced net out-migration, from 1985 to 1995 and from 1999 to 2005. Fourth, Gansu province experienced continuous net outmigration from 2000 to 2015.

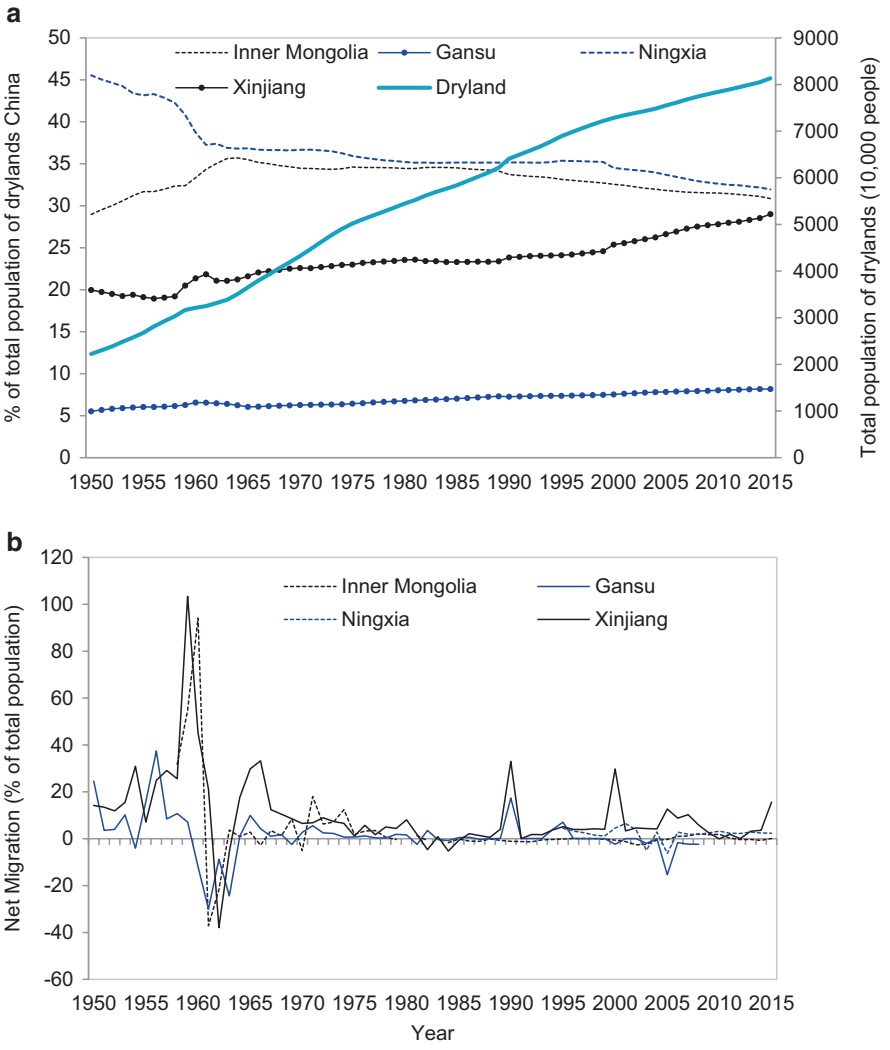

Fig. 7.2 Population dynamics of drylands China and its provinces, 1950–2015: (**a**) Total population change; (**b**) Net migration at the provincial and regional levels

7.3.2 Urban Population Change and Urban Built-Up Land in the Provinces in Drylands China

Urbanization in drylands China generally followed the national trend (Fig. 7.3). However, while the region was ahead of the country in terms of its urbanization ratio from 1965 to 1999, it fell behind the national average from 2000 on. Among the four provinces, Inner Mongolia was the most urbanized province and maintained

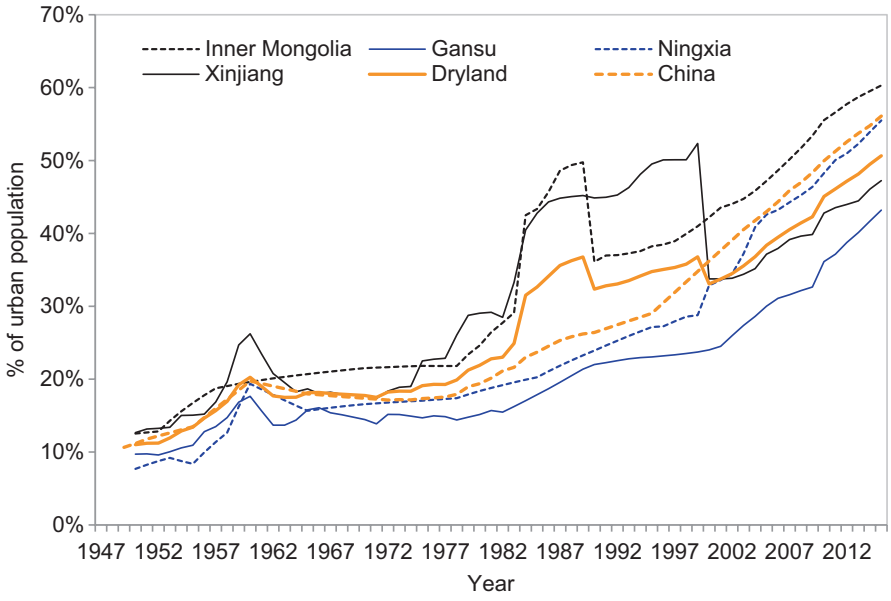

Fig. 7.3 Proportion of urban population of Inner Mongolia, Gansu, Ningxia, Xinjiang, drylands China, and China from 1947 to 2015

Table 7.3 Urban built-up area in the drylands provinces and region at four epochs. The annual expansion rate of urban built-up area of a period is calculated by first dividing the expanded area of a period by the urban built-up area at the beginning period, then dividing the outcome by the number of years in the period

	Urban built-up area (km^2)				Annual expansion rate			Expansion (times)
Year	1975	1990	2000	2014	75–90	90–00	00–14	75–14
Inner Mongolia	262	691	855	1284	10.9%	2.4%	3.6%	4.9
Gansu	231	379	446	606	4.3%	1.8%	2.6%	2.6
Ningxia	7	39	57	136	28.8%	4.4%	10.0%	18.4
Xinjiang	196	284	332	394	3.0%	1.7%	1.3%	2.0
Drylands China	696	1393	1689	2420	6.7%	2.1%	3.1%	3.5

its level above the national average, with Ningxia, Xinjiang, and Gansu trailing behind. While the four provinces started with small differences in their urbanization rates, from 7.7% for Ningxia and 12.7% for Xinjiang in 1950, the differences grew over the years, becoming 43.2% for Gansu and 60.3% for Inner Mongolia in 2015. Urban built-up land of the region expanded by 3.5 times from 1975 to 2014 (Table 7.3). However, wide variation exists, with Ningxia expanding the most (by 18.4 times), and Xinjiang expanding the least, by only two times.

7.3.3 *Urban Expansion in Drylands Provincial Capital Cities and Environmental Impacts*

All four provincial capitals experienced rapid expansion, although with distinct speeds and spatial patterns (Table 7.4). In 1975, Urumqi and Lanzhou had much larger urban built-up areas at 143.5 and 152.1 km^2, respectively, than those of Hohhot and Yinchuan at 26.1 and 4.4 km^2, respectively. Both cities remained on top in 2014 with their extended built-up areas of 213.8 km^2 and 199.4 km^2. When compared with the expansion rate, we found that Yinchuan, the city with the smallest urban built-up area in 1975 of 4.4 km^2, experienced the most dramatic expansion of a factor of 9.9 times, expanding its urban built-up land to 43.5 km^2 in 2014. In contrast, Urumqi and Lanzhou experienced expansion by factors of 1.5× and 1.3×, respectively, from 1975 to 2014 and Hohhot fell somewhere in the middle, expanding by 4.4 times, *i.e.* from 26.1 km^2 in 1975 to 121.6 km^2 in 2014. It is interesting to note that the capital cities usually showed a lower rate of urban land expansion than that of their respective provinces. While this trend echoes the findings of Xu and Zhu (2009) that large cities grew slower than small cities in China in the 1990s, it is in contrast with the findings of Fan et al. (2018a, b) who found that large cities grew faster than the country's average in Vietnam from 1990 to 2010.

Urban expansion at the provincial level had distinct speeds for different periods. Annual urban built-up land at the provincial level and for the region expanded the fastest from 1975 to 1990, followed by the period from 2000 to 2014, with 1990–2000 showing the slowest annual expansion rate (Table 8.3). Capital cities followed the same pattern except for Urumqi, whose annual expansion rate for 2000–2014 was slightly higher than that of 1990–2000 (Table 7.4).

Air quality indicators (AQIs) for the provincial capital cities illustrate urban environmental changes (Table 7.5). Overall, the cities seem to have divergent trends: Urumqi and Lanzhou generally improved their AQIs; whereas Yinchuan and Hohhot moved in the opposite direction. In terms of SO_2 concentrations, all cities reduced their pollutant levels by 2016, despite Hohhot and Yinchuan having higher levels in 2013. For NO_2, three cities had effectively stable levels from 2003 to 2016, but Urumqi showed a substantial decrease between 2013 and 2016. For PM_{10}, all cities reduced their average annual concentration levels. For $PM_{2.5}$, although China only began publishing values of $PM_{2.5}$ of cities in 2013, data from this short period revealed that all cities except Yinchuan decreased their concentration levels. In

Table 7.4 Urban land expansion in the provincial capital cities of drylands China

	Urban built-up area (km^2)				Annual rate			Expansion (times)
Year	1975	1990	2000	2014	75–90	90–00	00–14	75–14
Hohhot	26.1	75	86.8	121.2	12.5%	1.6%	2.8%	4.6
Lanzhou	152.1	178.7	185.7	199.4	1.2%	0.4%	0.5%	1.3
Yinchuan	4.4	18.1	24.0	43.5	20.8%	3.3%	5.8%	9.9
Urumqi	143.5	180.6	195.6	213.8	1.7%	0.8%	0.7%	1.5

Table 7.5 Selected air quality indicators of provincial capital cities

	1998	2003	2010	2013	2016
Annual average concentration of sulphur dioxide (SO_2) ($\mu g/m^3$)					
Hohhot	n.a.	39	49	56	28
Lanzhou	n.a.	86	59	33	19
Yinchuan	83	63	44	77	57
Urumqi	104	96	93	29	7
Annual Average concentration of nitrogen dioxide (NO_2) ($\mu g/m^3$)					
Hohhot	n.a.	46	40	40	42
Lanzhou	65	50	43	35	57
Yinchuan	n.a.	37	31	43	37
Urumqi	87	54	68	61	18
Annual average concentration of particulate matter (PM_{10}) ($\mu g/m^3$)					
Hohhot	n.a.	116	74	146	95
Lanzhou	632	174	150	153	132
Yinchuan	n.a.	132	90	118	111
Urumqi	504	127	140	146	55
Annual average concentration of $PM_{2.5}$ ($\mu g/m^3$)					
Hohhot	n.a.	n.a.	n.a.	57	41
Lanzhou	n.a.	n.a.	n.a.	67	54
Yinchuan	n.a.	n.a.	n.a.	51	56
Urumqi	n.a.	n.a.	n.a.	88	30
Days of air quality of Grade I and II (days) (% of the total year)					
		2003	2010	2013	2016
Hohhot		286 (82%)	346 (94%)	213 (58%)	283 (78%)
Lanzhou		207 (57%)	236 (65%)	193 (53%)	243 (67%)
Yinchuan		291 (80%)	328 (90%)	249 (68%)	252 (69%)
Urumqi		282 (77%)	262 (72%)	184 (50%)	330 (90%)

Source: China Statistical Yearbook, various years

China, a city's air quality, indicated by the overall air pollution index (AQI), is categorized into one of five grades. While Grades I and II refer to excellent and fine air quality, Grades III, IV, V represent light, medium, and heavy degrees of air pollution. Each pollutant has a calculated AQI and the overall AQI is the maximum AQI of all the pollutants included. The overall AQI was calculated based on the AQIs of SO_2, NO_2, and PM_{10} until 2013, when it expanded to include other three pollutants: CO, $PM_{2.5}$, and O_3. In terms of number days of air quality with grades I and II, Hohhot and Yinchuan decreased their values while Lanzhou and Urumqi increased their values from 2003 to 2016.

Urumqi has made the most impressive progress among the four cities and had the best overall air quality in 2016. It had the largest number of days of air quality of Grades I and II (90% of the year), as well as the lowest concentrations of SO_2, NO_2, PM_{10}, and $PM_{2.5}$ in 2016. In contrast, it was the city with the worst air quality in 2003, as indicated by highest concentrations of SO_2, NO_2, and the second lowest number of days of air quality of Grades I and II (Table 7.5).

7.4 Discussion

7.4.1 Possible Drivers for Population Dynamics

Although confirming specific driving factors behind the observed population changes is beyond the scope of this chapter, we can identify possible factors influencing migration; namely, migration policies for the Han ethnicity, occurrence of natural disasters, and economic opportunities. First, the general increasing population of the region and the migrant dynamics (Fig. 7.2) confirmed that the central government's policy to migrate Han Chinese from inland was effective, especially in Xinjiang, whose Han population increased from 7% in 1953 to 32% in 1964, and further increased to 60% in 1982. Second, the great famine from 1958 to 1962 caused massive internal migration as people sought means of survival (Dikötter 2010; Sternberg 2017), and drylands China was no exception to this trend. Migration is a common disaster coping strategy, both in drylands (Lioubimtseva and Henebry 2009) and in temperate climates (Gráda and O'Rourke 1997). Third, the emigration occurring in Gansu and Inner Mongolia after economic reforms may be associated with the level of economic development of these two provinces and the prospects for economic opportunities in other provinces. Gansu's low level of economic development likely contributed to the emigration; it had the lowest GDPpc in China with US$4163, or 51% of the national average of US$8130 in 2016.

7.4.2 Urban Expansion

The economic reforms of 1978 may have stimulated urban expansion nationwide, including in drylands China. However, the stagnant pattern in the 1990s contrasts with the period after 2000, appearing to confirm that the region benefited from the West Development Program, a central government initiative launched in 2000 (Fan and Qi 2010; Park et al. 2017; Schneider et al. 2005).

The spatial patterns of the urban expansion (Fig. 7.4) show a leapfrogging of traditional physical obstacles, such as mountains, to urban growth. After 2000, Lanzhou and Urumqi developed substantial urban areas beyond prior physical barriers (Fan and Qi 2010; Fan et al. 2013, 2014, 2016, 2018a, b).

We recognize that ethnic minorities are an important component of the drylands region, although we did not attempt in this chapter to link the ethnic minority populations with their spatial pattern aggregations or their influences on urbanization dynamics. Although a suite of factors contribute to regional ethnic conflicts, an intermingled spatial pattern of ethnic populations may lead to better understanding between the Han and ethnic minorities, as can be seen in Inner Mongolia and Hohhot (Fan and Qi 2010; Fan et al. 2016; Wang 1997).

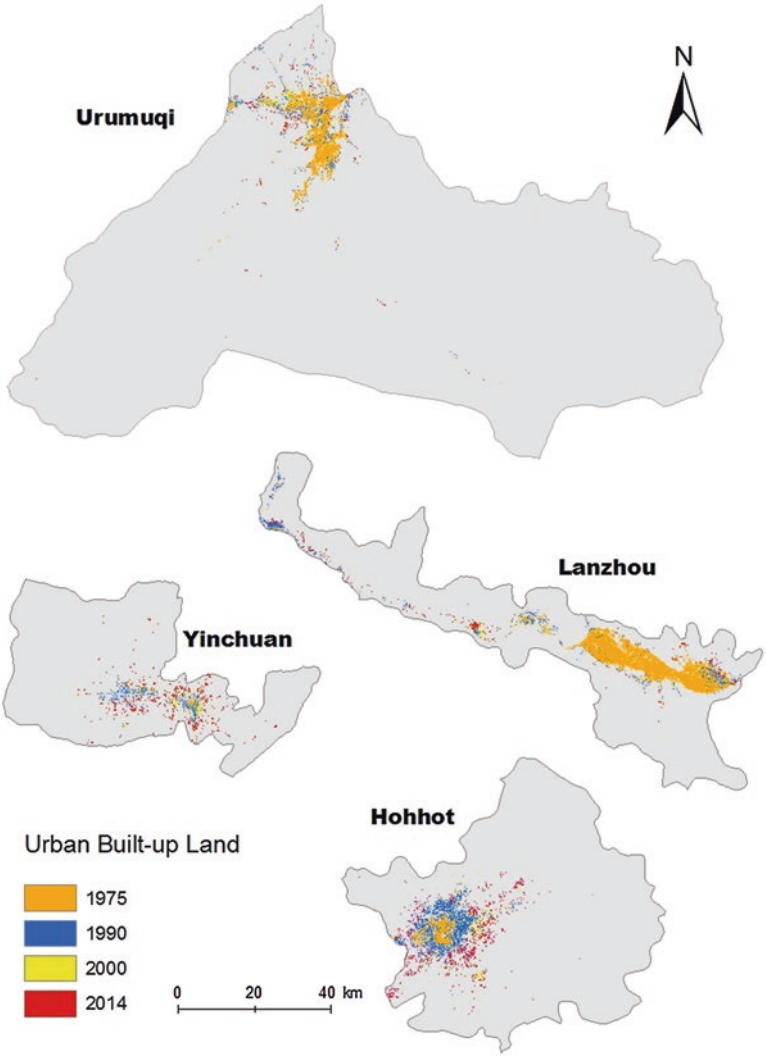

Fig. 7.4 Spatial extent of urban land expansion in the provincial capital cities of drylands China. The gray boundaries are the administrative boundaries of four cities. The four colors of orange, blue, yellow and red represent the urban built-up land in 1975, 1990, 2000, and 2014, respectively

7.4.3 Urbanization in the Context of Drylands

Drylands have specific vulnerability-creating mechanisms that threaten the wellbeing of humans and ecosystems alike (Safriel et al. 2005; Sietz et al. 2011). For example, according to global categorizations of drylands vulnerability (Sietz et al. 2011), drylands in Asia have a large range from the extremely vulnerable Afghan

deserts to the least vulnerable drylands in industrialized nations such as Israel. In the middle are the drylands with modest vulnerability, such as those in China, where poverty is relatively low and threats arise primarily from water stress, soil degradation, and food insecurity driven by climatic factors.

The overall climatic trend in Asian drylands is characterized by more extreme climatic events, higher average temperatures, and lower but uncertain precipitation amounts, except in Xinjiang Province, with a general impact on higher average temperature for drylands cities (Abdullaev and Sokolik 2020, Chap. 6; Cherednichenko et al. 2015; Groisman et al. 2020, Chap. 2; Henebry et al. 2020, Chap. 3; Hijioka et al. 2014; Lioubimtseva and Henebry 2009; Qi et al. 2012). Complex interactions of climate, ecosystems, and society make it difficult to develop adaptation strategies for the drylands in Asia (Chen et al. 2020, Chap. 10; Ford et al. 2015; Lioubimtseva and Henebry 2009; Qi et al. 2012, 2020, Chap. 5; Sokolik et al. 2020, Chap. 4; Spaeth et al. 2020, Chap. 8). When we compared our findings with other major cities in drylands Asia, we found that major cities in China's drylands are usually smaller in urban built-up area than other major cities in drylands Asia, with the exception of Kabul (Fig. 7.5). Urumqi, the city with the largest urban built-up area in drylands China, had an urban built-up area that was less than 1/8 that of Istanbul, 1/5 that of Teheran, and 1/4 that of Tashkent in 2014, the three largest cities in the region. However, they shared a similar trend of rapid urbanization with other cities in drylands Asia in terms of the increase in urban built-up area from 1975 to 2014 (Fig. 7.5). Changing climate, coupled with political and policy changes, led to dramatic increases of intensified human activities and further caused degradation of ecosystems of the drylands region (Qi et al. 2012). Urbanization can be viewed as one effective adaptive strategy to deal with these changes as cities are often considered as lands of hope for rural-to-urban migrants pushed by the destitution of rural areas. We echo the conclusion of Portnov and Safriel (2004) who based their research on the Negev region, Israel: urbanization, if properly managed and regulated, may be a better future development scenario than agriculture development as it has the potential to reduce the spatial extent of the disturbed area, minimizing the anthropogenic impact on desert environments.

7.5 Conclusions

Drylands of western China, an extensive region with a variable environment, has experienced dynamic migration patterns along with dramatic urban expansion in the past six decades. This chapter assessed population dynamics and migration from the middle of the twentieth century until 2015 and urbanization after the beginning of economic reforms in China. From 1950 to 2015, drylands in China increased their total population by 3.6 times, from 22 million in 1950 to 81 million in 2015, and experienced migrant inflow during most years. Three out of the four provinces, *i.e.*, Gansu, Inner Mongolia, and Xinjiang, experienced a huge outflow of migrants in the late 1950s and early 1960s. After the economic reforms, Inner Mongolia had

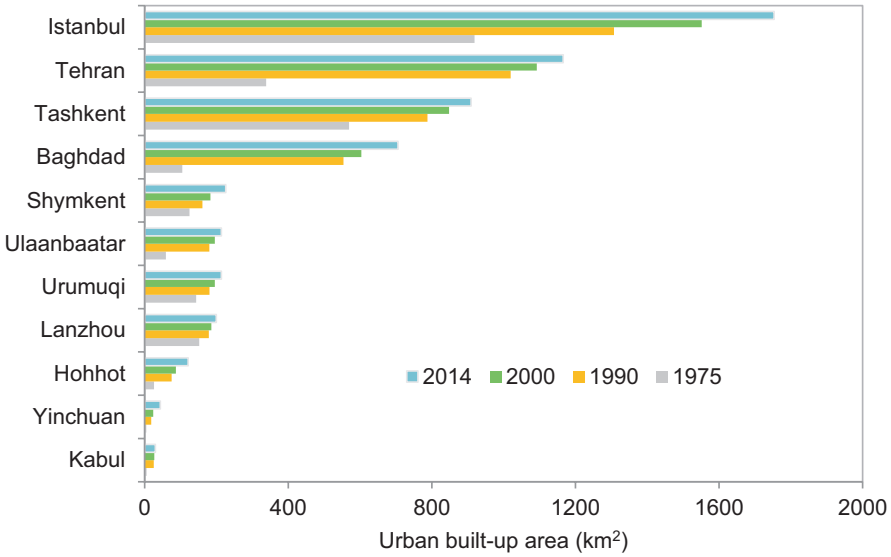

Fig. 7.5 Urban expansion of major cities in Asian Drylands Belt (ADB)

two extended periods totaling 16 years of net out-migration, whereas Gansu province experienced continuous net out-migration from 2000 to 2015. Urbanization of the drylands region generally followed national trends but switched from falling above the national average from 1965 to 1999 to below the national average after 2000. The region's urban built-up land expanded by a factor of 3.5 times from 1975 to 2014. Although all four provincial capitals of drylands China experienced rapid urban expansion, they showed a lower rate of expansion of urban built-up area than that of their respective provinces. Furthermore, the four cities appear to have divergent urban environmental changes, as while Urumqi and Lanzhou generally improved their air quality, Yinchuan and Hohhot illustrated an opposite trend.

Acknowledgements We would like to acknowledge the financial support from the National Aeronautics and Space Administration (NASA)'s Land-Cover and Land-Use Change (LCLUC) Program through its two grants to Michigan State University (NNX15AD51G and NNX09AI32G). We appreciate the help from Dr. Rong Zhang of East China Normal University and Dr. Yaowen Xie from Lanzhou University on population data of Xinjiang and Gansu. We are thankful for the constructive comments and edits provided by Dr. Geoffrey Henebry. We thank Connor Crank for editing the manuscript. Any opinions, findings, and conclusions or recommendations expressed in this paper are those of the authors and do not necessarily reflect the views of NASA.

References

Abdullaev SF, Sokolik IN (2020) Assessment of the influence of dust storms on the cotton production in Tajikistan. In: Gutman G et al (eds) Landscape dynamics of drylands across greater Central Asia: people, societies and ecosystems. Springer, Cham

Bai Y, Shang Z, Niu D (2008) Study on land use structure and driving factors in Lanzhou. J Huaihai Inst Technol 17:81–84

Bontemps S, Defourny P, Radoux J, Van Bogaert E, Lamarche C, Achard F, Mayaux P, Boettcher M, Brockmann C, Kirches G, Zülkhe M (2013) Consistent global land cover maps for climate modelling communities: current achievements of the ESA's land cover CCI. In Proceedings of the ESA Living Planet Symposium, Edinburgh, pp 9–13

Chen H, Gao Y (2007) A preliminary study on land use/cover change of Yinchuan city. Res soil water Conserv 14:95–99

Chen J, Wan S, Henebry G, Qi J, Gutman G, Sun G, Kappas M (eds) (2013) Dryland East Asia: land dynamics amid social and climate change. Walter de Gruyter, Berlin

Chen J, Ouyang Z, John R et al (2020) Social-ecological systems across the Asian Drylands Belt (ADB). In: Gutman G et al (eds) Landscape dynamics of drylands across greater Central Asia: people, societies and ecosystems. Springer, Cham

Cherednichenko A, Cherednichenko EN, Vilesov VS (2015) Climate change in the city of Almaty during the past 120 years. Quat Int 358:101–105

Deng X, Huang J, Rozelle S, Uchida E (2008) Growth, population and industrialization, and urban land expansion of China. J Urban Econ 63(1):96–115

Dikötter F (2010) Mao's great famine: the history of China's most devastating catastrophe, 1958–1962. Bloomsbury Publishing, New York

Dong W, Zhang X (2010) City profile: Urumqi. Cities 28:115–125

Dong W, Zhang X, Wang B et al (2006) Analysis of landuse expansion and spatial differentiation of Urumqi. Sci China Ser D Earth Sci 36:148–156

Dong W, Zhang X, Wang B, Duan Z (2007) Expansion of Urumqi urban area and its spatial differentiation. China Sci D Geogr Sci 50:159–168

Du G (2003) Analysis of Hohhot's land use change. Sci Econ Inn Mong 1:87–89

Du L (2007) Land use/cover change in Yinchuan city based on RS technology. Arid L Geogr 30(4):585–589

Fan P, Qi J (2010) Assessing the sustainability of major cities in China. Sustain Sci 5(1):51–68

Fan P, Qi J, Chen X et al (2013) Urban expansion and environment change in dryland East Asia. In: Dryland East Asia (DEA): land dynamics amid social and climate change. HEP/De Gruyter, Beijing/Berlin, pp 81–104

Fan P, Xie Y, Qi J et al (2014) Vulnerability of a coupled natural and human system in a changing environment: dynamics of Lanzhou's urban landscape. Landsc Ecol 29(10):1709–1723

Fan P, Chen J, John R (2016) Urbanization and environmental change during the economic transition on the Mongolian Plateau: Hohhot and Ulaanbaatar. Environ Res 144:96–112

Fan P, Ouyang Z, Duong ND et al (2018a) Urban landscape, economic development, environmental and social changes in transitional economies: Vietnam after Doimoi. Landsc Urban Plan.

Fan P, Wan G, Xu L et al (2018b) Walkability in urban landscapes: a comparative study of four large cities in China. Landsc Ecol 33:323–340

Food and Agriculture Organization of the United Nations (FAO) (2018) Definitions of drylands and dryland farming. Available at http://www.fao.org/docrep/012/i0372e/i0372e08.pdf

Ford JD, Berrang-Ford L, Bunce A et al (2015) The status of climate change adaptation in Africa and Asia. Reg Environ Chang 15:801–814

Gaubatz P (1999) China's urban transformation: patterns and processes of morphological change in Beijing, Shanghai and Guangzhou. Urban Stud 36(9):1495–1521

Gráda CÓ, O'Rourke KH (1997) Migration as disaster relief: lessons from the Great Irish Famine. Eur Rev Econ Hist 1(1):3–25

Groisman PY, Bulygina ON, Henebry GM et al (2020) Dry land belt of Northern Eurasia: contemporary environmental changes. In: Gutman G et al (eds) Landscape dynamics of drylands across greater Central Asia: people, societies and ecosystems. Springer, Cham

Hang F, Chang T (2006) Research into urban land expanding change and its driving force in Urumqi. J Chongqing Technol Bus Univ 16(1):47–49

Henebry GM, de Beurs KM, John R et al (2020) Recent land surface dynamics across the Eurasian Drylands. In: Gutman G et al (eds) Landscape dynamics of drylands across greater Central Asia: people, societies and ecosystems. Springer, Cham

Hijioka Y, Lin E, Pereira JJ et al (2014) Asia. (Cambridge, United Kingdom and New York, NY, USA: In: Climate change 2014: impacts, adaptation, and vulnerability. Part B: regional aspects. Contribution of Working Group II to the Fifth Assessment Report of the Intergovernmental Panel on Climate Change [Barros, V.R., C.B. Field, D.J. Dokken, M.D. Mastra)

Huang H, Zhang Q (2009) Landuse change and ecological environmental impact in Lanzhou, a study based on RS and GIS. Soil Water Conserv China 9:57–59

Klotz M, Kemper T, Geiß C et al (2016) How good is the map? A multi-scale cross-comparison framework for global settlement layers: evidence from Central Europe. Remote Sens Environ 178:191–212

Li F, Tan H (2009) Analysis of temperature contrast and observation between urban and outskirt areas of Yongning county. Ningxia Eng Technol 8(4):303–309

Li X, Zhang Q, Fu X (2008) Studies on driving forces of land utilizing changes in Hohhot city. Anhui Agric Sci Bull 14(9):61–63

Li X, Messina JP, Moore NJ et al (2017) MODIS land cover uncertainty in regional climate simulations. Clim Dyn 49:4047–4059

Liang X, Cao Y, Zhou W (2010) Analysis on change in land use and its driving forces in Lanzhou city. Resour Dev Mark 26(10):876–879

Lioubimtseva E, Henebry GM (2009) Climate and environmental change in arid Central Asia: impacts, vulnerability, and adaptations. J Arid Environ 73(11):963–977

Long H, Zou J, Liu Y (2009) Differentiation of rural development driven by industrialization and urbanization in eastern coastal China. Habitat Int 33(4):454–462

Luo G, Feng Y, Zhang B, Cheng W (2010) Sustainable land-use patterns for arid lands: a case study in the northern slope areas of the Tianshan Mountains. J Geogr Sci 20(4):510–524

Ma LJ (2002) Urban transformation in China, 1949–2000: a review and research agenda. Environ Plan A 34(9):1545–1569

Park H, Fan P, John R et al (2017) Urbanization on the Mongolian Plateau after economic reform: changes and causes. Appl Geogr 86:118–127

Pesaresi M, Ehrilch D, Florczyk AJ et al (2016) GHS built-up grid, derived from Landsat, multitemporal (1975, 1990, 2000, 2014). European Commission, Joint Research Centre (JRC) [Dataset] PID. Available at: http://data.europa.eu/89h/jrc-ghsl-ghs_built_ldsmt_globe_r2015b

Portnov BA, Safriel UN (2004) Combating desertification in the Negev: dryland agriculture vs. dryland urbanization. J Arid Environ 56(4):659–680

Qi J, Chen J, Wan S, Ai L (2012) Understanding the coupled natural and human systems in Dryland East Asia. Environ Res Lett 7(1):015202

Qi J, Kulmatov R, Bubochova T et al (2020) The complexity and challenges of water-energy-food systems in Central Asia. In: Gutman G et al (eds) Landscape dynamics of drylands across greater Central Asia: people, societies and ecosystems. Springer, Cham

Ren C, Wu D, Dong S (2006) The influence of urbanization on the urban climate environment in Northwest China. Geogr Res 25(2):233–241

Safriel U, Adeel Z, Niemeijer D et al (2005) Dryland systems. In: Millennium ecosystem assessment ecosystems and human well-beings: current state and trends, vol 1, Chapter 22. Available at: https://www.millenniumassessment.org/documents/document.291.aspx.pdf

Schneider A, Seto KC, Webster DR (2005) Urban growth in Chengdu, Western China: application of remote sensing to assess planning and policy outcomes. Environ Plan B Plan Des 32(3):323–345

Schneider A, Friedl MA, Potere D (2010) Monitoring urban areas globally using MODIS 500m data: new methods and datasets based on urban ecoregions. Remote Sens Environ 114(8):1733–1746

Sheng Y (2004) Characteristics of the timing and spatial change and analysis on driving factors in land use of Hohhot. J Inn Mong Norm Univ 33(3):313–316

Sietz D, Lüdeke MK, Walther C (2011) Categorisation of typical vulnerability patterns in global drylands. Glob Environ Chang 21(2):431–440

Sokolik IN, Shiklomanov A, Xi X et al (2020) Quantifying the anthropogenic signature in drylands of Central Asia and its impact on water scarcity and dust emissions. In: Gutman G et al (eds) Landscape dynamics of drylands across greater Central Asia: people, societies and ecosystems. Springer, Cham

Spaeth KE, Weltz MA, Guertin DP et al (2020) Hydrology and erosion risk parameters for grasslands in Central Asia. In: Gutman G et al (eds) Landscape dynamics of drylands across greater Central Asia: people, societies and ecosystems. Springer, Cham

Sternberg T (2017) Climate hazard crises in Asian societies and environments. Routledge, New York

Wang J (1997) Concerning the ethnic moving and living structures in the urban area of Hohhot. Northwest Minor Res 2:7–29

Wang L, Chen X, Pang F et al (2007) Research on the process and social driving forces of land use change in Lanzhou city. J Northwest Norm Univ 43(2):88–92

Xie Y, Hannum E (1996) Regional variation in earnings inequality in reform-era urban China. Am J Sociol 101(4):950–992

Xiong H, Zou G, Cui J (2010) Evolution of urban land spatial structure in Urumqi based on GIS. Geogr Sci 30(1):86–91

Xu Z, Zhu N (2009) City size distribution in China: are large cities dominant? Urban Stud 46(10):2159–2185

Yue W, Liu Y, Fan P (2013) Measuring urban sprawl and its drivers in large Chinese cities: the case of Hangzhou. Land Use Policy 31:358–370

Zhang K, Song S (2003) Rural–urban migration and urbanization in China: evidence from time-series and cross-section analyses. China Econ Rev 14(4):386–400

Zhang Q, Ma J, Zhao C (2005) The change of land use and its progress in Lanzhou based on GIS and RS. J Arid L Resour Environ 19(1):96–100

Zhang J, Chang X, Li J, Cai M (2008) Land use change and its ecological effect in Hohhot city based on 3S technology. Chinese J Ecol 27(12):2184–2187

Zhen Y, Niu S, Liu H et al (2007) Study on mechanism of landuse conversion in metropolitan area: a case study of Lanzhou metropolitan area, China. IEEE Int Geosci Remote Sens Symp IGARSS 2007:2170–2173

Zhu Z, Zhang X (2010) Study on the land use temporal dynamics in Yinchuan city. J Anhui Agric Sci 38(13):6796–6799

Chapter 8
Hydrology and Erosion Risk Parameters for Grasslands in Central Asia

Kenneth E. Spaeth, Mark A. Weltz, D. Phillip Guertin, Jiaguo Qi, Geoffrey M. Henebry, Jason Nesbit, Tlektes I. Yespolov, and Marat Beksultanov

8.1 Introduction

The Republic of Kazakhstan, located in the center of the Eurasia is the ninth largest country in the world (2.7 million km^2) and was the second largest republic in the former Soviet Union. The land area of Kazakhstan extends about 3000 km from the Caspian Sea to the Altai Mountains on the eastern fringe, and 1600 km from the western-Siberian lowlands to the Tianshan Mountains on the southern border. Four major ecoregions are represented in Kazakhstan: steppe (25% of land area),

K. E. Spaeth (✉)
USDA-Natural Resources Conservation Service, Central National Technology Support Center, Fort Worth, TX, USA
e-mail: ken.spaeth@ftw.usda.gov

M. A. Weltz · J. Nesbit
USDA-Agricultural Research Service, Great Basins Research, Reno, NV, USA
e-mail: Mark.Weltz@ars.usda.gov; Jason.Nesbit@ars.usda.gov

D. P. Guertin
Natural Resources and the Environment, University of Arizona, Tucson, AZ, USA
e-mail: dpg@email.arizona.edu

J. Qi · G. M. Henebry
Department of Geography, Environment, and Spatial Sciences, Center for Global Change and Earth Observations, Michigan State University, East Lansing, MI, USA
e-mail: qi@msu.edu; henebryg@msu.edu

T. I. Yespolov
Kazakh National Agrarian University, Almaty, Kazakhstan
e-mail: rector@kaznau.kz

M. Beksultanov
AgriTech Hub Kaz, Almaty, Kazakhstan
e-mail: maratb@precisionagro.com

G. Gutman et al. (eds.), *Landscape Dynamics of Drylands across Greater Central Asia: People, Societies and Ecosystems*, Landscape Series 17,
https://doi.org/10.1007/978-3-030-30742-4_8

semidesert (25%), desert (40%), and mountains (7%) (Ryabushkina et al. 2008). Kazakhstan ranks as the fifth largest country in terms of range and pastureland. The area of focus on this paper is the Kazakh steppe (also known as the Kirghiz steppe), a vast temperate grassland with interspaced savannas and shrublands in northern Kazakhstan (Fig. 8.1). It is the largest region of dry steppe rangeland and covers approximately 804,500 km^2. Historically, nomadic herders used the Kazakh steppe for grazing animals. While Kazakhstan was part of the Soviet Union, about 40% of the land area was cultivated (the *Virgin Lands* program) after 1950 (Schillhorn-van-Veen et al. 2003). During this time, the nomadic life style began to be replaced by collective state managed farms (kolkhoz). During the 1950s and 1960s, significant wind and water erosion degraded many of these cultivated areas, many of which were largely abandoned by the 1990s following independence. Today, the Kazakh steppe is fragmented with a mosaic of different land uses.

After independence from the Soviet Union at the end of 1991, several laws were enacted in Kazakhstan to regulate land use and ownership, mostly arable lands, but some of these laws have been applied to range and pasturelands. However, there is apparently minimal specific oversight as to management of special issues specific to

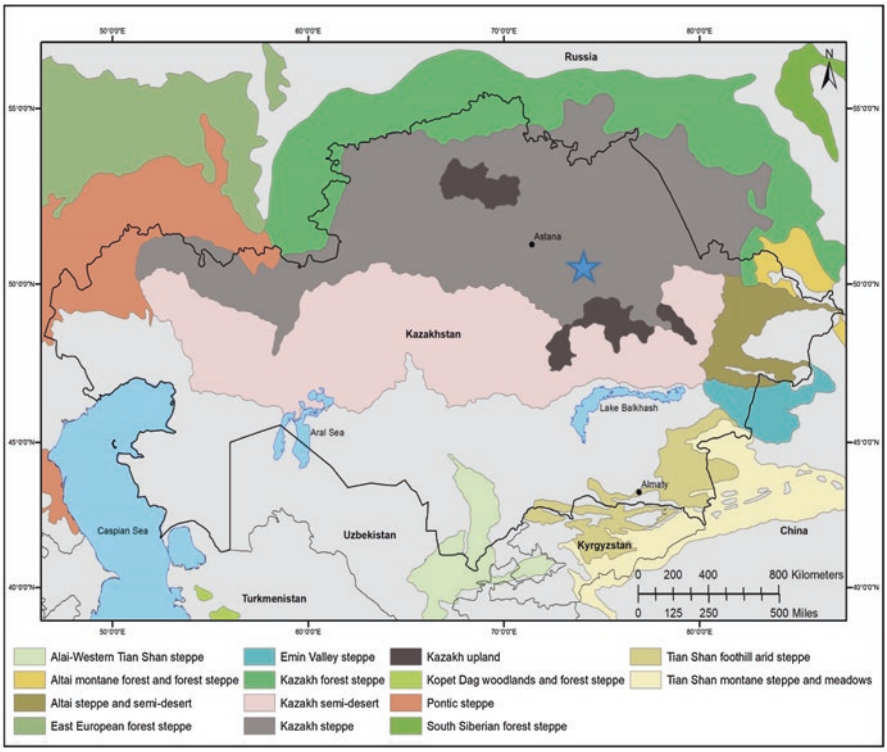

Fig. 8.1 Map of major steppe biomes in Central Asia. Blue star designates location of Yntaly, in the Karagandy Province, Kazakhstan

rangelands – Schillhorn-van-Veen et al. (2003) state that: "Consequently, the rangeland resources are currently used without proper regulation or oversight. The new Land Code (2003) allows private ownership of arable land as well as for much of the rangeland [today the majority of the rangeland is non-private] … the Government is facing the question of institutional oversight of the property both privately and state owned to assure its long-turn efficient use from ecological and economic points of view [the Land Law 2003 recognizes some lands used traditionally for grazing and classifies about 17 million ha as commons]".

Large tracts of rangeland still remain in government control and ownership with various estimates of rangeland degradation: 60% of Kazakhstan's arid areas (desert zone), or 30% of the pastureland are degraded due to overgrazing (Kharin et al. 1986). Schillhorn-van-Veen et al. (2003) estimated that 30–40% of the Nations rangeland were degraded. Robinson et al. (2003) concluded that these estimates are probably lower since the independence of Kazakhstan as livestock numbers had decreased significantly since gaining independence. They estimated that the range was in good condition overall. Robinson et al. (2003) stated that there is a void in the literature regarding Kazakhstan's rangeland. At present, the Government is aware of the repercussions of past land policies and is concerned with land degradation and restoration activities as well as how these lands are managed into the future. Without national level information of rangeland conditions, it is challenging to devise effective policies on rangeland management and planning. The Kazakh Ministry of Agriculture is focused on the well-being of its rangeland resources for long-term sustainability with increased conservation management focused on restoration, extended livestock production, and international markets (*cf.* Qi et al. 2020, Chap. 5). Climate change is also playing a key role in the land management and rangeland grazing potentials. Given the ongoing changes in regional climate change, especially the warming trend (*cf.* Henebry et al. 2020, Chap. 3) and changing precipitation patterns (*cf.* Groisman et al. 2020, Chap. 2), the Kazakh government has issued a number of adaptation policies to cope with water stress. These policies and potentially increasing uncertainties in agriculture, particularly crops and pastures, may further result in agricultural abandonment and land use conversion to grazing lands (*cf.* Qi et al. 2020, Chap. 5; Kappas et al. 2020, Chap. 9). Yet there is no national level source of rangeland health/condition information for future land use planning, due to the lack of technical capabilities for holistic rangeland assessments.

Throughout the world, rangelands are dynamic and commonly influenced by many different perturbations, natural and anthropogenic, which influence rangeland ecosystem function over a wide range of spatial and temporal scales (Williams et al. 2016). Climatic extremes such as drought and periods of intermittent above average precipitation can have profound influences on vegetation composition and biotic integrity, soil nutrient fluxes, soil surface stability, and hydrology and erosion processes. Considering climate extremes with other disturbances such as natural (*e.g.*, insect and plant diseases), wildfire, and diversity of grazing practices, the matrix of influencing factors on rangeland community functions becomes quite complex. In addition to vegetation composition changes, runoff and soil loss are effective quantitative indicators of current management impacts (Weltz and Spaeth 2012).

These hydrologic indicators have been used to infer impacts of vegetation changes due to grazing and drought on water availability and quality, forage availability for domestic livestock and/or wildlife, which ultimately influence the protective capacity of sustainability of the plant community (Weltz and Spaeth 2012; Williams et al. 2016; Hernandez et al. 2017). In this chapter, we examine potential hydrologic and water erosion dynamics on vegetation class 38 of the Atlas of Kazakhstan (2014), Kazakh steppe (*Stipa capillata, Festuca valesiaca, Artemisia frigida, and A. schrenkiana*) with several vegetation state changes. Our objective is to introduce a hydrology and erosion modeling method for holistic rangeland assessment to demonstrate feasibility and usefulness of this technology for rangeland management decision making.

8.2 Methods

8.2.1 Study Area

The Kazakh steppe is representative of a semi-arid, continental climate, and average precipitation ranges from 200 to 400 mm from south to north. Average temperatures range from 20 to 26 °C in July to −12 °C to −18 °C in January. The flora of the Kazakhstan is diverse, with over 13,000 species, of which 5754 are vascular plants (Ministry of Environmental Protection 2009). In the National Atlas of the Republic of Kazakhstan, there are 23 represented plant community associations for the dry temperate dry steppes and dry steppes on chestnut soils, which dominate the Kazakh steppe. The site for this study was near Yntaly, in the Karagandy Province, Kazakhstan (Fig. 8.1). The site is vegetation classification 38, Kazakh steppe (*Stipa capillata, Festuca valesiaca*, *Artemisia frigida, and A. schrenkiana*) (Atlas of Kazakhstan 2014) (Fig. 8.2). According to the United States system of soil nomenclature, on-site classification was a mollisol with a silty clay loam texture.

8.2.2 Data and Methods

At each study site, slope, aspect, vegetation classification, five clip quadrats for production estimates, brief description of soil profile with surface soil texture identification, and rangeland health assessment (Pellant et al. 2020) were made. Plant species foliar cover and ground cover parameters were determined from a 0.16 m^2 macroplot consisting of two 45.7 m transects aligned north to south and east to west (Table 8.1). The line point intercept method was used at every 0.9 m along the transects for a total of 100 intercept points. The methodology is according to the USDA-Natural Resources Conservation Service rangeland Natural Resources Inventory studies (USDA-NRCS 2019).

Fig. 8.2 Dry steppes on chestnut soils, #38 soil vegetation classification, Kazakh steppe, fescue-feathergrass (*Festuca valesiaca/Stipa capillata/Artemisia frigida, A. schrenkiana*; Atlas of Kazakhstan 2014). (Photo of historic reference plant community. Photo by Spaeth 2018 at Yntaly site)

Table 8.1 On-site measured field data for parameterization of the Rangeland Hydrology and Erosion Model

	S1	S1b	S2
Average annual precipitation (mm year^{-1})	359	359	359
Soil texture	Silty clay loam	Silty clay loam	Silty clay loam
Soil water saturation %	25	25	25
Slope length (meters)	50	50	50
Slope shape	Uniform	Uniform	Uniform
Slope steepness %	1 and 15	1 and 15	1 and 15
Bunch grass foliar cover %	60	45	35
Forbs and/or annual grasses foliar cover %	11	11	20
Shrubs foliar cover %	11	11	11
Sod grass foliar cover %	0	0	0
TOTAL FOLIAR COVER %	82	67	66
Basal cover %	3	2	1
Rock cover %	0	0	0
Litter cover %	31	25	10
Biological crusts cover %	0	0	0
Total GROUND cover %	34	27	11

Data represents separate model runs at 1% and 15% slopes

The Rangeland Hydrology and Erosion Model (RHEM v2.3, update 4) was used to evaluate runoff and erosion risk for different vegetation conditions representing a historic plant community reference state, a transitional state, with higher bare ground, and a degraded state with introduced annual weedy species on the site with two slope designations (1 and 15%) (Hernandez et al. 2017) (Fig. 8.3). In the U.S., government land management agencies and private land users are now using the concept of ecological sites that contain state and transition models, which are diagrammatic portrayals with narratives and identification of specific environmental drivers – states can change as a result of a natural or anthropogenic disturbance event, or lack of a natural event) (Westoby et al. 1989; Bestelmeyer et al. 2017) (Fig. 8.4). State and transition models are commonly used in conservation planning and for assessment and monitoring vegetation changes and health status of

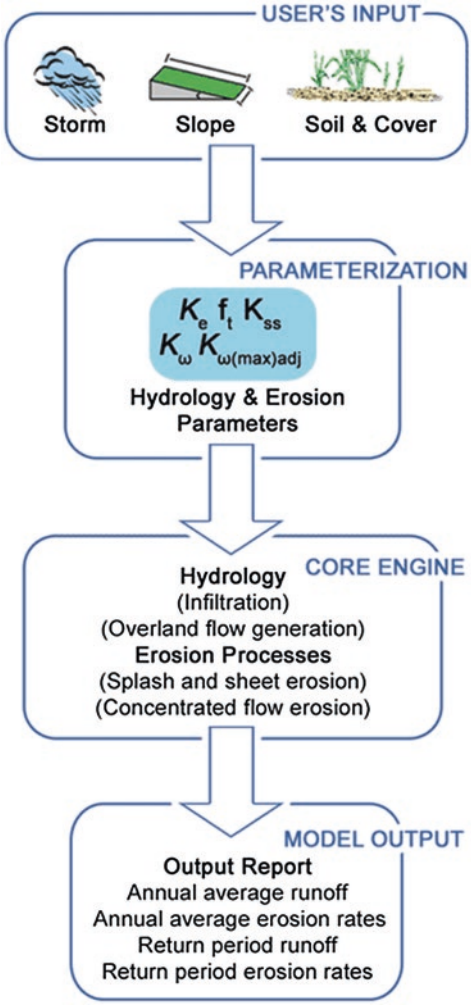

Fig. 8.3 A flowchart of Rangeland Hydrology and Erosion Model (RHEM), from https://apps.tucson.ars.ag.gov/rhem/about

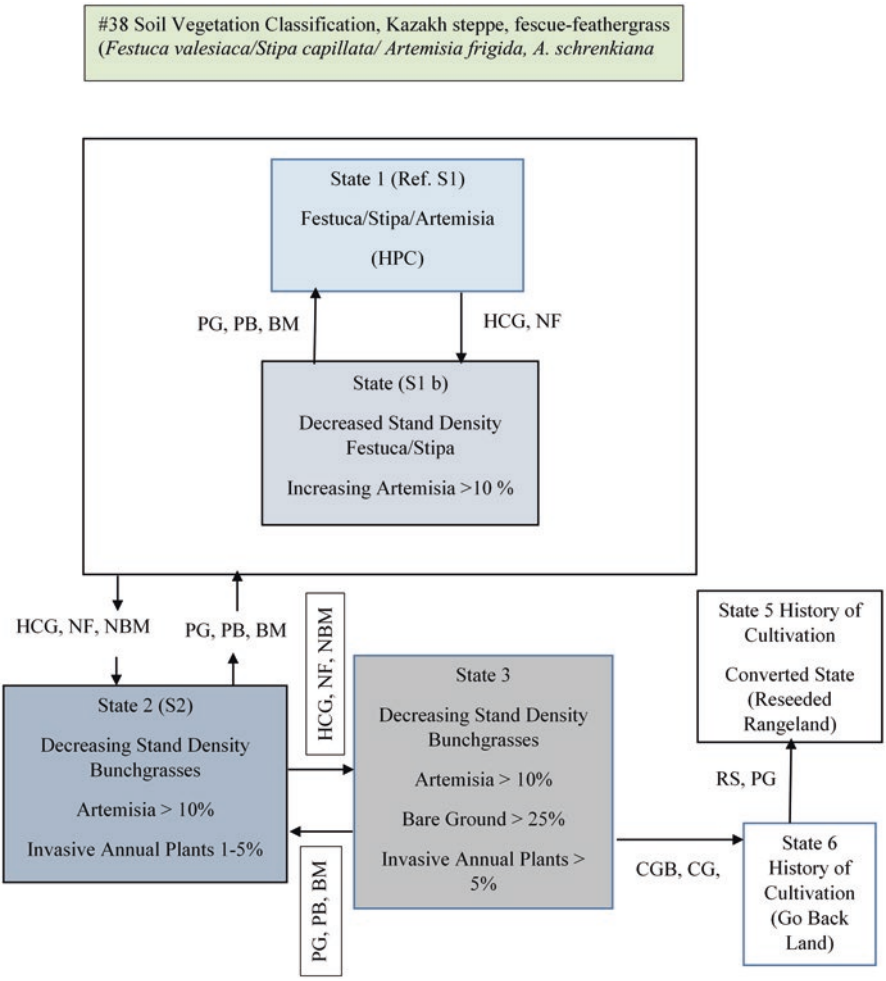

Fig. 8.4 State and transition diagram for #38 soil vegetation classification, Kazakh steppe, fescue-feathergrass (*Festuca valesiaca/Stipa capillata/Artemisia frigida, A. schrenkiana.* (*HPC* Historic Plant Community, *PG* Prescribed Grazing, *PB* Prescribed Burning, *BM* Brush Management, *HCG* Heavy Continuous Grazing, *NF* No Fire, *NBM* No Brush Management, *RS* Rangeland Seeding, *CGB* Cultivation Go-back, *CG* Continuous Grazing)

rangeland ecological sites (Carpenter and Brock 2006; Forbis et al. 2006; King and Hobbs 2006; Bestelmeyer et al. 2004, 2009).

The Rangeland Hydrology and Erosion Model was developed in a coordinated project between three USDA agencies: Agricultural Research Service (ARS), Natural Resource Conservation Service (NRCS), and the U.S. Forest Service (USFS) (Wei et al. 2009; Nearing et al. 2011). The RHEM model is designed for government agencies, land managers, and conservationists who need sound, science-based technology to model and predict runoff and erosion rates on rangelands and

to assist in assessing rangeland conservation practice effects. The RHEM model is a physically based erosion prediction tool for rangeland applications. It is based on fundamentals of infiltration, hydrology, plant science, hydraulics, and erosion mechanics. The RHEM model was developed from rainfall simulation experiments conducted at more than 25 geographic sites, which represented grassland, shrubland, and woodland sites throughout the western U.S (Nearing et al. 2011). Site environmental variables are used as RHEM model inputs [soil texture, slope length, slope steepness, slope shape, dominant plant life form, percentage of canopy cover, and percentage of ground cover by component (rock, litter, basal area, and microbiotic crusts)]. Climate (precipitation intensity, duration, and frequency) is estimated with the Climate stochastic weather generator (CLIGN, Nicks et al. 1995) containing 300 years of daily precipitation data. The RHEM model provides estimates of the average annual soil loss during a 300-year time span and for 2-, 10-, 25-, 50-, and 100-year return runoff events, which provide an assessment of site vulnerability from heavier than average rainfall storm events and the consequences of accelerated soil loss from raindrop splash and sheet-flow, and rill soil-erosion processes.

8.3 Results and Discussion

Vegetative cover and biomass have a major effect on hydrology and soil loss as indicated by numerous field studies (Tromble et al. 1974; Wood and Blackburn 1981; Gifford 1985; Blackburn et al. 1986; Thurow et al. 1986; Wilcox et al. 1988; Abrahams and Parsons 1995; Spaeth et al. 1996; Weltz et al. 1998; Williams et al. 2014; Nouwakpo et al. 2018). In addition, rainfall simulation experiments have shown that plant life form and individual species (taxa) also can have a profound influence on hydrology and erosion (Dee et al. 1966, Spaeth et al. 1996; Pierson et al. 2002). Levels of foliar cover necessary for site protection against accelerated soil erosion on rangelands vary from 20% in Kenya (Moore et al. 1979) to 100% for some Australian conditions (Costin et al. 1959). Most studies indicate that cover of 50–75% is probably sufficient (Wood and Blackburn 1981; Gifford 1985; Weltz et al. 1998; Pierson et al. 2011; Pierson and Williams 2016; Williams et al. 2014, 2016; Cadaret et al. 2016a, b) to prevent degradation from accelerated soil erosion processes.

On the Yntaly site, three vegetation states were identified: a reference state (Ref S1) representing the historic plant community dominated by *Stipa capillata;* a state phase with a history of heavier grazing, and higher bare ground (S1b); and a completely transitional state where introduced weedy grasses and forbs were present (S2). According to RHEM estimates at 1% slope, for Ref S1, about 22% of the total annual precipitation (rainfall) is lost through runoff with 82% foliar cover and 34% ground cover. Average soil loss was estimated as 0.4 t ha^{-1} $year^{-1}$ for this site (Table 1). These estimates are considered baseline and represent values expected for a *Stipa* bunchgrass plant community. Soil loss tolerance rate (T) was estimated < than 4.5 t ha^{-1} $year^{-1}$. The stability in hydrologic function in Ref S1 is

due to dominance of bunchgrass foliar and ground cover with no connected bare interspaces.

On the transitional phase (S1b) runoff was about 24% of total annual precipitation with 67% foliar cover, 27% ground cover, and 0.6 t ha^{-1} $year^{-1}$ soil loss (Fig. 8.5). On the degraded site (S2), foliar cover was 66% and ground cover was 11%; bunchgrasses decreased from 60% to 35% and forbs increased from 11% to 20% compared to state 1 (Table 1). Annual soil loss on S2 was estimated at 1.2 t ha^{-1} $year^{-1}$ at 1% slope (Fig. 8.5). This value is still under T; however, when the storm frequencies are examined, the 25, 50, and 100 storms can produce more than 1.0 t ha^{-1} $year^{-1}$ from a single storm. As indicated by RHEM, as slope increases, so does runoff and soil loss. In comparison, on 15% slopes, runoff on Ref S1 was 24% of the total annual precipitation, with 3.1 t ha^{-1} $year^{-1}$ soil loss. For state S1b, runoff was 26% of the total precipitation with soil loss of 6.5 t ha^{-1} $year^{-1}$ (1.4 times > T). On S2, runoff was 31% of the total precipitation with 19.6 t ha^{-1} $year^{-1}$, 4.3 times greater than T (Fig. 8.5). This level of soil erosion is unsustainable and will eventually result in loss of productivity and livestock carrying capacity.

When properly managed, *Stipa* bunchgrass plant communities representative of vegetation states Ref S1 and S1b provided adequate cover at 1–6% slopes with foliar plant cover of 82 and 67% to maintain soil loss below 4.5 t ha^{-1} $year^{-1}$ (allowable T) (Fig. 8.6c). Soil loss values for vegetation state Ref S1 remained less than T at slopes up to 15%; however, S1b soil loss exceeded T at slopes 6–15%, and state S2 exceeded T at greater that 3% slopes (Fig. 8.6c).

High intensity convective thunderstorms are typically associated with accelerated runoff, as rainfall intensity is greater than infiltration capacity. These types of storms, especially intense storms with 5, 10, 25, 50, and 100 year return intervals can cause rills, gullies, and irreparable soil loss. The probability of formation of gullies is increased under conditions of low cover and net annual primary production. The reduction in production also results in reduced aggregate stability. Heavy continuous grazing can result in, soil compaction with a corresponding increase in runoff and potential for soil loss, Long-term average soil loss on rangelands is usually not a concern on sites with adequate foliar and ground cover; however, it is the rare high intensity storms where high runoff and erosion can occur, which initiates increased water flow patterns, plant pedestalling, rills, and gullies (Weltz and Spaeth 2012).

The RHEM model indicates that high intensity convective storms can have a significant impact on this site. During 10, 25, 50, and 100 year storms, there are bursts of high intensity rainfall and soil loss. On 1% slopes this can facilitate soil loss >1 t ha^{-1} $year^{-1}$ for a single storm event on the degraded site (S2) (Fig. 8.6a). As slope increases, so does the incidence of accelerated runoff and erosion. RHEM estimates on 15% slopes shows that S2 exceeds T for the 2 through 100 year storm events (Fig. 8.6b). If the site is allowed to deteriorate to a point where considerable soil loss has occurred, an ecological and hydrologic threshold will be crossed, and depending on the site, restoration may not be possible by management alone (Weltz and Spaeth 2012). On S1b, soil loss is close to T for the 25 year storm and exceeds T for the 50 and 100 year storm frequencies. For Ref S1, soil loss remained below T

a)

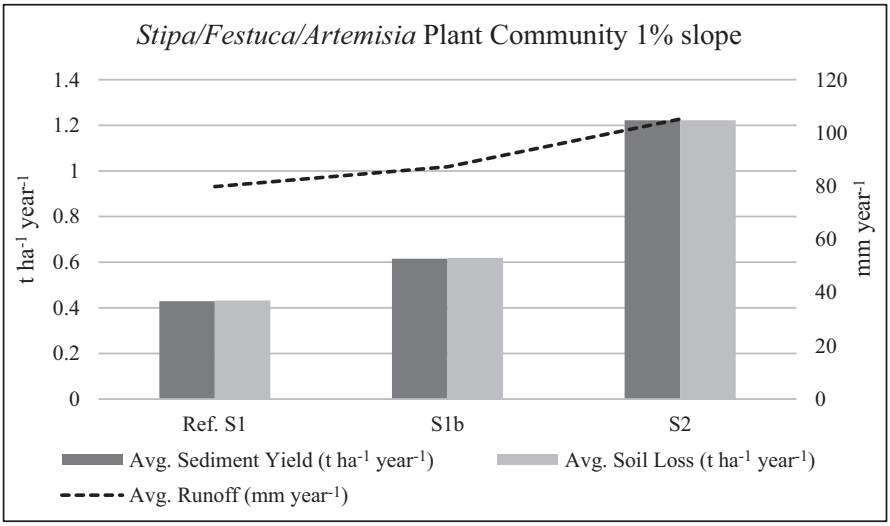

b)

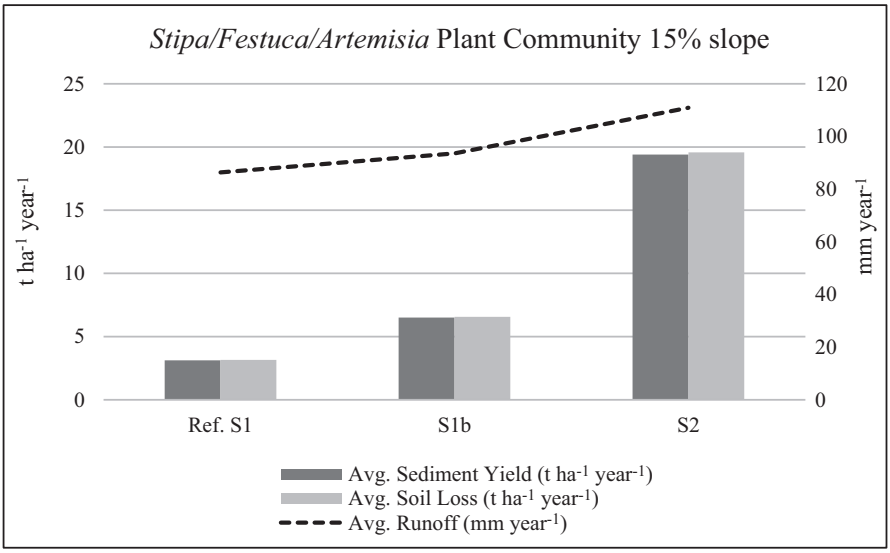

Fig. 8.5 Rangeland Hydrology and Erosion Model estimates for reference vegetation state, overgrazed state with native plants similar to reference state, and degraded state. (**a**) Average sediment yield (t ha^{-1} year^{-1}), average soil loss (t ha^{-1} year^{-1}), with average runoff (mm year^{-1}). (Ref. *S1* Reference plant community, *S1b* Native plant cover with reduced foliar and ground cover; and *S2* degraded grassland community with reduced plant cover and invasive annual species. Slope = 1%. (**b**) runoff and erosion at 15% slope)

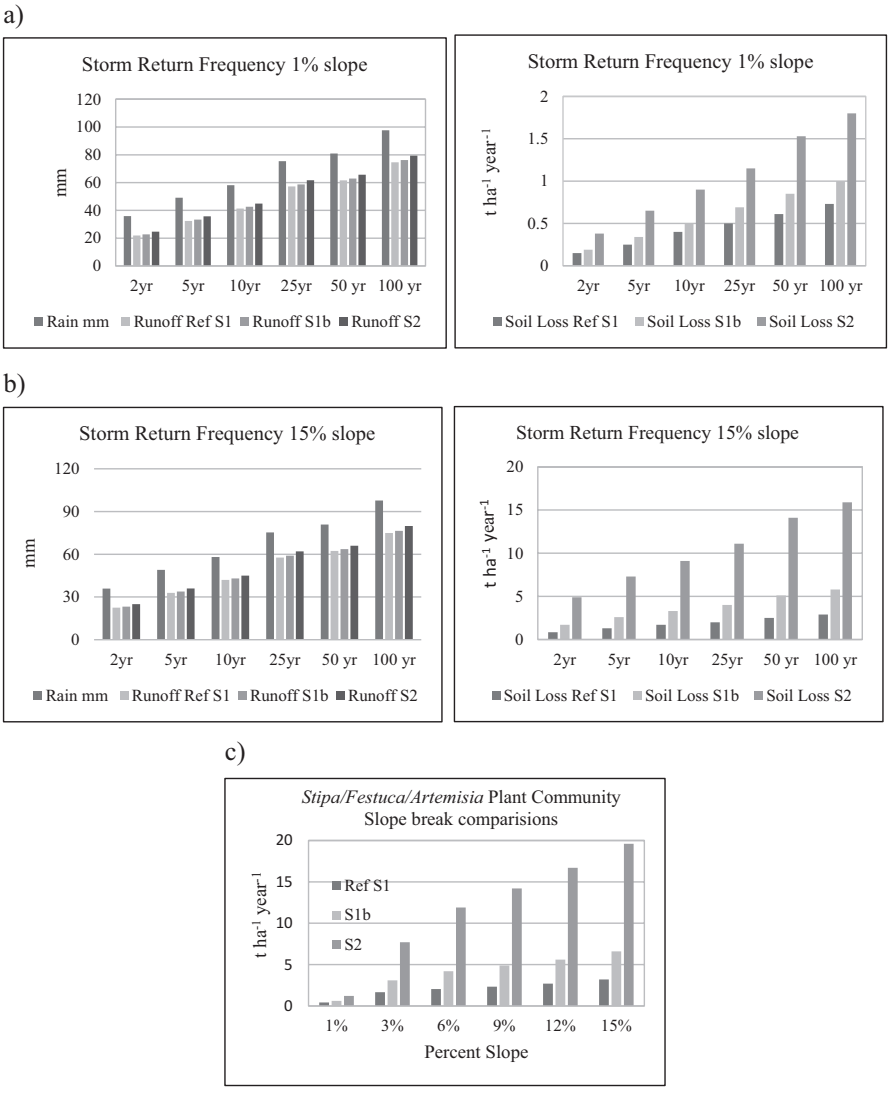

Fig. 8.6 (**a**, **b**) Rainfall, runoff, and soil loss for design storm events; and soil loss at 1% and 15% slopes. (**c**) RHEM soil loss estimates for incremental 3% slope increases

for the 2 through 100 year storms. In Fig. 8.7, probabilities of yearly soil loss potentials are given. For example, for Ref S1 (1% slope), there is a 50% chance that soil loss will be less than 0.4 t ha^{-1} year^{-1}, a 30% chance that soil loss is between 0.4 and 0.6 t ha^{-1} year^{-1}, a 15% chance that soil loss will be between 0.6 and 0.9 t ha^{-1} year^{-1}, and a 5% chance that soil loss will exceed 0.99 t ha^{-1} year^{-1}. For state S1b, there is a 55% chance that soil loss can exceed 0.99 t ha^{-1} year^{-1}. For the degraded state (S2), there is a 98% chance that soil loss will exceed 0.99 t ha^{-1} year^{-1} (Fig. 8.8).

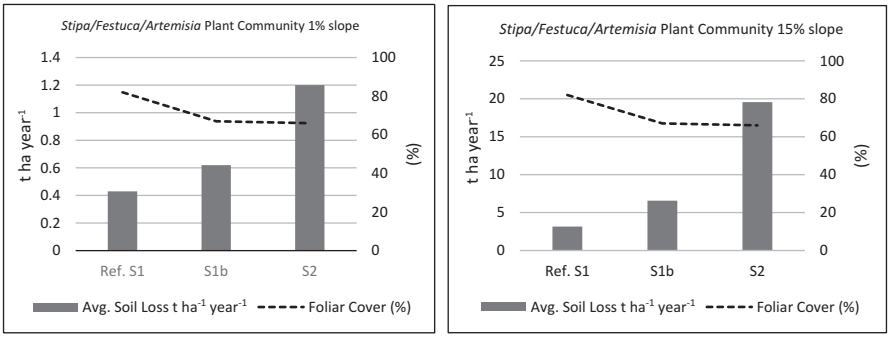

Fig. 8.7 Average RHEM estimated soil loss and foliar plant cover for reference state (Ref S1), state S1b, and state S2 at 1 and 15% slopes

In summary, foliar and ground cover are important elements in maintaining low runoff and soil loss from overland flow. In addition to foliar and ground cover, species life form and individual species can be highly correlated with infiltration, runoff, and erosion. On the Yntaly site, bunchgrasses were the dominant life form; however, on the more degraded states, foliar and ground cover was reduced with an increase in weedy forb species for states S1b and S2. This reduction was caused by heavier grazing. Over time, consistent continuous heavy grazing will cause a transition where bunchgrasses are reduced and weedy forbs increase. The shrub component can also increase; however, shrub cover was consistent at 11% cover for all three states in this study. On steeper sites, it is imperative that adequate cover of bunchgrasses be maintained to provide low potential soil loss from water erosion. On steeper slopes, the transition from a stable grassland plant community to an unstable hydrologic condition with lower plant cover and undesirable species can occur quickly. This can be documented by observing gap frequency between plants and the connectivity of flow paths as bunchgrasses are replaced with single stem forbs. The distance between plant stems increases resulting in concentrated flow and accelerated soil erosion.

Actual degradation on rangelands in Kazakhstan has been estimated at 30–60% (Kharin et al. 1986; Schillhorn-van-Veen et al. 2003). These estimates may or may not be representative of actual conditions as many of these estimates are based on coarse level remote sensing activities without any of sufficient validation of estimates via field sampling. For example, the author found many of the *Stipa* grasslands in the Kazakh steppe were undergrazed because of a lack of adequate livestock watering facilities. Rangelands in and near villages tend to be overgrazed, yet the open range at greater than 8 km from villages are not grazed at regular intervals (Fig. 8.9). Haying may occur on areas that are not directly grazed by livestock and used as supplemental winter feed.

These site-level results clearly demonstrate the usefulness of the modeling approach for holistic rangeland condition assessments; however, these site-level results may or may not the same in other geographic areas within the country, as the

a)

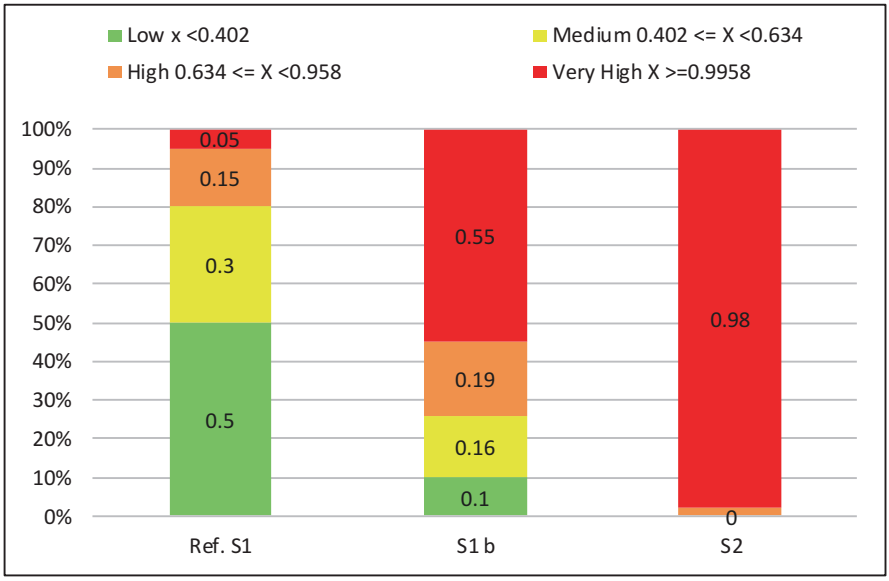

b)

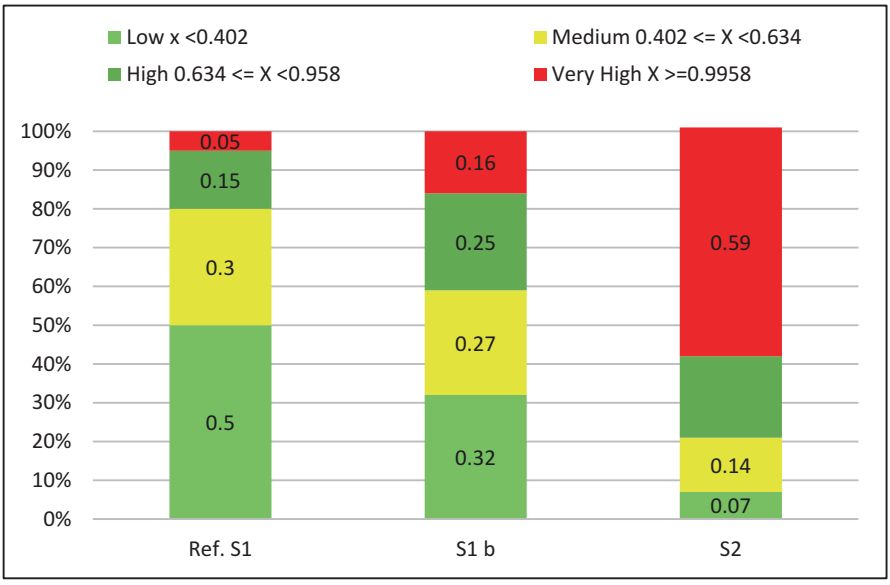

Fig. 8.8 (**a**) Probability of occurrence of yearly soil loss t ha^{-1} year^{-1} for states Ref. S1, S1b, and S2, at 1% slope. (**b**) Probability of occurrence of yearly soil loss t ha^{-1} year^{-1} for states Ref. S1, S1b, and S2, at 15% slope

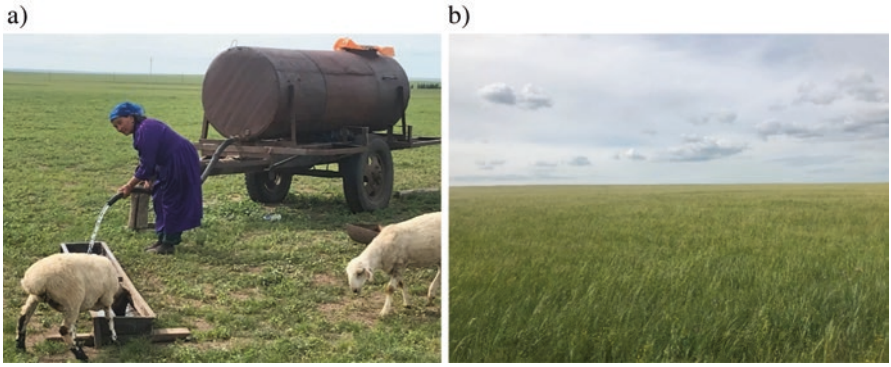

Fig. 8.9 (**a**) *Stipa* grassland, water provided at 3 km from village, (**b**) Ungrazed *Stipa* grassland 8 km from village. (Photos by Spaeth)

soil types, climate conditions, management practices, and plant communities vary greatly across the Asian steppe. The analysis presented here is site specific to *Stipa* dominated rangeland plant communities and national policies cannot, and should not, be based on just one or even several site analyses. The generalizability of this and similar additional studies can be validated by scaling up the method from site-level to regional and national levels, using geospatial and remote sensing technologies, which remain for future projects and programs.

It would be propitious for Kazakhstan and other Eurasian countries that possess vast grassland areas, to adapt a three-tier approach to gathering critical information on status of plant diversity, protective vegetative cover, and condition of the rangeland for grazing and other uses. Remote sensing studies have been conducted in Asian countries; however, correlations between imagery with field observation has been limited. It is imperative to have reliable resource information of rangeland resources (range health and conditions) before programs are implemented to expand livestock enterprises. A robust three-tier methodology for rangeland resource assessment would include three assessment protocols that would be cross calibrated: (1) a field protocol [can be based on similar National Resource Inventory (NRI) protocols used by USDA Natural Resources Conservation Service-NRCS on rangeland] to collect vital rangeland resource data; (2) on-site drone surveillance correlated with field sample – to expand the extent of the field based sample, and (3) analyzing from remote sensing imagery with the intent to correlate all three assessment protocols. This set of three resource assessment protocols enacted regionally or throughout a country could provide vital needed resource information so that realistic and effective levels of rangeland and soil health can be determined. Accurate resource inventory information on rangeland health, vegetation composition, and use of erosion tools such as RHEM are integral to grazing management program developments to enhance the probability of achieving sustainable grazing systems that are robust and sustainable and can endure the variability in climate that is inherent on rangelands.

Acknowledgements We would like to acknowledge the AgriTech Hub and Kazakh Agrarian University for hosting the USDA and University of Arizona team in Kazakhstan. The field trips throughout Kazakhstan and workshops at the University have been valuable experiences in providing firsthand information preparatory to this chapter.

References

Abrahams AD, Parsons AJ (1995) Effects of vegetation change on interrill runoff and erosion, Walnut Gulch, southern Arizona. Geomorphology 13:37–48

Atlas of Kazakhstan (2014) The national atlas of the Republic of Kazakhstan**.** Institute of Geography**.** https://ingeo.kz/?p=3643&lang=en

Bestelmeyer BT, Herrick JE, Brown JR et al (2004) Land management in the American southwest: a state-and-transition approach to ecosystem complexity. Environ Manag 34:38–51

Bestelmeyer BT, Tugel AJ, Peacock G et al (2009) State-and-transition models for heterogeneous landscapes: a strategy for development and application. Rangeland Ecol Manag 62:1–15

Bestelmeyer BT, Ash A, Brown JR et al (2017) State and transition models: theory, applications, and challenges. In: Briske (ed) Rangeland systems processes, management and challenges. Springer Open, Cham, pp 303–346

Blackburn WH, Thurow TL and Taylor CA (1986) Soil erosion on rangeland. Symposium on the use of cover, soils, and weather data in rangeland monitoring, Orlando, Florida, February 12, 1986. Texas Agr. Experiment Station TA-2119

Cadaret EM, McGwire KC, Nouwakpo SK et al (2016a) Vegetation canopy cover effects on sediment erosion processes in the Upper Colorado River Basin Mancos Shale Formation, Price, Utah. Catena 147:334–344

Cadaret EM, Nouwakpo SK, McGwire KC et al (2016b) Vegetation effects on soil, sediment erosion, and salinity transport processes in the Upper Colorado River Basin Mancos Shale formation. Catena 147:650–662

Carpenter SR, Brock WA (2006) Rising variance: a leading indicator of ecological transition. Ecol Lett 9:308–315

Costin A, Wimbush D, Kerr D and Day L (1959) Studies in catchment hydrology in the Australian Alps. 1. Trends in soils and vegetation. CSIRO Aust. Div. Plant Ind. Tech Pap. No. 13

Dee RF, Box TW, Robertson E (1966) Influence of grass vegetation on water intake of Pullman silty clay loam. J Range Manag 19(2):77–79

Forbis TA, Provencher AL, Frid L, Medlyn G (2006) Great basin land management planning using ecological modeling. Environ Manag 38:62–83

Gifford GF (1985) Cover allocation in rangeland watershed management (a review). In: Jones EB, Ward TJ (eds) Watershed management in the eighties, proceedings of a symposium. ASCE, New York, pp 23–31

Groisman PY, Bulygina ON, Henebry GM et al (2020) Dry land belt of Northern Eurasia: contemporary environmental changes. In: Gutman G et al (eds) Landscape dynamics of drylands across greater Central Asia: people, societies and ecosystems. Springer, Cham

Henebry GM, de Beurs KM, John R et al (2020) Recent land surface dynamics across the drylands of Greater Central Asia. In: Gutman G et al (eds) Landscape dynamics of drylands across greater Central Asia: people, societies and ecosystems. Springer, Cham

Hernandez M, Nearing MA, Hamdan OZ et al (2017) The rangeland hydrology and erosion model: a dynamic approach for predicting soil loss on rangelands. Water Resour Res 53:9368–9391

Kappas M, Degener J, Klinge M et al (2020) A conceptual framework for ecosystem stewardship based on landscape dynamics: case studies from Kazakhstan and Mongolia. In: Gutman G et al (eds) Landscape dynamics of drylands across greater Central Asia: people, societies and ecosystems. Springer, Cham

Kharin NG, Orlovskii NS, Kogai NA, Makulbekova GB (1986) Contemporary status of and prognosis for desertification in the USSR arid zone. Problems of Desert Dev 5:58–68
King EG, Hobbs RJ (2006) Identifying linkages among conceptual models of ecosystem degradation and restoration: towards an integrative framework. Restor Ecol 14:369–378
Ministry of Environmental Protection (2009) Republic of Kazakhstan, Ministry of Environmental protection. The fourth National Report on Progress in implementation of the convention on biological diversity. Republic of Kazakhstan, Astana
Moore E, Janes E, Kinsinger F et al (1979) Livestock grazing management and water quality protection. EPA 910/9–79-67, US Environmental Protection Agency and USDI Bureau of Land Management
Nearing MA, Wei H, Stone JJ et al (2011) A rangeland hydrology and erosion model. Biol Eng Trans 54:1–8
Nicks AD, Lane LJ, Gander GA (1995) Chapter 2, weather generator. In: Flanagan, Nearing (eds) USDA-water erosion prediction project: hillslope profile and watershed model documentation. USDA Agricultural Research Service, West Lafayette, pp 2.1–2.22
Nouwakpo SK, Weltz MA, Green CHM, Arslan A (2018) Combining 3D data and traditional soil erosion assessment techniques to study the effect of a vegetation cover gradient on hillslope runoff and soil erosion in a semi-arid catchment. Catena 170:129–140
Pellant M, Shaver PL, Pyke DA et al (2020) Interpreting indicators of rangeland health., Version 5. Tech 7 Ref 1734-6, U.S. Department of the Interior, Bureau of Land Management, National Operations 8 center, Denver
Pierson F, Williams C (2016) Ecohydrologic impacts of rangeland fire on runoff and erosion: a literature synthesis. Gen. Tech. Rep. RMRS-GTR-351. U.S. Department of Agriculture, Forest Service, Rocky Mountain Research Station, Fort Collins
Pierson FB, Spaeth KE, Weltz ME, Carlson DH (2002) Hydrologic response of diverse western rangelands. J Range Manag 55:558–570
Pierson FB, Williams CJ, Hardegree SP, Weltz MA (2011) Fire, plant invasions, and erosion events on western rangelands. Rangeland Ecol Manag 64:439–449
Qi J, Kulmatov R, Bubochova T et al (2020) The complexity and challenges of water-energy-food systems in Central Asia. In: Gutman G et al (eds) Landscape dynamics of drylands across greater Central Asia: people, societies and ecosystems. Springer, Cham
Robinson S, Milner-Gulland EJ, Alimaev I (2003) Rangeland degradation in Kazakhstan during the Soviet era: re-examining the evidence. J Arid Environ 53:419–439
Ryabushkina N, Gemedjieva N, Kobaisy M, Cantrell CL (2008) Brief review of Kazakhstan flora and use of its wild species. Asian and Australas J Plant Sci Biotech 2:64–71
Schillhorn-van-Veen TW, Alimaev I and Utkelov B (2003) Kazakhstan: rangelands in transition: the resource, the users and sustainable use, World Bank
Spaeth KE, Pierson FB, Weltz MA, Awang JB (1996) Gradient analysis of infiltration and environmental variables as related to rangeland vegetation. Trans ASAE 39:67–77
Thurow TL, Blackburn WH, Taylor CA (1986) Hydrologic characteristics of vegetation types as affected by livestock grazing systems, Edwards Plateau, Texas. J Range Manag 39:505–509
Tromble JM, Renard KG, Thatcher AP (1974) Infiltration for three rangeland soil-vegetation complexes. J Range Manag 27(4):318–321
USDA-NRCS (2019) Handbook of protocol procedures for the on-site rangeland National resource inventory studies, Washington, DC
Wei H, Nearing MA, Stone JJ et al (2009) A new splash and sheet erosion equation for rangelands. Soil Sci Soc Am J 73:1386–1392
Weltz M, Spaeth K (2012) Estimating effects of targeted conservation on nonfederal rangelands. Rangel J 34:35–40
Weltz MA, Kidwell MR, Fox HD (1998) Influence of abiotic and biotic factors in measuring and modeling soil erosion on rangelands: state of knowledge. Soil Erosion on Rangeland J Range Manage 51:482–495

Westoby M, Walker B, Noy-Meir I (1989) Opportunistic management for rangelands not at equilibrium. J Range Manag 42:266–274

Wilcox BP, Wood MK, Tromble JA (1988) Factors influencing infiltrability of semiarid mountain slopes. J Range Manag 41:197–206

Williams CJ, Pierson FB, Robichaud PR, Boll J (2014) Hydrologic and erosion responses to wildfire along the rangeland-xeric forest continuum in the western US: a review and model of hydrologic vulnerability. Int J Wildland Fire 23:155–172

Williams CJ, Pierson FB, Spaeth KE et al (2016) Incorporating hydrologic data and ecohydrologic relationships into ecological site descriptions. Rangeland Ecol Manag 69:4–19

Wood MK, Blackburn WH (1981) Grazing systems: their influence on infiltration rates in the rolling plains of Texas. J Range Manag 34:331–335

Chapter 9
A Conceptual Framework for Ecosystem Stewardship Based on Landscape Dynamics: Case Studies from Kazakhstan and Mongolia

Martin Kappas, Jan Degener, Michael Klinge, Irina Vitkovskaya, and Madina Batyrbayeva

9.1 Introduction

Central Asia's countries, including Mongolia, have been undergoing an extensive transformation of land cover (biophysical attributes of the earth's surface) and land use (human purpose-oriented land) change over the 19th, 20th and 21st centuries. Satellite remote sensing in combination with intensive field research has been an important approach in monitoring these land-cover and land-use changes in Central Asia.

Most landscapes of Central Asia belong to the category of drylands, which include arid, semi-arid and dry-sub-humid ecosystems. Many people live in these landscapes at subsistence level (Millennium Ecosystem Assessment 2005a) and these systems play also a role in storing terrestrial carbon (mostly soil-carbon; Millennium Ecosystem assessment 2005b). Moreover, these landscapes support a huge amount of the world's livestock (Allen-Diaz et al. 1996) and own areas with high biodiversity (Myers et al. 2000).

The most important transformations are triggered by the following changes such as land abandonment (e.g. in the twentieth century) and re-cultivation, new agricultural expansion in combination with increase and decrease of land-use intensity. But also processes of land degradation and vegetation recovery are important indicators of changing ecosystem conditions and land dynamics. A trend that exists in all Central Asian countries is the depletion of rural areas and the growth of cities known

M. Kappas (✉) · J. Degener · M. Klinge
Cartography, GIS & Remote Sensing Department, Institute of Geography, Georg-August University, Goettingen, Germany
e-mail: mkappas@uni-goettingen.de; jdegener@uni-goettingen.de

I. Vitkovskaya · M. Batyrbayeva
The National Centre of Space Researches and Technologies, Almaty, Kazakhstan

G. Gutman et al. (eds.), *Landscape Dynamics of Drylands across Greater Central Asia: People, Societies and Ecosystems*, Landscape Series 17,
https://doi.org/10.1007/978-3-030-30742-4_9

as the process of urban sprawl and contraction (see also Chap. 1, Henebry et al. 2020a). Given the importance of Northern Eurasia for global ecosystem and climate processes, improved characterization of land cover and land-cover change in the region is a scientific priority. This region is the largest landmass out of the tropics, the largest terrestrial reservoir of organic carbon, an area of active land-use changes and socio-economic transformations, and a major source of uncertainty in many global-scale estimates. The important role humans play in land-cover dynamics is widely recognized, however quantitative understanding of this role remains a challenge. Availability and quality of social science data is a cause for concern and methods for combining the remotely sensed and social science data need to be developed further so that robust projection of future changes in land cover and land use can be made (see Chap. 10 of this book, Chen et al. 2020).

In the last decades, huge data sets about the stage of the Eurasian drylands were created that help in studying landscape dynamics. In the last years, a lot of research focused on land-cover and land-use change in Central Asia and documented the underlying trends (e.g., Chen et al. 2020). One major and challenging question remained in this connection, namely the question of the stability, persistence, resistance, resilience and recovery of ecosystems in the different landscapes of Central Asia. It is evident that there is a need for dynamic system-related research to deliver a framework for future oriented decision tools.

Hereinafter the current chapter will provide an overview of important concepts underpinning the study of landscape dynamics and alternative concepts of system thinking and landscape equilibrium. Existing frameworks for the assessment of social-ecological-systems (SES), system thinking and new combined ecologic key concepts will be used. Finally, the theory of spatial and temporal scaling of disturbance regimes and the influence on equilibrium/non-equilibrium dynamics are highlighted. At the end of the chapter, two case studies (i.e., Kazakhstan and Mongolia) will underpin the dynamics of important state variables such as NDVI.

9.2 Landscape Dynamics and Ecosystem Stewardship

At the beginning, an elementary conceptual framework for investigating landscape dynamics is used. In this simple framework, system dynamics is characterized as a curve over time in a state variable. State variables are any variables that describe the state or condition of the system at a single point in time. They are in general present measures of system structures or functions. For example, NDVI, GPP, NPP, fPAR, or LAI are all examples of potential state variables. The progression of a state variable might fluctuate over time in response to disturbance and succession processes and fluctuate within a “natural range of change or variability”. This range of variability is also called as the “normal multiple states operating range” of a state variable (see also Chap. 3 of this book, Henebry et al. 2020b, where important ECV’s of Eurasia and their natural range of variability are analyzed). It is important to note that this range of variability is relative to a specific spatial and temporal scale.

Under human influence, the course of the state variable could change its behavior and develop a new range of variability. In Fig. 9.1a, there is a simple model shown for assessing the outcome of human activities on system dynamics. In Fig. 9.1b, two alternative human-altered curves of the state variable are drawn. The question is whether the system condition drawn by each curve is "normal" in reference to the natural range of change. In both cases, the dynamics of the state variable are modified (dampened.) In the first case (red curve), the state variable remains within its natural range of change, while in the second case (blue curve), the state variable moves to an equilibrium state outside of its natural range of change. In both cases, it is open whether the curves show a "resilient" system. This is not easy to answer in either case.

Thinking in system dynamics automatically brings up the question of scale because the range of change in any state variable can only be seen in reference to a specific spatial and temporal scale. For example, as the spatial extent of the system grows up (i.e., coarser scale), the expected range of variability is likely to go down

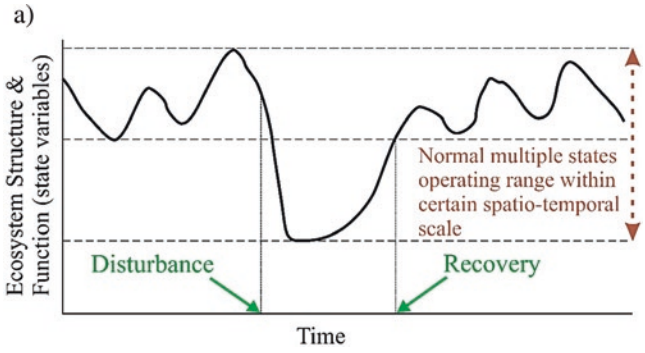

Fig. 9.1a Landscape Dynamics Concept: Variation of a state variable after disturbance and recovery. The state variable range is between normal multiple states and within a certain spatio-temporal scale

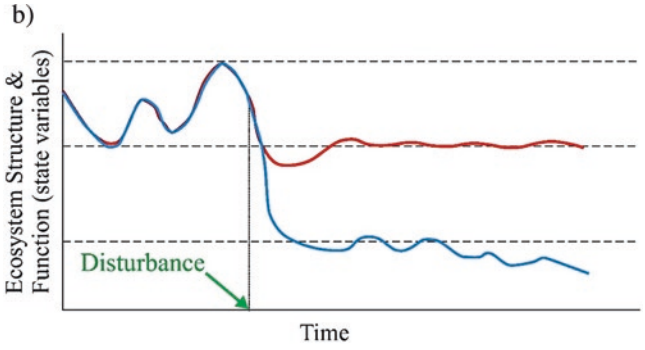

Fig. 9.1b Red curve: State variable is within 'normal' operating range; Blue curve: State variable moves outside of its natural range of change

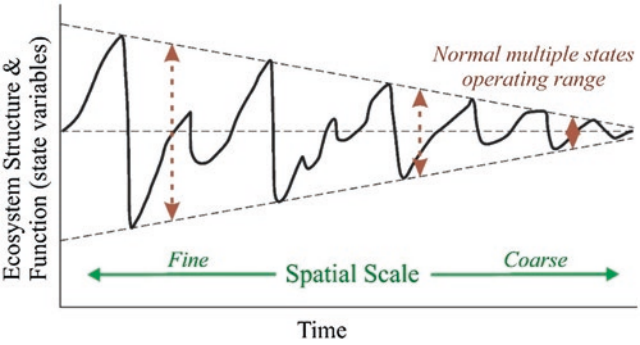

Fig. 9.2 Landscape changes under different spatial scale: Increasing the scale dampens the change

as the system increasingly is able to incorporate the disturbances. This is called as the balance of disturbance against succession in relation to Watt's unit pattern (Watt 1947). A central question is how this scaling relationship changes under a human-modified disturbance regime. For example, if the human-altered curve looks like the one in Fig. 9.2, it is shown that the range of change is increasingly dampened as the spatial scale increases.

A major question understanding landscape dynamics is whether recent trends in state variables (e.g. NDVI, LAI or populations) are biologically significant and signal the need for corrective action. For example, if the curve is decreasing (e.g., population decrease), we might think that immediate management action is needed. An understanding of system dynamics may reveal that the decrease is perfectly natural and within the range of natural change.

A quantitative understanding of system dynamics can be important for giving a reference framework for interpreting measures of landscape structure, because in most cases it is difficult or even impossible to determine the ecological significance of a derived value of a landscape metric without understanding its natural range of change.

In landscape dynamics, many expressions have been defined to explain the state of a landscape over time. Moreover, these expressions describe, how the landscape state changes, and how the trajectory of change for the landscape system will response to a disturbance. Discovering system state changes requires identifying state variables that are representative of the system state. Keeping in mind that it is extremely difficult to identify state variables that are sensitive enough to fine-scale changes in ecosystem states and that can be used to detect system changes due to a human activity.

In the following, the most important system descriptors are shortly explained that offer a conceptual frame for the study of systems dynamics:

The term *"Stability"* means the tendency of a system state variable or an entire landscape system to shift away from a stable state but only within defined bounds. In the case of a landscape systems, which are ecological systems, stability refers not to stagnation of all state variables but to variations within defined borders. A system

gets unstable when the system or state variables cross some thresholds from which a recovery to the former state is either impossible or develops only over relatively long periods. Therefore, we call a system "persistent" when the system remains in a defined state. *Persistence* is the length of time a system stays in a defined state but within some variations. The term *resistance* describes the capacity of a system to absorb or alter disturbances and protect the system from larger perturbations. Resistance mechanisms can be seen as a filter that diminish the impact of large disturbances. Another important term is "*Resilience"*. Resilience is the capability to return to the initial state after a disturbance. The resilience is related to the borders in state space in which a system will vary. If the system crosses these borders, the system will change to another state with new system state borders. Most important is that a resilient system is able to support the same key processes as before the disturbance and after recovering. The system integrity is preserved. The *"Recovery"* of the system describes the speed with which a landscape system returns to the initial state after a disturbance.

Stability of landscape systems can be obtained in different ways: Systems, which changed relatively easily, have therefore a low resistance but will return to the initial system state quickly. These systems have a rapid recovery time and high resilience and are mostly characterized by low biomass.

Other systems, which own a high resistance to disturbance and have a high persistence (stay in a stable state for long time), are mostly characterized by high biomass.

Changes in landscapes are natural processes and take place constantly. A simple concept of order is that of balance or equilibrium in the sense of constancy. This means that are no great changes over time. However, this is a very theoretical concept and disturbances and change are integral parts of landscape dynamics and make this concept of equilibrium unrealistic. Nevertheless, Turner et al. (1993) reviewed several concepts of landscape equilibrium.

First, the "shifting mosaic steady-state concept" (Bormann and Likens 1979) is introduced, which means that vegetation existing at individual patches in the landscape changes, but looking over a long time period or large area, the vegetation of the landscape is relatively constant or in an equilibrium. This concept describes a balance between disturbance (creation of new patches, e.g. by fire) and succession (e.g. regrowth of old patches). New patches inside the landscape system are balanced after disturbance by the maturation of old patches (by succession). The entire landscape system remains in a "steady-state" or "equilibrium" situation. The "shifting mosaic steady-state concept" is usable when the disturbances are small and frequent in a large area of a mostly homogeneous habitat. That's why larger areas show a more stable mosaic in the landscape than small areas. In the last years, stable mosaics could be identified over large areas. Therefore, the concept supposes that influences of topography, soils, soil moisture or other landscape factors have an effect on disturbance frequency or recovery time inside the landscape. A major challenge of this concept is that it is scale-dependent. The right choice of temporal and spatial scales to examine these landscape mosaics is challenging.

State-and-Transition Models (STMs) have emerged as the leading conceptual framework to describe vegetation dynamics over a range of management and restoration scenarios (Asefa et al. 2003; Chartier and Rostagno 2006; Quetier et al. 2007; Tietjen and Jeltsch 2007; Sankaran and Anderson 2009; Standish et al. 2009). These STM models are mostly qualitative models that show potential alternative stable vegetation states based on a particular combination of site conditions (e.g., soil, soil moisture) and climate. Further, they give an idea about possible transitions between states. These transitions indicate thresholds between alternative stable states that are normally viewed as irreversible without intensive management inputs.

These models also are useful for communicating complex ecosystem dynamics to diverse stakeholders in a simple form (mostly flowcharts). The major weaknesses in these models and other related conceptual models is that they have limited predictive capability. Further, they do not address management uncertainty and have only restricted ability to link management issues to multiple ecological processes in a quantitative way that foster ecosystem and landscape change. These constraints limit application of these models to scenario analysis and evaluation of landscape dynamics. The two case studies about Kazakhstan and Mongolia focus on the vegetation dynamics as an important state variable providing an overview about possible transitions between long-term states of vegetation cover.

9.3 Case Study from Kazakhstan

Most of the territory of the Republic of Kazakhstan, located in the arid and semi-arid zones, is vulnerable to the observed climate changes. The period 2004–2014 for the territory of Kazakhstan is characterized by an increase of continentality of climate and, as a consequence, an increase of situations with adverse and extreme weather events, among which the most dangerous is the drought.

The III-VI National Communication of the Republic of Kazakhstan to the UN Framework Convention on Climate Change was prepared in the framework of a joint project of the United Nations Development Program in Kazakhstan and the Ministry of Environment and Water Resources of the Republic of Kazakhstan. This National Communication synchronizes the timing of the submission of National Communications with other countries and includes reports for the period 2006–2012. The document is intended for government agencies, scientific and public organizations.

As noted in the National Communication of the Republic of Kazakhstan (2013), the increases in mean annual and seasonal surface air temperatures, especially in the summer months, are observed ubiquitously. Particularly rapid rates of warming began in the 1980s, which led to a high frequency of warm years. On average in Kazakhstan in all years in the period 1997–2010 (14 consecutive years), the average annual air temperatures were above the climatic norm calculated for the period 1971–2000 by 0.3–1.4 °C. The average annual air temperature increased at a rate of

0.28 °C every 10 years. More significantly, average annual temperatures increased in the north, west and south of Kazakhstan – by 0.30–0.37 °C/10 years, in other regions by 0.25–0.29 °C/10 years. Increasing temperature due to climate change contributes to expansion of dry areas and increase of frequency of droughts, which negatively affects crop yields. Due to climate change it is expected that the frequency of strong and medium droughts will change. Precipitation distribution for the territory of Kazakhstan has significant spatial irregularity. The average annual rainfall (without snow) in the territory of Kazakhstan ranges from 130 to 1600 mm and in general rainfall decreases from north to south. In the north oblasts (*e.g.*, Kostanai, Akmolinsk, North Kazakhstan oblast), rainfall is about 400 mm, in the central belt (semiarid steppe zone) – up to 300 mm and in the south (desert) – up to 150 mm. The deficit of precipitation is the most important component of the drought. According (III – VI National Communication 2013) the expected climate change in the near decade will reduce the moisture availability for agricultural crops, enhance of aridity, shift of the zones with sufficient humidification towards northern latitudes and decrease in grain yields.

The system of vegetation monitoring in Kazakhstan is based on traditional methods using the data of ground meteorological network and remote sensing data. Network of meteorological stations is rare and measurements are spatially interpolated across large area. Satellite observing systems do not have these disadvantages, enabling regular monitoring of ground surface in different parts of the spectrum and across large areas, including sparsely populated, inaccessible places. In addition, the accumulated long time series of satellite data allow us to evaluate not only the current state of the vegetation, but variation and changes through different periods. At the present time detection of vegetation changes in the Republic of Kazakhstan, the estimation of the scale of these changes, and the ability to forecast of further development have practical significance and require special attention. Forecasting of future changes is done empirically on the basis of past changes.

9.3.1 The Study Area

Kazakhstan is a transcontinental country, located on the border of Europe and Asia between N40°32′ – N55°16′ and E46°30′ – E87°18′. At 2.72 km^2, Kazakhstan is the ninth largest country on the planet. The territory of the Republic is characterized by a latitudinal distribution of natural areas with different vegetation productivity. Most of the country belongs to arid and semi-arid areas: 44% of Kazakhstan territory is desert; 14% is semi-desert; 26% is steppe; 4.6% is forests. Arable land is primarily located in northern Kazakhstan where rainfed agriculture is the dominant land use. Most of the pastures are located in central and southern Kazakhstan. State of vegetation is highly dependent on weather and climatic conditions. The overall goal of the Kazakhstan study is to derive the best possible vegetation cover of Kazakhstan territory including arid and semi-arid zones, which is largely affected by the stress depending on weather and climatic conditions.

9.3.2 Methods

The Long-term series of differential and integral vegetation indices calculated from NOAA and MODIS satellite data of low space resolution (1000 m and 250 m, respectively) for the growing season (April–September) of 2000–2016 were used for monitoring the natural and agricultural vegetation of Kazakhstan's arid and semi-arid areas.

Vegetation indices, such as the NDVI (Rouse et al. 1973) and the VCI (Kogan 1990), enable monitoring of the state and development of the vegetated land surface at specific periods. They are typically composited in time to minimize obscuring cloud cover, e.g., 10-day maximum NDVI composites. Integrated vegetation indices (IVI) are summarize effectively used for the analysis of long-term changes in productivity of vegetation (Spivak et al. 2012). Index IVI characterizes the amount of green biomass accumulated during the vegetation season and is calculated by summing the NDVI- composites in each pixel. Index IVCI (Integral Vegetation Conditions Index) is used for the analysis of inter seasonal variations of the effect of weather conditions influence on the state of vegetation. Values of VCI, IVCI less than 30% are a good indicator of drought because a decrease of yield is noted equal or more 20% in this case (Kogan 1990).

Vegetation indices used in the space monitoring of the vegetation cover in Kazakhstan are presented in Table 9.1. Time series of vegetation indices calculated

Table 9.1 Vegetation indices used in space monitoring of vegetation cover in Kazakhstan (in each pixel)

Name	Formula	Period	Function
NDVI (normalized differential vegetation index)	$\mathrm{NDVI} = \frac{NIR - RED}{NIR + RED}$	10-day composites	Indicator of photosynthetically active biomass. Estimation of the state of vegetation
VCI (vegetation condition index)	$\mathrm{VCI} = \frac{NDVI_i - NDVI_{\min}}{NDVI_{\max} - NDVI_{\min}}$	10-day composites across multiple years	The index characterizes the state of the vegetation in comparison with the perennial values of the extremes of NDVI. Can be used as an indicator of moisture
IVI (integral vegetation index)[a]	$\mathrm{IVI} = \sum_{t}^{27} NDVIt$ t- number of 10-days in a vegetation season	Season	Analysis of seasonal variation in the state of the vegetated land surface
IVCI (integral vegetation condition index)	$\mathrm{IVCI} = \frac{IVI_i - IVI_{\min}}{IVI_{\max} - IVI_{\min}}$	Multiple seasons	Analysis of inter-seasonal variation of seasonality in the vegetated land surface

[a]Mathematically, the calculation of this index corresponds to the definition of the integral of NDVI within the specified limits. Physically, the meaning of this index can be interpreted as the accumulation of values NDVI

from NOAA and MODIS satellite data for vegetation seasons (April–September) 2000–2016 are used to describe the state of the vegetated land surface and its variation and change over large areas (Ogar and Bragina 1999; Spivak et al. 2009, 2017).

9.3.3 *Long-Term Changes in the Integral Vegetative Index (IVI) across Kazakhstan*

Kazakhstan is characterized by latitudinal temperature and precipitation gradients that define yield zones of vegetation productivity. The vegetation cover of Kazakhstan is also characterized by a pronounced latitudinal sequence of the location of zones of different productivity, associated with the geographical features of the location of the republic. When moving from south to north, there is a change of vegetation types from desert to forest-steppe. Accordingly, the density and productivity of vegetation cover changes.

Zonation of Kazakhstan was carried out according to the values of the normalized integral vegetation index IVI, which were calculated on the basis of satellite data for the period 2000–2016. A similar variant of zoning showed that the selected zones almost coincide with natural geographic zones. Thus, the zone with the values of the normalized index IVI equal to (0; 0.1), practically coincides with desert zones and desert steppes with very low productivity of vegetation; (0.1; 0.2) – semi-deserts with low productivity; (0.2; 0.3) – dry steppe and moderately dry steppe with average productivity; (0.3; 0.4) – arid and moderately arid steppes with moderate productivity; more 0.4 – forested steppe with high productivity. For example, Fig. 9.3 shows the location of five productivity zones over several years with contrasting weather conditions: the growing season of 2002 was one of the most favorable (wet) for the reporting period, 2008 – one of the unfavorable (arid).The quantitative sizes of zones with high and low productivity essentially depend on seasonal weather conditions.

Long-term dynamics of areas of zones with different vegetation productivity are shown in Fig. 9.4. According to the remote sensing data for the period of 2000–2016, there is a negative trend in the areas of high productivity zones; on the contrary, zones with low productivity have tend to increase their area. This principle of zoning showed a strong dependence of the changes of areas of highlighted zones, and their movement in the latitudinal direction due to the weather conditions of each year. In years with favorable weather conditions, a significant increase in the areas of high productivity zones and a reduction in the areas of low productivity zones are observed. At the same time, in the average range of values of normalized IVI (0.2–0.3), no significant changes in the area of the zone occur. In dry years, there is a spatial expansion of areas with low productivity and, as a result, the middle zone moves to the north.

The overlapping of the boundaries of the zone with the values of the normalized IVI index (0.2–0.3) for all the years of observation reveals an interesting pattern.

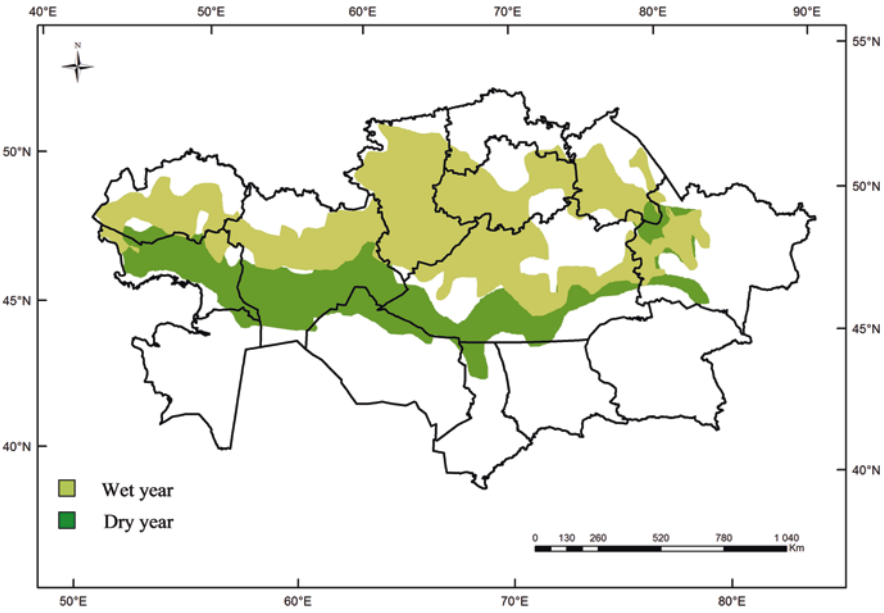

Fig. 9.3 Location of the zone with the normalized value of IVI (0.2–0.3) in the territory of Kazakhstan for various weather conditions

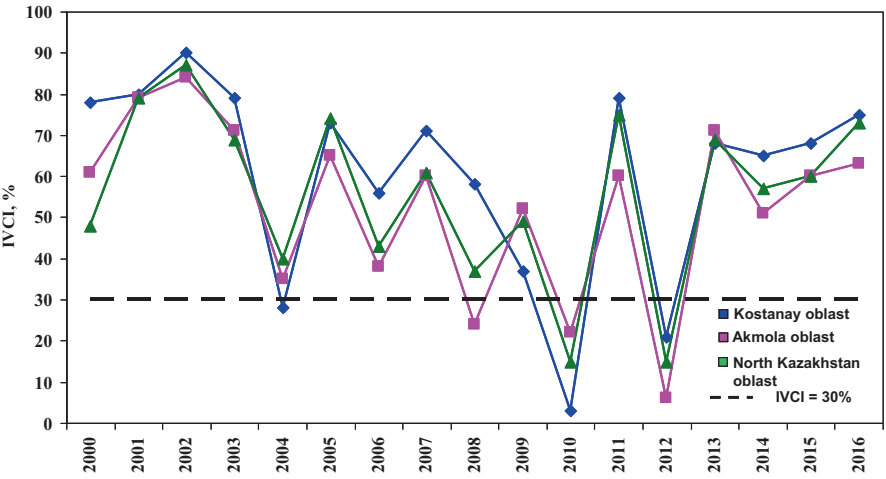

Fig. 9.4 Dynamics of the integral index of vegetation conditions on crop main oblasts of Kazakhstan for the period 2000–2016

The locations of this zone are determined in the latitudinal direction for different years, differing in weather conditions: for all years favorable for vegetation, the zone (0.2–0.3) is between 46° and 49° N and for all unfavorable (arid) years he lies

between 47°30′ and 54° N. The locations of the middle zone with IVI = (0.2–0.3) are shown for examples of wet (2002) and dry (2004) growing seasons (Fig. 9.3).

An IVCI value of 30% indicates drought. Thus, according to the remote sensing data, dry, low productivity years are 2008, 2010, 2012 for Akmolinsk oblast, 2004, 2010, 2012 for the Kostanay oblast, and 2010, 2012 for North-Kazakhstan oblast. Similar decrease of IVI and IVCI values are celebrated for all oblasts of Kazakhstan for period 2000–2016. Values of coefficient in the equations of the linear trend factically shows the rate of decrease of IVCI. Calculation of the coefficients in the equations of the linear trend of long-term changes of IVCI values and zoning of the territory of Kazakhstan by the their values were executed in the scale of oblasts of Kazakhstan (Fig. 9.5a) and of districts of the three north oblasts: Akmolinsk, Kostanay and North-Kazakstan (SKO) (Fig. 9.5b).

As the results of the calculation of the coefficients of the linear trend, the rate of deterioration in the condition of vegetation is more pronounced in the western regions of the republic. There is a positive trend of increasing of zones areas with IVCI <30%, which characterizes the growing impact of drought conditions on vegetation productivity in Kazakhstan. The results of calculation of areas of plots with low values IVCI for some regions of Kazakhstan are shown in Fig. 9.6.

Digital matrices of IVCI index allow visualization of the location of the plots with oppressed vegetation with indication of their geographic coordinates, as well as the definition of the areas of these sites. Digital map of frequency of low index values is formed by long-term values of satellite index IVCI to assess the probability of occurrence of droughts in Kazakhstan. This map was built for the time period of 2000–2016 with annual update. In Fig. 9.7 a schematic map of drought frequency after an algorithm of Spivak et al. (2010) is shown, where according to seasonal

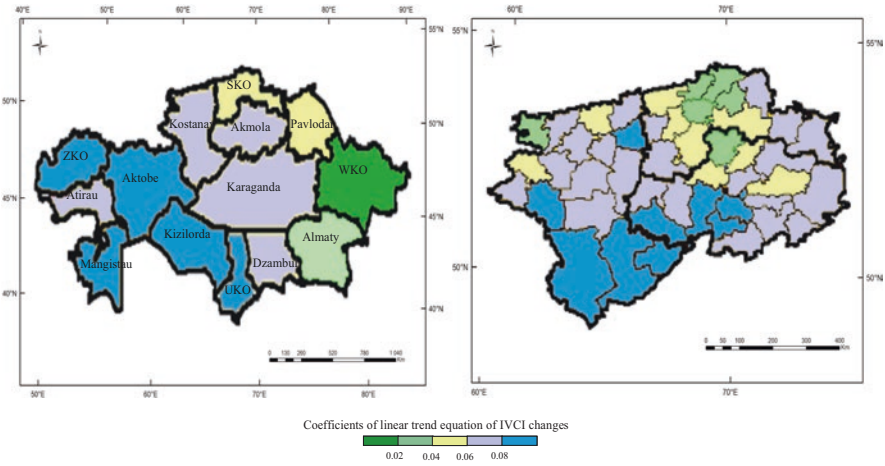

Fig. 9.5 Zoning of the Kazakhstan territory by the values of the coefficients in linear trend equations of long-term changes of IVCI (**a** – scale of oblasts; **b** – scale of districts within the three-oblast region of Akmolinsk, Kostanay, and North-Kazakstan)

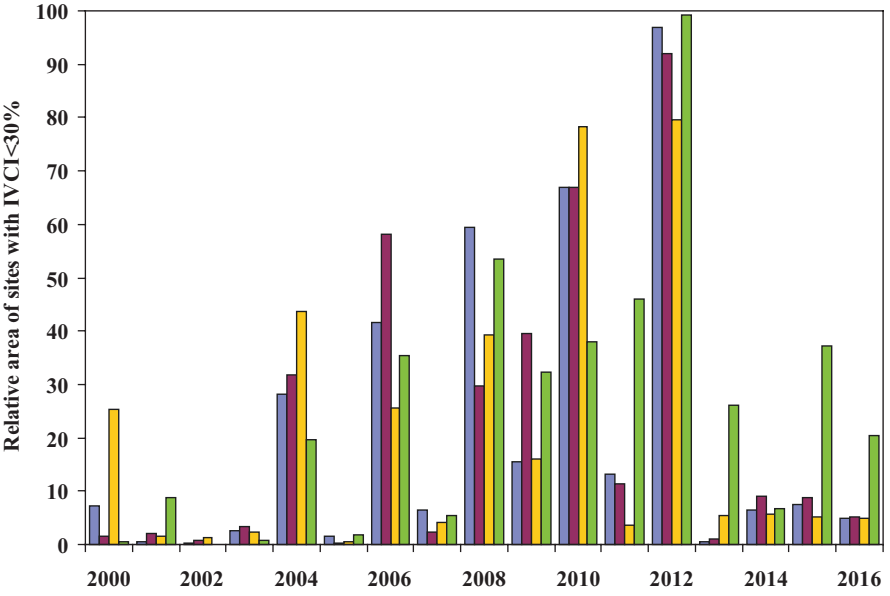

Fig. 9.6 The relative area in oblasts with IVCI values <30% as a function of time

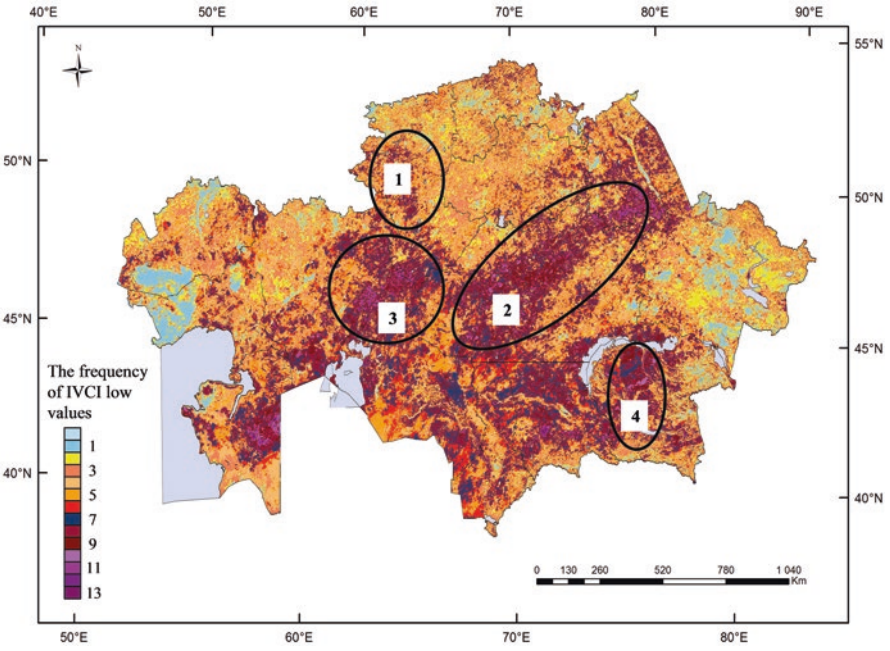

Fig. 9.7 The schematic map of frequency of droughts (IVCI <30%) during 2000–2016

digital maps IVCI each pixel is assigned to value of 1, if IVCI <30% (1), and value of 0 assigned, if IVCI >30%; (2) such binary cards are summed over a certain time period; (3) the final map shows the frequency of occurrence of index values less 30%.

Detected areas with a maximum frequency of dry conditions in 2000–2016 are in the map-scheme (Fig. 9.7). These include: (1) the western part of Kostanai region; (2) land on the borders of Akmola and Karaganda oblasts and the East Kazakhstan region; (3) land on the border of Kostanay, Aktobe and Kyzylorda oblasts; (4) Pribalkhashie. High degree of mosaic of the distribution of this index makes it difficult to identify areas subject to arid conditions. In this regard, zoning of the territory of the northern regions of Kazakhstan (regional scale) was carried out according to the values of IVCI <30% for 2000–2016. This made it possible to identify groups of regions with different degrees of risk of arid states (see Fig. 9.8).

VCI values of less than 30% correspond to the stress state of vegetation, characteristic of drought foci. (Kogan 1990). VCI-techniques are mainly used for monitoring of drought conditions in Kazakhstan. A drought can have different impact on the productivity of vegetation. After Spivak et al. (2009, 2017), it was proposed to estimate the intensity of drought on a three-point scale: $0.2 \leq$ VCI <0.3 indicates moderate drought; $0.1 \leq$ VCI <0.2 indicates severe drought; and VCI <0.1 indicates a very strong drought. Analysis of remote sensing data shows that areas of lots with a very strong damage of vegetation sharply increase as result of increasing drought duration.

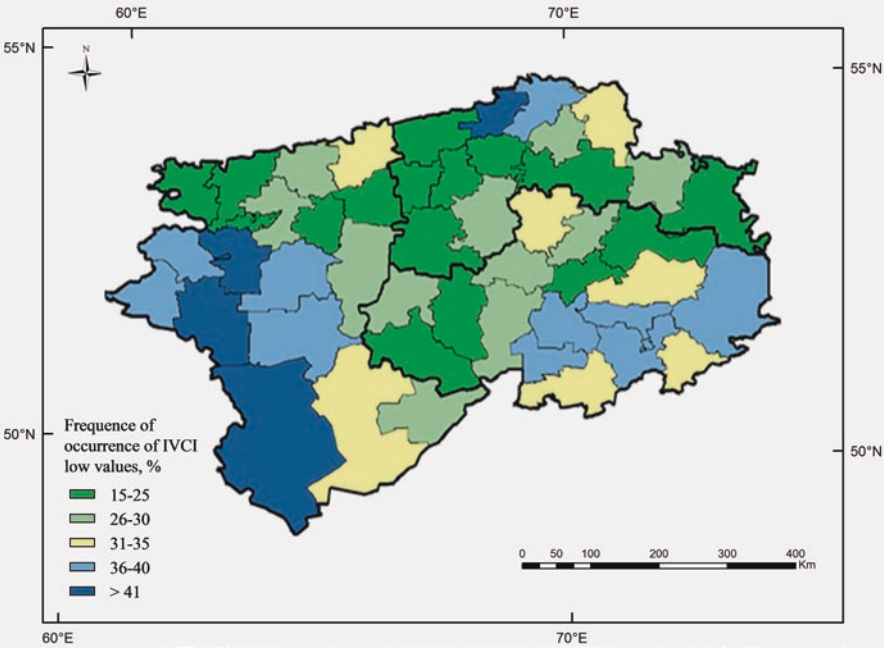

Fig. 9.8 Zoning of the northern oblasts of Kazakhstan according to the values of the frequency of occurrence of low IVCI values (May–August, 2000–2017)

Thus, using the example of Kostanay region, the diagram of changes in the characteristics of areas with low VCI values for arid 2012 is shown in Fig. 9.9. A more stringent condition VCI < 0.1 of the time period 2000–2016 becomes significant for the entire territory of the Republic actually since 2006. This fact indicates an increase in the frequency of dry years in the second half of the period under review. This is also confirmed by the negative trend in long-term changes of the integral index IVI, IVCI, both for Kazakhstan and for its individual parts (region, district) (Fig. 9.10).

To interpret the analysis of vegetation indices VCI/IVCI, the results of monitoring of the vegetation state and its dependence on weather conditions according to the data of remote sensing are compared with long-term statistical data on the yield of grain crops. Such a comparison of the time series of crop production and IVCI for the period 2000–2013 was performed for the northern regions of Kazakhstan. It is here that the main part of the production of grain crops is located in the non-irrigation zone of the republic. IVCI values are calculated for May–August of each growing season. The correlation coefficients between the two data sets are calculated on examples of regional and district levels (see Table 9.2).

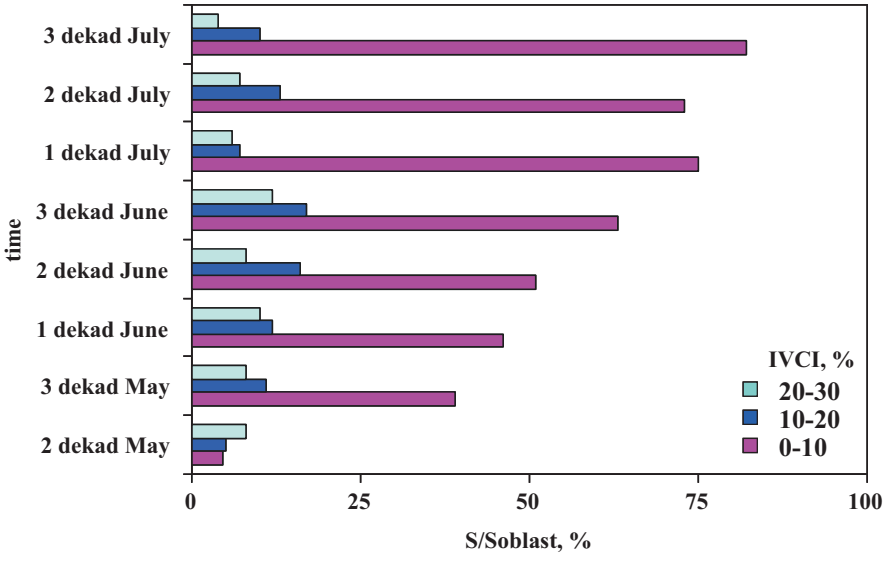

Fig. 9.9 Area of Kostanay oblast with low values of VCI indicating different levels of drought in 2012. Note that more than 50% of the oblast was in the very severe drought category by the second dekad of June and progressed to more than 80% of the oblast by the third decade of July 2012

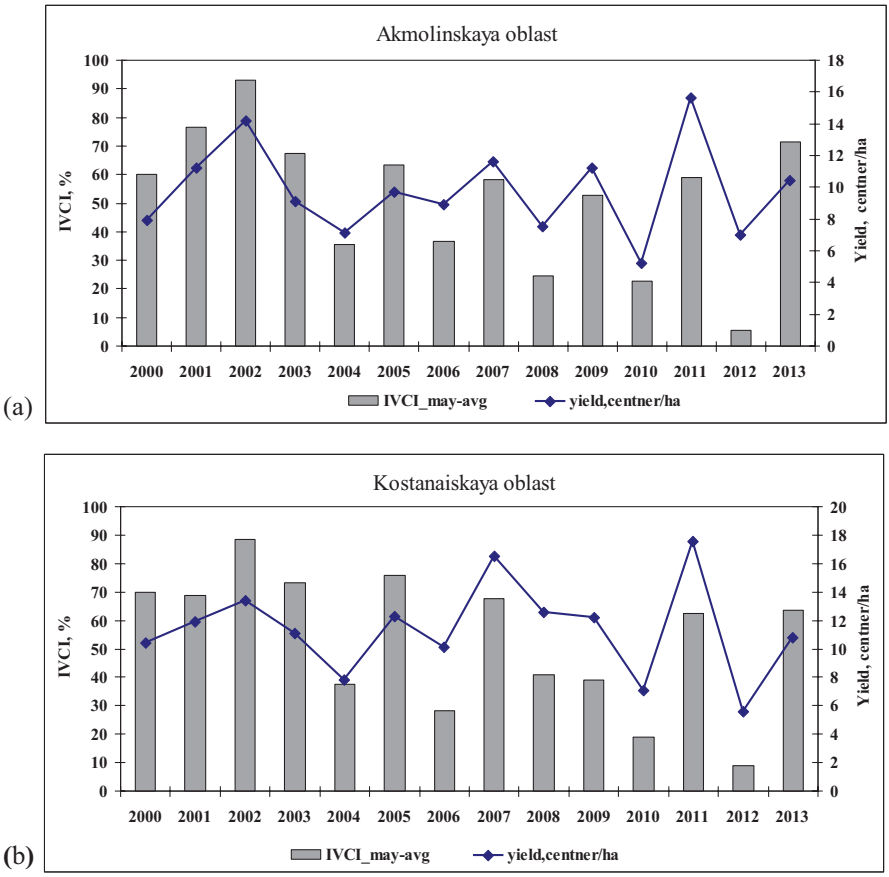

Fig. 9.10 Long-term statistical data on grain yield and values of the integral index of vegetation conditions IVCI in the territory of Akmola (**a**) and Kostanay (**b**) regions

Table 9.2 Values of correlation coefficients and closeness of the relationship between statistical data on the yield of grain crops and IVCI

Territory	Correlation coefficient	Closeness
Akmola region	0.71	Strong
Accol district	0.63	Moderate
Zhaksy district	0.58	Moderate
Kostanay region	0.66	Strong
Kamysty district	0.78	Strong
Denisov district	0.67	Strong

9.3.4 Spatiotemporal Changes of the Steppes

The steppe zone for Kazakhstan's agriculture plays an important role. It is here that the main grain lands of the Republic and pastures are located. The steppe zone covers more than two thirds of the Republic territory. These lands are traditionally used for rainfed agricultural production, making them highly vulnerable to climatic variation and extremes.

Climate change scenarios for the territory of Kazakhstan based on the use of the IPCC AR5 model show an increase in average annual temperatures (The III-VI National Communication 2013). For precipitation, the presence of such a clear trend is not noted, but their redistribution is predicted. Such changes have a negative impact on climate-dependent sectors of the economy, especially agriculture. One of the negative consequences could be a reduction in the yield of some crops, in particular, grains. Due to the change in the temperature the boundaries of the moisture zones will shift to the north by an average of 50–100 km and, at the maximum, of 350–400 km. Accordingly, it is projected that the zone of insufficient precipitation, where most of the commodity crops are grown in Kazakhstan (irrigated farming), will increase from 6% to 23%. Experts predict that crop losses of up to 30% are possible due to climate change.

The steppe zone of Kazakhstan is the most vulnerable from among all natural zones in the Republic to the effects of arid conditions, which intensify the processes of aridization and desertification. Space monitoring of the steppe and dry steppe zone of Kazakhstan is of special interest. The object of the research are space-temporal changes in the spectral characteristics of the vegetation cover of the steppe zone of Kazakhstan. To determine the patterns of their changes, depending on the state of the vegetation cover in different agro-climatic zones, including dry conditions, a territory was selected as a transect with a width of 100 km and a length of 730 km (Fig. 9.11). The allotted territory is located on the border of the main grain-bearing oblasts – Kostanay, Akmola, North-Kazakhstan and includes areas with natural vegetation of almost all subzones of the steppe zone of Kazakhstan.

The differences of coefficients in the linear trend equations relatively deviation of IVI from the mean multiyear value for each selected section are shown in Fig. 9.12. The coefficient in the linear trend equation of the multi-year variation IVI can serve characterizes the intensity of the changes that occur.

9.3.5 Summary

The analysis of changes in vegetation indices (differential – NDVI, VCI and integral – IVI, IVCI), computed from satellite data over the territory of Kazakhstan for the period 2000–2016, shows:

- values of integrated indices of vegetation have an expressed tendency to decrease;

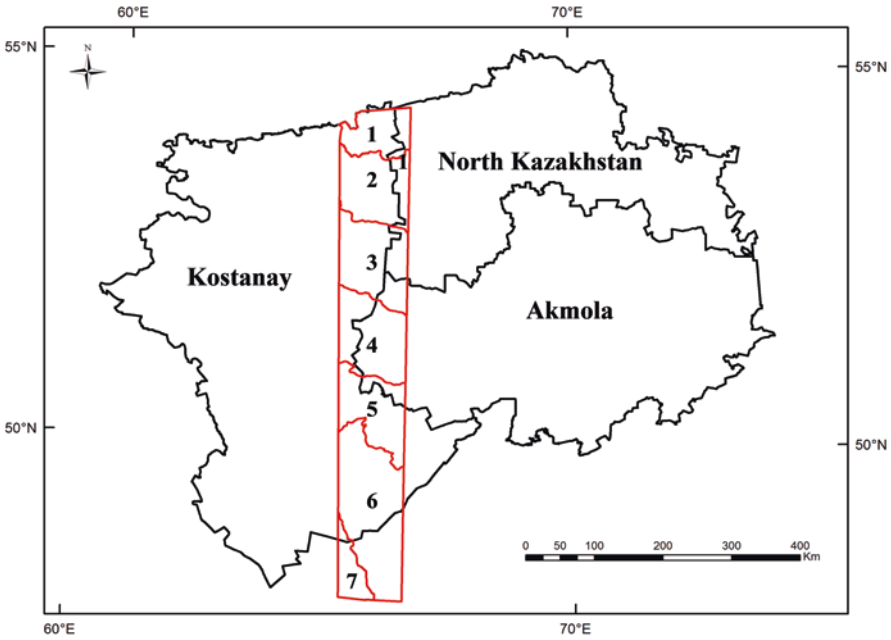

Fig. 9.11 Subzones of steppe region of Kazakhstan within the limits of the transect: 1 = forested steppe; 2 = moderately arid steppes; 3 = arid steppe; 4 = moderately dry steppes; 5 = dry steppe; 6 = desert steppes; 7 = northern desert

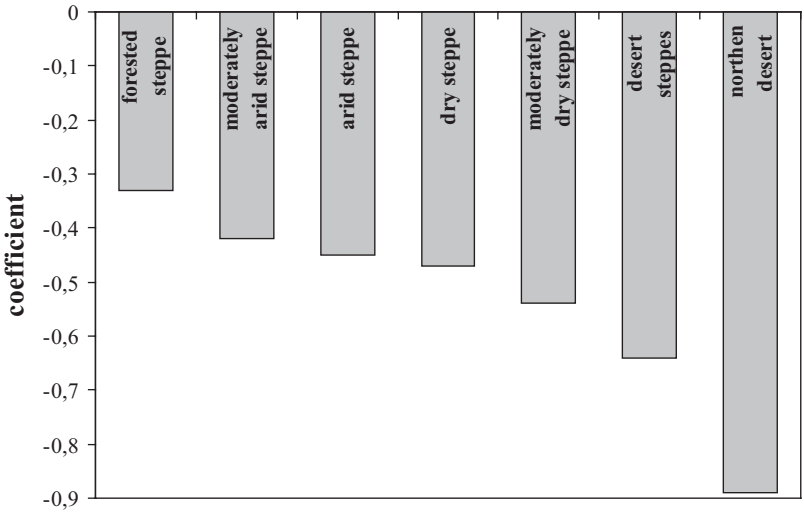

Fig. 9.12 Coefficient in the linear trend equations of the relative deviation from the IVI long-term average (characteristic of a sensitivity of vegetation to weather changes)

- an increase in the areas of plots with low IVCI values (<30%) during the observation period is noted;
- analysis of the distribution of the VCI index for the territory of Kazakhstan for the range (0–0.3), which is an indicator of arid conditions, revealed a positive tendency to increase the areas with low VCI values (<0.1) for the whole territory of the Republic since 2006;
- comparison of the time series of the integral index of vegetation conditions and yield of grain crops shows a fairly high correlation. Low yields coincide with the droughts (IVKI <30%);
- according to the zoning of the steppe zone of Kazakhstan on the state of vegetation based on satellite information, since 2004, the growth of areas with low productive vegetation located between 48°N and 53°N parallels has been recorded.

Analysis of vegetation indices showed the intensification of the stress effect of aridity on the vegetation cover of the steppe zone of Kazakhstan in 2000–2016. Such information is important in the study of the processes of aridization and desertification in the Republic.

9.4 Case Study Mongolia

Mongolia is a country of fragile ecosystems, a continental climate, relatively high altitudes and is occasionally described as being quite sensitive to climatic changes (Dagvadorj et al. 2014). Climate Change affects the environment, water supply, desertification and natural disasters that already led to financial, environmental and human losses. An average increase of annual mean air temperatures in Mongolia of 2.14 °C between 1940 and 2008 as compared to 0.85 °C worldwide from 1880–2012 is impressive evidence for the change that Mongolia has already undergone. Increased occurrences of drought, water sources depletion and decreasing biological diversity, all benefiting the process of desertification, accompany these changes (Dagvadorj et al. 2014; UNCBD 2014). The process of land degradation in these arid or semiarid environments is further affected by human activities that may include overstocking and overgrazing, undergrazing at more remote locations, switching from sheep to goat herding or deforestation (UNCCD 2012; Rosales and Livinets 2005; Dorj et al. 2013).

Mongolia's steppe grasslands include one of the largest grassland ecosystem complexes of the world. Over 70% of Mongolia is built up by three major ecological zones: the desert-steppe, steppe and mountain steppe. These grasslands support most of Mongolia's domestic livestock (camels, cattle, yaks, horses, sheep and goats). To date, relatively little is known about the vegetation composition and dynamics of these ecosystems. Three national-scale classifications of Mongolia's vegetation (Hilbig 1995; Ulziikhutag 1989; Yunatov 1977) are available, of which only the first is in English. The scientific data situation about the response of

Mongolian grassland vegetation to increasing grazing intensity or the effect of grazing removal is scarce. A few studies (Chogni 1989; Tserendash and Erdenebaatar 1993) concentrate on the impact of grazing intensity or removal grazing, but these studies were mostly conducted in the mountain-steppe and steppe zones in the center or north of Mongolia. Studies about grazing and climate influences on the composition of desert-steppe grasslands in southern Mongolia are so far non-existent. Moreover, Mongolia as a country at the southern edges of the Eurasian cryosphere, is a country partly under the influence of permafrost. Three basic forms of frozen soils (permafrost, sporadic permafrost, and seasonal frozen soil) exist in Mongolia. The spatial distribution of these "permafrost types" is determined by annual mean air temperature. Frozen soils may have influence on the phenological shifts of dry and cold grasslands in Mongolia (Sun et al. 2015). Frozen soils play a decisive role in storing water from precipitation of the previous autumn for the subsequent grass green-up in the next year.

In contrast, long-term (1982–2010) NDVI development in the region, evaluated using AVHRR (1982–2006) and MODIS (2000–2010) data, describe an upward trend in vegetation greenness until the mid to late 1990s (Bao et al. 2014). During the 2000s this trend apparently reversed in coherence with a significant decline in precipitation in the same period. The authors attribute the decline on 60% of the landmass to a hotter and drier climate that is associated with drought stress. (Eckert et al. 2015) reported mostly positive significant trends on 50% of Mongolia's surface between 2001–2011 using the MODIS 16-day composite vegetation indices product. They also conclude that precipitation changes during this time are related to changes in NDVI, though identifying further areas where deforestation and mining are predominant factors in declining NDVI's. The largest part of the country has none or a positive trend, while negative trends are clustered to the far west and the Dundgovi province. The study could however only identify significant trends for about 50% of the country due to the relative short time-series. Chu and Guo (2012) used a similar 12-year MODIS time-series from 2000–2011 to characterize vegetation responses to climate change in the Hövsgöl area, northern Mongolia. They concluded that the growing season that normally starts in late April and ends in late October, with full growth in July, does begin earlier in more recent years. They therefore assumed that NDVI dynamics in the research area are mainly controlled by the pattern of temperature variations rather than due to precipitation. Purevsuren et al. (2012) used SPOT VEGETATION data for a short time-period (2003–2009) and they also detected a slight increase in NDVI during this time-span. They also concluded that NDVI and precipitation are well correlated in wet years but quite weak during dry years, if at all. Several studies exist in which the suitability of NDVI is raised for various vegetation related changes and responses in Mongolia (Nandintsetseg et al. 2010; Zhang et al. 2009; Iwasaki 2009; Adyasuren et al. 2005; Javandulam et al. 2005) or Central Asia in general (Yu et al. 2003; Yu et al. 2004; Vostokova and Gunin 2005; Huang and Siegert 2006; Dulamsuren et al. 2016).

A common feature of these studies is the use of rather short time-series (< 10 years), the use of similar remote sensing products (mostly MODIS and GIMMS) or that the end of the considered time-series lies somewhere between 2006 and

2010. As such we will evaluate if there is again a trend reversal towards a positive NDVI development in Mongolia as indicated by previous studies mentioned above. To achieve this we incorporated more recent years of available NDVI data of SPOT-VGT data in combination with the ERA-interim climate data-set in a comparably high resolution of 0.125 degrees and a modern 4D-var sampling technique. The driving environmental factors for the purported changes are then assessed and discussed. The assessment is done on an annual and monthly basis.

9.4.1 Study Area

Mongolia is situated at the northern fringe of Central Asia in the transition zone between the Siberian Taiga to the north and the Gobi Desert in the south (Fig. 9.13). Spatially it extends from 87°45′E to 119°56′E and from 41°34′N to 52°09′N and covers a total area of 1,562,950 km^2. The wide basins of the interior drainage system lie at elevations between 900 and 1500 m asl with the lowest areas below 720 m asl. The mountains are shaped by pronounced flat planation surfaces in elevations between 2500 and 3500 m asl, while the highest peaks rise above 4000 m asl. There are four main mountain regions in Mongolia. The Mongolian Altai in the west (highest peak is Tavan Bogd, 4374 m asl), the Gobi Altai in the south (Ikh Bogd, 3957 m asl), the Khangai Mountains in the center (Otgon Tenger, 3964 m asl) and the Khentei Mountains in the northeast (Asralt Kharj khan, 2799 m asl). Modern glaciation occurs exclusively within the Mongolian Altai with a small ice field at Otgon Tenger as the sole exception.

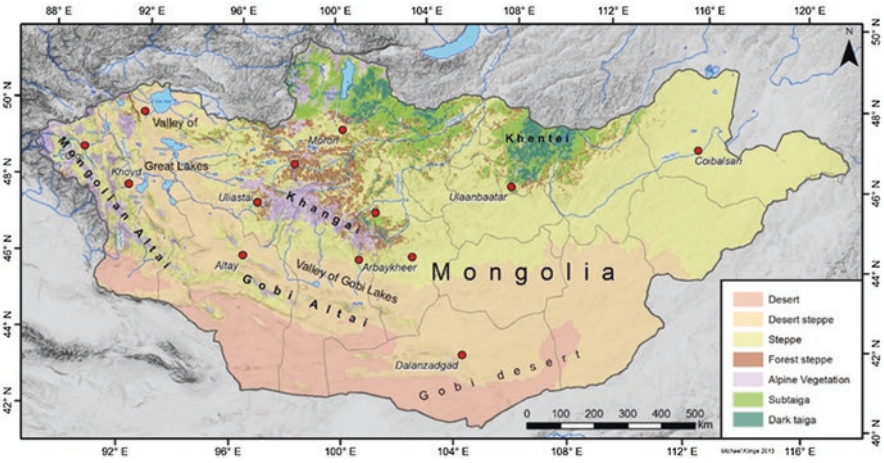

Fig. 9.13 General vegetation units of Mongolia. (Changed by M. Klinge using original data from Hilbig 1995; Vostokova and Gunin 2005; Dulamsuren et al. 2016)

The largest lake in Mongolia is Uvs Nur (3585 km^2), which is situated in the northern part of the "Valley of Great Lakes". Large lakes like Khiargas Nur (1365 km^2), Khar Nur (918 km^2) and Khar Us Nur (934 km^2) are distributed throughout this north to south trending endorheic basin too. This catchment area lies east of the Altai mountain range, which is drained by the Khovd Gol, and in the west of the Khangai Mountains, which are drained by the rivers Tes and Zavkhan Gol. Large dune fields exist in the east of the lakes. The west to east trending "Valley of Gobi Lakes" with Bon Cagan Nur (269 km^2) and Orog Nur (106 km^2) lies between the Khangai Mountains and the Gobi Altai in the south. Lake Khovsgol Nur (2723 km^2) in northern Mongolia drains to the Selenge river, which together with the Orchon river is flowing into lake Baikal in Siberia.

The climate of Mongolia is characterized by high continental semi-arid to arid conditions. In wintertime the Siberian high pressure cell produces cold and dry weather with few snowfall and average temperatures between −15 and −30 °C. The main rainy season occurs from June to August during a short summer period, induced by westerlies and cyclone precipitation, but is soon ending when the dry season starts again in autumn. Mean summer temperatures range between 10 and 27 °C. The mean annual precipitation is below 50 mm in the interior basins, around 125 mm in the southern desert and up to 350 mm in the northern steppes, while it increases to more than 500 mm in the high mountains. There is a great annual variation of precipitation in the amount and spatial pattern which is strongly influencing the density of the vegetation cover (Barthel 1983). In accordance with these climatic environments a latitudinal zonation of the vegetation exists, which is modified by an altitudinal zonation in the relief (Fig. 9.1a). In northern Mongolia taiga vegetation with mixed needle and deciduous broadleaf forests occurs. The vegetation belt in the middle of Mongolia consists of steppe, crop- and grasslands in the basins and forest steppe in the mountain area. In this forest boundary ecotone of semiarid climate conditions the relief is controlling the spatial vegetation pattern. While the deciduous needleleaf forests, consisting of larch trees (*Larix sibirica*), are exclusively growing on northern aspect slopes, the south facing slopes are covered by steppe vegetation. The southern part of Mongolia consists of desert steppe and sparse desert vegetation. Sand dune, playas and takirs are widely distributed. In the high mountains dense alpine meadow vegetation occurs between forest steppe and the periglacial zone of frost debris. The main perennial rivers are accompanied by floodplain meadows and forests.

9.4.2 Materials and Methods

SPOT VGT satellite data: The satellite data used in this case study primarily consists of SPOT VEGETATION 10-daily NDVI atmospherically corrected composites at 1 km resolution for the time January first 1999 to December 31st 2013, equaling 540 distinct time-steps. In addition, the SAVI was calculated from raw SPOT-VGT reflectance data to verify the NDVI signal in areas with sparse vegetation (Huete

1988). These were re-sampled to monthly rasters using the maximum value of all three. The annual means were calculated from the 12 re-sampled rasters. In a first step pixel based NDVI trends were calculated by estimating the coefficients of a linear regression where the Mann-Kendall trend test indicated a significant trend.. As the sole consideration of monthly NDVI values and annual means might not be sufficient, a seasonal evaluation of NDVI changes was additionally executed. This includes the consideration of the winter months only (November–March) to detect possible NDVI changes that occur when no vegetation is present and those months that can be generally described as the growing period (May–September) (Dagvadorj et al. 2014; Wang et al. 2007; Suttie and Reynolds 2003). For each combination, the linear regression and the Mann-Kendall test were calculated on a pixel-by-pixel basis. For each pixel the best combination (lowest p-Value, most positive or negative r-value) and the corresponding value are determined and logged.

AVHRR satellite data: To evaluate the validity of the SPOT-VGT data-set it was compared against the GIMMS AVHRR Global NDVI-3G dataset. The AVHRR data was atmospherically corrected as well and features a resolution of 0.0833 degrees, making it more coarse than the SPOT-VGT data (by about a 1D factor of 10). For a direct comparison in the form of a regression analysis the AVHRR data was re-sampled to match the resolution of the SPOT-VGT data. In a first step both datasets where cropped to the same extent before the AVHRR data was actually re-sampled using a spline interpolation by the order of 3. The original dataset covered the time from 1982–2012 in a bi-monthly resolution. The monthly maximum values and from this derived annual means from 1999–2012 were then used for the comparison. If p-values are mentioned in regard to the comparison of both data-sets, these refer to a simple two sided t-test with H0 being the slope of the regression line is equal to zero. Significance is assumed for $\alpha < 0.05$, meaning that if $p < 0.05$ the correlation at a certain pixel is considered significant.

Climate data: The dataset used to investigate climate induced changes to the NDVI is the ERA-interim data-set (Berrisford et al. 2011; Dee et al. 2011). This was chosen over the NCEP/NCAR Reanalysis products for its higher spatial resolution (here 0.125 degrees) and more modern sampling technique, as the longer temporal series of the NCEP, going back until 1948, was not necessary for this approach. We did use monthly data from January 1999 until December 2013 to cover the same period as our NDVI data-set. Temperatures were calculated from the "Monthly Means of Daily Means", precipitation from the "Synoptic Monthly Means" section of the ECWMF website as no pre-computed daily means were available. The daily 8 synoptic mean values were added to form a monthly mean value. This was done by adding together the synoptic monthly means at time 00, step 12 and time 12, step 12, as suggested by the ECWMF. The original ERA-interim units for temperature (Kelvin) and precipitation (mm/day) were maintained. A possible source of error might be found in the context of the used climate dataset. Though the confidence in this kind of data has steadily risen in the past years and it is more often regarded as equivalent to observational data, this is not always justified (Dee et al. 2011). Validation of ERA-interim data for Mongolia is however sparse. A comparison of soil moisture on the Mongolian Plateau did show that ERA-interim data is capable

of representing temporal dynamics, though slightly overestimating it (Wen et al. 2014). Global assessments of the quality of ERA-interim precipitation data (Lorenz and Kunstmann 2012) conclude that it is still the most reliable data-set in areas with a large number of gauges. Though this is not given to the same extent in Mongolia as in Europe or North America, regions that were pointed out as problematic were mostly parts of Africa and South America.

We included a validation of the ERA-interim dataset used in this publication with monthly data from 4 weather stations in Mongolia (Matthew et al. 2012). Figure 9.14 displays the monthly correlations between both data sources. From this, it should be clear that the ERA-interim dataset is well suited to depict the temperature development in the study area. For precipitation it is always more difficult to be reliably reproduced in models, which is also the case for ERA-interim. Though not as good as for temperature, the precipitation data is in general agreement for Bulgan or Choir, a bit worse for Dalanzadgad station and worst at the Altai station. The agreement for all stations mostly diminishes when precipitation becomes rather low, in these cases ERA-interim sometimes returns precipitation while none was reported by the station data. The rather weak correlation for the Altai station was also to be expected, as apart from the low overall precipitation, relief influences complicate its translation into the ERA model.

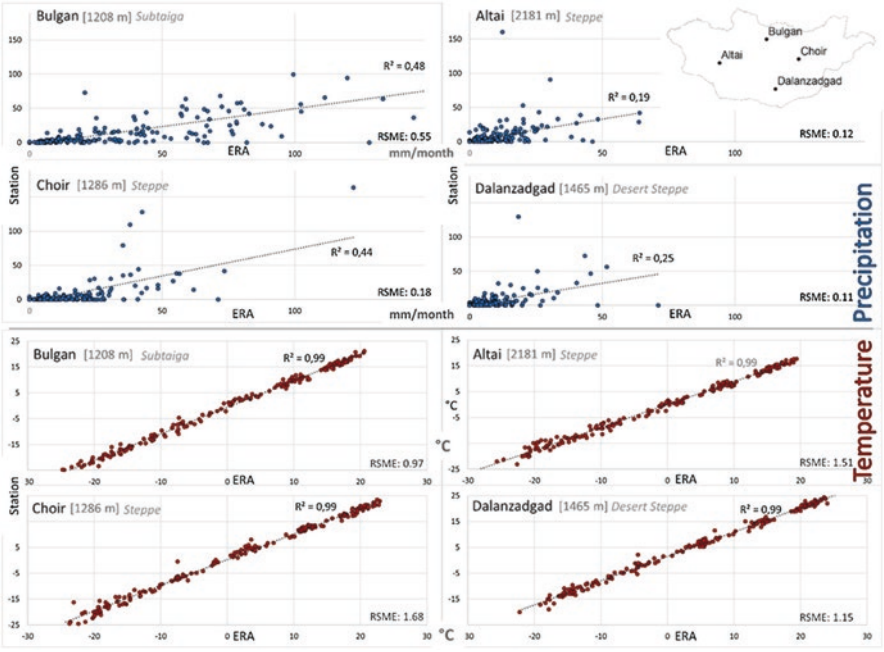

Fig. 9.14 Correlation analysis between monthly ERA-interim and local weather station data for precipitation (top) and temperature (bottom) data for 1999–2013. ERA-interim units (x-axis) are in average mm/day and K, while station units are total mm/month and average °C (y-axis)

Mann-Kendall trend test: This study combines two approaches to determine the significance and strength of existing trends. The Mann-Kendall (MK) test for trends is first applied to determine which locations have a significant trend. MK can assess if any monotonic trend exists within the data (positive or negative, without regarding it to be a linear trend) and is also a non-parametric test. We assumed existing trends for $p < 0.05$.

As Mann-Kendall only ascertains the level of confidence that any trend is existent within the data, it does not give information on its strength or direction. We therefore used the r-value of a linear regression to approximate the strength and direction of each pixel where MK was significant.

Exemplary Points A–E As a map-only depiction of trends hides the underlying changes and is limited to 1 value per pixel, we chose 5 exemplary points in Mongolia to highlight annual values and their progression. Figure 9.15 shows where these points are located, Fig. 9.23 gives in-detail NDVI, temperature and precipitation

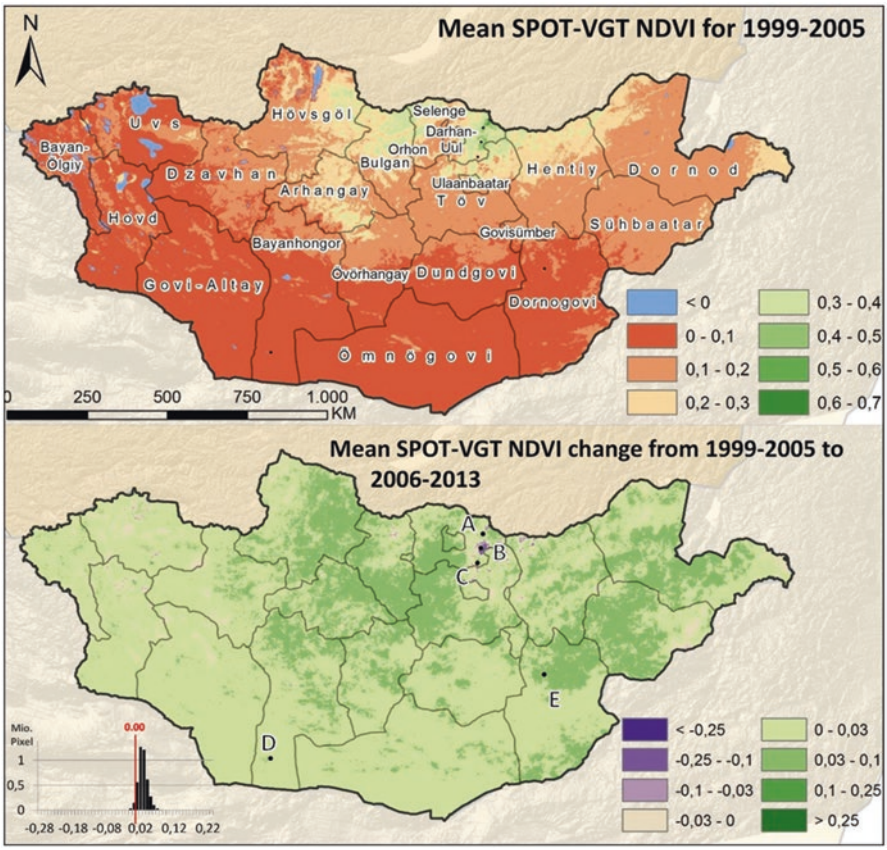

Fig. 9.15 Top: Mean annual NDVI Values from SPOT-VGT data for the years 1999–2005 Bottom: NDVI change in absolute values from mean 1999–2005 to mean 2006–2013

information for each point. All points where chosen at locations with strong and highly significant trends. After identifying these locations, the exact points where chosen in their respective centers. Points A and B lie within the areas of strongest NDVI decline. While A was chosen for its location at the largest absolute NDVI decline in Mongolia, B lies within the largest contiguous area of decline. C is located in the vicinity of A and B, but shows a significantly positive NDVI trend, and can as such be seen as a contrast to A and B. All three points are located in an area that is dominated by forest. D and E were chosen for their location in the center of the largest continuous areas of positive NDVI trends in Mongolia. While D lies in the midst of the desert, E lies in a transition zone commonly labeled as Desert Steppe.

9.4.3 Results

As a consequence of the prevailing arid climate, Mongolia consists of vast areas of land that stay well below annual average NDVI values of 0.2 (see Fig. 9.15). About 48% of the total land area are even below 0.1 while less than 4%, mostly within the northern mountainous area, show annual NDVI averages of >0.3. Thus even small differences on the annual scale might be an indication for an apparent change within the area. A rough comparison of the first (1999–2005) and subsequent half (2006–2013) of the time-series gives an initial impression of supposed NDVI changes. In this comparison (Fig. 9.15) almost all of Mongolia shows an increase in annual mean NDVI, on average by 0.02. Parts with a negative development are scattered throughout western Mongolia and to a lesser extent in the far east. However, these declines are mostly fairly below −0.10. Another small area (about 620 km^2) in the Selenge province north of Ulaanbaatar shows an average decline in NDVI of around −0.10 that is selectively as low as −0.27. To give a better impression of the inter-annual dynamics, results were not only calculated spatially but also for five point locations (compare Fig. 9.15 and Fig. 9.23).

9.4.4 Annual and Monthly NDVI Trends

Though small in absolute numbers, the NDVI in Mongolia generally shows a rising trend during the presented time period, thus Mongolia is getting greener on average. This paragraph's scope is to determine if this is a significant trend or rather an anomaly, if it is valid for entire country or only parts and if it is detected throughout the year or just on a monthly basis. While Fig. 9.15 gives an impression of the absolute change in NDVI, around 0.01–0.08 between both half's of the time-series, Fig. 9.16 describes trends on an annual basis. This was done spatially on a pixel by pixel basis. A Mann-Kendall test to determine significant trends within the data (top), regardless of strength and direction, was applied first to account for trends in general.

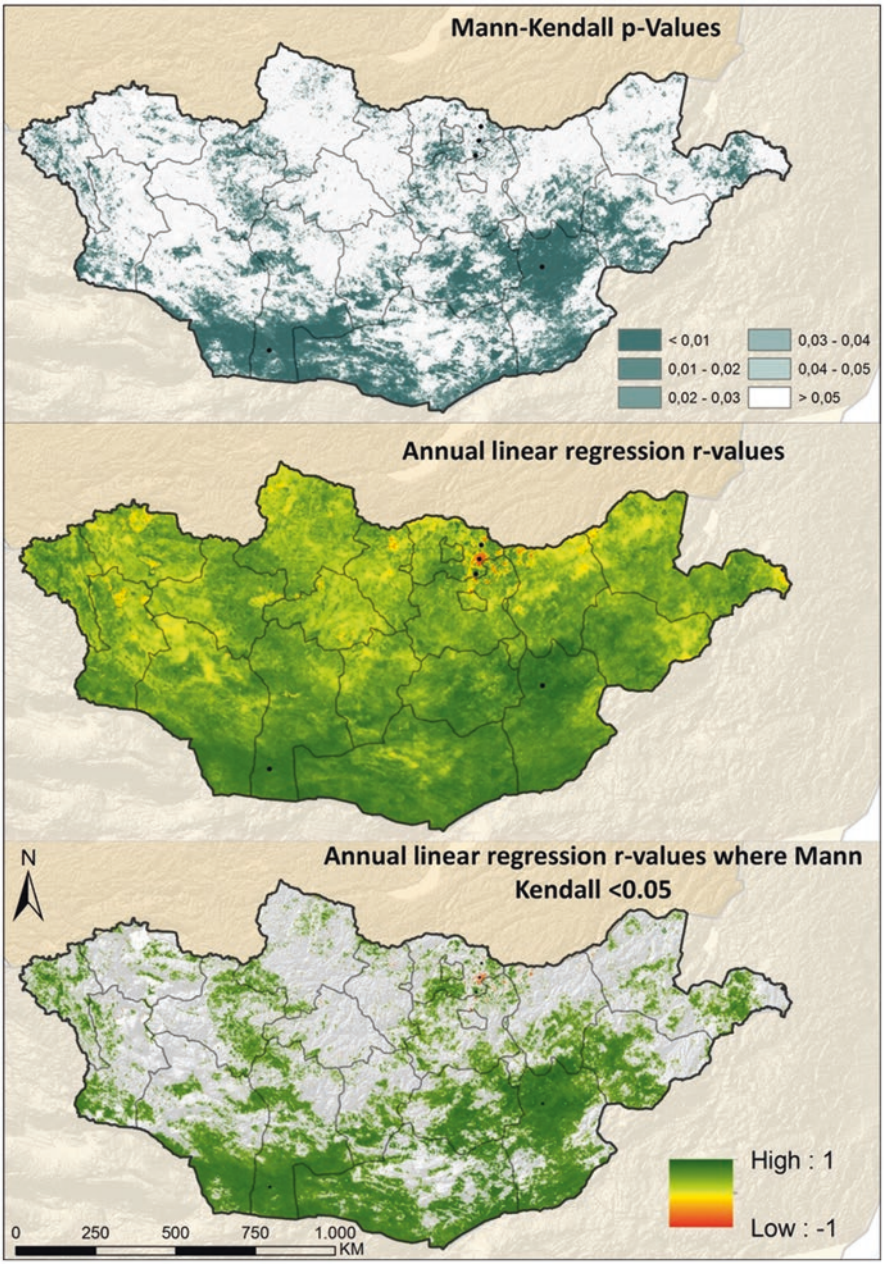

Fig. 9.16 Trend of annual mean NDVI values from 1999–2013. Top: R-values of a pixel-based linear regression. Middle: Mann-Kendall trend test significance. Bottom: r-values of the linear regression where Mann-Kendall is significant for $\alpha = 0.05$

To give an impression of the quality and direction of trends a linear regression was conducted (middle). Finally, both calculations were intersected (bottom) so only r-values at locations with significant trends remain in the map. A significant annual trend is detected on about one third of the Mongolian landmass. In accordance with the basic mean value comparison between 1999–2005 to 2006–2013 these trends are mostly positive. The only coherent area with a negative development is the aforementioned area north of Ulaanbaatar with r-values generally well below −0.5. However, the other areas with a slighter negative development, *e.g.* those to the west, do not show up as being significant.

The strongest and most extensive indication of a positive NDVI development can be found in the Gobi desert, namely in the south of the provinces Govi-Altay, Bayanhongor and Ömnögovi as well as the northern part of Dornogovi. Most of the area south of Govi-Altay is a strictly protected area (national conservation area or national park). Here most areas show Mann-Kendall p-values <0.01 (highly significant) an r-values >0.8. Locations D and E are located in these areas. Though the changes during these 15 years are small in absolute numbers, they are quite obvious and well enough described linearly. If trends are estimated on a monthly basis (Fig. 9.17) it becomes evident that the described annual trends can largely be attributed to positive changes in the time from March to June with average r-values of 0.66. These are closely followed by July to November (also February) with average r-values of 0.62 while December and January averages around 0.48. April is clearly the one month with the strongest and most widespread uptrend. Not only are the average r-values at 0.68 the highest of all months but it is also the month with the largest area of significant changes in NDVI. Half of Mongolia is affected, almost twice as much as in March, May or June, while >99% of these areas show a positive trend. Interestingly, there is even a significant increase in NDVI from December to February, mostly in the southern part of the country. The trends are comparably weak and cover only small areas but are clearly present in the data. This is interesting, as temperatures in these areas are well below freezing during this period and one would not assume large scale vegetation growth in this period.

9.4.5 Seasonal NDVI Trends

If the months are combined into seasons, e.g. winter (November–February) and growing season (May–September) as shown in Fig. 9.18, considerable trends exist throughout the growing season. About 40% of Mongolia is affected by a mostly positive trend which is distributed throughout the entire country. Though sparse, significant trends occur during the winter season as well. Then only about 5% of the country is affected with a clear concentration on the southern desert parts.

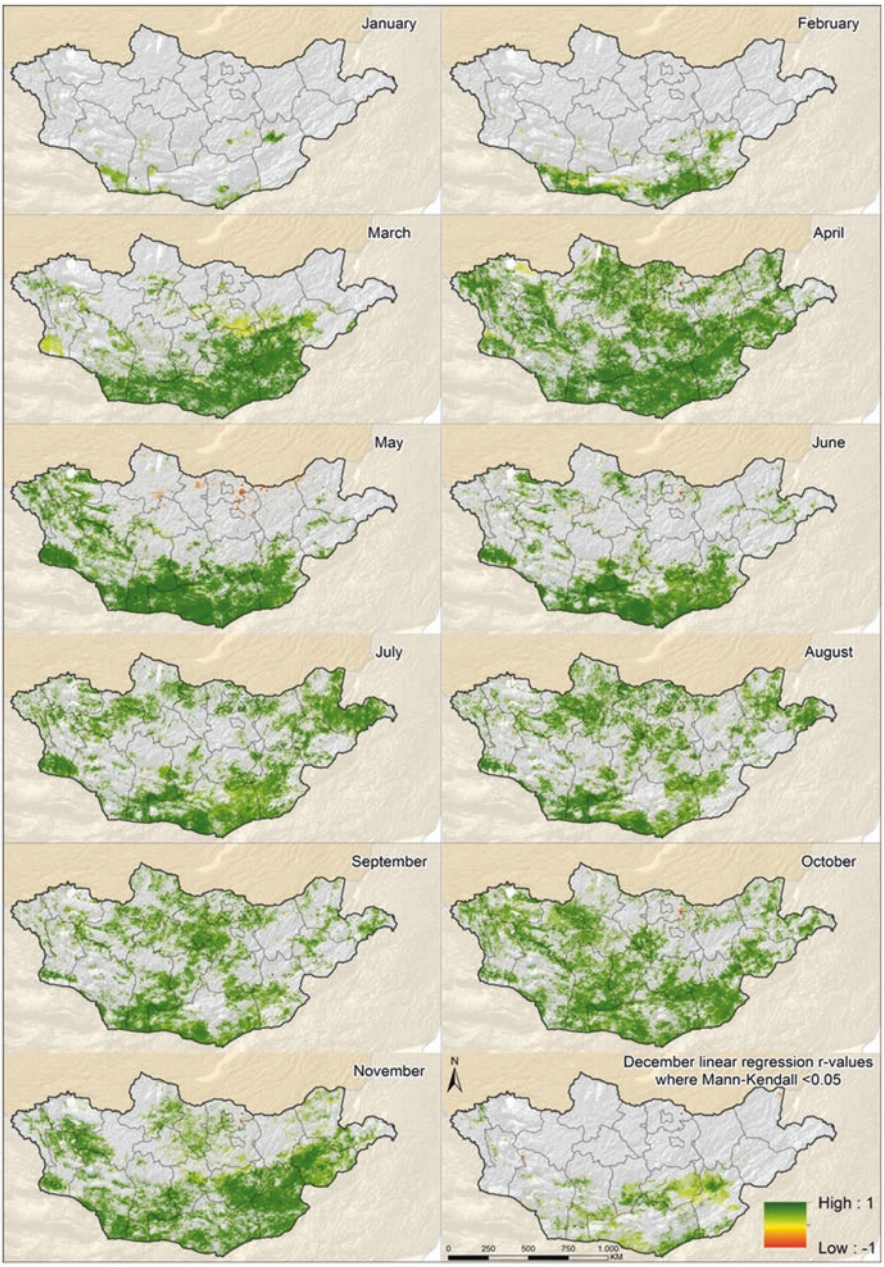

Fig. 9.17 Trends of maximum NDVI values from 1999–2013 by month. Each month shows the r-values of a linear regression where Mann-Kendall is significant for $\alpha = 0.05$

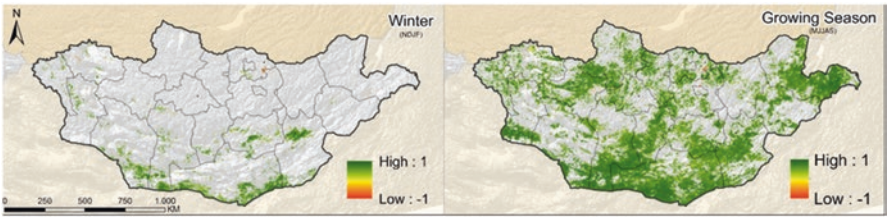

Fig. 9.18 r-values of the pixel based linear regression where Mann-Kendall indicated significant trends during winter (left) and growing period (right)

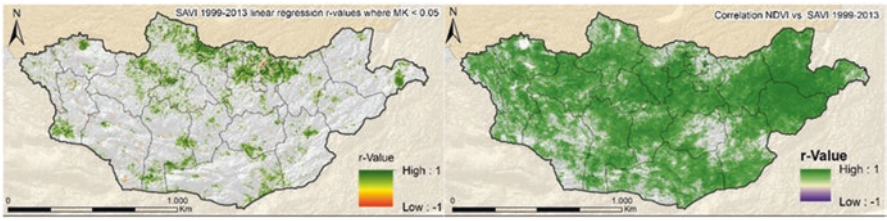

Fig. 9.19 Left: linear regression r-values of annual mean SAVI trends from 1999–2013 where Mann-Kendall $\alpha < 0.05$. Right: r-values for correlation analysis between SPOT-VGT NDVI and SAVI for 1999–2013 where $\alpha < 0.05$

9.4.6 SAVI Changes and Trends

The SAVI was calculated from raw SPOT-VGT reflectance data to verify the NDVI signal in areas with sparse vegetation like the Gobi desert, because background soil brightness can heavily influence NDVI values (Huete 1988).

A cross-validation of the SPOT-VGT NDVI with SAVI values (see Fig. 9.19) mostly agrees with the NDVI changes. There exists a significant correlation between both indices for 78% of Mongolia, of which >99% represent a positive correlation ($r > 0.5$). There are two larger areas where the SAVI returns a different signal than the NDVI: namely in the southern desert areas, as well as the eastern part of the Dundgovi province. However, if the SAVI data is probed for trends using the Mann-Kendall trend test, significant SAVI trends are only detected for about 13% of Mongolia as compared to 33% for the NDVI during the same period. This area reduction is most prominent in the southern desert and steppe areas.

9.4.7 Climatic Trends

The scope of this paragraph is to address presumed climatic changes during the 15 years that are used to analyze potential influences on a locally changing NDVI. The presence or lack of any trends during these years should not be regarded

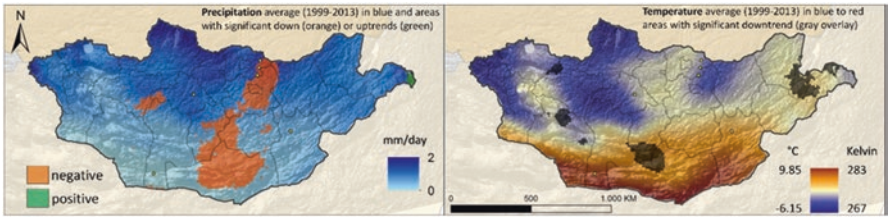

Fig. 9.20 Top: Average daily precipitation (mm/day) for 1999–2013 with annual trends orange/green) superimposed. Bottom: Average Temperature (K) for 1999–2013 with annual trends (gray) superimposed. Trends are assumed to be significant for Mann-Kendall $\alpha = 0.05$ and always negative for temperature

as a description of a long term climate change in Mongolia, as this would at least involve a testing against 30-year climate normal. It should be noted that since 1940 Mongolia has undergone an extensive rise in temperatures (+2.14 °C) and region specific changes in precipitation (1).

Between 1999 and 2013 Mongolia as a whole features no significant trends in temperature or precipitation on an annual basis (Fig. 9.23 bottom right). However, some parts of the country do (Fig. 9.20). The annual mean temperature trend is here negative in general, meaning that it is getting slightly cooler. This affects only a few distinct clusters throughout Mongolia with an average decline of 0.08 K per year. The precipitation trend is concentrated in a more contiguous north-south corridor in the center of Mongolia, though two smaller spots in the west and far east exist. Only the small far eastern part shows increasing precipitation while the larger areas get drier. Figure 9.23 gives a more detailed description of the annual sequence of temperature, precipitation and NDVI at five distinct locations as well as for the Mongolian Average. For none of the five chosen points a significant trend in temperatures exists (see also Table 9.3 – right side). However, sites B and C do show a significant downtrend in precipitation for $\alpha = 0.05$, while site A only slightly fails to be significant. However, the downtrend at site A is still stronger than at D or E. At location A and B, though still relatively weak, there is also a correlation to be found between NDVI and precipitation ($r^2 = 0.27$ and $r^2 = 0.23$). Especially at A the role of precipitation as the major influence on NDVI seems quite unlikely. Not only is the decline in NDVI incomparably steeper, but even gets contradictive from 2007 to 2009 when precipitation is slightly rising and NDVI values decline drastically from 0.46 to 0.29. This also constitutes the largest difference between any 2 years at the selected locations. At B the downtrend in NDVI is more moderate but still not really explicable through changes in temperature or precipitation. For example in years with a local minimum in precipitation (2005 or 2010) the NDVI is actually rising.

Figure 9.21 gives an overview how climatic variables and NDVI values are connected during years 1999–2013 within the different vegetation zones. 1000 random samples were distributed throughout every vegetation zone and probed monthly for their NDVI, temperature and precipitation. We further sub-divided the points into three groups of 5 years each, to highlight changes in the shown relationships during

Table 9.3 Correlation between NDVI and temperature and between NDVI and precipitation for the time-series for each point (for points refer to Fig. 9.2)

	NDVI ↔ Temp. correlation		NDVI ↔ Precip. correlation		NDVI ↔ Temp. *shifted* correlation		NDVI ↔ Precip. *shifted* correlation		*Temperature trend*		*Precipitation trend*	
Points	r-value	r^2	r-value	r^2	r-value	r^2	r-value	r^2	MKp	r-value	MKp	r-value
A	0.48	0.23	0.52	0.27	0.22	0.05	0.49	0.24	0.32	0.07	0.09	−0.52
B	−0.02	0.00	0.48	0.23	−0.01	0.00	0.46	0.21	0.55	0.04	0.01	−0.57
C	−0.12	0.02	−0.40	0.16	−0.33	0.11	−0.64	0.41	0.55	0.02	0.02	−0.59
D	−0.27	0.07	0.03	0.00	−0.44	0.19	0.33	0.11	0.49	0.04	0.62	−0.16
E	0.08	0.01	−0.04	0.00	0.02	0.00	0.17	0.03	0.77	0.01	0.77	−0.14
F	0.17	0.03	0.47	0.22	−0.20	0.04	−0.13	0.02	0.28	0.11	0.69	−0.12

The center part gives the respective values if the NDVI series is shifted by +1 year. Right side: Statistical evaluation of temperature and precipitation time-series. MK p = Mann-Kendall p-Value, r-value = Coefficient of Correlation

our period of interest. However, there is no clear difference present, though the maximum of precipitation is a little higher in the earlier years in the Desert and Desert Steppe and the years 2004–2008 have slightly elevated maximum temperatures.

The strongest relationship between precipitation and NDVI can be found in the Steppe areas, followed by the bordering Desert Steppe and Forest Steppe. While desert areas seem to indicate a relationship as well, their values are generally too small, and as such within the error margins of the NDVI and precipitation datasets, that no strong relationship is apparent. Alpine Vegetation shows a very weak NDVI response to precipitation increases while Subtaiga and Dark Taiga are more or less free of direct influences. However, these last two, and here especially the Subtaiga, show an increase in NDVI with increasing temperatures. This is similarly true for Forest Steppe. The Desert Steppe also shows a connection, which this is directed downwards, meaning that increases in temperature here lead to a reduction in NDVI. It should be noted however that there is a considerable amount of noise, and while these connections exists, they are relatively weak.

Lastly locations D and E are both located within a warmer and dry environment, though the climate at E can be interpreted as slightly milder. The significant rise in NDVI values is visually perceivable and not linked to the annual behavior in precipitation patterns. No correlation exists between the two parameters at either of both locations. This is especially remarkable for D, as in the years 1999–2002 about no NDVI signal at all is detected, combined with a lack of precipitation. From 2003–2008 a ‘normal’ and expectable pattern can be seen: even slight precipitation leads in the year or in the year to follow to an emerging NDVI. After 2009 however, though about no annual precipitation is detected, NDVI values continue to rise to a frail 0.04 annual average in 2013. The site at E behaves similar, however the slightly higher precipitation causes also higher NDVI values. By pure correlation there seems to be no connection between precipitation and NDVI pattern at neither of the

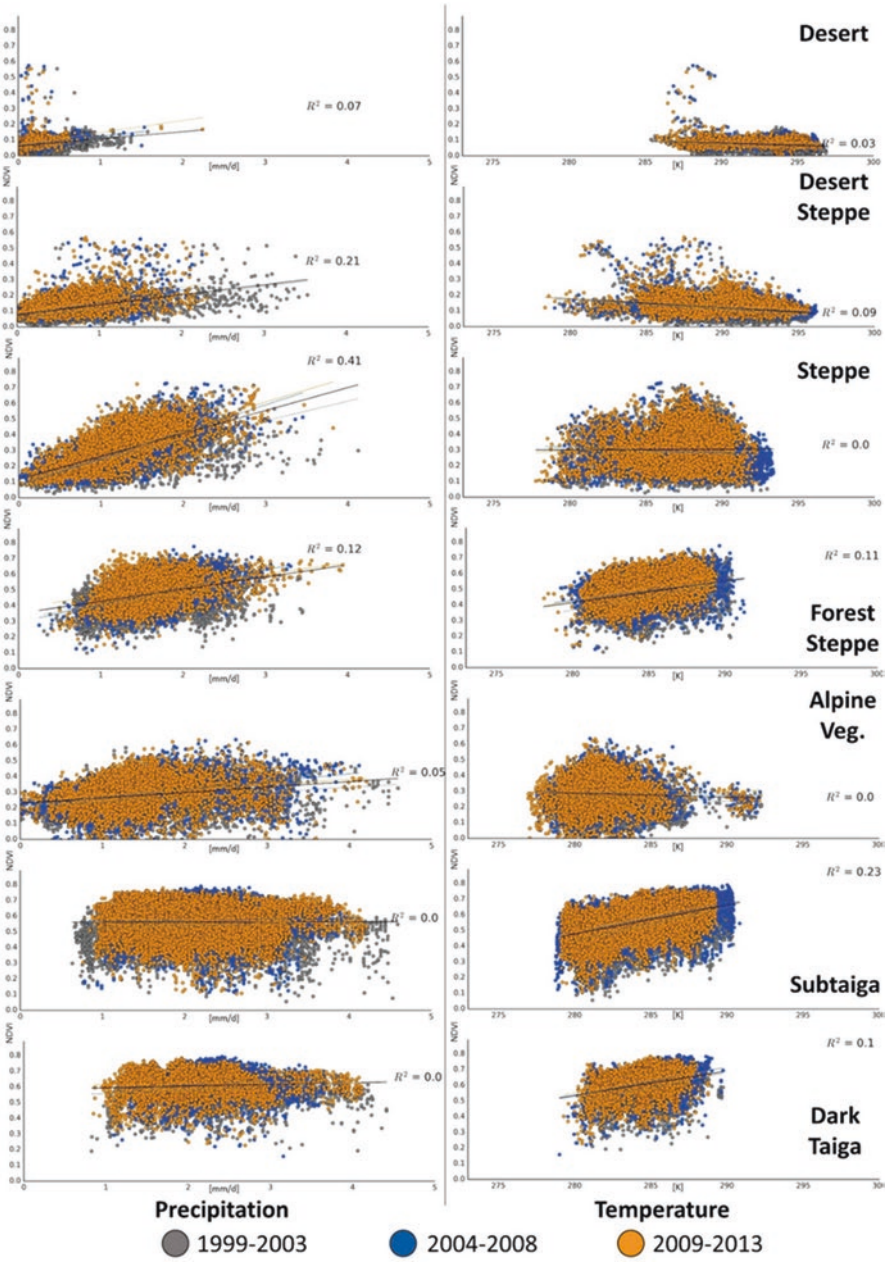

Fig. 9.21 Scatterplot between NDVI values and precipitation (left) and temperature (right) by general vegetation units for the main vegetation period (May–September). Each vegetation unit is represented by 1000 randomly distributed dots, where each dot represents the growing periods average NDVI vs. average climate variable. Points are distinguished into three different time periods, given R^2 values represent the entire 15 years

two sites. Figure 9.22 shows trends distinguished on a monthly basis. Generally, temperature changes only occur from January to July, varying largely in their spatial extent and location. With the exception of March and April, which have the smallest area featuring a trend (only at 3 or 6 pixels), these temperature trends are negative, i.e. it is getting colder. Monthly precipitation is decreasing at most significant trend sites, when April, May and August are largely affected. In May, almost a quarter of the country sees a decline in precipitation of up to −0.1 mm/day p.a. Furthermore, one must consider Dzud-events, extreme winters and following summer droughts, as at least three of those are reported during the time-span of this study (1999–2002, 2005 and 2009). Dzud events have a severe impact on the present vegetation (John et al. 2013). However, these events are not clearly visible in the presented climatic data, possibly obscured by the computation of annual means using January to December instead of a winter to summer mean. These Dzud events however appear to be visible in the SPOT-VGT NDVI series, even for the Mongolian annual average (Fig. 9.23).

9.4.8 Comparison of SPOT VGT and AVHRR

AVHRR NDVI data is used to validate the SPOT-VGT signal over the area of Mongolia. Figure 9.24 gives an overview on trends that can be detected using AVHRR. Long-term positive trends (1982–2012) only exist on 0.1% of Mongolia.

When NDVI values of SPOT-VGT and AVHRR are compared against each other on a pixel-by-pixel basis their annual means (see Fig. 9.24) show a positive correlation ($r > 0.3$) on 61% of the Mongolian territory. 31% of all pixels do not seem to correlate at all ($0.3 > r > -0.3$) and only 8% are negatively correlated. These correlations are significant for 40% of all pixels when $\alpha = 0.05$ and would only see a negligible rise to 50% if α was assumed to be 0.1. Generally, both data-sets agree well in the northern part of Mongolia, where in most provinces >70% of all pixels correlate positively. The best agreement can be found in the north-east (Hentiy and Sühbaatar region) with >95% positive correlation. Here almost all of these correlations are continuously significant. Greater areas with no disagreement are found on a north-west to south-east axis through the country, with the most western Sum, Bayan-Ölgiy, featuring nearly 60% of pixels with no agreement. However, this is the only province with a disagreement on more than half of its area. The two next biggest provinces, Hovd and Govi-Altay, show a disagreement on 45% of their area.

However, there exists a relatively small stripe of significant and strong negative correlations as well in the south western borderlands of Mongolia, namely in the south of Hovd, Govi-Altay, Bayanhongor and Ömnögovi. This correlation is almost entirely significant and generally features r-values <-0.5. This means that the strong positive trends that are described in this area using SPOT-VGT are not present in the AVHRR data. Even worse, the AVHRR data shows a strong negative trend in this area, even if the longer time series 1982–2012 is regarded.

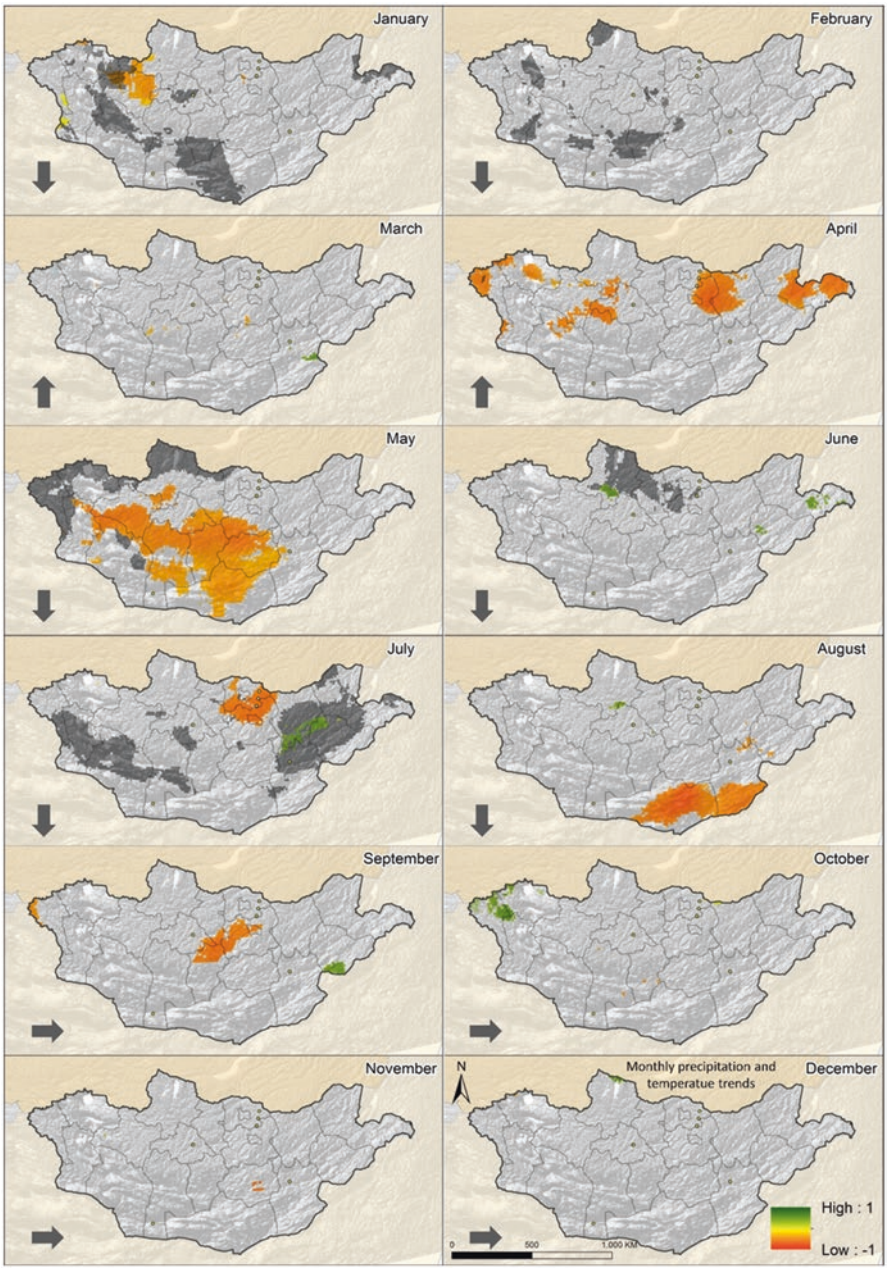

Fig. 9.22 Trends of average precipitation values from 1999–2013 by month. Each month shows the r-values of a linear regression where Mann-Kendall is significant for $\alpha = 0.05$. Gray overlays indicate temperature trends, while the gray arrows explain if the monthly temperature trend is generally positive, negative or absent

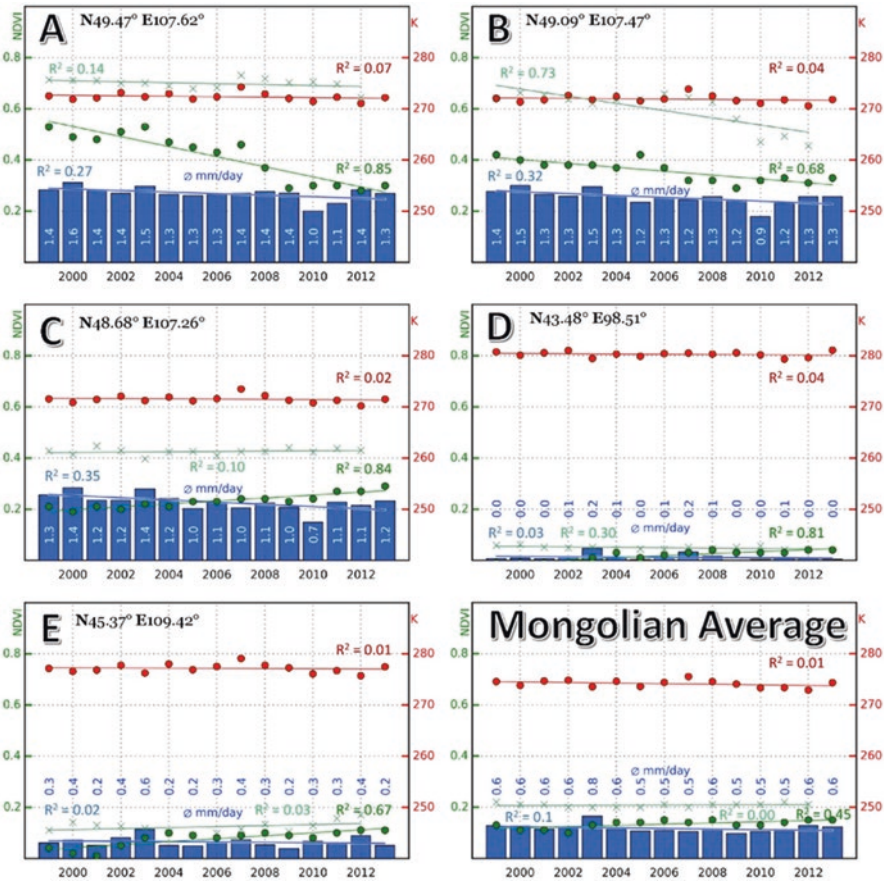

Fig. 9.23 Point based diagrams and Mongolian average of the annual NDVI (dark-green dots is SPOT-VGT), temperature (red) and precipitation (blue) development (1999–2013). Light-green crosses indicate AVHRR NDVI values and range from 1999–2012

9.5 Discussion

While, based on the SPOT-VGT data, Mongolia is getting greener on average, the question remains as to why? No clear correlation between annual climatic averages and the inter-annual NDVI changes could be established. Even more, if a precipitation trend is detected at all, its general direction is downward, not upward as for the NDVI. However, as we could show in Fig. 9.21, NDVI and precipitation are positively correlated in the Desert Steppe and Steppe, which is exactly where we detected large areas of NDVI increases. No significant precipitation or temperature changes could be detected on an annual basis. As annual averaging might conceal intra-annual changes we also applied a monthly climate analysis. While most months during the vegetation period from May–September show no significant cli-

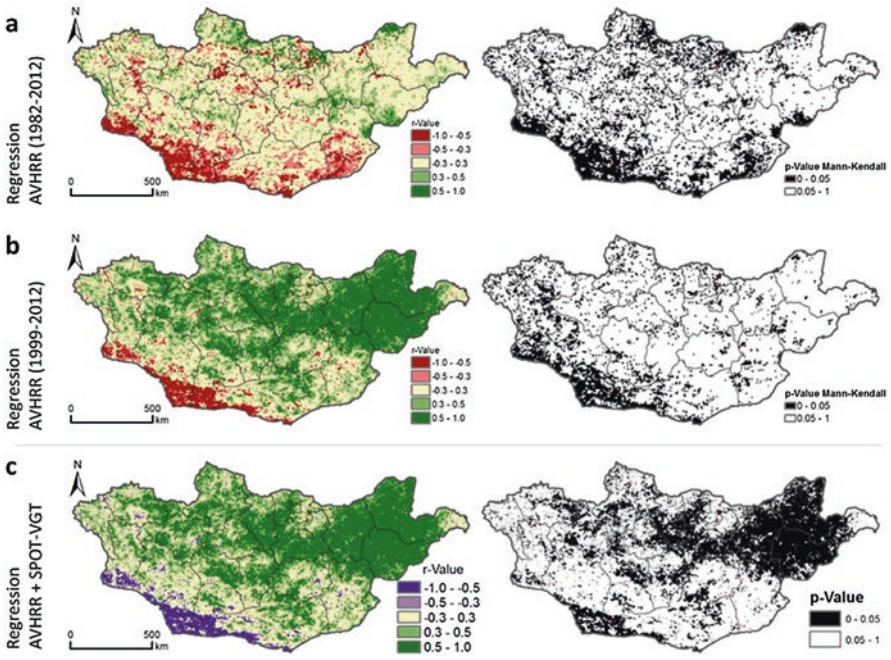

Fig. 9.24 (**a, b**) AVHRR regression trends over Mongolia for a long (1982–2012) and short (1999–2012) period. (**c**) shows a direct regression analysis between AVHRR and SPOT-VGT data for 1999–2012. Left: regression analysis r-. Right: corresponding p-values. Black colors indicate significant correlations

matic changes in places where NDVI trends were detected, July does. In eastern Mongolia, declining temperatures happen along with a small core area of rising precipitation. While the area of significant precipitation changes is too small to account for all of the NDVI rises alone, a decline in temperature could be the dominant factor here. Figure 9.21 shows a very weak negative correlation between the Desert Steppe NDVI and temperature values. Declining temperatures will reduce evapotranspiration and lead as such to an increased water availability. As precipitation or water availability is clearly the dominating factor in these zones, increases in water availability, regardless of the source, are bound to increase the NDVI. This effect may also be responsible for the small scale NDVI increases on the eastern slopes of the Gobi Altai, where July temperatures are decreasing as well and no change in precipitation pattern could be discovered.

While this explains the NDVI rise in eastern Mongolia and the eastern Gobi Altai, the other region of large scale increase, the southern desert region, shows no climatic changes, even when evaluated on a monthly basis. Furthermore, while the NDVI trend in the east could be confirmed using AVHRR data, this not only fails in the south, but both sensors are diametrically opposed in their results. Also, this trend is not apparent in the SPOT-VGT SAVI data (Fig. 9.19), which is much more suitable for areas of sparse vegetation. As such, before diving into possible environmen-

tal reasons for a greening, the robustness and validity of the SPOT-VGT NDVI time series should be put under scrutiny. A single sensor may create biases of its own, which is why we applied a comparison to data derived from AVHRR. As they show a strong agreement for 61% of Mongolia during their time of overlap (1999–2012) we assume that the positive trend in the eastern part is not an artifact from the SPOT sensor. Though the long-term downward trend seen in AVHRR seems to turn into a positive trend in recent years, we acknowledge that a time-series of 15 years (SPOT-VGT) may be too short to capture any sustainable trends. An example for this might be a study from (Zhao and Running 2010) that reported reductions in global carbon between 2000–2009, which was later shown to be due to artifacts in their NPP model (Samanta et al. 2011). The matter becomes even more crucial when we have to consider that the SPOT-VGT data product is a combination of two different sensors, for which it has been reported before that the break between these, which occurred in 2003, resulted in a more positive NDVI trend as compared to MODIS or AVHRR (Fensholt et al. 2009). SPOT-VGT NDVI values before 2003 seem to be systematically lower. If only the data from the more recent SPOT-VGT2 are considered, overall significant trends are reduced, as can be seen in Fig. 9.25.

This almost entirely cancels the positive trends found in southernmost Mongolian desert. NDVI values are reported to be 3,4% higher in SPOT-VGT2 as compared to SPOT-VGT1 due to their different spectral response functions (Fensholt et al. 2009). This difference seems to become much more severe around NDVI values of 0 though, as Point D in Fig. 9.23 illustrates, where NDVI values are generally <0 before 2003 and generally >0 after. Therefore we conclude that the SPOT-VGT time-series from 1999–2013 is not reliable for areas of very low NDVI and at least biased towards positive trends for areas of larger NDVI.

We therefore conclude that there is no strong positive NDVI trend in the southern desert area, but rather an artifact from the break between two sensors. Though there

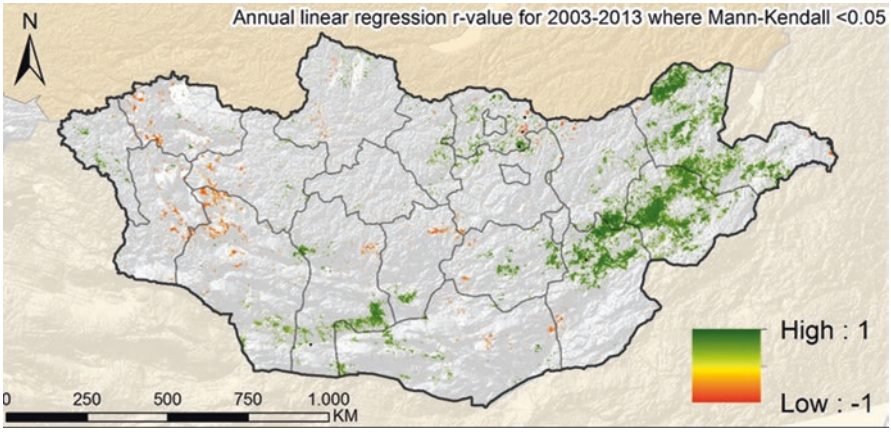

Fig. 9.25 Annual linear regression r-values for the period 2003–2013 where Mann-Kendall p-values are below 0.05

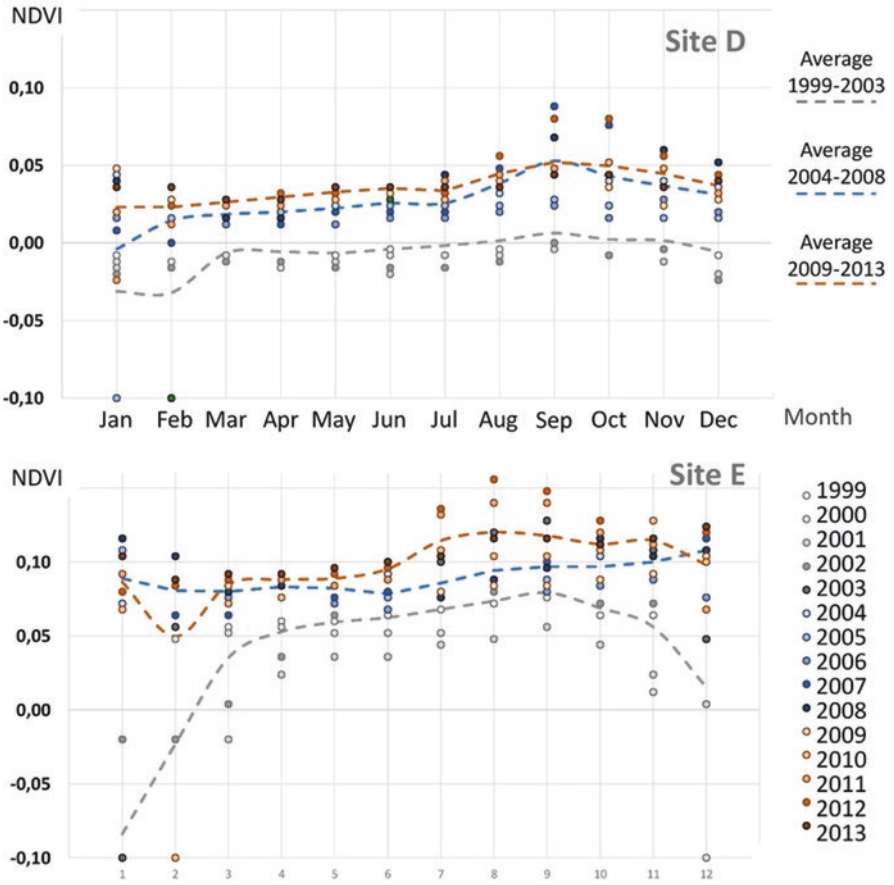

Fig. 9.26 Monthly NDVI values at site D and E for the years 1999–2013

might be an increase even if the data before 2003 is excluded, as displayed in Fig. 9.26 at site D, it is not strong enough to be significant. However, the eastern part of the Gobi Altai, large parts of eastern Mongolia as well as the seamline between desert and steppe in the south, retain a strong positive trend during these 10 years that cannot be explained by the shift between the 2 sensors. As such, we assume that regardless of the drawbacks due to the sensors flaws, there are significant NDVI trends in Mongolia that are mostly positive.

A third area of interest is found primarily north-east of the capital Ulaanbaatar, where significant positive and negative NDVI trends are found close together in the Sub- and Dark Taiga. This area is part of a belt that runs through the center of Mongolia, in which precipitation significantly declines on an annual basis. Mainly the months of April and July show the greatest declines. However, as shown in Fig. 9.21, NDVI values in these regions are predominantly affected by temperature rather than precipitation and there are no large-scale temperature changes that might

be responsible here. As environmental factors seem far-fetched to explain the changes happening here, we would like to present another possibility. This greater area, as it harbors more than half of the Mongolian population, is predestined for being under a strong human influence. As the area consists mostly of forest, Eckert et al. (2015) describe that forest fires in this region are a main reason for NDVI changes similar to those described in our study. Points A, B and C (Fig. 9.23) are single pixels in this area, all located within a 50 km radius, that allow for an inter-annual analysis of the events. A and B feature significant NDVI declines, while C shows significant increases. For A and B a one-time event, as would be evidence to a forest fire, is not visible in the data. For example Site B consists of a rather continuous decline in NDVI. Site A does show signs of a single event as the NDVI drops drastically between 2 years 2007 and 2009. Here the question remains as to why the NDVI drops in 2 consecutive years if a single event is responsible? To take a closer look at the environmental changes at these locations, Landsat images of several years are compared in Fig. 9.27. As of August 2002, the area seems more or less undisturbed. Until June 2003 a small forest area east of location A gets lost to what looks like a fire event. This overall picture remains until May 2007. Unfortunately, the images of the crucial year of 2008 were not available. However, in 2009 a large fire event around location A becomes visible. The last image of July 2007 does not show these burnt-down areas, however the image quality is rather bad due to clouding. In accordance with the NDVI data it is also more likely that the fire event took place in 2008. This would explain the 2-year-drop in NDVI, as e.g. a fire in August 2008 would mean high NDVI values before and low after the event, thus averaging in the annual perspective to a value between that of 2007 and 2009. As it turns out the location of B was chosen rather "lucky", as it is located right between two major fire events. One occurring between May and July of 2007, where a large area south/east of B was affected. Between 2007 and 2009 another large event did happen to the north/west. Both fires might have only partly affected the NDVI development at site B what might explain the lack of sharp inter-annual drops. While negative NDVI changes in the greater vicinity of both sites seem to be a consequence of forest fires by large, logging done by humans might aid to the general trend of deforestation.

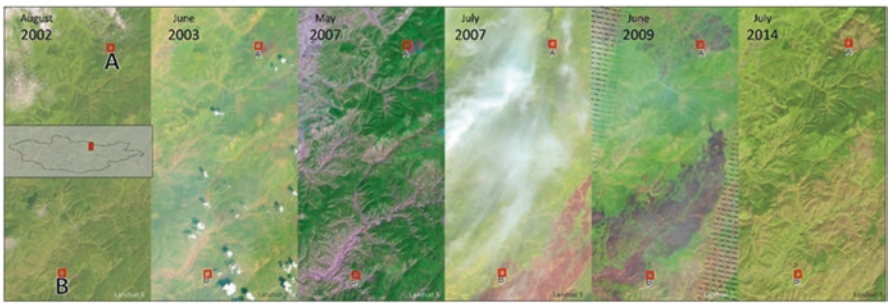

Fig. 9.27 Locations A and B in Landsat images for different years. Red rectangles indicate the extent of one SPOT-VGT NDVI pixel (i.e. the area within each rectangle is used for the values in Fig. 9.22)

C and similar sites in the vicinity are interesting for their strong positive trend while being surrounded by areas of absent or negative change. Even more, there is a steady and significant downtrend in precipitation and no trend in temperatures, while the NDVI is steadily increasing. All considered, it is highly unlikely that solely changes in the climatic parameters are responsible for this change. The causing factor might be related to human activity, normally leading to deforestation though.

What is remarkable is the close distance to the Gorkhi Terelj National Park. In the years 1995–2002 the German GTZ (now GIZ, the German government's program for technical cooperation) established an initial program "Nature Conservation and Buffer Zone Development Project" in the area. Until at least 2008 several related programs did follow. Within those, fire management concepts were established with local communities that were later expanded to account for climate change and biodiversity. In the course of these programs forest user groups in the Mandal Sum developed a management plan that was approved by local authorities (Jamsranjav 2012). This area coincides very well with the area of detected NDVI rise in recent years. The human influence here can also be seen in official data from 1998. It suggests that only one fifth of the forest area here could be classified as natural forest. Another fifth is logged, another open stand and a close quarter of forest area burned (the remaining constituting of shrubs and regenerating forest) (Tanaka et al. 2008). The potential to improve forest quality and quantity through elaborated management plans is thus largely present and seems to be a good explanation for the positive NDVI development in a rather highly populated area. However, as of now, no local observations are available to validate this hypothesis. Optical evaluation of Landsat imagery for sample site C is also inconclusive.

While we discussed the significant changes in NDVI, we mostly omitted the fact that almost all of Mongolia shows some positive NDVI response in the years since 1999. Though this is often not significant, probably due to the shortness of the time-series, there still seems to be a shift towards an increased greening. This is also present in the AVHRR time-series, which shows a long-term down-trend in NDVI but indicates a turning of this in recent years. Other publications have noticed this shift as well (Eckert et al. 2015) and reported it for up to 50% of Mongolia. Apart from the local climatic factors, we want to argue for another and perhaps more subtle underlying effect that may partially cause this emergent greening: atmospheric CO_2 and its associated fertilization effect. Several studies indicate a connection between rising atmospheric CO_2 and plant growth in arid environments (Berry and Roderick 2002; Higgins and Scheiter 2012). In the years from 1999 to 2013 global mean CO_2 concentrations rose quite linearly from 368 to 397 ppm, or roughly 2 ppm per year (Scripps 2016). A correlations of atmospheric CO_2 levels with NDVI values at site and E returns an r-value of 0.83. As the vegetation in the affected areas mostly consists of grasses which are C3-plants (Ehleringer and Cerling 2002), an increase in biomass through elevated atmospheric CO_2 levels is feasible. This trend will continue for some time, as it is expected that these plants might benefit from CO_2 increases up to 1000 ppm. Furthermore, the water saving aspect (increase in water-use-efficiency) due to elevated CO_2 can be strong enough to counteract the

otherwise negative effects of water scarcity (Morgan et al. 2004). As we could show, precipitation or water availability is directly affecting NDVI values in all of the Steppe areas (Fig. 9.21) and as such, an increased water-use-efficiency should lead to increasing NDVI values.

There are examples where even under increased summer drought stress some Grasslands showed an increase in biomass simply due to changes in the surrounding CO_2 concentrations (Taube and Herrmann 2009). Especially within warm and arid environments, where water plays a crucial part for primary production, the CO_2-fertilization effect should be particularly pronounced. Donohue et al. (2013) showed that an increase in atmospheric CO_2 in warm and arid environments of 14% between 1982–2010 helped to increase green foliage cover on a global average by 11%. This increase did also occur within their study in southern Mongolia and they concluded "that the fertilization effect is now a significant land surface process".

One study for northern China seems to indicate indeed a trend reversal in more recent years, as NDVI data from 1982–2010 shows close to zero trends but a decrease in earlier years (Peng et al. 2011). However, there is still no clear consensus at what is currently happening as a study covering the period 1982–1999 reported a significant rise in NDVI (Piao et al. 2006) while another reported a decline, if 1997–2006 is regarded (Park and Sohn 2010). In a global study by Zhu et al. (2016) Mongolia is among the few countries that saw a negative LAI trend for 1982–2009, which was attributed to negative climatic impacts. At the same time 25–50% of the global vegetated area did show a greening that was directly attributed to CO_2 -fertilization effects. As such, we might now see that the fertilization effect is now beginning to surpass the impact of detrimental climatic changes of the past 30 years. If this holds true, this initial greening we described above will continue in the future and will then be detectable with much higher confidence than we are able to now due to the shortness of the NDVI series.

9.6 Summary

While long-term NDVI trends in Mongolia, typically analyzed using AVHRR starting from the early 1980s and MODIS data after 1999, have often been described as negative, we could show that this is not true anymore in recent years. We could identify positive significant trends in small areas around the capital Ulaanbaatar that we attributed towards a change in human practices within these forest areas. Near these locations the only significant NDVI declines for Mongolia could be identified as well. We attributed these to fire events that temporarily reduced the forest cover. A rather large scale rise was identified in eastern Mongolia, where increasing precipitation and decreasing temperatures in July increased water availability and as such NDVI values. We also attributed the smaller scale increases on the eastern slopes of the Gobi Altai to decreasing July temperatures, though the connection here is weaker. Apart from theses significant changes, weak NDVI increases can be found in other parts of Mongolia as well. However, they fail to be statistically sig-

nificant and as such must remain speculative. We attribute this in part to the general shortcomings of trend studies and the length of our datasets in particular. While the significant trends we described above are found under almost all tested conditions, many other trend locations disappear if the length of the NDVI series is changed (Fig. 9.24 a-b), different sensors are considered (Figs. 9.16 and 9.24), only the most recent SPOT sensor is analyzed (Fig. 9.25) or if different indices are considered (Fig. 9.19).

9.7 Outlook

The case study from Mongolia shows that there are major research gaps existing in relation to landscape dynamics assessments in Central Eurasia. The development of a new method for ecosystem state assessment that combines breakpoint analysis (tipping points), ecosystem response categorization and traditional trend analysis is needed.

A GIS based mapping and assessment tool that can serve for largescale assessment of change in ecosystem functioning that enables the detection of turning (tipping) points in ecosystem functioning over Eurasia should be established. Beside timing, occurrence and type of abrupt shift, the analysis of spatial variability of the type / timing of trend shift as well as in the direction of change is of high relevance for ecosystem assessment studies. Accurate assessment of environmental changes and land dynamics calls for long-term, high quality, continuous, harmonized Earth Observation time series (both climate and vegetation datasets). Further important is more research on scale implication (spatial resolution, observation period). At which scale can be a reliable indicator of ecosystem functioning derived? The Mongolia case study discusses this scale problem. Further, the comprehensive attribution of drivers remains a big challenge (co-occurrence of global and local drivers) that cannot be performed without additional data on the drivers and expert knowledge. Both case studies show that land-use change modelling is a highly dynamic field of research with many new developments. The main current developments presented in these special case studies concern progress in

- The modelling of drivers of land-use change.
- Modelling of scale dependency of drivers of land-use change.
- Modelling progress in predicting location versus quantity of land-use change.
- The incorporation of biophysical feedbacks in land-use change models.

Much of the interest in landscape dynamics is coming from the desire to understand how human activities have influenced landscapes, and how this understanding can inform future land planning and ecosystem stewardship for the drylands of Eurasia. Much of the focus has been on how anthropogenic changes in disturbance

regimes that have altered landscape patterns and dynamics. For instance, changes in fire disturbance regimes due to altered climate conditions or fire suppression activities, and the impacts of forest management activities and land use activities, e.g. logging, have received high attention.

Eurasia, as shown in this book, is a unique region from an ecological point of view with a remarkable mix of climatic and edaphic conditions, vegetation types and land use patterns. Over the twentieth century, drastic changes, both natural and anthropogenic are studied, that profoundly affected landscapes and their ecosystem functioning: Successive institutional changes with large impact on the agricultural sector/landscape, global warming and major droughts (e.g. mid/end-1990s, 2010). We have many reports of greening due to global warming, crop intensification or land abandonment. Other reports tell us of browning due to droughts or land abandonment. One important question that arises when dealing with landscape dynamics is whether changes in ecosystem functioning is only a gradual process? With the increased length of EO time series, we have more and more the possibility to differentiate between gradual and abrupt changes (tipping points). Tipping points in time series (e.g. vegetation cover) can be caused by climate extremes (e.g. severe droughts, floods, etc.), land-cover change, climate / human -induced land degradation or combinations of all. Also data artefacts in the time series (e.g. continuity issues related to changes in platforms/sensors/pre-processing/etc.) could cause such breakpoints in time series and are misleading in the final assessment.

Therefore a new ecosystem-state assessment method for Eurasia that reveals turning points in Eurasian ecosystem functioning must and could be developed in the future. Land dynamics research requires new sophisticated datasets: Long-term, high quality/continuous, global time series; trade-off between length of the observation period and spatial resolution; a common and clear selection of the method for trend assessment (OLS, Mann-Kendall, Thiel-Sen, etc.). Here we have to keep in mind that different methods may lead to different results (e.g. look of the different results in the Mongolia case study using different sensors or length of time series). We have also to focus on the attribution of changes to extricate anthropogenic (local) and climate (regional-global) drivers. To achieve a better ecosystem stewardship, we have to combine historical retrospective studies and spatial modeling to derive important insights in landscape dynamics. As a major outlook of this book, the development of a new method for ecosystem state assessment, which combines tipping point analysis, ecosystem response categorization and traditional trend analysis, is necessary for framing new ecosystem stewardship.

Acknowledgments We would like to thank the German Academic Exchange Service (DAAD) for funding the International German Alumni Summer School Mongolia 2015 “Large scale natural landscapes in Mongolia under the pressure of climate change and competition for land and resources’’. This summer school enabled research on vegetation dynamics over Mongolia.

References

Adyasuren T, Sugita M, Erdenetuya M (eds) (2005) Assessment of pastureland change using remote sensing data in eastern steppe zone of Mongolia

Allen-Diaz B, Chapins FS, Diaz S et al (1996) Rangelands in a changing climate: impacts, adaptation and mitigation. In Watson et al (eds), *Climate change impacts, adaptation and mitigation*, pp. 131–158. Cambridge University Press, Cambridge

Asefa DT, Oba G, Weladji RB, Colman JE (2003) An assessment of restoration of biodiversity in degraded high mountain grazing lands in northern Ethiopia. Land Degrad Dev 14:25–38

Bao G, Qin Z, Bao Y et al (2014) NDVI-based long-term vegetation dynamics and its response to climatic change in the Mongolian Plateau. Remote Sens 6(9):8337–8506

Barthel H (1983) Die regionale und jahreszeitliche differenzierung des klimas in der Mongolischen Volksrepublik. Stud Geogr 34:3–91

Berrisford P, Dee D, Poli P et al (2011) ERA report series: 1 The ERA-Interim archive Version 2.0. 09.12.2014. Available online: http://old.ecmwf.int/publications/library/do/references/show?id=90276. Accessed 9.Dec 2014

Berry L, Roderick ML (2002) CO_2 and land-use effects on Australian vegetation over the last two centuries. Aust J Bot 50(4):511

Bormann FH, Likens GE (1979) Pattern and process in a forested ecosystem: disturbance, development, and the steady state based on the Hubbard Brook ecosystem study. Springer. ISBN 0387903216, 9780387903217

Chartier MP, Rostagno CM (2006) Soil erosion thresholds and alternative states in northeastern Patagonian rangelands. Rangeland Ecol Manag 59:616–624

Chen J, Ouyang Z, John R et al (2020) Social-ecological systems across the Eurasian drylands. In: Gutman G et al (eds) Landscape dynamics of drylands across greater Central Asia: people, societies and ecosystems. Springer, Cham

Chogni O (1989) Methods for the protection and restoration of pasture. In: Tserendolam R, Tserendash S (eds) Current state of natural pasture use and protection, Proceedings of a scientific conference (in Mongolian). Ulaanbaatar, pp 12–14

Chu T, Guo X (2012) Characterizing vegetation response to climatic variations in Hovsgol, Mongolia using remotely sensed time Series Data. In: Dagvadorj et al. (UNEP) Mongolia Assessment Report on Climate Change 2009. http://www.unep.org/climatechange/adaptation/ScienceandAssessments/MongoliaAssessmentReport/tabid/29575/Default.aspx

Dagvadorj D, Batjargal Z, Natsagdorj L (2014) Mongolia Second Assessment Report on Climate Change 2014 (MARCC-2014) Ministry of Environment and Green Development of Mongolia

Dee DP, Uppala SM, Simmons AJ et al (2011) The ERA-interim reanalysis: configuration and performance of the data assimilation system. Q J Roy Meteor Soc 137(656):553–597

Donohue RJ, Roderick ML, McVicar TR, Farquhar GD (2013) Impact of CO_2 fertilization on maximum foliage cover across the globe's warm, arid environments. Geophys Res Lett 40(12):3031–3035

Dorj O, Enkhbold M, Lkhamyanjin S et al (2013) Mongolia: country features, the main causes of desertification and remediation efforts. In: Heshmati GA, Squires VR (eds) Combating desertification in Asia, Africa and the Middle East. Springer, Dordrecht, pp 217–228

Dulamsuren C, Klinge M, Degener J et al (2016) Carbon pool densities and a first estimate of the total carbon pool in the Mongolian forest-steppe. Glob Chang Biol 22:830–844

Eckert S, Hüsler F, Liniger H, Hodel E (2015) Trend analysis of MODIS NDVI time series for detecting land degradation and regeneration in Mongolia. J Arid Environ 113:16–28

Ehleringer J, Cerling T (2002) C3 and C4 photosynthesis. In: Encyclopedia of global environmental change. The earth system: biological and ecological dimensions of global environmental change, vol 2. Wiley, Chichester, pp 186–190

Fensholt R, Rasmussen K, Nielsen TT, Mbow C (2009) Evaluation of earth observation based long term vegetation trends—intercomparing NDVI time series trend analysis consistency of Sahel from AVHRR GIMMS, Terra MODIS and SPOT VGT data. RSE 113(9):1886–1898

First National Communication of the Republic of Kazakhstan under the United Nations Framework Convention on Climate Change (2013). Almaty, p 74

Henebry GM, Chen J, Gutman G, Kappas M (2020a) Multiple perspectives on Eurasian drylands. In: Gutman G et al (eds) Landscape dynamics of drylands across greater Central Asia: people, societies and ecosystems. Springer, Cham

Henebry GM, de Beurs KM, John R et al (2020b) Recent land surface dynamics across the Eurasian drylands. In: Gutman G et al (eds) Landscape dynamics of drylands across greater Central Asia: people, societies and ecosystems. Springer, Cham

Higgins SI, Scheiter S (2012) Atmospheric CO_2 forces abrupt vegetation shifts locally, but not globally. Nature 488(7410):209–212

Hilbig W (1995) The vegetation of Mongolia. SPB Academic Pub, Amsterdam

Huang S, Siegert F (2006) Land cover classification optimized to detect areas at risk of desertification in North China based on SPOT VEGETATION imagery. J Arid Environ 67(2):308–327

Huete AR (1988) A soil-adjusted vegetation index (SAVI). Remote Sens Environ 25:295–309

Iwasaki H (2009) NDVI prediction over Mongolian grassland using GSMaP precipitation data and JRA-25/JCDAS temperature data. J Arid Environ 73(4–5):557–562

Jamsranjav J (2012) Key elements for success and weakness of community based conservation in Mongolia

Javandulam T, Tateishi R, Sanjaa T (2005) Analysis of vegetation indices for monitoring vegetation degradation in semi–arid and arid areas of Mongolia. Int J Environ Stud 62(2):215–225

John R, Chen J, Ou-Yang ZT et al (2013) Vegetation response to extreme climate events on the Mongolian Plateau from 2000 to 2010. Environ Res Lett 8(3)

Kogan F (1990) Remote sensing of weather impacts on vegetation in non-homogeneous areas. Int J Remote Sens 11:1405–1419

Lorenz C, Kunstmann H (2012) The hydrological cycle in three state-of-the-art reanalyses: intercomparison and performance analysis. J Hydrometeorol 13(5):1397–1420

Matthew MJ, Durre I, Korzeniewski B et al (2012) Global historical climatology network – daily (GHCN-daily), version 3. NOAA National Climatic Data Center

Millennium Ecosystem Assessment (2005a) Ecosystems and human Well-being: desertification synthesis. World Resources Institute, Washington, DC

Millennium Ecosystem Assessment (2005b) Ecosystems and human well-being: current state and trends. Island Press, Washington, DC

Morgan JA, Pataki DE, Körner C, Clark H et al (2004) Water relations in grassland and desert ecosystems exposed to elevated atmospheric CO_2. Oecologia 140(1):11–25

Myers N, Mittermeier RA, Mittermeier CG et al (2000) Biodiversity hotspots for conservation priorities. Nature 403:853–858

Nandintsetseg B, Shinoda M, Kimura R, Ibaraki Y (2010) Relationship between soil moisture and vegetation activity in the Mongolian steppe. SOLA 6:29–32

Ogar NP, Bragina TM (1999) Transformation of ecosystems and their components: basic terms and concepts. In: Transformation of natural ecosystems and their components during desertification. Almaty, pp 28–32

Park HS, Sohn BJ (2010) Recent trends in changes of vegetation over East Asia coupled with temperature and rainfall variations. J Geophys Res 115(D14)

Peng S, Chen A, Xu L, Cao C (2011) Recent change of vegetation growth trend in China. Environ Res Lett 6(4):44027

Piao S, Mohammat A, Fang J et al (2006) NDVI-based increase in growth of temperate grasslands and its responses to climate changes in China. Global Environ Chang 16(4):340–348

Purevsuren T, Hoshino B, Ganzorig S, Sawamukai M (2012) Spatial and temporal patterns of NDVI response to precipitation and temperature in Mongolian steppe. http://hdl.handle.net/10659/3449

Quetier F, Thebault A, Lavorel S (2007) Plant traits in a state and transition framework as markers of ecosystem response to land-use change. Ecol Monogr 77:33–52

Rosales M, Livinets S (2005) Grazing and land degradation in CIS countries and Mongolia: Food and Agriculture Organization of the United Nations. Proceedings of the electronic conference on grazing and land degradation in CIS countries and Mongolia. Available at: http://www.fao.org/fileadmin/templates/lead/pdf/e-conf_05%E2%80%9306_background.pdf

Rouse JW, Haas RH, Schell JA, Deering DW (1973) Monitoring vegetation systems in the great plains with ERTS. In: Proceedings of the third ERTS symposium (NASA SP-351), pp 309–317

Samanta A, Costa MH, Nunes EL et al (2011) Comment on drought-induced reduction in global terrestrial net primary production from 2000 through 2009. Science 333(6046):1093

Sankaran M, Anderson M (2009) Management and restoration in African savannas: interactions and feedbacks. In: Hobbs, Suding (eds) New models for ecosystem dynamics and restoration. Island Press, London, pp 136–155

Scripps (2016) Homepage of the Scripps CO_2 program. Available at: http://scrippsco2.ucsd.edu

Spivak L, Terekhov A, Vitkovskaya I, Batyrbayeva M (2009) Use of long-term satellite data of different resolution for a complex assessment of the vegetation cover of the territory of Kazakhstan. Modern problems of remote sensing of earth from space. Moscow IKI RAS 6(2):450–458

Spivak L, Vitkovskaya I, Batyrbaeva M, Terekhov A (2010) Detection of desertification zones using multi-year remote sensing data. In: NATO science for peace and security, series C: environmental security use of satellite and in-situ data to improve sustainability. Springer, pp 235–241

Spivak L, Vitkovskaya I, Batyrbayeva M, Terekhov A (2012) The experience of land cover change detection by satellite data. Front Earth Sci Higher Education Press/Springer, Berlin/Heidelberg 6(2):140–146

Spivak L, Batyrbaeva M, Vitkovskaya I (2017) The system of space monitoring of vegetation and drought conditions in Kazakhstan based on long-term series of remote sensing data. In: Ground-space monitoring of dynamics of geospheres. Almaty pp. 174–189

Standish RJ, Cramer VA, Yates CJ (2009) A revised State-and-Transition model for the restoration of woodlands in Western Australia. In: Hobbs, Suding (eds) New models for ecosystem dynamics and restoration. Island Press, London, pp 169–188

Sun Z, Wang Q, Xiao Q et al (2015) Diverse responses of remotely sensed grassland phenology to interannual climate variability over frozen ground regions in Mongolia. Remote Sens-Basel 7(1):360–377

Suttie JM, Reynolds SG (eds) (2003) Transhumant grazing Systems in Temperate Asia. FAO Plant Production and Protection Series No 31

Tanaka T, Jayakumar R, Erdenechimeg B (2008) Proceedings of the UNESCO chair workshop on sustainable groundwater management in arid and semi-arid regions: IHP VII | Technical Document in Hydrology | No. 1

Taube F, Herrmann A (2009) Relative benefit of maize and grass under conditions of climatic change. In: Schwarz (ed) Optimierung des Futterwertes von Mais und Maisprodukten, vol 331 of Landbauforschung/Sonderheft, vol VTI, Braunschweig, pp 115–126

Tietjen B, Jeltsch F (2007) Semi-arid grazing systems and climate change: a survey of present modelling potential and future needs. J Appl Ecol 44:425–434

Tserendash S, Erdenebaatar B (1993) Performance and management of natural pasture in Mongolia. Nomad People 33:9–15

Turner MG, Romme WH, Gardner RH et al (1993) A revised concept of landscape equilibrium: disturbance and stability on scaled landscapes. Landsc Ecol 8(3):213–227

Ulziikhutag N (1989) Survey of Mongolian vegetation provinces (in Mongolian). Ulsiin Khevleliin Gazar, Ulaanbaatar

UNCBD (2014) Mongolia's fifth national repo on implementation of convention of biological diversity. Available at: https://www.cbd.int/doc/sworld/mn/mn-nr-05-en.pdf

UNCCD (2012) United Nations Convention to Combat Desertification. Available at: www.unccd.int

Vostokova EA, Gunin PD (2005) Ecosystems of Mongolia. Atlas. Russian Academy of Sciences, Moscow

Wang C, Wang S, Zhou H, Glindemann T (2007) Effects of forage composition and growing season on methane emission from sheep in the Inner Mongolia steppe of China. Ecol Res 22(1):1011–1021

Watt AS (1947) Pattern and process in the plant community. J Ecol 35(1/2):1–22.

Wen X, Lu H, Li C et al (eds) (2014) SPIE Asia Pacific remote sensing, SPIE proceedings, SPIE

Yu F, Price KP, Ellis J, Shi P (2003) Response of seasonal vegetation development to climatic variations in eastern Central Asia. Remote Sens Environ 87(1):42–54

Yu F, Price KP, Ellis J, Kastens D (2004) Satellite observations of the seasonal vegetation growth in Central Asia: 1982–1990. Photogramm Eng Remote Sens 70(4):461–469

Yunatov AA (1977) Fundamental characteristics of the vegetation of the Mongolian People's Republic (in Mongolian). Ulsiin Khevleliin Gazar, Ulaanbaatar

Zhang X, Hu Y, Zhuang D et al (2009) NDVI spatial pattern and its differentiation on the Mongolian Plateau. J Geogr Sci 19(4):403–415

Zhao M, Running SW (2010) Drought-induced reduction in global terrestrial net primary production from 2000 through 2009. Science 329(5994):940–943

Zhu Z, Piao S, Myneni RB et al (2016) Greening of the Earth and its drivers. Nat Clim Chang 6:791–795.

Chapter 10
Social-Ecological Systems Across the Asian Drylands Belt (ADB)

Jiquan Chen, Zutao Ouyang, Ranjeet John, Geoffrey M. Henebry, Pavel Ya. Groisman, Arnon Karnieli, Steven Pueppke, Maira Kussainova, Amarjargal Amartuvshin, Askarbek Tulobaev, Tlektes I. Yespolov, Connor Crank, Ameen Kadhim, Jiaguo Qi, and Garik Gutman

10.1 Social-Ecological Systems of the Asian Drylands Belt

Drylands are defined according to the aridity index, the ratio between average annual precipitation and potential evapotranspiration (PET). This identifies four biomes: the hyper-arid, arid, semi-arid, and dry sub-humid (Safriel 2009). Asian drylands extend across an immense landscape that stretches westward from Mongolia to the eastern shores of the Mediterranean Sea. As the largest drylands system on the planet, they account for over 30% of total global drylands (Henebry et al. 2020,

J. Chen (✉) · Z. Ouyang · G. M. Henebry · S. Pueppke · C. Crank · A. Kadhim · J. Qi
Department of Geography, Environment, and Spatial Sciences, Center for Global Change and Earth Observations, Michigan State University, East Lansing, MI, USA
e-mail: jqchen@msu.edu; yangzuta@msu.edu; henebryg@msu.edu; pueppke@msu.edu; crankcon@msu.edu; ghadhban@msu.edu; qi@msu.edu

R. John
Department of Biology, University of South Dakota, Vermillion, SD, USA
e-mail: ranjeet.john@usd.edu

P. Y. Groisman
North Carolina State University at NOAA National Centers for Environment Information, Asheville, NC, USA

P.P Shirshov Institute for Oceanology, RAS, Moscow, Russia

Hydrology Science and Services Corp., Asheville, NC, USA
e-mail: Pasha.Groisman@noaa.gov

A. Karnieli
Jacob Blaustein Institutes for Desert Research, Ben-Gurion University of the Negev, Beersheba, Israel
e-mail: karnieli@bgu.ac.il

G. Gutman et al. (eds.), *Landscape Dynamics of Drylands across Greater Central Asia: People, Societies and Ecosystems*, Landscape Series 17,
https://doi.org/10.1007/978-3-030-30742-4_10

Chap. 1). The Asian Drylands Belt (ADB), a neologism form in recent literature (Qi et al. 2017; Groisman et al. 2017, 2018), refers to the Asian region where arid and semi-arid biomes predominate. This region is broadly defined as "Greater Central Asia or GCA" in this book (Henebry et al. 2020, Chap. 1) and includes three subregions: Central Asia Core (CAC), Drylands East Asia (DEA), the Middle East (ME). In contrast to sub-tropical drylands such as the Sahara Desert, and except some marginal areas, the ADB belongs to the cold deserts category, which is typical of high latitudes where the intra-annual variation in solar energy creates definable extreme cold vs. extreme hot seasons (Warner 2004).

The ADB covers a land area of 15.4 million square kilometers and is the home to more than 645 million people. It encompasses approximately 10.3% and 8.6% of the global land area and population, respectively. Drylands, including barrens, grasslands, savannahs, shrublands, and croplands, account for over 95% of the total land area. Grasslands and barrens occupying 37.3% and 41.6% of the total, respectively, and thus predominate. Several large forest patches (<1% of the total ADB land area) can nevertheless be found in the mountains of northeastern Inner Mongolia, southwestern Tibet, northern Mongolia and Kazakhstan, and along the northern coasts of Turkey.

For purposes of statistical analysis, this chapter considers the ADB to be composed of 22 political entities in 17 countries, with six provinces of China considered as separate entities due to their large areas (Fig. 10.1). The 22 entities are further aggregated into Dryland East Asia, Central Asia Core, and the Middle East (Table 10.1). We exclude several Asian countries from our synthesis of the social-ecological systems (SES) in the ADB because of either their low latitude (*e.g.*, Saudi Arabia) or a small portion of dryland coverage (*e.g.*, India, Russia). Although the country with the largest proportion of the land area of the ADB is Kazakhstan (2.7 million km^2 or 17.5% of the total), the country with the highest population of citizens residing in the ADB is Pakistan (197 million or 30.5% of the total). Both of these countries are landlocked, and indeed, all of the Central and East Asian countries lying within the ADB lack access to the sea. Kazakhstan and Mongolia rank as the two largest such countries in the world.

On average, the ADB receives 307 mm precipitation and loses 249 mm through evapotranspiration (ET), yielding an annual water surplus of 58 mm for recharging

M. Kussainova · T. I. Yespolov
Kazakh National Agrarian University, Almaty, Kazakhstan
e-mail: maira.kussainova@kaznau.kz; rector@kaznau.kz

A. Amartuvshin
Department of Economics, University of the Humanities, Ulaanbaatar, Mongolia

A. Tulobaev
Kyrgyz-Turkish Manas University, Bishkek, Kyrgyz Republic
e-mail: askarbek.tulobayev@manas.edu.kg

G. Gutman
Land-Cover/Land-Use Change Program, NASA Headquarters, Washington, DC, USA
e-mail: ggutman@nasa.gov

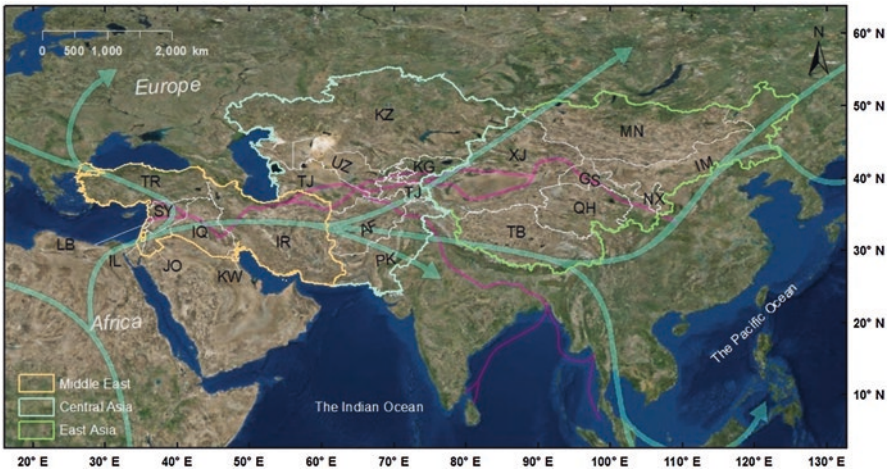

Fig. 10.1 The Asian drylands Belt (ADB) served as a major land base for the establishment of the Silk Road (pink) and the spread of *Homo sapiens* (cyan). This region includes 17 countries in three sub-regions: Central Asia Core (CAC), and Drylands East Asia (DEA) and Middle East (ME). The six provinces in China are treated as distinct political entities for the convenience of statistical analysis. Data sources for the Silk Road and human spread are, respectively, from http://www.arcgis.com/home/item.html?id=1ea892441f974ecda84a87449f936104 and https://www.arcgis.com/home/item.html?id=07166c922d3d4af29ef710a14727fdf3

groundwater and stream flows. The spatial distribution of this water balance is highly heterogeneous. Jordan and Kuwait in ME receive <100 mm annual precipitation, whereas Xinjiang and Mongolia receive 134 mm and 196 mm, respectively. Water deficit, the negative difference between precipitation and ET, occurs in most entities of Drylands East Asia (Chen et al. 2013), with Qinghai (−136 mm), Gansu (−134 mm) and Xinjiang (−105 mm) showing the largest deficits. Water surplus, a positive difference between precipitation and ET, occurs in Tibet (120 mm) and Ningxia (28 mm) (Table 10.1). High elevation terrain in Tajikistan, Pakistan, Afghanistan, and Kyrgyzstan accounts for water surpluses in Central Asia Core (Table 10.1). Countries in the Middle East have the greatest range in annual water balance, which ranges from −51 mm in Jordan to 434 mm in nearby Lebanon (Table 10.1). Due to this pervasive water limitation, gross primary production (GPP) is low, averaging only 215 gC/m^2. Countries in the Middle East have a higher average value (589 gC/m^2) than those in Central (184 gC/m^2) or Drylands East Asia (204 gC/m^2) (Table 10.1), but variation of GPP across entities is substantial, with coefficients of variation of 32%, 59%, and 83% for Drylands East Asia, Central Asia Core, and the Middle East, respectively, and 66% overall (Table 10.1).

The ADB has always played a critical role in human civilization and societal development. After having emerged from Africa, *Homo sapiens* used the area as a major migratory route across Eurasia. Some of humanity's earliest societal organizations arose around the Fertile Crescent 9500 years ago. Diamond (1997) suggested that the long, east-west axis across Eurasia at approximately 40°N, the approximate center of ADB, is fundamental to human development. It was the route

Table 10.1 Socioeconomic and environmental state of 22 political entities in the Asian Drylands Belt (ADB)

Region	Political entity	Area (km^2)	POP (10^6)	POP_d (per km^2)	LSK (10^6)	LSK_d (per km^2)	GDP (10^9 $)	GPP (gC/m^2)	ET (mm)	Precip (mm)	LSK_{pc}
Central Asia Core (CAC)	Afghanistan (AF)	652860	35.53	54.42	29.265	44.8	35.65	57.2	190	342	0.824
	Kazakhstan (KZ)	2699700	18.04	6.68	25.605	9.4	192.00	225.9	182	270	**1.419**
	Kyrgyzstan (KG)	199951	6.20	32.33	7.087	35.5	11.70	318.6	330	422	**1.143**
	Pakistan (PK)	770880	197.02	255.57	131.341	164.6	414.00	329.6	154	324	0.667
	Tajikistan (TJ)	138786	8.92	64.28	6.546	45.7	14.31	121.5	297	477	0.734
	Turkmenistan (TM)	469930	5.76	12.25	18.315	37.3	42.47	102.0	110	169	**3.180**
	Uzbekistan (UZ)	425400	32.39	76.13	24.735	55.1	85.18	129.4	154	190	0.764
	Mean			**71.67**	**34.700**	**56.1**	**113.62**	**183.5**	**202**	**313**	**1.247**
	STD			**85.14**	**43.540**	**49.9**	**146.39**	**108.6**	**81**	**114**	**0.893**
	CV (%)			**118.8**	**125.5**	**89.0**	**128.8**	**59.2**	**39.9**	**36.3**	**71.6**
Drylands East Asia (DEA)	Gansu (GS)	453700	26.10	57.53	24.147	53.1	87.58	268.1	456	322	0.925
	Inner Mongolia (IM)	1183000	25.20	21.30	95.242	80.5	250.51	314.3	310	263	**3.779**
	Mongolia (MN)	1553560	3.08	1.98	36.336	23.4	11.72	181.9	259	196	**11.797**
	Ningxia (NX)	66399	6.75	101.66	4.693	70.7	36.67	164.2	286	314	0.695
	Qinghai (QH)	720000	5.93	8.24	19.763	27.4	29.14	183.4	466	330	**3.333**
	Tibet (TB)	1228400	3.31	2.69	23.065	18.8	10.57	197.6	442	562	**6.968**
	Xinjiang (XJ)	1664897	23.98	14.40	35.394	21.3	115.31	120.4	239	134	**1.476**
	Mean			**29.69**	**34.09**	**42.2**	**77.36**	**204.3**	**351**	**303**	**4.139**
	STD			**37.00**	**28.97**	**25.7**	**85.90**	**65.6**	**100**	**135**	**4.015**
	CV (%)			**124.6**	**85.0**	**60.8**	**111.0**	**32.1**	**28.4**	**44.7**	**97.0**
Middle East (ME)	Iran (IR)	1628760	81.16	49.83	82.601	50.1	838.0	122.1	194	214	**1.018**
	Iraq (IQ)	434320	38.27	88.13	12.957	29.6	194.0	120.0	113	155	0.339
	Israel (IL)	21640	8.70	402.61	1.041	50.3	213.0	245.1	257	256	0.120
	Jordan (JO)	88780	9.70	109.29	3.110	34.8	32.6	84.9	118	67	0.321
	Kuwait (KW)	17820	4.14	232.13	0.696	39.1	0.0	127.3	59	In 99	0.168
	Lebanon (LB)	16250	6.08	374.30	1.093	105.1	549.5	574.7	303	737	0.180
	Syria (SY)	183630	18.27	99.49	21.649	116.9	96.9	157.5	172	286	**1.185**
	Turkey (TR)	769630	80.75	104.91	41.168	52.5	994.0	588.6	379	616	0.510
	Mean			**182.60**	**20.539**	**59.8**	**364.8**	**252.5**	**199**	**304**	**0.405**
	STD			**137.57**	**28.765**	**32.8**	**382.0**	**208.5**	**107**	**244**	**0.405**
	CV (%)			**75.3**	**140.0**	**54.8**	**104.7**	**82.6**	**54.0**	**80.2**	**100.0**
ADB	**Mean**			98.64	29.357	53.0	193.4	215.2	249	307	1.888
	STD			115.25	33.225	36.3	273.2	141.4	117	170	2.733
	CV (%)			116.8	113.2	68.5	141.3	65.7	47.0	55.2	144.7

Six provinces of China are considered as equivalent entities in this chapter because of their large land areas.

POP: population, *LSK* livestock, *GDP:* gross domestic production in constant 2005 US dollars, *GPP:* gross primary production of ecosystems, *ET:* average evapotranspiration in 2017, *precip:* average precipitation in 2011, LSK_{pc}: livestock per capita.

Note that Livestock accounts for only cattle, horses, asses, mules, camels, sheep and goats; the area, POP, LSK, and GDPpc are from the World Bank (https://data.worldbank.org/indicator) for 2017.

for domestication and movement of plants and animals that began in the Fertile Crescent and ushered in agriculture. The ADB was *a significant route for dissemination of foodstuffs in prehistory* (Jones et al. 2016; Spengler et al. 2014) *and* became an important trade route between the East and West as early as 200 years BCE. It was eventually traversed by the Silk Road (Elisseeff 2001; Williams 2014) and defended by portions of the Great Wall of China. Almost all of today's major religions—Christianity, Islam, Judaism, Hinduism, Buddhism, and Daoism—either originated in the ADB or have become entwined with the region over the past 3500 years.

The ADB witnessed the Mongol invasion into Central Asia and Europe, the rise and spread of the Ottoman Empire throughout Western Asia and the Middle East, the conquest of Central Asia by Russia, and the Great Game as Russia and the British Empire struggled for regional influence during the nineteenth century. More recently, the ADB experienced the rise and fall of the Soviet Union and the ascent of China as a world power. The Soviet-Afghan War of 1979–1981, the Iran-Iraq War of 1980–1989, and Operation Desert Storm in 1992 were all fought in the territory of the ADB. The ongoing Syrian Civil War and numerous localized armed conflicts continue to trouble the region. In short and by virtue of its geography and location, the ADB has long been a crossroads of culture, tradition, religion, economy, infrastructure building, and political conflicts (Wittfogel 1957; Carrère d'Encausse 2009; Frankopan 2017).

There can be no doubt that history and tradition have shaped the function and dynamics of the social, economic, and ecological systems of the ADB. From a human-nature relationship perspective, wars and internecine conflicts as early as the Mongolian expansion and the Ming dynasty wars were likely responsible for sharp increases in global CO_2 concentrations because they promoted large-scale changes in demography and agricultural practices (Pongratz et al. 2011). Human activities continue to be responsible for major changes in global greenhouse trace gases, mostly through agricultural development (Ruddiman 2006). The ecosystem and societal consequences triggered by the collapse of the former Soviet Union have been dramatic and direct across Central Asia (de Beurs and Henebry 2004), Eastern Europe (Baumann et al. 2015), and Mongolia (Chen et al. 2015b). As a result of its long history and a high number of large-scale institutional shifts, the structure, function, and dynamics of the SES across the ADB are arguably more diverse and complex than those of any other region in the world.

Today, the 22 political entities within the ADB are characterized by distinct peoples, societies, governance, and economic structures. Lack of access to the sea has made them more self-sustaining, as they struggled with difficulties in transportation across rugged terrain. Despite the harsh environment and its vastness, the ADB supports a population of over 645 million humans, with a population density (POP_d) almost double that of the global average of 51 persons per km^2 (Table 10.1). As is the case with other statistical attributes, population density within the ADB varies significantly from region to region, ranging from 183 persons per km^2 in the Middle East to just 30 persons per km^2 in Drylands East Asia (much higher population densities characterize areas of Drylands East Asia that lie outside the limits of the ADB). Tibet supports only three persons per km^2, but Israel's population density is 130-fold higher. Average annual gross domestic production per capita

(GDP_{pc}) for the ADB is $9712 in US dollars, but this measure varies, too. The figures for Central Asia Core, Drylands East Asia, and the Middle East are $3122, $12,382 and $13,143, respectively. Afghanistan has the lowest value at $586 and Israel the highest at $40,270 (Table 10.1).

Most ADB countries are well endowed with grassland, and so their primary economies traditionally depended on grazing animals. Animal husbandry remains a major component of the region's economy despite recent economic diversification. The average livestock density across the ADB, currently 53 animal units/km^2, is remarkably consistent across the region, ranging from 42 units/km^2 in Drylands East Asia to 56 units/km^2 in Central Asia Core to 53 units/km^2 in the Middle East. The coefficients of variation for these numbers in the three sub-regions are high (Table 10.1) and evident for significant country-to-country variability. Although Pakistan, Syria and Lebanon harbor 100 animal units/km^2, Kazakhstan with its seemingly endless steppes has only nine animal units/ km^2. The ratio of livestock (LSK) to people is an indicator of the importance of the pastoralist livelihood. This value (LSK: POP) is greater than unity in 10 of 22 political entities of the ADB, with a trend from higher values in Drylands East Asia toward lower values in the Middle East. Large pastoral entities such as Mongolia and Tibet have 7 to >10 animals per capita, but smaller, richer countries such as Israel and Kuwait have less than one animal per five residents (Table 10.1).

China and its neighbors share some of the world's majestic mountain ranges, including the Altay, Greater Khingan, Karakoram, Kunlun, Pamir, and Tianshan mountains. Other ranges, including the western Himalayas of Pakistan, the Hindu Kush mountains of Afghanistan and Pakistan, the Urals in northwestern Kazakhstan, and the Zagros mountains of Iran, Iraq, and southeastern Turkey also characterize the region and are important sources of water inflows to the surrounding lowlands. The inflows arise from glacial melt and seasonal melting of snow cover at lower elevations in the mountainous terrain. The Yangtze River, Yellow River, and Mekong River all originate in the Qinghai-Tibetan Plateau in southwestern ADB. These rivers are among the longest waterways in the world and supply water primarily to political entities outside of the ADB in South and Southeast Asia.

The Tigris–Euphrates river system connects Syria, Iraq, Turkey, and Iran and serves as the major domestic water source for these countries. The Amu Darya and the Syr Darya both flow into the Aral Sea and drain parts of Afghanistan, Kazakhstan, Kyrgyzstan, Tajikistan, Turkmenistan, and Uzbekistan. Farther north, the Irtysh River flows across Mongolia, China, Kazakhstan, and Russia. The transboundary nature of so many of the region's rivers underscores the importance of compacts and other transnational agreements in defining water distribution and use in the arid drylands. This is particularly the case for irrigation, industrial, municipal, and instream uses, but also for flood control, natural hazard mitigation, and fisheries management (Bernauer and Siegfried 2012; Graham et al. 2017; Pueppke et al. 2018; Rahaman 2012).

Although the ADB borders the Mediterranean Sea to the west, the Black Sea to the northwest, and the Persian Gulf to the southwest, most of the region lies within the continental interior. Indeed, the Eurasian Pole of Inaccessibility, i.e., the part of Eurasia most distant from the sea, lies in far northwestern Xinjiang, more than

2500 km from the ocean. Many large freshwater lakes in the ADB characterize closed, endorheic basins, including Lake Balkhash in Kazakhstan (16,400 km^2), high mountain Lake Issyk-Kul in Kyrgyzstan (6200 km^2), Urmia Lake in Iran (6000 km^2), Sargamysh Lake in Uzbekistan and Turkmenistan (5000 km^2), and Qinghai Lake in western China (4500 km^2). The Dead Sea between Jordan and Israel is the deepest and most hypersaline lake in the world (420 m below the sea level). Other saline lakes, including the Caspian Sea and the Aral Sea, also lie within Central Asia. Diversion of the Amu Darya and Syr Darya rivers for agriculture is an example of mismanagement at a large scale in use of the region's scarce water supplies. This led to the loss of most of the surface area of the Aral Sea during the latter half of the twentieth century (Micklin 1998, 2007).

10.2 Variability and Changes in Temperature and Precipitation

Three major types of climate characterize the ADB, which generally lies within the temperate zone. A Mediterranean climate with mild winters and hot summers dominates along the coasts of the Black and Eastern Mediterranean Seas, but most of the ADB is located inland and farther east in areas that are distant from the Atlantic and Pacific Oceans and isolated from the Indian Ocean. In these inland areas, the climate is continental, with cold winters and hot summers. Only in the easternmost ADB are the hot, dry summers replaced by relatively humid climatic conditions that, when the abundance of solar radiation is mitigated by atmospheric moisture from the Pacific Ocean, leading to monsoons (Groisman et al. 2018, Chap. 2). Temperatures of the ADB exhibit extremely high spatial and temporal variability. Spatial temperature variations are exacerbated in montane areas, and high solar radiation and deficit of atmospheric and soil moisture exaggerate temporal variations, both diurnally and seasonally (Groisman et al. 2018). Atmospheric teleconnections also influence the spatial and temporal patterns of temperature and precipitation (Henebry et al. 2013; de Beurs et al. 2018).

Changes in climate and related atmospheric processes across the ADB have been well documented (IPCC 2013). The surface air temperature across the region was stable from the beginning of the twentieth century until the mid-1960s, but has increased significantly over the five subsequent decades (Groisman et al. 2018). These changes were most rapid during the winter and spring seasons, which experienced calculated mean rates of change of 1.8 °C and 1.6 °C per century, respectively. The temperature variability is higher in winter when a linear trend explains 23% of the variation. The slightly smaller linear warming trend explains 37% of the variation in spring. For autumn and summer seasons, the warming signals have been much smaller in the autumn and summer, just 0.7 °C and 0.4 °C per century, respectively. The autumn and summer increases are also evident only across the past three decades.

We performed a nonparametric trend analysis of mean annual precipitation (MAP) and meant annual temperatures (MAT) from the CRU4.01 climate dataset over an interval from 1961 to 2016 (https://crudata.uea.ac.uk/cru/data/hrg/cru_ts_4.01/). This allowed us to obtain spatially explicit Theil-Sen slopes that indicate trends. We partitioned the trend images to distinguish pixels that showed non-significant trends from those showing significant trends on the basis of changes exceeding either one or two standard deviations (SD), respectively. This allowed us to partition the dataset pixels into five classes: −2 SD, −1 SD, no significant change, +1 SD, and + 2 SD. Subsequent analysis revealed several hotspots of change.

Our analysis of the long-term change in MAP between 1961 and 2016 confirms that more than three-quarters of the land in the ADB experienced no significant trend in precipitation (Table 10.2). This is in agreement with the results of Groisman et al. (2018), who stated that "Atmospheric precipitation, its amount (totals), form (frozen, mixed or liquid), intensity (for rainfall), intra-seasonal distribution, and their systematic changes (trends) remain the most variable characteristics … systematic continent-wide reduction in the near-surface wind speeds may 'increase' the observed cold season precipitation while the ground-true precipitation is unchanged or even decreased." Our analysis nevertheless confirms that a drying trend is evident in 12.8% of the ADB and a wetting trend evident in 8.4% of the region.

Significantly, there exist major differences among the three sub-regions. Over 90% of lands in Drylands East Asia show no change in MAP, but 7.7% experienced

Table 10.2 Amount of land area (in percentage of the total of the ADB or one of its three sub-regions) that has experienced an increase (+) or decrease (−) from the linear changing trends during 1981–2016 for mean annual temperature (MAT, °C) and mean annual precipitation (MAP, mm)

Region	Variable	−2SD	−1SD	NS	+1SD	+2SD
ADB	MAT	0.06	0.14	7.11	38.24	54.46
	MAP	0.54	12.28	77.20	7.83	0.54
Central Asia Core (CAC)	MAT	0.01	0.20	4.89	55.57	39.32
	MAP	0.00	2.93	72.90	19.19	4.98
Drylands East Asia (DEA)	MAT	0.18	0.17	16.20	50.41	33.03
	MAP	0.34	7.72	90.46	1.48	0.34
Middle East (ME)	MAT	0.00	0.05	2.22	13.96	83.77
	MAP	1.17	23.88	71.02	2.66	1.27

1SD and 2SD denote the changes with one or two standard deviations, whereas NS stands for no change. See Fig. 10.2 for their spatial distributions across the Asian Drylands Belt (ADB)

reductions. Nearly 75% of the area of both Central Asia Core and the Middle East also shows no change, but the remaining land in Central Asia Core is getting wetter while that in the Middle East is receiving less precipitation. There are hotspots of change, both wetting and drying, across the ADB. The former is concentrated in the northeast Mongolian Plateau and western Tibet, along the Tigris River, and in the coastal Mediterranean region, while the latter exist in central Tibet, central parts of Central Asia Core, and western Turkey (Fig. 10.2a).

Our analysis confirms that average warming, *i.e.,* no significant change in dataset pixels, is limited to a few locations in the ADB. They account for just 7.1% of the land, mostly on the Tibetan Plateau and the northern parts of the Mongolian Plateau, as well as in Kazakhstan (Fig. 10.2b). Three large belts characterized by significant positive trends in MAT are apparent. One of these hotspots is centered on the Gobi Desert in the southwest of the Mongolian Plateau in Inner Mongolia and Mongolia; the second runs northwest from the Taklimakan Desert of Xinjiang to the Betpaqdala Desert, Aral Sea, and the Caspian Sea; the third also extends in a southeast-northwest direction and covers the majority of the countries in the Middle East. The geographical extent of these hotspots is evidence that more than half of the land area in the ADB has experienced significant warming since 1961. Although 84% of the land area in the Middle East falls into this category, the corresponding figures for Drylands East Asia and Central Asia Core are just 33% and 39%, respectively (Table 10.2). All of Israel, Jordan, Kuwait, and Lebanon lies within a hotspot, but just 0.6% of Turkmenistan, 5.8% of Gansu, and 6.9% of Qinghai are so located.

Comparison of MAP and MAT maps permits identification of zones experiencing undesirable climatic trends. Areas that are warming and drying represent especially serious concerns because they are expected to become increasingly arid. Tibet, southern Kazakhstan, and western Turkey all fall into this category. Several other areas experiencing no significant changes in temperature while receiving more rainfall may benefit from climate change. These include western Tibet, northern and northeastern Mongolia, and northeastern Inner Mongolia.

10.3 Divergent Dynamics in Land Cover

The surface of the ADB is dominated by desert areas that are collectively referred to as barrens. These areas represent 41.2% of the landmass of the ADB, the most expansive such area on earth except Antarctica (Chen et al. 2013; Groisman et al. 2018). The Gobi Desert of southern Mongolia and northwestern China is well known, as is the Judean Desert, parts of which are 304 m below sea level at the planet's lowest point of land (Niemi et al. 1997). Other barrens including the Betpaqdala Desert of south-central Kazakhstan, the Karakum Desert of Turkmenistan, the Kyzylkum Desert of Kazakhstan, Uzbekistan, and Turkmenistan, the Taklimakan Desert of northwest China, and the Thar Desert of Pakistan and India cover large areas of the ADB. Syria, Jordan, and Iraq are also largely deserts.

The ADB also harbors the most extensive zone of grasslands on earth (Suttie et al. 2005), accounting for 37.3% of the region. Other major cover types include

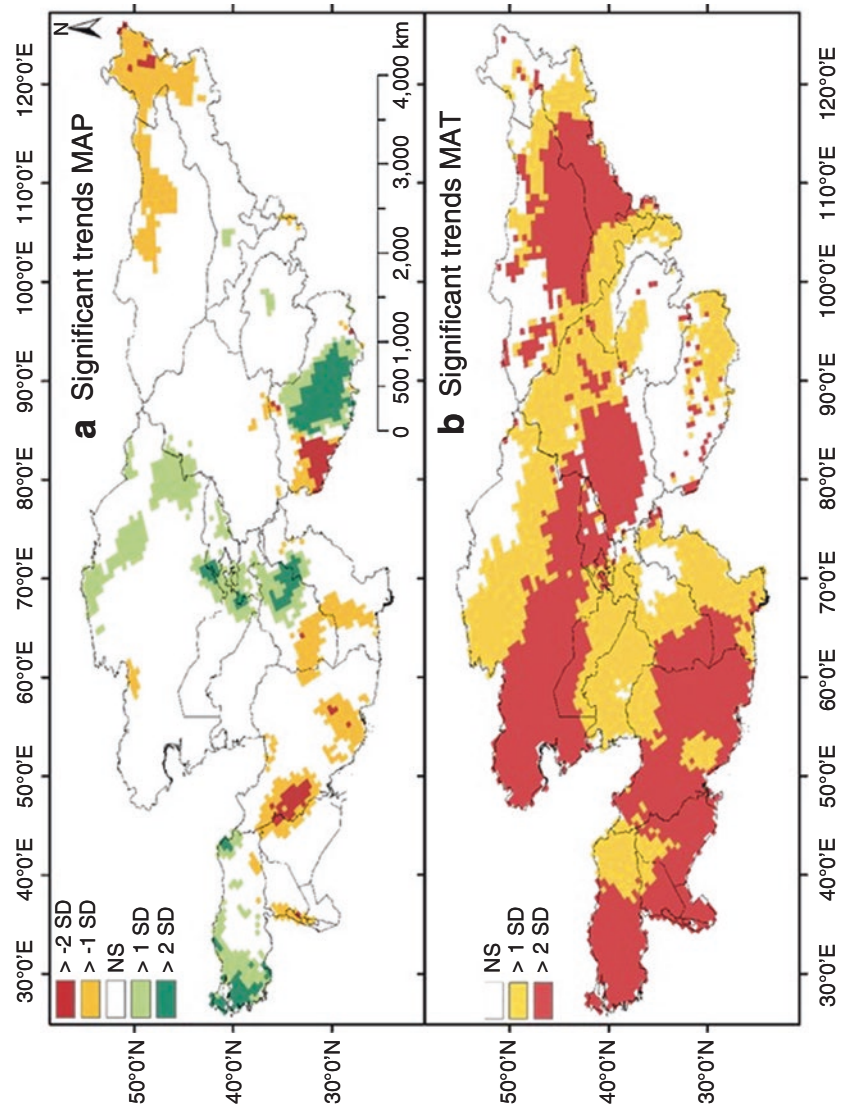

Fig. 10.2 Land area with significant (*i.e.*, >1 and 2 standard deviations from the mean) non-parametric trends of: (**a**) mean annual precipitation (MAP), and (**b**) mean annual temperature (MAT) from 1981 to 2016. These data were from the CRU4.01 gridded climate database (https://crudata.uea.ac.uk/cru/data/hrg/cru_ts_4.01/)

croplands (9.8%), and shrublands/savannas (7.2%). Although forests are a relatively minor feature of the ADB, extending across only 1% of the total area, they are important features of Tibet, Inner Mongolia, Turkey, and Gansu. Forests cover more than 3.5% of the land area in each of these entities, and since each is a large territory, the total amount of forest area is substantial, about 190,000 km^2 (also see Henebry et al. 2020, Chap. 3; Kappas et al. 2020, Chap. 9)

The relationship between grasslands, barrens, and natural other areas varies in the three sub-regions of the ADB. Although Lebanon and Turkey have substantial grasslands, many Middle East countries are mostly desert (Table 10.3a). Indeed, Jordan, Syria, and Kuwait have almost no natural grass cover at all. The combination of barrens and grasslands dominates in Central Asia Core, typically constituting from 65% to almost 90% of the land area of individual countries. The ratio of the two land cover types varies, such that Pakistan has relatively large barren areas, while Kazakhstan and Kyrgyzstan are both characterized by extensive grassland areas. The Drylands East Asia sub-region is also dominated by grasslands and barrens, which make up more than 80% of the landmass of the region's political entities (Table 10.3a). Ningxia is unique in having a few barren areas (4.6%); conversely, almost 75% of Xinjiang falls into this category.

Croplands are a minor feature of the landscape of most ADB countries, comprising 10% of the total or less—often much less (Table 10.3a). Just four countries, all in the Middle East (Israel, Lebanon, Syria, and Turkey) have more than one-quarter cropland. Between these two extremes lie entities such as Gansu, Ninjia, Pakistan, and Uzbekistan with cropland areas of 10–20%. Uzbekistan, a desert country, is noteworthy for extensively irrigated croplands, most of which are dedicated to the production of cotton (Zanca 2011). With few exceptions, snow and water are minor landscape features of the entities in the ADB (Table 10.3a). Only Uzbekistan has more than 4% of its surface area covered with water, and snow is for the most part associated with mountainous countries and regions of western China.

Land cover changes in the ADB have been dramatic during the 15-year period that ended in 2016 (Fig. 10.3, Table 10.3a), with 5.6% of the land experiencing cover change during this period (Groisman et al. 2018; Henebry et al. 2020, Chap. 3; Kappas et al. 2020, Chap. 8). Seven zones across the ADB have experienced rapid land cover change and have been identified by Groisman et al. (2018) as hotspots of land cover change. These zones include: (1) areas adjacent to the Caspian Sea in Turkmenistan, Uzbekistan and southwestern Kazakhstan; (2) the periphery of the Drylands East Asian drylands of western Xinjiang; (3) the eastern limits of the Gobi desert in Inner Mongolia and Mongolia; (4) the Hetao region next to the Yellow River; (5) tree-covered zones of northeast Inner Mongolia; (6) forested areas of northern Mongolia; and (7) northwestern Kazakhstan.

We used the most recent NASA MODIS land cover product (MCD12Q1 V6; available online at https://earthdata.nasa.gov/) and the IGBP land cover scheme at 500-m spatial resolution and annual temporal resolution to comprehensively evaluate land cover and land cover change in the ADB over a 15-year period from 2001 to 2016 (Fig. 10.4). Overall, the relative proportion of land covered by barrens is decreasing in the ADB, except for Kazakhstan, Uzbekistan, Turkmenistan, and Syria, which saw no reductions between 2001 and 2016. Lebanon and Turkey wit-

Table 10.3a Composition and change of land cover from 2001 to 2016 across the political entities of the Central Asia Core (CAC)

P. entity	Year	Forests	Shrublands	Savannas	Grasslands	Wetlands	Croplands	Urban	Mosaic	Snow	Barren	Water
Afghanistan (AF)	2001	201.25 (0.03)	46517.25 (7.25)	4553.5 (0.71)	240692.25 (37.50)	12.5 (0)	20589 (3.21)	899.75 (0.14)	0 (0.00)	2407 (0.38)	325647 (50.74)	314.75 (0.05)
	2016	193.25 (0.03)	63964.25 (9.97)	4838.25 (0.75)	247144.25 (38.51)	32.5 (0.01)	19222.5 (2.99)	917 (0.14)	0 (0.00)	3098.75 (0.48)	302383 (47.11)	40.5 (0.01)
	Δ	−0.04	0.38	0.06	0.03	1.60	−0.07	0.02		0.29	−0.07	−0.87
Kazakhstan (KZ)	2001	12821.75 (0.47)	2340.75 (0.09)	15444.75 (0.57)	2318210.75 (85.23)	8784.5 (0.32)	143071.25 (5.26)	3530 (0.13)	201.5 (0.01)	1361.5 (0.05)	154828.5 (5.69)	59375.5 (2.18)
	2016	10407.75 (0.38)	6224 (0.23)	18120.25 (0.67)	2306996 (84.82)	8728.75 (0.32)	139397.75 (5.12)	3637.5 (0.13)	582.25 (0.02)	7385.75 (0.27)	158884 (5.84)	59606.75 (2.19)
	Δ	−0.19	1.66	0.17	0.00	−0.01	−0.03	0.03	1.89	4.42	0.03	0.00
Kyrgyzstan (KG)	2001	382.75 (0.20)	7.25 (0.00)	1308 (0.67)	144706.5 (73.93)	161.75 (0.08)	12354 (6.31)	1855 (0.95)	13.75 (0.01)	3451.25 (1.76)	24781.25 (12.66)	6709.25 (3.43)
	2016	278.75 (0.14)	20.25 (0.01)	1542.75 (0.79)	143323 (73.22)	153.5 (0.08)	13579.25 (6.94)	1878.25 (0.96)	38 (0.02)	4192 (2.14)	24028.75 (12.28)	6696.25 (3.42)
	Δ	−0.27	1.79	0.18	−0.01	−0.05	0.10	0.01	1.76	0.21	−0.03	0.00
Pakistan (PK)	2001	1522.5 (0.17)	102003.5 (11.71)	18432.75 (2.12)	119440.25 (13.71)	542.75 (0.06)	161840.5 (18.57)	6262.5 (0.72)	719.25 (0.08)	8643.25 (0.99)	448668 (51.49)	3266 (0.37)
	2016	1776 (0.20)	122226 (14.03)	22407.25 (2.57)	114709.5 (13.16)	1009 (0.12)	176182.5 (20.22)	6410 (0.74)	1415.25 (0.16)	10568.25 (1.21)	411191.25 (47.19)	3446.25 (0.40)
	Δ	0.17	0.20	0.22	−0.04	0.86	0.09	0.02	0.97	0.22	−0.08	0.06
Tajikistan (TJ)	2001	5.5 (0.00)	2432 (1.72)	266.25 (0.19)	63857.5 (45.09)	21 (0.01)	6455.25 (4.56)	1235.75 (0.87)	0 (0.00)	7551.25 (5.33)	59004 (41.66)	797.5 (0.56)
	2016	1.5 (0.00)	3240.5 (2.29)	335.75 (0.24)	62000.5 (43.78)	25.25 (0.02)	7786 (5.50)	1246 (0.88)	0 (0.00)	8727.75 (6.16)	57441.5 (40.56)	821.25 (0.58)
	Δ	−0.73	0.33	0.26	−0.03	0.20	0.21	0.01		0.16	−0.03	0.03
Turkmenistan (TM)	2001	0 (0.00)	76855.25 (16.35)	4.75 (0.00)	112341.5 (23.90)	122.75 (0.03)	14170.25 (3.01)	1702.25 (0.36)	0 (0.00)	4.25 (0.00)	261199.75 (55.56)	3733.75 (0.79)
	2016	0 (0.00)	94160.75 (20.03)	6.5 (0.00)	94646.25 (20.13)	143 (0.03)	14805.75 (3.15)	1705.5 (0.36)	0 (0.00)	381.5 (0.08)	260303.25 (55.37)	3982 (0.85)
	Δ		0.23	0.37	−0.16	0.16	0.04	0.00		88.76	0.00	0.07
Uzbekistan (UZ)	2001	0 (0.00)	12823.5 (2.87)	150 (0.03)	195265.75 (43.65)	387 (90.09)	46618 (10.42)	10500.75 (2.35)	0 (0.00)	46.25 (0.01)	162568.75 (36.34)	18955 (4.24)
	2016	0 (0.00)	22835.75 (5.11)	206.5 (0.05)	180735.25 (40.40)	917.5 (0.21)	47616.75 (10.65)	10599.25 (2.37)	0 (0.00)	2158 (0.48)	163108.75 (36.46)	19137.25 (4.28)
	Δ		0.78	0.38	−0.07	1.37	0.02	0.01		45.66	0.00	0.01

Land cover data were from the MODIS MCD12Q1. The unit for each cover type is a square kilometer. The numbers in the parentheses represent the relative percentage composition (%) at the country level; Δ represents the change of the cover type during the 15 years (%)

Table 10.3b Drylands East Asia (DEA)

P. entity	Year	Forests	Shrublands	Savannas	Grasslands	Wetlands	Croplands	Urban	Mosaic	Snow	Barren	Water
Gansu (GS)	2001	15036.75	291.75	9967.5	155507	186.5	49382	1682.75	2525.5	66.5	169387.25	88
		(3.72)	(0.07)	(2.47)	(38.48)	(0.05)	(12.22)	(0.42)	(0.62)	(0.02)	(41.92)	(0.02)
	2016	17297.25	546.25	13143	151917.25	283.25	52069.25	1707.5	3211.75	520.5	163329.5	96
		(4.28)	(0.14)	(3.25)	(37.59)	(0.07)	(12.88)	(0.42)	(0.79)	(0.13)	(40.42)	(0.02)
	Δ	0.15	0.87	0.32	−0.02	0.52	0.05	0.01	0.27	6.83	−0.04	0.09
Inner Mongolia (IM)	2001	39990	565.25	87682.75	658897.25	300.75	58573	3148.25	1283.5	0.25	296642.25	2932.75
		(3.48)	(0.05)	(7.62)	(57.29)	(0.03)	(5.09)	(0.27)	(0.11)	(0.00)	(25.79)	(0.26)
	2016	55117.5	1082.5	91499.5	646214.5	513.75	65458.25	3285.25	3257.25	13.75	280896.5	2677.25
		(4.79)	(0.09)	(7.96)	(56.190	(0.04)	(5.69)	(0.29)	(0.28)	(0.00)	(24.43)	(0.23)
	Δ	0.38	0.92	0.04	−0.02	0.71	0.12	0.04	1.54	54.00	−0.05	−0.09
Mongolia (MG)	2001	10265.5	897.5	41607.5	979743.75	504.75	307	1008	0	99.75	516879	12067.75
		(0.66)	(0.06)	(2.66)	(62.67)	(0.03)	(0.02)	(0.06)	(0.00)	(0.01)	(33.06)	(0.77)
	2016	15016.75	954.75	50399.75	997436.75	688.5	578.25	1010.5	0	171.5	485424.75	11699
		(0.96)	(0.06)	(3.22)	(63.80)	(0.04)	(0.04)	(0.06)	(0.00)	(0.01)	(31.05)	(0.75)
	Δ	0.46	0.06	0.21	0.02	0.36	0.88	0.00		0.72	−0.06	−0.03
Ningxia (NX)	2001	71.5	357.75	8.5	38178.25	17.25	10130.5	432.5	0	0	2355.5	3.25
		(0.14)	(0.69)	(0.02)	(74.05)	(0.03)	(19.65)	(0.84)	(0.00)	(0.00)	(4.57)	(0.01)
	2016	159	642	23.25	37074.75	41	11938.5	488	0	0	1185.25	3.25
		(0.31)	(1.25)	(0.05)	(71.91)	(0.08)	(23.16)	(0.95)	(0.00)	(0.00)	(2.30)	(0.01)
	Δ	1.22	0.79	1.74	−0.03	1.38	0.18	0.13			−0.50	0.00
Qinghai (QH)	2001	97.75	9.25	699	447067.5	94.75	6066.5	790.5	0	2302.5	247570.5	10131
		(0.01)	(0)	(0.10)	(62.54)	(0.01)	(0.85)	(0.11)	(0.00)	(0.32)	(34.63)	(1.42)
	2016	97.25	10.5	692	454079.5	162.75	5219.75	796.25	0	3249.75	239962.25	10559.25
		(0.01)	(0)	(0.1)	(63.52)	(0.02)	(0.73)	(0.11)	(0.00)	(0.45)	(33.57)	(1.48)
	Δ	−0.01	0.14	−0.01	0.02	0.72	−0.14	0.01		0.41	−0.03	0.04
Tibet (TB)	2001	72841.25	6541.5	10813	632510	933.25	1349.75	89.25	204.5	16877	440490.75	20310.5
		(6.06)	(0.54)	(0.90)	(52.58)	(0.08)	(0.11)	(0.01)	(0.02	(1.40)	(36.62)	(1.69)
	2016	73084.75	8493.25	12843	646793	800.75	908.25	90	192.5	14212.25	424264	21279
		(6.08)	(0.71)	(1.07)	(53.77)	(0.07)	(0.08)	(0.01)	(0.02)	(1.18)	(35.27)	(1.77)
	Δ	0.00	0.30	0.19	0.02	−0.14	−0.33	0.01	−0.06	−0.16	−0.04	0.05
Xinjiang (XJ)	2001	2092.75	465	3424.5	369550.75	876	45574.75	2737.5	203.25	12634	1193036.5	5494.5
		(0.13)	(0.03)	(0.21)	(22.59)	(0.05)	(2.79)	(0.17)	(0.01)	(0.77)	(72.92)	(0.34)
	2016	1621.75	652	4876.5	370789.5	940.25	68611	2748.75	333.5	21052.25	1158823.5	5640.5
		(0.10)	(0.04)	(0.30)	(22.66)	(0.06)	(4.19)	(0.17)	(0.02)	(1.29)	(70.83)	(0.34)
	Δ	−0.23	0.40	0.42	0.00	0.07	0.51	0.00	0.64	0.67	−0.03	0.03

Table 10.3c The Middle East (ME)

Country	Year	Forests	Shrublands	Savannas	Grasslands	Wetlands	Croplands	Urban	Mosaic	Snow	Barren	Water
Iran	2001	12292.75	178417.25	7295	347287.25	433.75	77464.25	8186.5	112.75	0.25	985497	5932.75
(IR)		0.76)	(10.99)	(0.45)	(21.40)	(0.03)	(4.77)	(0.50)	(0.01)	(0.00)	(60.72)	(037)
	2016	10576.5	200338.25	9428.75	339239.75	790.25	73980	8371.5	171.25	30.25	976161.25	3831.75
		(0.65)	(12.34)	(0.58)	(20.90)	(0.55)	(4.56)	(0.52)	(0.01)	(0.00)	(60.15)	(0.24)
	Δ	−0.14	0.12	0.29	−0.02	0.82	−0.04	0.02	0.52	120.00	−0.01	−0.35
Iraq	2001	0 (0.00)	27784.5	1032.75	54075.25	251.75	44297.75	3542.5	154.75	0	302227.5	4424.75
(IQ)			(6.35)	(0.24)	(12.35)	(0.06)	(10.12)	(0.81)	(0.04)	(0.00)	(69.03)	(1.01)
	2016	0 (0.00)	28662.5	820.75	64474	772.75	47256.25	3714.25	126.75	0	287384.75	4579.5
			(6.55)	(0.19)	(14.73)	(0.18)	(10.79)	(0.85)	(0.03)	(0.00)	(65.64)	(1.05)
	Δ		0.03	−0.21	0.19	2.07	0.07	0.05	−0.18		−0.05	0.03
Israel	2001	4.5	1759.5	244.5	5632.75	4.5	5558	1402.25	3	0.00	11584.25	620.5
(IL)		(0.02)	(6.56)	(0.91)	(21.01)	(0.02)	(20.73)	(5.23)	(0.01)		(43.20)	(2.31)
	2016	12.25	1960.75	296.5	5402.75	4.75	5615.75	1457.25	7.75	0.00	11435.75	620.25
		(0.05)	(7.31)	(1.11)	(20.15)	(0.02)	(20.94)	(5.43)	(0.03)		(42.65)	(2.31)
	Δ	1.72	0.11	0.21	−0.04	0.06	0.01	0.04	1.58		−0.01	0.00
Jordan	2001	0 (0.00)	5201	26.25	1487.75	0	2239.75	810.25	4 (0.00)	0	79108	450.75
(JO)			(5.82)	(0.03)	(1.67)	(0.00)	(2.51)	(0.91)		(0.00)	(88.56)	(0.50)
	2016	0 (0.00)	6062.25	6	1194.25	0	2358.75	821.25	0.75	0	78433.75	450.75
			(6.79)	(0.01)	(1.34)	(0.00)	(2.64)	(0.92)	(0.00)	(0.00)	(87.80)	(0.50)
	Δ		0.17	−0.77	−0.20		0.05	0.01	−0.81		−0.01	0.00
Kuwait	2001	0 (0.00)	17 (0.10)	0 (0.00)	128.5	0.25	6	536	0	0 (0.00)	16692	33.5
(KW)					(0.74)	(0.00)	(0.03)	(3.08)	(0.00)		(95.86)	(0.19)
	2016	0 (0.00)	44 (0.25)	0 (0.00)	238.75	0	13	568.75	0	0 (0.00)	16514.25	34.5
					(1.37)	(0.00)	(0.07)	(3.27)	(0.00)		(94.84)	(0.20)
	Δ		1.59		0.86	−1.00	1.17	0.06			−0.01	0.03
Lebanon	2001	34.25	2504.5	589.25	4063.25	20.75	2322	443.25	0.5	0	199.5	21
(LB)		(0.34)	(24.56)	(5.78)	(39.84)	(0.20)	(22.77)	(4.35)	(0.00)	(0.00)	(1.96)	(0.21)
	2016	51 (0.50)	2596.5	735.5	3904.75	9.75	2327.75	459.25	2.5	0	90.25	21
			(25.46)	(7.21)	(38.29)	(0.10)	(22.82)	(4.50)	(0.02)	(0.00)	(0.88)	(0.21)
	Δ	0.49	0.04	0.25	−0.04	−0.53	0.00	0.04	4.00		−0.55	0.00
Syria	2001	213	27147.75	871	9048.5	66	44312.25	2676.75	813.5	0.00	101633.25	820.5
(SY)		(0.11)	(14.47)	(0.46)	(4.82)	(0.04)	(23.62)	(1.43)	(0.43)		(54.17)	(0.44)
	2016	76.5	27627.75	834.25	9337.75	85.75	38688.25	2737.5	862.75	0.75	106610.25	741
		(0.04)	(14.73)	(0.44)	(4.98)	(0.05)	(20.62)	(1.46)	(0.46)		(56.83)	(0.39)
	Δ	−0.64	0.02	−0.04	0.03	0.30	−0.13	0.02	0.06		0.05	−0.10
Turkey	2001	37470	17758	91307	397929.75	1823.5	203790.25	8961.75	3306.75	123	5645.25	8745.75
(TR)		(4.80)	(2.28)	(11.70)	(51.01)	(0.23)	(26.12)	(1.15)	(0.42)	(0.02)	(0.72)	(1.12)
	2016	43958.25	15854.75	94541.25	379671.75	3408	211157	9328.75	5495.5	242	4239	8964.75
		(5.64)	(2.23)	(12.12)	(48.67)	(0.44)	(27.07)	(1.20)	(0.70)	(0.03)	(0.54)	(1.15)
	Δ	0.17	−0.11	0.04	−0.05	0.87	0.04	0.04	0.66	0.97	−0.25	0.03

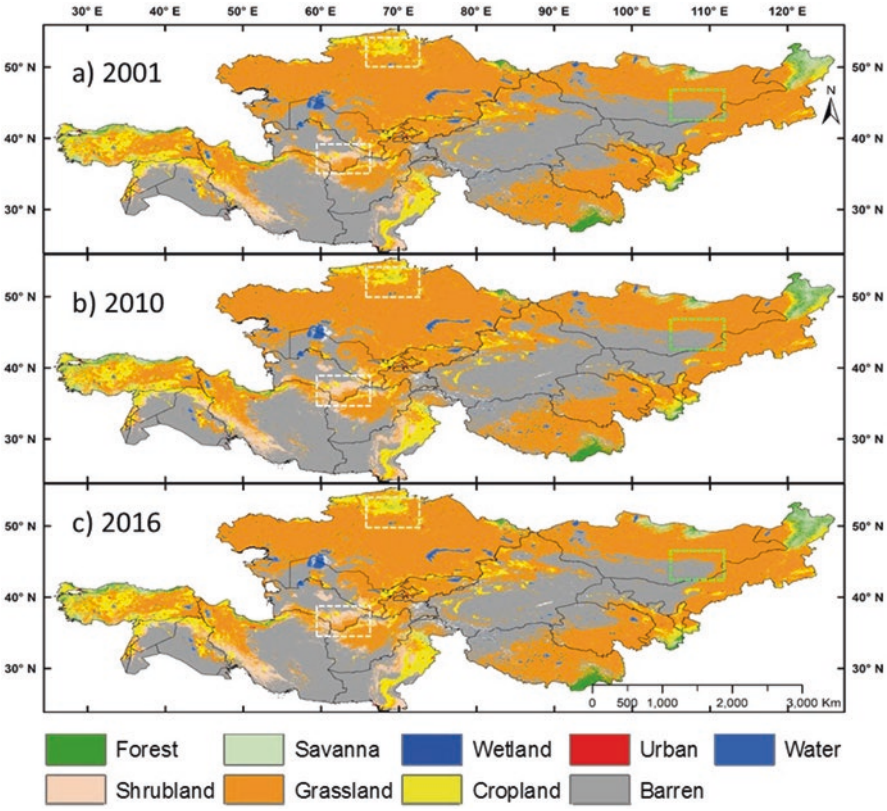

Fig. 10.3 MODIS derived land cover (MCD12Q1) in 2001 (**a**), 2010 (**b**) and 2016 (**c**), highlighting "hotspots" of land use change in Kazakhstan, Turkmenistan and Mongolian Plateau. Non-parametric trend analysis was performed on the mean annual precipitation (MAT) and mean annual temperature (MAT) for the CRU4.01 climate dataset during 1961–2016 to generate the spatially explicit Theil-Sen slopes

nessed the greatest reduction in a barren land, 55% and 25%, respectively (Table 10.3c). Shrinkage of barren land was a modest 8% in Pakistan and 7% in Afghanistan, but an impressive 50% in China's Ningxia Province (Table 10.3b). Grassland coverage did not generally change to a significant extent, but Turkmenistan and Jordan experienced reductions of 16% and 20%, respectively. Grassland coverage in Kuwait expanded by 86% and in Iraq by 19%.

Loss of barren and grassland areas was often coupled with gains in shrublands, savannas, and/or mosaics of cropland and natural vegetation. Shrubland areas increased in all entities except Turkey (−11%), with Kazakhstan, Kyrgyzstan, Uzbekistan, Kuwait, and the Chinese administrative districts experiencing the greatest increases. Savannas also increased in most entities, with significant decreases recorded only in Iraq (−21%) and Jordan (−77%). The cropland-natural vegetation mosaic (CNVM) class expanded in most entities from 2001 to 2016, doubling or

Fig. 10.4 Percentage of land cover change from 2001 to 2016. The blue (red) dots represent the increases (decreases) by IGBP land cover type

even tripling in the area in Kazakhstan, Kyrgyzstan, Pakistan, Inner Mongolia, Israel, and Lebanon. CNVM was reduced only in Iraq, Jordan, and Tibet. Interpreting change in CNVM (*i.e.*, Mosaic) is nevertheless challenging because it is a composite cover class that can include several types of agricultural land use, including fallow croplands.

Variations in cropland area were apparent across the entire ADB. Cropland expanded greatly in Kuwait (117%), but contracted in Syria (13%), likely as a result of civil instability and armed conflict. The extent of croplands in Central Asia Core increased in Tajikistan (20%), Kyrgyzstan (10%), and Pakistan (9%) but decreased in Afghanistan (7%). Across the Drylands East Asia, large increases in cropland occurred in Mongolia (88%), Xinjiang (51%), and Ningxia (18%), but there were also decreases in Qinghai (14%) and Tibet (33%). Urban expansion was evident in all three sub-regions, but the change in areal extent was minimal (<1%).

10.4 Interrelationships Among SES Indicators

Understanding the interrelationships among the key measures of social, economic, and ecological systems, *i.e.* the three pillars of sustainability, is a precondition for exploring the direct and indirect regulative mechanisms for a social-ecological system (Ostrom et al. 1999; Turner et al. 2016). Using Inner Mongolia and Mongolia as two macrosystems, Chen et al. (2015b) proposed a framework to connect the dots representing social, economic, and ecosystem functions and land use to understand the livestock (LSK) dynamics. Using widely available measures, the authors examined the ratios among net primary production (NPP), gross domestic production (GDP), human population (POP) and LSK over 60 years (1950–2010) to evaluate the interdependencies of the social, economic, ecological systems. This concept has been expanded to include the roles of policy and governance that may have affected those interrelationships (Chen et al. 2015a). The conceptual framework was also used to compare the urbanization processes in Inner Mongolia and Mongolia (Park et al. 2017) and the Asian portion of Russia (Fan et al. 2020), whereas Tian et al. (2018) examined the interrelationships on the Tibetan Plateau using structural equation models following the framework.

Following this school of thought, we performed a preliminary analysis of the interrelationships among key indicators of the social, economic, ecological systems by using national data for the 22 political entities within the ADB. There exist significant log-linear relationships among population, POP, LSK and GDP (Fig. 10.5a–c), but low correlations with gross primary production (GPP) (Fig. 10.5d–f). The relationship of GDP and LSK seems weak ($R^2 = 0.15$), likely due to the influence of obvious outliers (*i.e.*, Israel, Lebanon, and Kuwait), suggesting that LSK continues its historically important role in national economic development (Fig. 10.5a). A particularly interesting finding is that the log-transformed LSK values in entities in Central and East Asia were above the ADB average, which stresses the greater

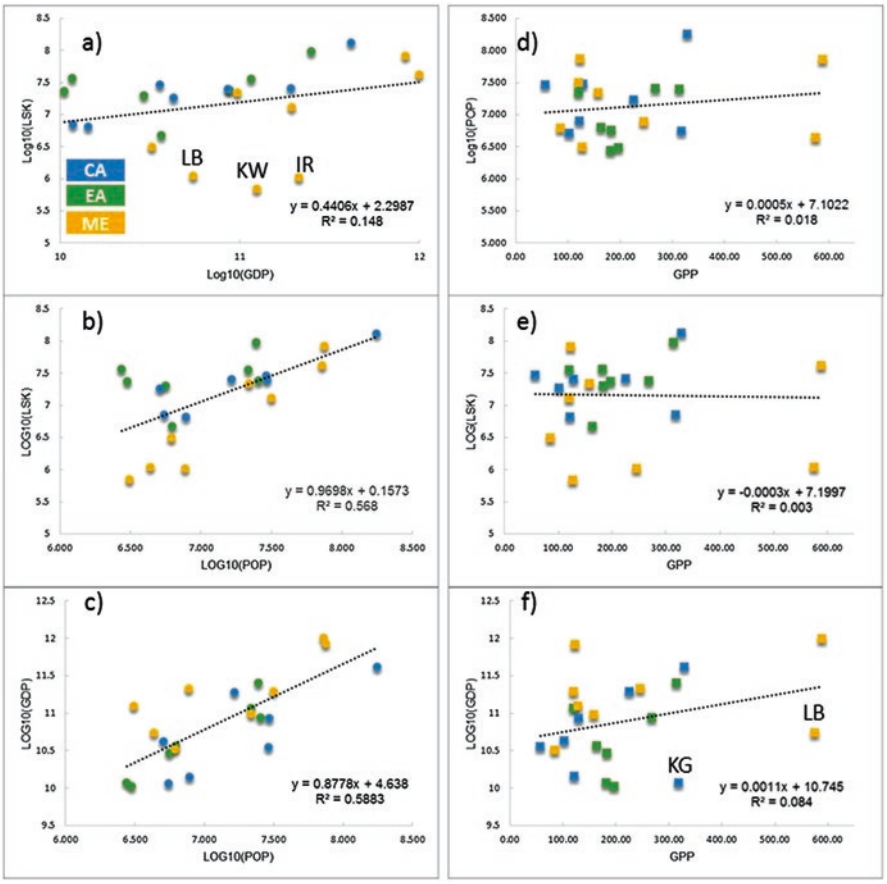

Fig. 10.5 Relationship between: (**a**) GDP and POP, (**b**) POP and Livestock, (**c**) GPD and LSK, (**d**) POP and GPP, (**e**) LSK and GPP, and (**f**) GDP and GPP in 2011 for the 17 countries in the Asian Drylands Belt (ADB). The values for the six provinces in China were scaled from the national average of China due to lack of provincial data

importance of LSK in total GDP compared to that in the Middle East. Similarly, the importance of livestock relative to population varies among the three sub-regions, with higher and lower values than the ADB mean for Drylands East Asia and the Middle East, respectively (Fig. 10.5b). Although further analysis is needed, this may partially due to a higher portion of herder population in Drylands East Asia and a lower workforce in the Middle East. As for the relationship between GDP and POP, the correlation is strong ($R^2 = 0.59$) and tight (Fig. 10.5c). The slope of this relationship is known as GDP per capita (note that we present the log-linear relationship, which is different from GDP_{pc}). This value is overall higher in the Middle East and lower in Central Asia Core, while entities in Drylands East Asia fall well below average, with the notable exceptions of Tibet and Mongolia.

It stands to reason that socioeconomic variables should be highly correlated with ecosystem production (e.g., GDP vs GPP), as nature provides a foundation for societal development, but these relationships are not significant in the ADB (Fig. 10.5d–f). There nevertheless exists a weak positive correlation between POP and GPP (Fig. 10.5d), as well as GDP and GPP (Fig. 10.5e). However, the slightly negative correlation between LSK and GPP is unexpected (Fig. 10.5f). The relationship between GDP and GPP—a potential indication of economic status based on natural production—might appear highly correlated when excluding Lebanon and Kyrgyzstan, two entities with low GDP (Fig. 10.5f). We also examined the correlations with precipitation, ET, and water deficit, but insignificant relationships were detected (data not shown). These weak, non-significant correlations suggest that the socioeconomic development of landlocked ADB entities does not rely solely on their natural resources, but rather can be driven by other forces. These might include connections with entities outside the country and could involve constraints with internal institutions. For example, the magnitudes of LSK, POP, and GDP in Inner Mongolia are much higher than those in Mongolia due to the influence of China (Chen et al. 2015a, 2018). The socioeconomic development of Kazakhstan, and likely other Central Asian republics, remains under the influence of another power: Russia (Mukhashbaeva and Chumachenko 2016).

In sum, there appear potential connections among the indicators of social, economic and ecological systems in the ADB, but the relationships are complicated, contingent, contextural, and vary substantially among the entities as well as among the three sub-regions. The macrosystem approach applied here would benefit from data at the sub-country level that considers land cover composition (*e.g.*, the dominance of grassland versus barrens), geographical settings (*e.g.*, mountain ranges and waterways) that provide water supply, global connections, and institutional structure and performance. Future investigations are needed to combine the macrosystem approach with a mechanistically based exploration by incorporating detailed data at finer spatial and temporal scales.

10.5 Priority Issues for the Sustainability of SES in the ADB

Sustainability has become a key focus of many governments and scientific communities, international agencies, political entities, and civil society in general. Despite the increasing number of scholarly investigations, the definition, measurement, and modeling of sustainability and implementation of sustainable practices remain ununited. Indeed, a Google literature search conducted in October of 2018 yielded 138 million URLs using a keyword of "sustainability methods." Ongoing challenges arise from debates about the types of system feedbacks (direct vs. indirect, linear vs. nonlinear), the roles of institutional constraints (*e.g.*, policy; Fernandez-Gimenez 2001; Chen et al. 2015a), the relative influence of legacy effects (*e.g.*, historical consequences; Costanza et al. 2007; de Beurs et al. 2017), and causal feedbacks with external forcings (*e.g.*, global climatic change, international trade, international polity, labor migration from ADB and remit-

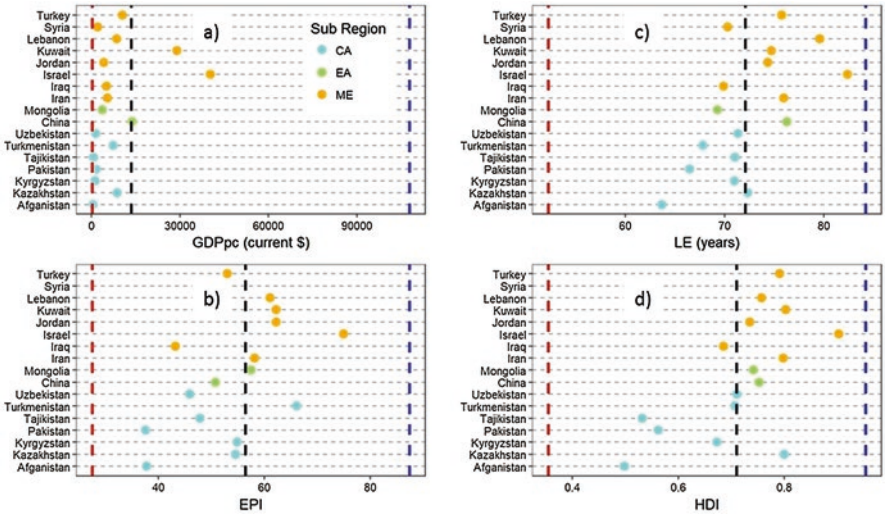

Fig. 10.6 State of major SES indicators for the 22 political entities in 2015 within the ADB, including gross domestic production per capita (GDP_{pc}), human development index (HDI), life expectancy (LE), and EPI (environmental performance index (EPI). The black line is the global average and the red and blue lines are the minimum and maximum values of global countries, respectively. The values for the six provinces in China were scaled from the averages of China (due to lack of provincial data). Data were from the 2017 year book of each province (http://www.stats.gov.cn/english/statisticaldata/annualdata/)

tances back to ADB, *etc*.) (Abdih et al. 2012b; Rubinov 2014; Bordachev et al. 2016; Mukhashbaeva and Chumachenko 2016).

To understand the relative positions of sustainability of the 22 political entities across the ADB, we examined the values of four critical measures for each entity in 2015 by using data from the World Bank (https://data.worldbank.org/indicator/NY.GDP.PCAP.CD), the United Nations Human Development Programme (http://hdr.undp.org/en/content/human-development-index-hdi) and the Environmental Performance Index (EPI; https://epi.envirocenter.yale.edu/): GDP_{pc}, environmental performance index (EPI), life expectancy (LE), and the human development index (HDI) (Fig. 10.6). These values are placed within the global context so that areas of improvement can be identified. Except for Israel and Kuwait, which have the highest GDP_{pc} in 2017, ADB entities fell below the global average value of $13,489 (Fig. 10.6a). Kazakhstan and Turkmenistan lead in Central Asia Core, while all others have a GDP_{pc} of near the global minimum ($212.50).

As assessed by EPI values, the environmental performance of entities in Central and East Asia (54.2) are lower than the global average (56.4), except for Turkmenistan (66.1) and Mongolia (57.5). An opposite trend is apparent for the Middle East, where the average EPI (59.3) is higher than the global average except for Turkey (53.0), Iraq (43.2), and likely Syria (no data was available due to conflict). Israel leads the Middle East with an EPI value of 75.0 (Fig. 10.6b). The life expectancy for the ADB is 72.5 years and reflects low values across Central Asia Core (69.1) and

most entities in the Middle East except for Israel at 82.4 years and Lebanon at 79.6 years (Fig. 10.6c). The HDI for the ADB averages 0.71 and is higher in the Middle East (0.75) than in Central Asia Core (0.64) or Mongolia (0.70) (Fig. 10.6d). Israel and Lebanon again lead the regional HDI at 0.90 and 0.80, respectively. With an HDI of 0.80, Kazakhstan is the only country in CA with an HDI greater than the global average (0.71), whereas Iraq is the only country in the Middle East with a lower-than-global-average HDI value (0.69).

These figures provide a snapshot of the major indicators for the 17 independent countries in the ADB. In sum, Israel leads the region by having the highest values of all four indicators, whereas Afghanistan and Pakistan have the lowest values. Israel and Kuwait were the only two countries with values of all indicators above the global average, while all other countries had most indicators below the average. Mongolia stands out as a country with a mixed performance. Its GDP_{pc}, EPI, and LEI values are below average, but its HDI value is above average. Conflict undoubtedly influences the four indicators, especially in Iraq, Afghanistan, Pakistan, and especially Syria, where complete data are not even available. The challenges facing the sustainability of SES in each country are different, but successful models within the ADB exist and can be adopted if there is strong support from citizens, sound government initiatives, and a favorable global environment and connections.

There are many challenges for achieving growth and sustainability of the SES in the ADB. Chen et al. (2018) identified five pressing issues for its sustainability on the Mongolian Plateau: (1) divergent and uncertain changes in social and ecological characteristics; (2) the declining prevalence of nomadism; (3) the consequences of rapid urbanization in transitional economies; (4) the unsustainability of large-scale afforestation efforts in the semi-arid and arid areas of Inner Mongolia; and (5) the role of institutional changes in shaping the SES on the Plateau. In considering the sustainability of livestock in the ADB, Qi et al. (2017) highlighted four main challenges: (1) achieving an agreeable balance of trade-offs among different ecosystem services, (2) balancing long- and short-term benefits, (3) bending the trajectory of consumption behaviors and culture, and (4) ensuring community participation, adaptation, and coordination. We now identify five additional concerns for the region, either entirely or in part:

10.5.1 Water Scarcity

Water is essential for the ecological and economic sustainability of all ecosystems, and by definition, it is scarce in drylands systems. Several major factors are likely to exacerbate future water scarcity in the ADB (Lattimore 1940; Micklin 1991, 2008; Qi and Kulmatov 2008; Smolyar et al. 2012; Qi et al. 2017). These include a rapid loss of glaciers, the disappearance of lakes (Micklin 1991; Qi and Kulmatov 2008), reduced stream flows (Dostaj et al. 2006; Kezer and Matsuyama 2006; Qi et al. 2012; Propastin 2013), increased abstraction of water for irrigation and direct human use, elevated loss due to ET (Jung et al. 2010), and reduction in groundwater

table. Coupled with these changes are lengthened and severe droughts and/or increased extreme precipitation events that can trigger large scale flooding and landslides in mountainous terrain. The likely loss of glaciers is a particularly serious concern that could tip the water balance of the ADB into a permanently unsustainable situation. Indeed, control of stream flows in upper reaches is becoming a critical issue in transboundary water disputes, such as those among the Central Asian republics (Yasinsky et al. 2010).

Dams and related forms of hydrological engineering by Turkey and Iran in the upper streams of the Euphrates-Tigris basin and by the Central Asian republics in the Tianshan mountains are widely recognized as sources of water conflicts within the ADB (Groisman et al. 2020, Chap. 2). Within the transboundary Shatt Al-Arab river system, the accessible downstream water is greatly influenced by increased water withdrawal and upstream water diversion, which has resulted in a significant decline in arable lands and saltwater intrusion at the delta (Singh 2005; Brandimarte et al. 2015). Four rivers, including the Euphrates (2800 km), Tigris (3000 km), Karun (867 km), and Karkheh (964 km), all originate in the mountains of Iran and Turkey and feed the Shatt Al-Arab basin, where transboundary water is shared by Turkey, Syria, Iran, Jordan, Saudi Arabia, and Iraq. The surface region is 938,305 km^2 (*i.e.*, the largest basin in southwestern Asia), with Iraq supplying 16% of the overall water to the basin (Al-Asadi 2017). Population growth, agricultural expansion, dam construction, climate change, and expanded irrigation systems are all putting an escalating demand for water supplies. While the regeneration of water from natural precipitation has been decreasing (Fig. 10.2a), downstream freshwater, especially near Basra in Iraq, has been severely affected by redirecting water to the Kashmir Channel inside Iran. These two coupled processes make the basin one of the major "hotspots" of drought within the ADB (Fig. 10.2a). To resolve the accessibility of freshwater downstream, inter-governmental cooperation for water use and management among Turkey, Iran, and Iraq is urgently needed with a goal of mutual benefit of all parties. These countries have organized conventions, signed treaties, and proposed various protocols to regulate water use, but none so far has been implemented (Abdullah et al. 2015; Beaumont 1996).

Redistribution of river water within the Shatt Al-Arab river system has directly altered vegetation, agriculture and, consequently, people and societies. The normalized difference vegetation index (NDVI) within the flood plains of the river declined from 1975 to 2017 (Fig. 10.7a). The change in NDVI (−0.004) along the Karun River, just upstream from its junction with the Shatt Al-Arab river is the result of slightly increased NDVI on the west bank of the river in Iraq and a decrease in NDVI on the east side in Iran, where military wastes have been deposited (Fig. 10.7a). Along the Karun River, changes in NDVI have opposite signs in Iran and Iraq (Fig. 10.7a). The average change in NDVI on Iraq side is −0.005, but it is +0.027 on Iran side (Fig. 10.7b). This is a direct result of water redirection from the Karun River into Iran's inland Kashmir Channel for irrigation. In short, the Iran government constructed engineering infrastructure since 2008 to withdraw water from the Karun River and divert it to the Kashmir Channel to promote large scale irrigation of agriculture fields (Hamid 2015). This greatly reduced the water flow of the Shatt al-Arab River, setting the stage for the catastrophic intrusion of high salinity water

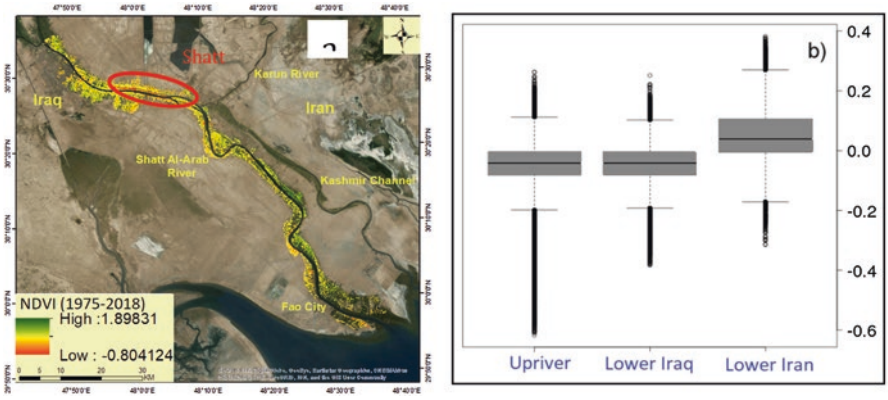

Fig. 10.7 Spatial change in NDVI between 1975 and 2017 in the Shatt Al Arab Region, showing the difference at the junction of the Karun River with the Shatt al Arab River. NDVI in the southwest of the region has declined more than that in the southeast and north of the region. The southwest region close to the Persian (Arabian) Gulf, which is affected by sea level rise, has less fresh water than that in the northern part of the region. The southeast part has a higher increase in NDVI because the Iranian Government withdraws more water from the Karun River for irrigation

from the Persian Gulf farther north into Fao City (Abdullah et al. 2015; Hamid 2015). Available water for Iraq's agricultural fields was further reduced. Water withdrawal by Iran must be reconsidered and renegotiated if the river is to be sustained as a source of water supplies for both countries, and for the sake of preserving the surrounding ecosystem and the societies that depend on it. This example demonstrates not only the importance of water use in drylands but also the importance of joint efforts by multiple governments when river basins are transboundary.

Similar challenges also characterize river basins dependent on glaciers on the Tianshan Mountains in Central Asia Core. The Ili River, for example, originates from the mountains of Xinjiang, China, and flows across an increasingly arid landscape before terminating in Kazakhstan's Lake Balkhash, which has no outlet to the ocean. The river has been extensively impounded and diverted over the past half-century to produce hydroelectric power and food on irrigated land (*e.g.*, Kulmatov et al. 2008; Pueppke et al. 2018; Qi et al. 2017). Water withdrawals are increasing to the extent that they are threatening the sustainability of the ecosystem, just as it is becoming stressed by altered inflows as glaciers retreat and disappear (Pueppke et al. 2018). As a consequence, the basin is undergoing dramatic changes in land use and land cover with significant implications for water, energy, and food systems (Amirgaliev et al. 2012; Graham et al. 2017; Pueppke et al. 2018; Qi et al. 2017). Human dimensions, especially the economic development policies both in China and Kazakhstan, are exacerbating this challenge and will remain a major driver of the future sustainability of the basin.

10.5.2 Intensified Land-Use and Land-Cover Changes

With continued population increases, economic development, and climatic changes, demands for land will be further intensified across the ADB (Henebry et al. 2020, Chap. 3). Major land demands will likely come from agricultural expansion (Spaeth et al. 2020, Chap. 8; Sokolik et al. 2020, Chap. 4), urban sprawl (*e.g.*, Fan et al. 2020, Chap. 7), promotion of livestock farming, and construction of major infrastructure such as roads and railroads (Chen et al. 2018). The United Nations Convention to Combat Desertification (UNCCD) predicts that desertification will also likely continue to expand (http://www.unesco.org/new/en/natural-sciences/environment/ecological-sciences/specific-ecosystems/drylands/). Each country will nevertheless have its unique trajectory of land-use change—its type, intensity, duration, and extent. Irrigated agricultural lands will likely expand, even though intensification of water use may occur. Turkey, for example, plans to upscale its Southeastern Anatolia Project, which was started 40 years ago. This project includes 22 large dams and 19 hydroelectric power stations in the upper Euphrates and Tigris rivers to store water during the rainy season and release it during the dry months. The new irrigation areas have been extended to over 18,000 km^2 (Ozdogan et al. 2006; Bilgen 2018). Similar large-scale projects have escalated in Chinese provinces (Wang and Jin 2006), Iran (Hamid 2015), Kazakhstan (FAO 2016), and other locations. Irrigation is essential to sustain national crop production in northern China (Wang et al. 2012), with high demands for use in Inner Mongolia, Gansu, Ningxia, and Xinjiang (*cf.* Fig. 10.3).

In addition to the rapid expansion of urban areas (Fan et al. 2020, Chap. 7), development of major rail and highway transportation systems (Chen et al. 2018) and industries such as mining and oil production will likely result in more land conversion. Before 1990, Inner Mongolia and Mongolia had comparable road transportation networks on the Mongolian Plateau. Today this vital infrastructure is much more advanced in Inner Mongolia, with paved roads and railroads at densities that are 13.2 and 5.7 times of those in Mongolia (Chen et al. 2018). Other infrastructure such as hay harvesting facilities, fenced grazing lands, feedstock importing and storage facilities, and gravel roads will almost certainly be substantially and extensively developed shortly in other ADB countries, especially in Central Asia Core. Kazakhstan is a case in point. Land-use/land-cover changes in this large, newly independent republics were triggered by dramatic socio-economic changes after the collapse of the Soviet Union in 1991. Differential effects are apparent. Land degradation in the Ust-Urt Plateau has been severe due to exploration and exploitation of the gas and oil reserves in the region. On the other hand, the Kyzyl-Kum Desert underwent rehabilitation processes due to a dramatic reduction in grazing pressure as food production shifted from herding to settled, crop-based agriculture (Karnieli et al. 2008). Mongolia has experienced similar drivers that include overgrazing, shifts from nomadic to pasture-based livestock production, the rapid expansion of mining land, and urbanization (Cao et al. 2013; Tuvshintogtokh and Ariungerel 2013; Chen et al. 2018).

10.5.3 Climatic Extremes and Climatic Change

Drylands are typically characterized by extreme climatic conditions, temporally and spatially. According to Mildrexler et al. (2006): "In 2004, the hottest spot on the Earth's surface was 68.0 °C, in the Lut desert of Iran's Kerman Province (30.1°N, 59.3°E). Described as the 'thermal pole of the Earth,' the Iranian deserts are regarded as among the hottest, driest desert regions in the world. In fact, the Lut is so inhospitable to life that not even bacteria can survive (http://www.wonderquest.com/; DesertDriest.htm). In 2005, the Lut desert reached 70.7 °C (29.9°N, 59.1°E) and again registered the hottest LST on Earth." The future climate of the ADB is nevertheless expected to be warmer, drier, and more even in distribution as compared to today. Importantly, climatic variation, especially extreme events such as droughts, extremely cold winters, and heatwaves from late spring through the summer, will escalate and threaten to tip ecosystem function and disrupt human wellbeing.

Periods of extremely low temperature and dry air are known as the *dzud* in Mongolia. They have been increasing in frequency and intensity on the Mongolian Plateau over the past 70+ years and will likely continue to increase with future atmospheric changes (Bayasgalan et al. 2009). The number of heatwaves in the Songnen plain of China has been increasing since the 1980s, and the rate of occurrence has increased since the 2010s to higher than ever before (Qu et al. 2016). These increases are coupled with droughts, which will likely exert strong effects on livestock mortality, human wellbeing, and local to national economies (Chen et al. 2018; Fernández-Giménez et al. 2012; John et al. 2016; North 1989). There is every reason to believe that these extremes will be further elevated across ADB landscapes as the climate changes. Of great concern is the observation that these climatic extremes often coincide in time and space, making their impact especially dangerous and life-threatening to humans. There is an urgent need to model and understand the consequences of joint forcing on ecosystems and societies, especially at broader spatial and temporal scales.

10.5.4 Globalization and Cross-Country Effects

ADB entities are not exempt from the rapid process of globalization that is occurring worldwide. Culture, market and trade, information technology, and labor migration from the ADB, as well as remittances back to the ADB, are among the key drivers of SES dynamics and functions. Among many pressing issues including the changes discussed in Sects. 9.1, 9.2, 9.3, 9.4, and 9.5, we emphasize the importance of human migration within (and outside) of the ADB, as well as remittances that interconnect SES measures.

In many developing economies in the ADB, workers migrate from rural to urban locations in search of gainful employment. Labor migration may be domestic—to a city in the same country—or international—to a city in another country. Labor migrants often remit a portion of their earnings to their families back home (Olimova and Olimov 2007; Abdih et al. 2012b). These remittances use the international

banking system and are typically in the form of money transfers between family members across national borders. They constitute a significant source of income in many developing countries and can exceed overseas development aid (Ratha 2016). Although remittances generally flow from stronger to weaker economies, counterflows can occur to assist dependent family members, *e.g.*, students studying abroad or emigrants in distress. In addition, some portions of the remittance are small business holders transferring capital and profit.

Understanding the bilateral flows of international remittances can shed light on the informal linkages between nations and the dependence of developing economies on the health of stronger economies. In 2015, the top five recipients of remittances were India, China, the Philippines, Mexico, and France, comprising 11.9%, 11.0%, 4.9%, 4.5%, and 4.0% of global remittances, respectively, for a total of more than US$210 billion or 36.3% of global remittances. The dependence of the recipient economies on remittances ranged widely from 9.8% of GDP for the Philippines to 0.6% for China. In contrast, the top five recipients of remittances in 2015 relative to GDP were Nepal, Liberia, Tajikistan, Kyrgyzstan, and Bermuda, comprising 32.2%, 31.2%, 28.8%, 25.7%, and 25.0% of GDP, respectively, for a total of just US$12.7 billion or less than 2.2% of global remittances (Ratha 2016). Note that two of these top five recipients are from Greater Central Asia.

There are three salient aspects of remittance networks. First, remittances appear to be strongly procyclical relative to sending-country income (Abdih et al. 2012b; Barajas et al. 2012). Second, remittances tend to be spent on the consumption of both imported and domestically produced goods, rather than on investments (Abdih et al. 2012b; Rubinov 2014). Third, shocks in the sending countries are transmitted via remittances both to the public finances—specifically, tax revenues—of receiving countries (Abdih et al. 2012b; Barajas et al. 2012) and to the families reliant on remittances (Akramov and Shreedhar 2012). Moreover, some studies have linked increased remittance inflows to decreases in institutional quality (increased corruption, lower government effectiveness), particularly when remittances constitute a high proportion of GDP (Abdih et al. 2012a; Ebeke 2012; Berdiev et al. 2013).

Within the ADB there is a variety of dependencies on remittances, but here we will contrast the remittance networks in the countries of former Soviet Central Asia Core (*i.e.*, Kazakhstan, Kyrgyzstan, Tajikistan, Turkmenistan, and Uzbekistan) with Mongolia. Since remittances flow from emigrants back to their country of origin, we speak first about emigration. Between 2013 and 2017 there were increases in emigrant populations in every country, but the magnitude of migrants from Central Asia was much larger than from Mongolia (Table 10.4). In 2017, the destination of most of the migrants from Central Asia was the Russian Federation, with Germany and Ukraine being top destinations outside of Greater Central Asia (Table 10.5). In contrast, the plurality of migrants from Mongolia went to the Republic of Korea with the Russian Federation placing second (Table 10.5). Destinations of Mongolian migrants were more diverse than those from Central Asia Core (Table 10.5). While the United States was a top ten destination for every Central Asian country, it did not attract more than 3% of the total, and it was not in the top ten for Mongolia (Table 10.5).

Table 10.4 Estimated stocks of emigrants from Central Asia and Mongolia. "n" indicates a number of emigrants, "Δ" indicates the difference between 2013 and 2017

	2013 (n)	2017 (n)	Δ (n)	Δ (%)
Kazakhstan	3,826,984	3,945,105	118,121	3.1
Kyrgyzstan	738,283	781,950	43,667	5.9
Tajikistan	607,802	638,249	30,447	5.0
Turkmenistan	249,523	258,256	8,733	3.5
Uzbekistan	1,912,897	2,071,103	158,206	8.3
Central Asia	**7,335,489**	**7,694,663**	**359,174**	**4.9**
Mongolia	74,847	81,311	6,464	8.6

Source: World Bank

Table 10.5 Emigrant stocks and destinations for the countries of former Soviet Central Asia and Mongolia in 2017. "n" indicates the number of emigrants

Nation	Emigration (n)	Rank										Top 5 ranks
		1st (%)	2nd (%)	3rd (%)	4th (%)	5th (%)	6th (%)	7th (%)	8th (%)	9th (%)	10th (%)	Sum (%)
Kazakhstan (KZ)	3,945,105	RU	DE	UA	UZ	BY	US	GR	BY	MA	TM	
		64.9	18.7	5.9	2.3	1.8	0.8	0.7	0.5	0.5	0.5	93.7
Kyrgyzstan (KG)	781,950	RU	DE	UA	UZ	TJ	KZ	US	BY	TR	AZ	
		75.7	10.7	3.6	1.9	1.5	0.9	0.8	0.7	0.5	0.4	93.4
Tajikistan (TJ)	638,249	RU	KZ	UA	DE	AF	UZ	BY	US	AZ	MA	
		73.1	5.9	4.8	4.6	3.9	2.4	0.9	0.7	0.5	0.4	92.3
Turkmenistan (TM)	258,256	RU	UA	UZ	DE	BY	TR	IR	KZ	IL	US	
		71.9	9.2	2.7	2.6	2.1	1.9	1.9	1.0	0.9	0.9	88.7
Uzbekistan (UZ)	2,071,103	RU	KZ	UA	TM	US	DE	TR	KR	IL	AZ	
		55.4	14.7	11.2	4.1	3.0	2.0	1.7	1.2	1.1	0.8	88.4
Mongolia (MG)	81,311	KR	RU	CZ	CN	UA	SE	AT	AU	UK	FR	
		33.4	26.0	7.0	5.6	5.4	3.2	2.6	2.6	1.8	1.8	77.5

Source: World Bank

The contrast between remittance inflows to Central Asia and Mongolia (Table 10.6) and remittance outflows from Central Asia and Mongolia (Table 10.7) illustrates the relative strength of national economies, but more importantly, differences among the countries. Kazakhstan is remarkable among the Central Asia Core for having 16 times more outflows than inflows. In contrast, Kyrgyzstan and Tajikistan have 5 times and 11 times more inflows than outflows, respectively. Since monetary transfers out of Turkmenistan and Uzbekistan are prohibited, there are data only on remittance inflows. Uzbekistan receives nearly as many remittances as Kyrgyzstan and Tajikistan combined, but its population and economy are much larger. Turkmenistan receives very little in remittances. Mongolia's ratio of inflows to outflows is closer to unity.

Remittance networks remain an understudied dimension of SES, but they form a critical dynamic in the ADB. However, the magnitudes of remittances into and out of the region are underestimated because the informal value transfer systems of

Table 10.6 Estimated remittances into Central Asia and Mongolia in 2014–2016. "$M" indicates millions of US$ Source: World Bank

Nation	2014 ($M)	2015 ($M)	2016 ($M)	Total ($M)
Kazakhstan	229	194	275	698
Kyrgyzstan	2,243	1,688	1,995	5,926
Tajikistan	3,384	2,259	1,867	7,510
Turkmenistan	30	16	9	55
Uzbekistan	5,828	3,062	2,479	11,369
Central Asia Core	**11,714**	**7,219**	**6,625**	**25,558**
Mongolia	255	261	260	776

Table 10.7 Estimated remittances out from Central Asia and Mongolia in 2014–2016. "$M" indicates millions of US$ Source: World Bank

Nation	2014 ($M)	2015 ($M)	2016 ($M)	Total ($M)
Kazakhstan	3,550	3,078	2,395	9,023
Kyrgyzstan	454	363	378	1,194
Tajikistan	304	165	87	556
Turkmenistan	0	0	0	0
Uzbekistan	0	0	0	0
Central Asia Core	**4,308**	**3,606**	**2,860**	**10,773**
Mongolia	337	228	171	735

hawala in the Middle East and hundi in South Asia do not use the international banking system (Abdih et al. 2012b; Ratha 2016).

10.5.5 Unforeseeable Institutional Changes and Shifts

These unknowns are perhaps the most critical change for the future because the ADB will likely remain at the center of recurring geopolitical conflicts, which will, in turn, affect the structure and function of the SES. Historical conflicts across the ADB have been massive and extensive, with significant enduring legacy effects (Chen et al. 2018). For example, without a strong Buddhism movement in western China, the sole dawn redwood (*Metasequoia glyptostroboides)*—one of the three living fossil trees that is responsible for all trees across the globe—next to a Buddhist temple would not be preserved (Shao et al. 2000). The Iran and Iraq war during 1980–1988 left the Shatt Al-Arab river region littered with the remnants of conflict. The legacy of the 8-year military operation, which was conducted in an area of about 120 km^2 (Fig. 10.7a) along the eastern border of Iraq with Iran, continues to threaten the ecosystems, people, and development of agricultural systems because the area remained restricted from human access (Mohammed 2008). Minefields, for

example, are significant obstacles for farmers and/or residents to rebuild agriculture or return to their homes.

Other evidence has also been reported showing the significance of institutional changes in societies and ecosystems. For example, Tajikistan and Afghanistan used to be part of Iran since the First Persian Empire until the nineteenth century, resulting in a large portion of the population speaking versions of Farsi. Similarly, the language and culture have remained strongly influenced by Russia after the collapse of the USSR in 1991. Much of the current livestock production in northern Kazakhstan depends on demand for meat in Russia. After a series of wars in Iraq, Afghanistan, Syria, and Pakistan, these countries remain on uncertain trajectories of future governance. China's recent Belt and Road Initiative (BRI) is expanding quickly through Central Asian countries, while Mongolia is extending its ties beyond Russia and China to Japan, South Korea, Australia, the USA, and the EU. Both efforts will cause substantial changes for the societies and natural landscapes, including the development of transportation corridors, increased mining, and urbanization). At the local scale, each government has its policies to promote its economic development and perceived wellbeing. One example is the large-scale planting of fast-growing poplar trees in the arid and semi-arid areas of Inner Mongolia (Chen et al. 2018).

10.6 Outlook

Global drylands cover about 40% of the Earth's total land surface, with the ADB serving as the largest such area. This region has an extremely high contrast of social, economic, cultural, traditional, governmental, climatic, and geophysical features. It also has historically been an important crossroads for human civilization and societal development. In recent decades, global environmental change has created different mosaics of temperature, precipitation, climatic extremes, and associated natural disturbances—dust storms, *dzuds*, heat waves, flood shortages, and landslides. Following a brief review of major historical events and biogeography of the ADB, we have provided summaries of relevant climatic and land use changes. Our macrosystem analysis of the interrelationships among the key indicators of social, economic, and ecological systems reveals the complexity and variety of SES structure and function across the region. While the need for in-depth analysis of the SES dynamics for the sustainability of ADB entities is apparent and urgent, the scientific community may face an extreme challenge in modeling and predicting the future. This is partially due to a lack of data (both availability and accessibility), unforeseeable institutional changes that could tip SES structure and function, and/or potentially greater influence from globalization or neighboring countries.

Here we have proposed a conceptual framework by including institutions as the essential foundation for understanding and modeling the SES in terms of the conventional three pillars of sustainability science (Clark and Dickson 2003; Kates et al. 2001; UNGA 2005): the social, economic, and ecological systems (Fig. 10.8). The pivotal role of institutional change on SES has been well described for socio-

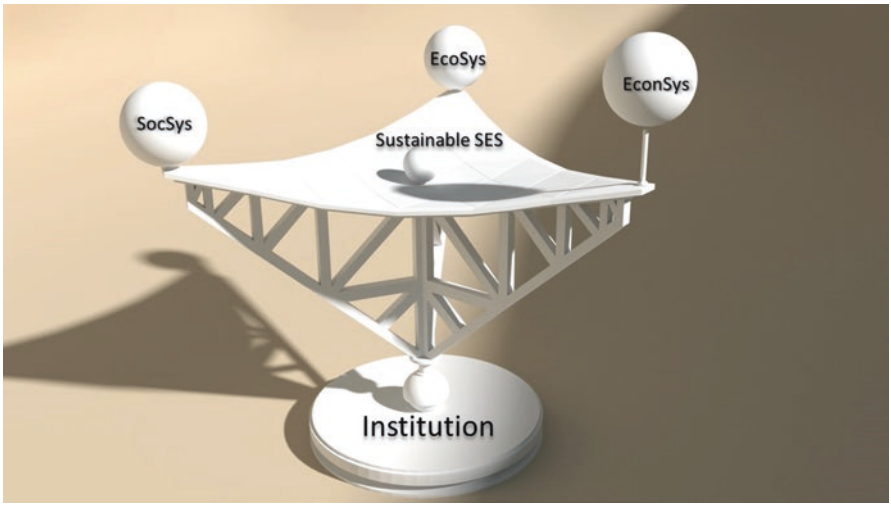

Fig. 10.8 The sustainability of social and ecological systems (SES) is conventionally conceptualized by the entangled elements of social systems (SocSys), economic systems (EconSys), and ecological systems (EcoSys). Institutions and their change serve as the foundation that determines the structure, function and dynamics of the three systems, as well as their interdependent relationships

economic aspects (North 1989; Ostrom 1986), but less so for ecosystem structure, function, and dynamics (Chen et al. 2015b, 2018). The inclusion of institutional change is critical at macro-scales because the complex interactions among elements of the three pillars develop within the context of geopolitical change, technological advancement, and regional environmental change. The ability of local populations to cope with or adapt to these changes is contingent upon local to national institutions (Lioubimsteva and Henebry 2009).

Integrating institutions into macrosystem analyses is challenging. We have endeavored to advance sustainability science by including institutions as the essential foundation of the three-pillared macrosystem because: (1) the sustainability of a macrosystem is maintained by the complex interactions and feedbacks among the entangled elements of the three pillars; (2) a major change in any of these elements can tip the balance and stability of a macrosystem; (3) while external driving forces (*e.g.*, geopolitical or climatic changes) play significant roles in the sustainability of a macrosystem, institutional shifts also have great potential to counteract external influences through adaptation. The direct and indirect effects on ecosystems and societies derived from the collapse of the former Soviet Union across Central Asia (de Beurs and Henebry 2004, 2008), Eastern Europe (Kuemmerle et al. 2008; Prishchepov et al. 2012), Drylands East Asia (Chen et al. 2013, 2018) have been reported. National and regional land use, ecosystem functions, and socioeconomic stability have been dramatically and directly altered. The reduction in livestock and herder practices in western Mongolia after 1992, when a large portion of its population migrated to central cities or other mining regions, is a vivid case in point (Park et al. 2017).

Quantitative examination of the three-pillared nature of sustainability rarely occurs. Disciplinary approaches have been occasionally investigated (Costanza et al. 2000; Fisher et al. 2008), but few have quantitatively addressed regulation of the complex interactions and feedbacks among the elements of the three-pillar system (Chen et al. 2015a; Fan et al. 2020). We have demonstrated that major policy shifts on the Mongolian Plateau, including those triggered by the collapse of the Soviet Union and China's elevated status in the World Trade Organization (WTO), have changed the empirical relationships among ecosystem production, population density, gross domestic production, livestock, and land use (Chen et al. 2015a). Although these relationships will undoubtedly be different when comparing the Middle East, Central Asia Core, and Drylands East Asia (Fig. 10.5), their inclusion as an institutional dimension of macrosystem analyses will be crucial for understanding the future of the ADB.

Acknowledgments We would like to acknowledge the financial support from the National Aeronautics and Space Administration (NASA)'s Land-Cover and Land-Use Change (LCLUC) Program (NNX15AD51G, NNX14AJ32G), and the "Dynamics of Coupled Natural and Human Systems (CNH)" Program of the NSF (#1313761). Any opinions, findings, conclusions or recommendations expressed in this chapter are those of the authors and do not necessarily reflect the views of NASA or the NSF.

References

Abdih Y, Chami R, Dagher J, Montiel P (2012a) Remittances and institutions: are remittances a curse? World Dev 40:657–666

Abdih Y, Chami R, Ebeke C, Barajas A (2012b) Remittances channel and fiscal impact in the Middle East, North Africa, and Central Asia. IMF Work Pap 12:1.

Abdullah AD, Masih I, van der Zaag P et al (2015) Shatt al Arab River system under escalating pressure: a preliminary exploration of the issues and options for mitigation. Int J River Basin Manag 13:215–227

Akramov KT, Shreedhar G (2012) Economic development, external shocks, and food security in Tajikistan. IFPRI Discuss Pap 60

Al-Asadi SAR (2017) The future of freshwater in Shatt Al- Arab river (Southern Iraq). J Geogr Geol 9:24.

Amirgaliev NA, Timirkhanov SR, Isbekov KB (2012) Fisheries in Kazakhstan: state and prospects. In: Water resources of Kazakhstan: assessment, forecast, management. UNDP Publication in Kazakhstan, Almaty, p 670

Barajas A, Chami R, Ebeke C, Tapsoba SJ-A (2012) Workers' remittances: an overlooked channel of international business cycle transmission? IMF Work Pap 12:1.

Baumann M, Radeloff VC, Avedian V, Kuemmerle T (2015) Land-use change in the Caucasus during and after the Nagorno-Karabakh conflict. Reg Environ Chang 15(8):1703–1716

Bayasgalan B, Gombluudev R, Oyunbaatar P et al (2009) Climate change and sustainable livelihood of rural people in Mongolia. In: Devissher et al (eds) The adaptation continuum: groundwork for the future. ETC Foundation, Leusden, pp 193–214

Beaumont P (1996) Agricultural and environmental changes in the upper Euphrates catchment of Turkey and Syria and their political and economic implications. Appl Geogr 16:137–157

Berdiev AN, Kim Y, Chang CP (2013) Remittances and corruption. Econ Lett 118:182–185

Bernauer T, Siegfried T (2012) Climate change and international water conflict in Central Asia. J Peace Res 49:227–239

Bilgen A (2018) The southeastern anatolia project (GAP) in Turkey: an alternative perspective on the major rationales of GAP. J Balkan Near East Stud 21:532–552.
Bordachev T, Wan Q, Small A (2016) Report: Russia, China, and USA in Central Asia: a balance of interests and opportunities for cooperation—valdai club. Moscow, Russia
Brandimarte L, Popescu I, Neamah NK (2015) Analysis of fresh-saline water interface at the Shatt Al-Arab estuary. Int J River Basin Manag 13(1):17–25
Cao J, Yeh ET, Holden NM et al (2013) The roles of overgrazing, climate change and policy as drivers of degradation of China's grasslands. Nomad People 17:82–101
Carrère d'Encausse H (2009) Islam and the Russian empire: reform and revolution in central Asia. I. B. Taurus, New York, p 267
Chen J, Wan S, Henebry G et al (2013) Dryland East Asia: land dynamics amid social and climate change. de Gruyter and Higher Education Press, Beijing, p 415
Chen J, John R, Shao C et al (2015a) Policy shifts influence the functional changes of the CNH systems on the Mongolian Plateau. Environ Res Lett 10:085003.
Chen J, John R, Zhang Y et al (2015b) Divergences of two coupled human and natural systems on the Mongolian Plateau. Bioscience 65:559–570
Chen J, John R, Sun G et al (2018) Prospects for the sustainability of social-ecological systems (SES) on the Mongolian Pateau: five critical issues. Environ Res Lett 13:123004.
Clark WC, Dickson NM (2003) Science and technology for sustainable development special feature: Sustainability science: the emerging research program. Proc Natl Acad Sci 100:8059–8061
Costanza R, Daly H, Folke C et al (2000) Managing our environmental portfolio. Bioscience 50:149–155
Costanza R, Graumlich L, Steffen W et al (2007) Sustainability or collapse: what can we learn from integrating the history of humans and the rest of nature? Ambio 36:522–527
de Beurs KM, Henebry GM (2004) Land surface phenology, climatic variation, and institutional change: analyzing agricultural land cover change in Kazakhstan. Remote Sens Environ 89:497–509
de Beurs KM, Henebry GM (2008) War, drought, and phenology: changes in the land surface phenology of Afghanistan since 1982. J Land Use Sci 3:95–111
de Beurs K, Ioffe G, Nefedova T, Henebry G (2017) Land change in European Russia: 1982–2011. In: Land-cover and land-use changes in eastern Europe after the collapse of the Soviet Union in 1991. Springer International Publishing, Cham, pp 223–241
de Beurs KM, Henebry GM, Owsley BC, Sokolik IN (2018) Large scale climate oscillation impacts on temperature, precipitation and land surface phenology in Central Asia. Environ Res Lett 13(6):065018.
Diamond J (1997) Guns germs and steel:the fates of human societies. W. W. Norton & Company, New York
Dostaj ŽD, Giese E, Hagg W (2006) Wasserressourcen und deren Nutzung im Ili-Balchaš Becken. ZEU, Giessen
Ebeke CH (2012) Do remittances lead to a public moral hazard in developing countries? An empirical investigation. J Dev Stud 48:1009–1025
Elisseeff V (2001) The Silk Roads: highways of culture and commerce. Berghahn Books, New York
Fan P, Ouyang Z, Chen J et al (2020) Population and urban dynamics in dryland China. In: Gutmann G et al (eds) Landscape dynamics of drylands across greater central Asia: people, societies and ecosystems. Springer, Cham
FAO (2016) AQUASTAT – FAO's information system on water and agriculture. Available at: http://www.fao.org/nr/water/aquastat/main/index.stm
Fernandez-Gimenez ME (2001) The effects of livestock privatization on pastoral land use and land tenure in post-socialist Mongolia. Nomad People 5:49
Fernández-Giménez ME, Batkhishig B, Batbuyan B (2012) Cross-boundary and cross-level dynamics increase vulnerability to severe winter disasters (dzud) in Mongolia. Glob Environ Chang 22:836–851.
Fisher B, Turner K, Zylstra M et al (2008) Ecosystem services and economic theory: integration for policy-relevant research. Ecol Appl 18:2050–2067

Frankopan P (2017) The silk roads: a new history of the world. Knopf Doubleday Publishing, New York
Graham NA, Pueppke SG, Uderbayev T (2017) The current status and future of Central Asia's fish and fisheries: confronting a wicked problem. Water (Switzerland) 9:01.
Groisman P, Shugart H, Kicklighter D et al (2017) Northern Eurasia Future Initiative (NEFI): facing the challenges and pathways of global change in the twenty-first century. Prog Earth Planet Sci 4:41
Groisman PY, Bulygina ON, Henebry G et al (2018) Dry land belt of northern Eurasia: contemporary environmental changes and their consequences. Environ Res Lett 13:115008.
Groisman PY, Bulygina ON, Henebry GM et al (2020) Eurasian drylands: contemporary environmental changes. In: Gutman G et al (eds) Landscape dynamics across drylands of greater central Asia: people, societies and ecosystems. Springer, Cham
Hamid RAM (2015) The concentration of salt in Shatt Al-Arab. J Basrah Res 39:229–252
Henebry G, De Beurs K, Christopher W et al (2013) Dryland east Asia in hemispheric context. In: Chen J et al (eds) Dryland east Asia: land dynamics amid social and climate change. de Gruyter, Berlin/Boston
Henebry GM, de Beurs KM, John R et al (2020) Recent land surface dynamics across the Eurasian Drylands. In: Gutman G et al (eds) Landscape dynamics of drylands across greater central Asia: people, societies and ecosystems. Springer, Cham
IPCC (2013) Climate change 2013: the physical science basis. Contribution of working group I to the fifth assessment report of the intergovernmental panel on climate change. IPCC, Cambridge/New York
John R, Chen J, Kim Y et al (2016) Differentiating anthropogenic modification and precipitation-driven change on vegetation productivity on the Mongolian Plateau. Landsc Ecol 31:547–566
Jones M, Hunt H, Kneale C et al (2016) Food globalisation in prehistory: the agrarian foundations of an interconnected continent. J Br Acad 4:73–87
Jung M, Reichstein M, Ciais P et al (2010) Recent decline in the global land evapotranspiration trend due to limited moisture supply. Nature 467:951–954
Kappas M, Degener J, Klinge M et al (2020) A conceptual framework for ecosystem stewardship based on landscape dynamics: case studies from Kazakhstan and Mongolia. In: Gutman G et al (eds) Landscape dynamics across drylands of greater central Asia: people, societies and ecosystems. Springer, Cham
Karnieli A, Gilad U, Ponzet M et al (2008) Assessing land-cover change and degradation in the central Asian deserts using satellite image processing and geostatistical methods. J Arid Environ 72(11):2093–2105
Kates RW, Clark WC, Corell R et al (2001) Sustainability science. Science 292:641–642
Kezer K, Matsuyama H (2006) Decrease of river runoff in the Lake Balkhash basin in Central Asia. Hydrol Process 20(6):1407–1423.
Kuemmerle T, Hostert P, Radeloff VC et al (2008) Cross-border comparison of post-socialist farmland abandonment in the Carpathians. Ecosystems 11:614–628
Kulmatov R (2008) Modern problems of using, protection and management of water and land resources of the Aral Sea basin. Environmental problems of Central Asia and their economic, social and security impacts. Collection of Articles, Springer, pp 24–32
Lattimore O (1940) Inner Asian frontiers of China. American Geographical Society, New York
Lioubimtseva E, Henebry GM (2009) Climate and environmental change in arid central Asia: impacts, vulnerability, and adaptations. J Arid Environ 73:963–977
Micklin P (1991) The water management crisis in Soviet Central Asia (the Carl Beck papers in Russian and east European studies). University of Pittsburgh Center for Russian and East European Studies, Pittsburgh
Micklin PP (1998) Desiccation of the Aral Sea: a water management disaster in the Soviet Union. Science 241(4870):1170–1176
Micklin PP (2007) The Aral Sea disaster. Annu Rev Earth Planet Sci 35:47–72
Micklin P (2008) Using satellite remote sensing to study and monitor the Aral Sea and adjacent zone. In: Environmental problems of central Asia and their economic, Social and security impacts. Springer, Dordrecht, pp 31–58

Mildrexler DJ, Zhao M, Running SW (2006) Where are the hottest spots on Earth? Eos 87:461–467.
Mohammed AJ (2008) Remnants of war in the province of Basra: a study of geography. Basra Stud J 5:115–150
Mukhashbaeva AK, Chumachenko TN (2016) Bilateral relations of Kazakhstan with the countries of Central Asia. Bull KaNPUR, Ser "International Life Polit" 105
Niemi TM, Ben-Avraham Z, Gat J (1997) The Dead Sea: the lake and its setting. Oxford University Press, New York
North DC (1989) Institutions and economic growth: an historical introduction. World Dev 17:1319–1332
Olimova S, Olimov M (2007) Labor migration from mountainous areas in the central Asian region: good or evil? Mt Res Dev 27:104–108
Ostrom E (1986) An agenda for the study of institutions. Public Choice 48:3–25
Ostrom E, Burger J, Field CB et al (1999) Revisiting the commons: local lessons, global challenges. Science 284:278–282
Ozdogan M, Salvucci GD, Anderson BT (2006) Examination of the Bouchet–Morton complementary relationship using a mesoscale climate model and observations under a progressive irrigation scenario. J Hydrometeorol 7(2):235–251.
Park H, Fan P, John R, Chen J (2017) Urbanization on the Mongolian Plateau after economic reform: changes and causes. Appl Geogr 86:118–127
Pongratz J, Caldeira K, Reick CH, Claussen M (2011) Coupled climate-carbon simulations indicate minor global effects of wars and epidemics on atmospheric CO_2 between ad 800 and 1850. The Holocene 21(5):843–851
Prishchepov AV, Radeloff VC, Baumann M et al (2012) Effects of institutional changes on land use: agricultural land abandonment during the transition from state-command to market-driven economies in post-Soviet Eastern Europe. Environ Res Lett 7:024021
Propastin P (2013) Assessment of climate and human induced disaster risk over shared water resources in the Balkhash Lake drainage basin. In: Climate change and disaster risk management. Springer, Berlin/Heidelberg, pp 41–54
Pueppke SG, Nurtazin ST, Graham NA, Qi J (2018) Central Asia's Ili River ecosystem as a wicked problem: unraveling complex interrelationships at the interface of water, energy, and food. Water 10:541
Qi J, Kulmatov R (2008) An overview of environmental issues in Central Asia. In: Environmental problems of central Asia and their economic, social and security impacts. Springer, Dordrecht, pp 3–14
Qi J, Bobushev TS, Kulmatov R et al (2012) Addressing global change challenges for Central Asian socio-ecosystems. Front Earth Sci 6:115.
Qi J, Xin X, John R et al (2017) Understanding livestock production and sustainability of grassland ecosystems in the Asian Dryland Belt. Ecol Process 6:22.
Qu L, Chen J, Dong G et al (2016) Heat waves reduce ecosystem carbon sink strength in a Eurasian meadow steppe. Environ Res 144:39–48
Rahaman MM (2012) Principles of transboundary water resources management and water-related agreements in central Asia: an analysis. Int J Water Resour Dev 28:475–491
Ratha D (2016) Migration and remittances factbook 2016, 3rd edn. World Bank Group, Washington, DC
Rubinov I (2014) Migrant assemblages: building postsocialist households with Kyrgyz remittances. Anthropol Q 87:183–215
Ruddiman WF (2006) The early anthropogenic hypothesis: challenges and responses. Rev Geophys 8(4):01749.
Safriel U (2009) Deserts and desertification: challenges but also opportunities. Land Degrad Dev 20:353–366
Shao G, Liu Q, Qian H et al (2000) The discoverer of *Metasequoia*: Zhan Wang. Taxon 49:593–601
Singh A (2005) One planet, many people: Atlas of our changing environment. UNEP, Nairobi

Smolyar VA, Burov BV, Mustafayev S (2012) Underground waters of Kazakhstan: security and use. In: Water resources of Kazakhstan: assessment, forecast, management. UNDP Publication in Kazakhstan, Almaty, p 402

Sokolik S, Xi X et al (2020) Quantifying the anthropogenic signature in drylands of Central Asia and its impact on water scarcity and dust emissions. In: Gutman G et al (eds) Landscape dynamics of drylands across greater Central Asia: people, societies and ecosystems. Springer, Cham

Spaeth K, Weltz MA, Guertin DP et al (2020) Hydrology and erosion risk parameters for grasslands in Central Asia. In: Gutman G et al (eds) Landscape dynamics of drylands across greater Central Asia: people, societies and ecosystems. Springer, Cham

Spengler R, Frachetti M, Doumani P et al (2014) Early agriculture and crop transmission among Bronze age mobile pastoralists of central Eurasia. Proc R Soc B Biol Sci 281:20133382.

Suttie JM, Reynolds SG, Batello C (2005) Grasslands of the world. FAO Publication, Rome

Tian L, Gong Q, Chen J (2018) Interdependent dynamics of LAI-albedo across the roofing landscapes: Mongolian and Tibetan plateaus. Remote Sens 10(7):1159.

Turner BL, Esler KJ, Bridgewater P et al (2016) Socio-environmental systems (SES) research: what have we learned and how can we use this information in future research programs. Curr Opin Environ Sustain 19:160–168

Tuvshintogtokh I, Ariungerel D (2013) Degradation of Mongolian grassland vegetation under overgrazing by livestock and its recovery by protection from livestock grazing. In: The Mongolian ecosystem network. Springer, Tokyo, pp 115–130

UNGA (2005) Resolution adopted by the General Assembly on 16 September 2005 60/1. 2005 World Summit Outcome

Wang XC, Jin PK (2006) Water shortage and needs for wastewater re-use in the north China. Water Sci Technol 53(9):35–44

Wang J, Rothausen SGSA, Conway D et al (2012) Chinas waterenergy nexus: Greenhouse-gas emissions from groundwater use for agriculture. Environ Res Lett 7:014035.

Warner TT (2004) Desert meteorology. Cambridge University Press, Cambridge

Williams T (2014) The silk roads: an ICOMOS thematic study. ICOMOS, Charenton-le-Pont, p 152

Wittfogel KA (1957) Oriental despotism: a comparative study of total power. Yale University Press, New Haven

Yasinsky VA, Mironenkov AP, Sarsembekov TT (2010) Water resources of transboundary rivers in the regional cooperation between the countries in Central Asia. Almaty, Kazakhstan

Zanca R (2011) Life in a Muslim Uzbek village: cotton farming after communism. Cengage Learning, Belmont, p 211

Index

G. Gutman et al. (eds.), *Landscape Dynamics of Drylands across Greater Central Asia: People, Societies and Ecosystems*, Landscape Series 17,
https://doi.org/10.1007/978-3-030-30742-4